

**On the development
of novel cocaine-analogues
for in vivo imaging of the
dopamine transporter status.**

Dissertation

zur Erlangung des Grades

"Doktor der Naturwissenschaften"

im Promotionsfach Chemie

am Fachbereich Chemie, Pharmazie und Geowissenschaften
der Johannes Gutenberg-Universität in Mainz

Patrick J. Riß
geb. in Aachen

Mainz, den 21.11.08

1 Abstract

The present thesis is concerned with the development of novel cocaine-derived dopamine transporter ligands for the non-invasive exploration of the striatal and extra-striatal dopamine transporter (DAT) in living systems. The presynaptic dopamine transporter acquires an important function within the mediation of dopaminergic signal transduction. Its availability can serve as a measure for the overall integrity of the dopaminergic system. The DAT is upregulated in early Parkinson's disease (PD), resulting in an increased availability of DAT-binding sites in the striatal DAT domains. Thereby, DAT imaging has become an important routine diagnostic tool for the early diagnosis of PD in patients, as well as for the differentiation of PD from symptomatically similar medical conditions. Furthermore, the dopaminergic system is involved in a variety of psychiatric diseases. In this regard, DAT-selective imaging agents may provide detailed insights into the scientific understanding of the biochemical background of both, the progress as well as the origins of the symptoms. DAT-imaging may also contribute to the determination of the dopaminergic therapeutic response for a given medication and thereby contribute to more convenient conditions for the patient.

From an imaging point of view, the former demands a high availability of the radioactive probe to facilitate broad application of the modality, whereas the latter profits from short-lived probes, suitable for multi-injection studies. Therefore, labelling with longer-lived ^{18}F -fluoride and in particular the generator nuclide ^{68}Ga is worthwhile for clinical routine imaging. In contrast, the introduction of a ^{11}C -label is a prerequisite for detailed scientific studies of neuronal interactions. The development of suitable DAT-ligands for medical imaging has often been complicated by the mixed binding profile of many compounds that interact with the DAT. Other drawbacks have included high non-specific binding, extensive metabolism and slow accumulation in the DAT-rich brain areas. However, some recent examples have partially overcome the mentioned complications. Based on the structural speciality of these leads, novel ligand structures were designed and successfully synthesised in the present work. A structure activity relationship (SAR) study was conducted wherein the new structural modifications were examined for their influence on DAT-affinity and selectivity. Two of the compounds showed improvements in *in vitro* affinity for the DAT as well as selectivity versus the serotonin transporter (SERT) and norepinephrine transporter (NET). The main effort was focussed on the high-affinity candidate PR04.MZ, which was subsequently labelled with ^{18}F and ^{11}C in high yield. An initial pharmacological characterisation of PR04.MZ in rodents revealed highly specific binding to the target brain structures. As a result of low non-specific binding, the DAT-rich striatal area was clearly visualised by autoradiography and μPET . Furthermore, the radioactivity uptake into the DAT-rich brain regions was rapid and indicated fast binding equilibrium. No radioactive metabolite was found in the rat brain. $[^{18}\text{F}]\text{PR04.MZ}$ and $[^{11}\text{C}]\text{PR04.MZ}$ were compared in the primate brain and the plasma metabolism was studied. It was found that the ligands specifically visualise the DAT in high and low density in the primate brain. The activity uptake was rapid and quantitative evaluation by Logan graphical analysis and simplified reference tissue model was possible after a scanning time of 30 min. These results further reflect the good characteristics of PR04.MZ as a selective ligand of the neuronal DAT. To pursue ^{68}Ga -labelling of the DAT, initial synthetic studies were performed as part of the present thesis. Thereby, a concept for the convenient preparation of novel bifunctional chelators (BFCs) was developed. Furthermore, the suitability of novel 1,4,7-triazacyclononane based N_3S_3 -type BFCs for biomolecule-chelator conjugates of sufficient lipophilicity for the penetration of the blood-brain-barrier was elucidated.

2 Table of Contents

1	Abstract	1
2	Table of Contents	2
3	Introduction	3
4	Manuscripts	16
4.1	A convenient chemo-enzymatic synthesis and ^{18}F -labelling of both enantiomers of <i>trans</i> -1-toluenesulfonyloxymethyl-2-fluoromethyl-cyclopropane	17
4.2	Synthesis and monoamine uptake inhibition of conformationally restricted 2 β -carbomethoxy-3 β -phenyl tropanes	34
4.3	<i>In vitro</i> , <i>ex vivo</i> and <i>in vivo</i> characterisation of [^{18}F]PR04.MZ in rodents: A selective dopamine transporter ligand for low concentration imaging.	58
4.4	Efficient [^{11}C]MeI methylation of PR04.MZ: A DAT-ligand for low concentration imaging	76
4.5	Comparison of [^{11}C]PR04.MZ and [^{18}F]PR04.MZ in <i>anubis papio</i> baboons: A selective high-affinity DAT-ligand for low concentration imaging of the extra-striate dopamine transporter	83
4.6	Efficient microwave-assisted direct fluorination of [^{18}F]PRD04 and [^{18}F]LBT999: Highly selective dopamine transporter ligands for PET	96
4.7	NODAPA-OH and NODAPA-(NCS) _n : Synthesis, ^{68}Ga -radiolabelling and <i>in vitro</i> characterisation of novel versatile bifunctional chelators for molecular imaging	108
4.8	Studies towards the synthesis of lipophilic bifunctional chelators for ^{68}Ga	115
4.9	Radioaktiv-markierte Cyclopropan-Derivate DAT-affiner Tropane	125
5	Summary and Conclusions	137
6	References	145

3 Introduction

The present thesis is concerned with design, preparation and biological evaluation of novel cocaine derivatives for the non-invasive exploration of the functionality of the human dopamine-transporter in high and low densities in the mammalian brain.

A historic progress in the methodological development of neuroscience has been made since Otto Loewi has discovered chemical neurotransmission in 1921.¹ In these days quantitative studies *in vivo* were mainly complicated due to the absence of a non-invasive method for quantitative monitoring of compounds within the living subject. Until the discovery of single photon emission computed tomography (SPECT) and the introduction of positron emission tomography (PET) by Michael Phelps and Ter-Pogossian in 1975,^{2,3} these examinations were restricted to invasive postmortem, *ex vivo* and *in vitro* studies. In contrast, the new imaging methods allowed the non invasive tracking and quantification of radioactive molecules in non-toxic, non-pharmacodynamic concentrations according to the tracer principle defined by Georg de Hevesy.⁴ Since then, the advances in technical, hardware and software equipment, the development of modern, non-invasive imaging techniques as well as the significant efforts in the development of radioactive probes for this purpose have contributed to impressive insights into the tissue distribution, metabolic rates and mechanisms of action of many biomolecules.⁵ In these terms, expanding George de Hevesy's tracer principle to living systems may be one of the greatest advances since Otto Loewi's days.

Although the modern radiological *in vivo* imaging modalities computer tomography (CT) and nuclear magnetic resonance imaging (MRI) provide superior lateral resolution (MRI, CT) and tissue contrast (MRI), their application is limited (today) to primary morphologic information. In contrast, the nuclear imaging methods SPECT and in particular PET provide quantitative information on the biochemical and physiological function of molecules, cells and tissues within the subject. Recently, this has led to the development of combined „multi-modality“ imaging approaches wherein nuclear and radiological imaging is fused (eg. PET/CT). Thereby, quantitative PET data and structural alignment information is collected in a single scanning procedure. Up to date PET/CT-scanners are prone to reliability, diagnostic information and time-effectivity of any given examination (Figure 1).

At this point the physico-technical equipment has evolved to a highly technical routine modality.⁷ However, this expensive equipment is completely useless without the continued influx of appropriate molecular probes, labelled with positron-emitting radionuclides, to meet the medicinal challenges of the present century.

The most versatile representative among these molecular imaging probes / tracers is the glucose surrogate 2-deoxy-2-[¹⁸F]fluoro-D-glucose ([¹⁸F]FDG), a fluorine labelled non-natural sugar derivative that can be applied as indicator for glucose transport and the glucose phosphorylation rate, based on the Sokoloff-correlation between metabolic trapping of 2-deoxyglucose⁸ and natural glucose metabolism inside the body.⁹ [¹⁸F]FDG is not only the most available and most cost-effective radiotracer for PET, but also provides the broad molecular diagnosis of a variety of indications related to glucose consumption.

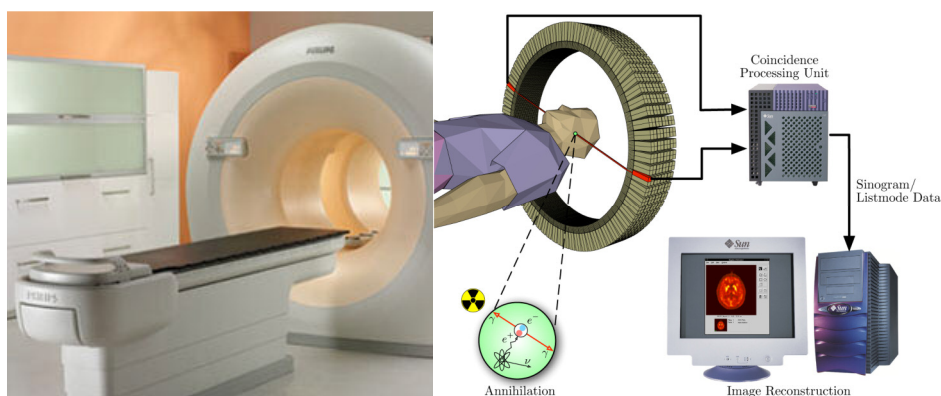


Figure 1: Philips® Gemini TF big bore PET/CT scanner (left), scheme of the theoretical background of positron emission tomography (right)⁶

It is, in addition, a highly relevant tool for diagnosing diseases of the human brain and the exploration of pharmacodynamic properties and mechanisms of action for multiple neuro-ligands and pharmaceuticals. However, full information on neuro-receptor related processes, availability and activity of a neuronal protein such as a trans-membrane receptor, an ion-channel, an extracellular or intracellular enzyme, or a neuronal trans-membrane transporter, can only be obtained with positron-emitter labelled true ligands or substrates of the system examined. Their development and characterisation is the domain of medicinal and radiopharmaceutical chemistry.

The development of appropriate ligands is often complicated by the discrete requirements for a dedicated PET-radioligand. In contrast to pharmaceutically relevant molecules, these structures have to be particularly selective for their biological target, because it is impossible to distinguish specific ligand-target interactions from ligand-binding to non-target regions and non-specific binding on the obtained images. For studies of the central nervous system (CNS), in particular, the radiotracer has to penetrate the blood-brain-barrier in sufficient concentration. Low non-specific binding is furthermore necessary for high tissue-to-non-target ratios which will result in a good visualisation within the PET images. In the end, the compound's metabolism has to be compatible with the duration of a PET examination. Furthermore, the presence of labelled metabolites within the brain, that have retained some biological activity, is disadvantageous for precise conclusions on the obtained data and thus has to be excluded. As a result, only a minority of the examined potential candidates are actually suited for initial human PET-studies.⁵

Nonetheless, multiple more or less selective radiotracers have already been developed for a variety of different neurotransmitter systems, for local energy consumption, metabolism, enzymatic activity, or drug-transport and uptake. In this regard the dopaminergic system has been studied most extensively. This is due to the fact that alterations in the dopaminergic system have been associated to a broad range of neurodegenerative or psychiatric diseases and disorders and even cancer (e.g. dopaminergic receptors in neuroendocrine excretion?). Dopamine itself is one of the most important neurotransmitters in the mammalian brain. Although this catechol amine was initially assigned as a metabolite of norepinephrine, its prominent role among the monoamines is well accepted today.¹⁰

The nigro-striatal pathway originates in the midbrain-located substantia nigra pars compacta and the involved DA-neurons project from there into the putamen and the caudate nucleus. These structures are located within the basal ganglia. Sometimes they are summarised as striatum. The nigro-striatal dopaminergic pathway is mainly relevant in the inhibition of acetyl-cholinergic neuronal excitations. Briefly, it mediates motor activity and movement. The movement constriction in Parkinson's disease (PD) is causally related to the downstream depletion of the DA biosynthesis in the striatum. The former, however, is initiated by the degradation of melanin containing dopaminergic neurons in the substantia nigra, due to the deposition of non-natural proteins. These downstream events are clinically established symptoms of PD, but the typical movement effects may also be related to other diseases. Therefore, specific alterations within the complex interactions in DA-neuronal terminals are utilised for the early diagnosis of PD and the differentiation of the disease from symptomatically similar diseases with PET.

In contrast to the nigro-striatal pathway, the meso-cortico-limbic pathway is related to mood, attention, and reinforcement. Sometimes it is referred to as the 'reward pathway'. The pathway originates in the (ventral) tegmental area, also located in the midbrain. The involved neurons project from there into the nucleus accumbens. The latter may be regarded as the central region of the corresponding pathway. DA-neurons project from there further on into some cortical regions. Pathologic alterations within this pathway have been associated with eating disorders, psychosis, and also the addictive component of drug abuse. Furthermore the transition of the acute reinforcing effects of several drugs, including cocaine and amphetamines, into mood affection may be found within this pathway.¹⁰

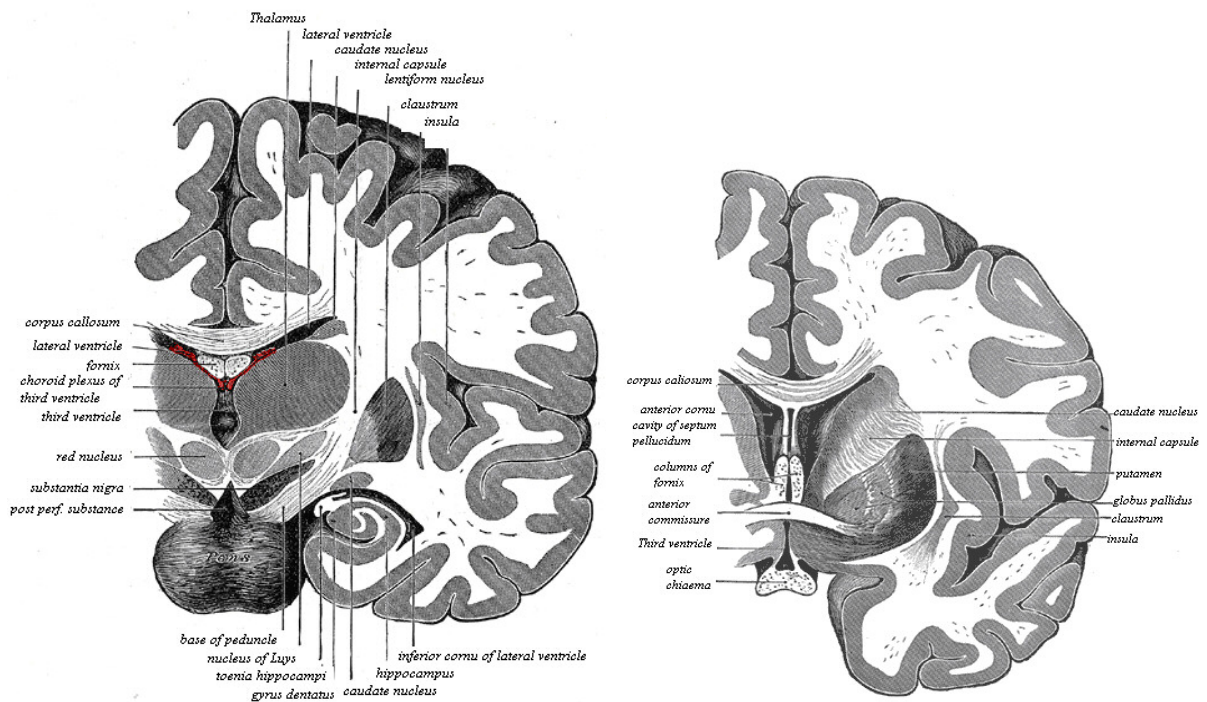


Figure 2: Schematic images of the basal ganglia in the human brain^{10g}

The tubero-infundibular pathway consists of dopaminergic neurons in the hypothalamus. The involved neurons project into the median eminence and into the subthalamic nucleus. Excreted DA effects adenylyl cyclase inhibition and thereby, the tubero-infundibular pathway mediates secretion of prolactin from the anterior pituitary gland.

Briefly, the overall process of DA-neurotransmission consists of six distinguishable biochemical processes (Figure 3):¹⁰

- a) DA is synthesised in two consecutive biotransformations from L-tyrosine. The latter is actively transported into the brain and subsequently hydroxylated by aromatic amino acid hydroxylase in the striatum to form L-DOPA. L-DOPA is then decarboxylated by aromatic amino acid decarboxylase (AADC) to DA.
- b) Free dopamine in the cytosol is taken up by the vesicular DA transporter (VMAT2) and transported into vesicles where it is stored until needed.
- c) The upstream axon of the neuron is excited by G-protein activation followed by sequential depolarisation of sodium and potassium channels. This leads to fast inversion of the overall cell charge that proceeds along the axon to the downstream terminals. The electrical signal reaches the terminal and calcium channels are opened. The influx of Ca(II) into the terminal leads to the fusion of the DA-containing vesicles with the cell membrane at the synaptic gap and subsequent excretion of the vesicularly stored dopamine into the synaptic gap. The amount of excreted neurotransmitter is proportional to the intensity of the electrical signal.
- d) The free dopamine in the synaptic gap crosses the approximately 0.02-0.04 μm broad gap via diffusion to the downstream neuron where it interacts with postsynaptic DA receptors. At present, five different dopaminergic receptor subtypes are distinguished. These are further partitioned into two main groups, the so called D₁-like receptors which include the D₁ and the D₅ subtype, and the so called D₂-like receptors which consist of D₂, D₃ and D₄ subtypes. The D₁-receptor is by far the most abundant subtype with a widespread distribution throughout the brain. D₁-like receptors are furthermore involved with excitatory effects on the adenylate cyclase, resulting in an elevation of the neuronal cyclic adenosine monophosphate (cAMP) concentration. In contrast, D₂-like receptors inhibit the adenylate cyclase, resulting in a decreased production of cAMP.^{10e} DA forms a complex with the receptor protein which is subsequently internalised into the neuron. In the case of G-protein coupled receptors (GPCR), this internalisation leads to G-protein complexation and inhibition of the adenylate cyclase. The signal is transduced from one neuron to another. In this regard, the signal intensity is proportional to the amount of internalised DA-receptor complexes.
- e) Loss of liberated DA from the synaptic gap via diffusion and/or enzymatic degradation by the monoamine oxidases (MAO) A and B.
- f) Simultaneously to the interaction of DA with presynaptic proteins such as the D₁-receptor DA can interact with the presynaptic DA-transporter DAT. The DAT is crucial for the mediation of DA signalling. The DA excreted into the synaptic cleft is recycled via the reuptake from the extracellular space back into the parent neuron, and restored in the vesicles by the VMAT. Thereby, the upstream neuron receives a feedback from the synaptic gap by binding to the autoreceptor and the further release of DA is terminated.

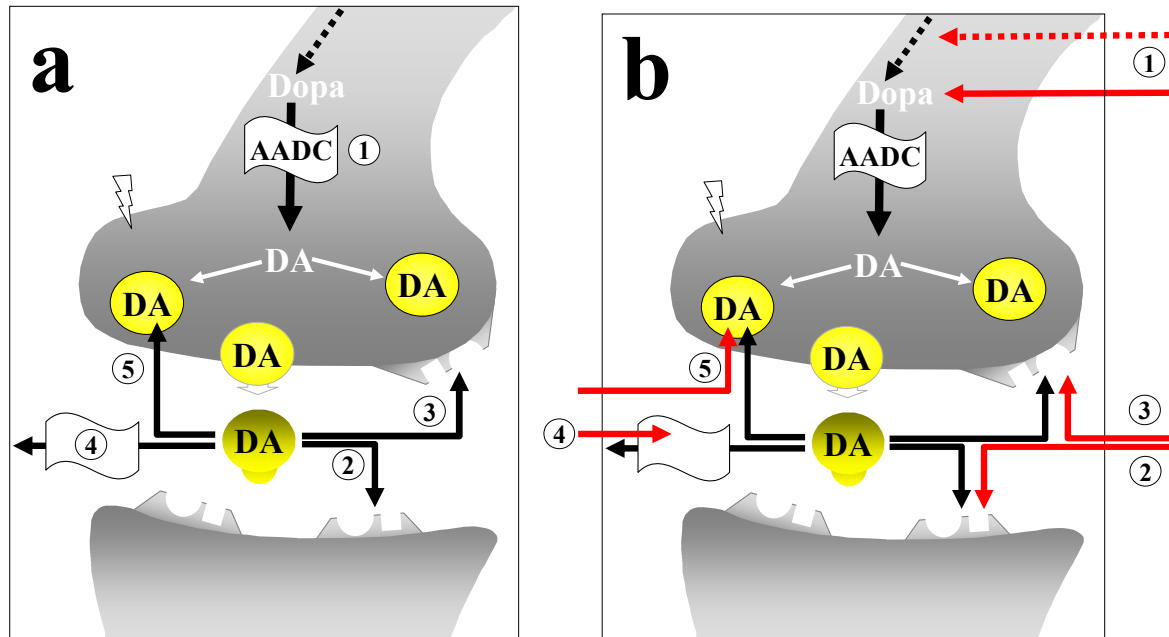


Figure 3: Principal processes at the presynaptic terminal and the synaptic gap of DA-neurons a): (1) DA biosynthesis, (2) release and diffusion to postsynaptic receptors, (3) interaction with receptors at the postsynaptic neuron, (4) loss of dopamine via diffusion or degradation, (5) reuptake into the presynaptic neuron.¹² b) red arrows: (1) visualisation of the DA-biosynthesis with 6-^[18F]-L-DOPA or 6-^[18F]-L-meta-tyrosine; (2) quantification of the DA-receptor availability with [¹¹C]raclopride or [¹⁸F]fallypride; (3) quantification of the DAT-availability with [¹²³I]DATscan (**5g**) or [¹⁸F]FECNT (**5k**); (4) quantification of the extracellular degradation of DA via monoamino oxidase activity with [¹¹C]harmine; (5) quantification of the VMAT2-activity with [¹¹C]dihydratotetrabenazine.^{12b}

Notably, the DAT is the primary site of action for the reinforcing effects of cocaine. In this regard, blockade of the transporter affects the prolonged exposure of the pre- and postsynaptic receptors to the neurotransmitter.¹³

Numerous studies with PET tracers, such as e.g. [¹¹C]raclopride or DAT ligands such as [¹¹C]D-threo-methyphenidate and [¹¹C]cocaine have contributed to the present understanding of the structure and function of the dopaminergic „reward-system“.¹³

In parallel, PET studies of the nigro-striatal pathways have particularly included exploration of striatal effects of several pathologies, such as PD and Huntington's Chorea. In this regard, two compound classes have emerged as clinically established tools for routine diagnostic applications.

On the one hand, the integrity of the DA-biosynthesis is monitored by 6-^[18F]-L-DOPA and 6-^[18F]-L-meta-tyrosine. 6-^[18F]-L-DOPA is transported into the brain and metabolised similar to L-DOPA by the AADC. The bulk of the resultant [¹⁸F]-DA is stored in the vesicles. The diagnostic discrimination between PD-positive and non-positive clinical evidence is obtained by the differential accumulation of ¹⁸F-radioactivity in the striatum. In PD-positive patients, the accumulation is drastically reduced compared to normal controls. However, this application lacks sensitivity in the early stage of the disease, when the downstream effects have not yielded a significant striatal effect.

In this regard, the early up-regulation of DA-receptors or DA-transporters can be used for a significantly more sensitive diagnosis.^{13b,c} Radio-labelled cocaine derivatives are clinically established markers for the integrity of DA-neurons in the striatum. Despite the fact of their clinical use, the main drawback of the established ligands include the lack of selectivity for the DAT, due to the close homology of the serotonin transporter SERT and the noradrenaline transporter NET. Many of these ligands furthermore display a slow equilibrium between binding of the ligand to the DAT and dissociation. The latter is, unfortunately, absolutely mandatory for quantification of the PET-data. In practice, this results in prolonged scanning periods with PET and/or long incubation times post injection (up to one day e.g. for [¹²³I]FP-β-CIT (DATscan[®])-SPECT). In consequence, unreasonable exposure of the patients to radiation dose and lower diagnostic throughput have to be taken into account.^{13b,c}

It has been proposed that the DAT may serve as an indicator on the integrity of the DA-system in general, as its availability is sensitive to minor changes within the system.^{14b} Unfortunately, studies of the DAT were often complicated by the absence of a suitable radiotracer. Considerable effort has already been spent on the development of DAT selective positron emitter labelled radioligands. The first attempts included [¹¹C]nomifensine, [¹⁸F]GBR13119 and [¹¹C]cocaine (Figure 4).¹⁴ Later on, *D-threo*-[¹¹C]methylphenidate, known as the ADHD-therapeutic Ritalin[®], was examined.^{14e}

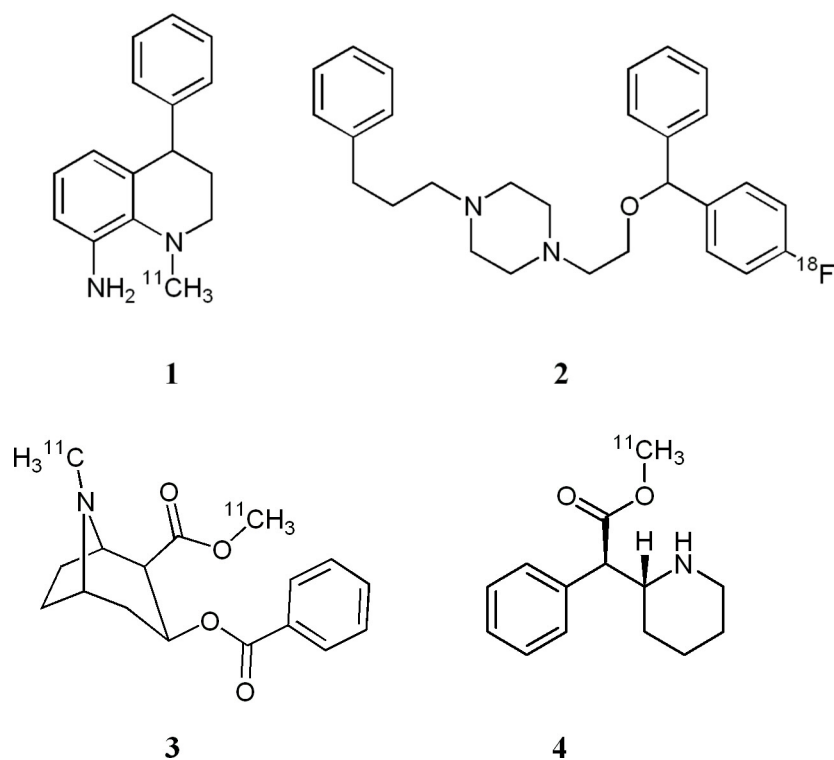


Figure 4: Structures of [¹¹C]nomifensine (1), [¹⁸F]GBR13119 (2), [¹¹C]cocaine (both variants) (3) and *D-threo*-[¹¹C]methylphenidate (4)

However, these early candidates suffered from low striatum to cerebellum ratios (1.5 to 2.4), fast washout and in particular from low selectivity for the DAT. Cocaine analogue phenyltropanes, with the metabolically sensitive benzoyl ester moiety replaced by a carbon-bound phenyl ring, proved to be a more promising lead. Representative derivatives from this

series include MCL-322, β -CFT, β -CIT, FE-CNT, and FP-CIT (Table 1). These compounds almost generally provide higher affinity to the DAT, resulting in higher specific to non-specific binding ratios. Although remarkable increases in striatum to cerebellum ratios were achieved, these candidates still suffer from low specificity, due to the inherent similarity of DAT, SERT and NET. Other drawbacks include the slow accumulation in the DAT rich brain regions, resulting in a slow binding equilibrium at the DAT (up to 120 min).

Despite its rather slow equilibrium and non-selective binding profile, [123 I]FP- β -CIT is the clinically established imaging agent for the early diagnosis of PD, and the differentiation of PD from symptomatically similar syndromes. Nevertheless, there are several attempts for the clinical establishment of a [18 F]fluorinated DAT-ligand for PET, particularly due to the relevance of the dopaminergic system in clinical research. The DAT may serve as an indicator for the dopaminergic contribution to a variety of neuro-degenerative and psychiatric diseases. Furthermore, DAT imaging agents can be used for the exploration of mechanisms of action of pharmaceuticals, with regard to the involvement of dopaminergic binding sites.

Compared to the semi-quantitative mathematical evaluation of SPECT-data, PET provides more accurate absolute quantification of the local dose concentration in the tissue. Furthermore the maximum lateral resolution of a clinical high-resolution PET/MR-scanner exceeds 4 mm, whereas the resolution of modern SPECT scanners is in the range of 1 cm. The main advantages of SPECT are the lower expenses for the acquisition of a camera and the readily available $^{99}\text{Mo}/^{99\text{m}}\text{Tc}$ -generator system, which facilitates the synthesis of multiple cost-effective radiotracers. The only drawback is the rather short half-life of molybdenum-99 (66 h) which results in a high logistic demand for the distribution and production of generator systems. However, the overall costs of a PET examination exceed the costs for a comparable SPECT-scan by far. Nevertheless, the particular advantage of SPECT is only applicable, when suitable technetium-99m labelled tracers have been developed. Otherwise, as in the case for DATscan, the radioactivity has to be prepared off-site and delivered on-site, similar to the satellite distribution systems for fluorine-18 radiopharmaceuticals.

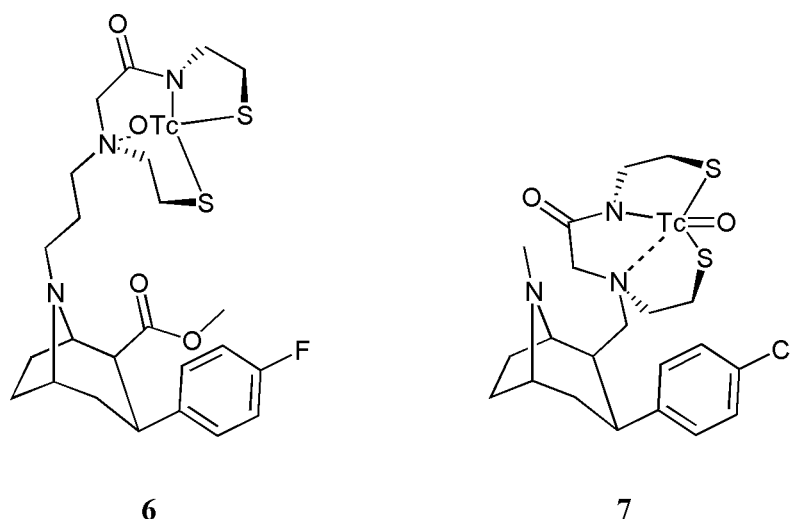


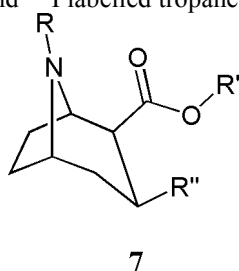
Figure 5: [$^{99\text{m}}\text{Tc}$]Technepine (**6**) and [$^{99\text{m}}\text{Tc}$]TRODAT-1 (**7**)¹⁵

Several groups have reported on the successfully synthesis of tropane derivatives, labelled

with ^{99m}Tc . Some of these were validated as selective DAT-imaging agents and applied in human SPECT studies, see figure 5 for representative examples. However, the preferred SPECT-tracer for this purpose remains [^{123}I]FP- β -CIT, as it is more sensitive for the diagnosis of PD and provides a faster equilibrium, resulting in much more convenient scanning protocols.¹⁵

However, although remarkable *in vitro* affinities and selectivities were found for these critically modified tropanes, these derivatives display slow, continuous accumulation in the DAT-rich brain areas, resulting in prolonged time-periods for the equilibration and poor sensitivity compared to [^{123}I]FP- β -CIT.

Table 1: Structural overview: ^{11}C , ^{18}F , ^{76}Br and ^{123}I labelled tropanes for DAT-imaging.



entry	common	R	R'	R''	reference
7a	β -CFT	[^{11}C]CH ₃	[^{11}C]CH ₃	4'-C ₆ H ₄ [^{18}F]F	16a-c
7b	β -CIT	[^{11}C]CH ₃	[^{11}C]CH ₃	4'-C ₆ H ₄ [^{123}I]I	16c-d
7c	β -IP-CIT	[^{11}C]CH ₃	CH(CH ₃) ₂	4'-C ₆ H ₄ [^{123}I]I	16e
7e	β -CPPIT	[^{11}C]CH ₃	CH ₃	4'-C ₆ H ₄ Cl	16f-g
7f	NS-2214	[^{11}C]CH ₃	CH ₃	2 β -3-phenyl-1,2-oxazol-5-yl	16h
7g	FP- β -CIT	[^{18}F]F(CH ₂) ₃	[^{11}C]CH ₃	4'-C ₆ H ₄ [^{123}I]I	16i-k
7h	FE- β -CIT	[^{18}F]F(CH ₂) ₂	[^{11}C]CH ₃	4'-C ₆ H ₄ [^{123}I]I	16l
7i	β -CDCT	CH ₃	[^{11}C]CH ₃	3',4'-C ₆ H ₃ Cl ₂	16m
7j	Altropane [®]	[^{123}I]I(CH ₂) ₂ CH ₂	[^{11}C]CH ₃	4'-C ₆ H ₄ F	16n
7k	FECNT	[^{18}F]F(CH ₂) ₂	CH ₃	4'-C ₆ H ₄ Cl	16o
7l	FE- β -CFT	[^{18}F]F(CH ₂) ₂	CH ₃	4'-C ₆ H ₄ F	16p
7m	FP- β -CMT	[^{18}F]F(CH ₂) ₃	CH ₃	4'-C ₆ H ₄ CH ₃	16o,r
7n	FP- β -CCT	[^{18}F]F(CH ₂) ₃	CH ₃	4'-C ₆ H ₄ Cl	16s
7o	FP- β -CBT	[^{18}F]F(CH ₂) ₃	CH ₃	4'-C ₆ H ₄ [^{76}Br]Br	16t
7p	MCL301	CH ₃	[^{18}F]F(CH ₂) ₂	4'-C ₆ H ₄ [^{123}I]I	16u
7q	MCL322	CH ₃	[^{18}F]F(CH ₂) ₂	4'-C ₆ H ₄ Br	16v
7r	FE@CIT	CH ₃	[^{18}F]F(CH ₂) ₂	4'-C ₆ H ₄ [^{123}I]I	16w-x
7s	FE- β -CT	CH ₃	[^{18}F]F(CH ₂) ₂	4'-C ₆ H ₄ Cl	16w-x
7t	FE- β -CMT	CH ₃	[^{18}F]F(CH ₂) ₂	4'-C ₆ H ₄ CH ₃	16y

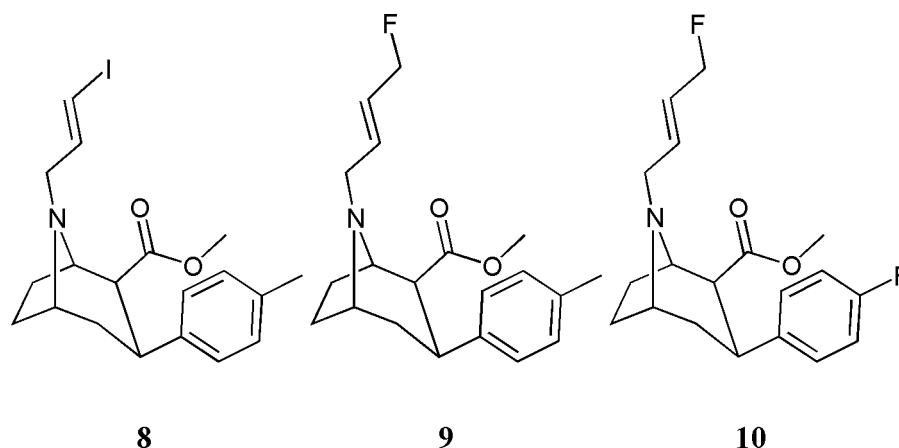


Figure 6: Structures of PE2I (8), LBT999 (9) and FBCFT (10)

Recent progress in this field was made in a modification of the highly suitable radioligands PE2I and Altoprane[®] (cf. Figure 6, Table 1). While the former facilitates labelling with iodine-123-125, the isosteric exchange of iodine for a fluoromethyl group in the novel candidates LBT999 and FBCFT enable fluorine-18 labelling. Its nuclide properties include one of the lowest β^+ energy of all PET nuclides, resulting in a high theoretical resolution and an increased availability. Furthermore, ¹⁸F provides a convenient half-life of approximately 109 min, which facilitates satellite distribution of the radioprobe. Therefore, fluorine-18 labelled probes for non-invasive quantitative visualisation of DAT-availability are of significant clinical relevance.

There is an interest in high-selective and high affinity radiotracers, suitable for the visualisation of both, the dopamine rich brain regions in the basal ganglia, as well as the lower-density extrastriatal DAT populations. The DAT is located on DA-neurons, as well as in the surrounding glia cells and on blood platelets. Highest DAT densities can be found in the caudate-putamen. The DAT is present in lower densities in the amygdala, subthalamic nuclei and in particular in the substantia nigra and the tegmental area, brain regions where the dopaminergic signal pathways originate.

Cocaine itself is rapidly metabolised *in vivo* due to ester cleavage by the enzyme acetylcholine esterase. Therefore, it displays a rapid pharmacokinetic profile of fast accumulation, washout from the brain and renal excretion. Interestingly, the main metabolite of cocaine, methyl ecgonine, can be found in remarkable concentration during the annual environmental monitoring of the river Rhine.^{17a}

An improvement concerning metabolic stability has been made by Clarke and co-workers,^{17b} who found, that the substitution of the benzoyl ester moiety for phenyl yielded a drastically increased biological half-life, while retaining the biological activity profile. Compounds derived from this lead are long-lasting monoamine uptake inhibitors. Considerable effort has been spent during the last decades to optimise the selectivity profile of compounds derived from this lead. This is due to the fact that natural cocaine exhibits a mixed binding profile with equal inhibition potencies at all three monoamine transporters. (DAT, SERT, NET).

Although a variety of more or less selective DAT ligands have been found within these investigations, only a minority among the former contained fluoride in a position, accessible for high yield routine batch production of radiotracers *via* nucleophilic substitution with [¹⁸F]fluoride.¹⁸ Furthermore, most of the ligands studied so far required long scanning periods until equilibrium was reached. In contrast, more promising candidates with respect to equilibrium suffered from lower DAT-affinity, resulting in low target-to-reference ratios and poor visualisation of extrastriatal DAT-domains. Therefore, the development of fluorinated DAT-ligands suitable for the exploration of both, striatal and extra-striatal DAT-populations is still an ongoing process, with significant issues not yet being solved.

More recent promising candidates include FECNT (**7k**), which's utility is somewhat limited due to a blood-brain-barrier penetrating metabolite and LBT-999 (**9**), a fluorinated derivative of the iodine-bearing congener PE2I (**8**).

For these reasons, the present thesis is concerned with the design, synthesis, radio-labelling and both, *in vitro* and *in vivo* characterisation of improved DAT-ligands, based on cocaine. Apart from differential labelling, the novel tracers should possess at least a selectivity factor of ten for the DAT, exhibit a high affinity in the low nanomolar range and low non-specific binding. Finally they should provide a sufficiently fast equilibrium and visualise the relevant striatal and extra-striatal DAT.

Concerning the choice of the radionuclide used, the present work is concerned with structural modifications of the known lead to obtain DAT-ligands that provide the possibility to be labelled with ¹⁸F and ¹¹C, and, as a vision, with ⁶⁸Ga. The ¹¹C is superior to ¹⁸F, due to the fact that its half-life enables multi-injection or multi-tracer studies in one subject on the same day or in close sequence (sometimes multiple injections within two hours). In contrast to the short-lived carbon isotope, fluorine-18 enables longer scanning periods of up to 9 h (5 half-lives) compared to 100 min with carbon-11, while multiple injections per day are excluded. Furthermore, ¹⁸F-radioactivity can be transported to distant PET-facilities in a so called *satellite* distribution system. This is the particular feature of ¹⁸F as a nuclide for clinical routine applications.

With regard to radionuclide availability, radionuclide generators have proven their value for routine applications of therapeutic or diagnostic radionuclides.^{5c} Those space-saving devices consist of a “longer”-lived mother nuclide, which continuously decays to the medically relevant daughter nuclide. The latter can be separated from the mother nuclide, extracted in reasonable time-intervals and subsequently it can be used for labelling or direct application. As a result, generator derived nuclides provide readily available, cost-effective alternatives to the elaborate and expensive production of radio-nuclides via a cyclotron or a reactor. Compared to the technical equipment needed for the production of relevant radio-nuclides, i. e. fluorine-18, the overall expenses for the acquisition and operation of such a generator system is usually significantly less expensive. However, the main drawback of the generator idea is the requirement of a suitable mother-daughter system, which is rarely present among the known radionuclides. Nevertheless, in most cases, where a suitable mother nuclide can be obtained or produced, the extensive use of the derived generator system is of great importance for both, availability of the clinical high quality diagnosis, as well as cost-effectivity for each particular examination. At this point it is worthwhile to mention, that all PET and SPECT-facilities that do not possess radionuclide production facilities, rely on the constant supply with all relevant radiotracers, resulting in a high logistic demand and extended amortisation times for the data acquisition equipment.

Due to the high clinical relevance of an available DAT-ligand for routine diagnosis, the development of a DAT-ligand suitable for labelling with generator produced ^{68}Ga was also considered. Recent improvements of commercial $^{68}\text{Ge}/^{68}\text{Ga}$ generator systems and post-processing of the eluates led to a renaissance of gallium-68 as a promising PET nuclide.¹⁹ It has been hypothesised, that a ^{68}Ga -labelled tropane might be of high clinical impact as a routine marker for the early diagnosis of PD.

This would require the following achievements:

- the successful synthesis of a charge free, lipophilic ^{68}Ga -chelate with low molecular weight. It has to be kinetically inert and thermodynamically stable for the duration of a PET-examination.
- the introduction of a suitable complex precursor in a non-pharmacophore region of the ligand-structure.
- sufficient affinity and selectivity of the obtained Ga-complex-tropane conjugate for the DAT
- a method for the introduction of ^{68}Ga from aqueous media into a water insoluble labelling precursor

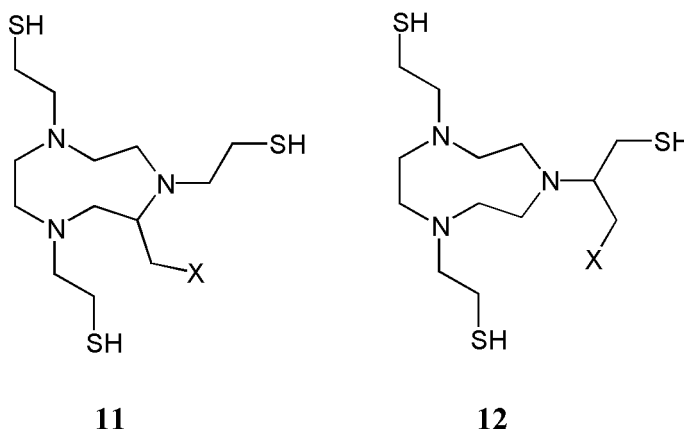


Figure 7: Backbone-branched chelator for lipophilic bifunctional ^{68}Ga -chelates (**11**) and pendant arm branched chelator for lipophilic bifunctional ^{68}Ga -chelates (**12**).

Although several metal-containing DAT-ligands have been reported, the transfer from the transition metal Tc to the main group metal Ga generates several inherent issues to be addressed.

First of all, there are no suitable lipophilic, bifunctional chelators for Ga described in literature. Therefore, the initial requirement for the development of appropriate lipophilic Ga-chelate-tropane conjugates is the successful synthesis and characterisation of lipophilic bifunctional chelators (Figure 7). This is particularly complicated due to the inherent sensitivity of carbon-bound sulphur to oxidative degradation, which necessitates a corresponding protective group strategy and limits the storability of the obtained intermediates and products.

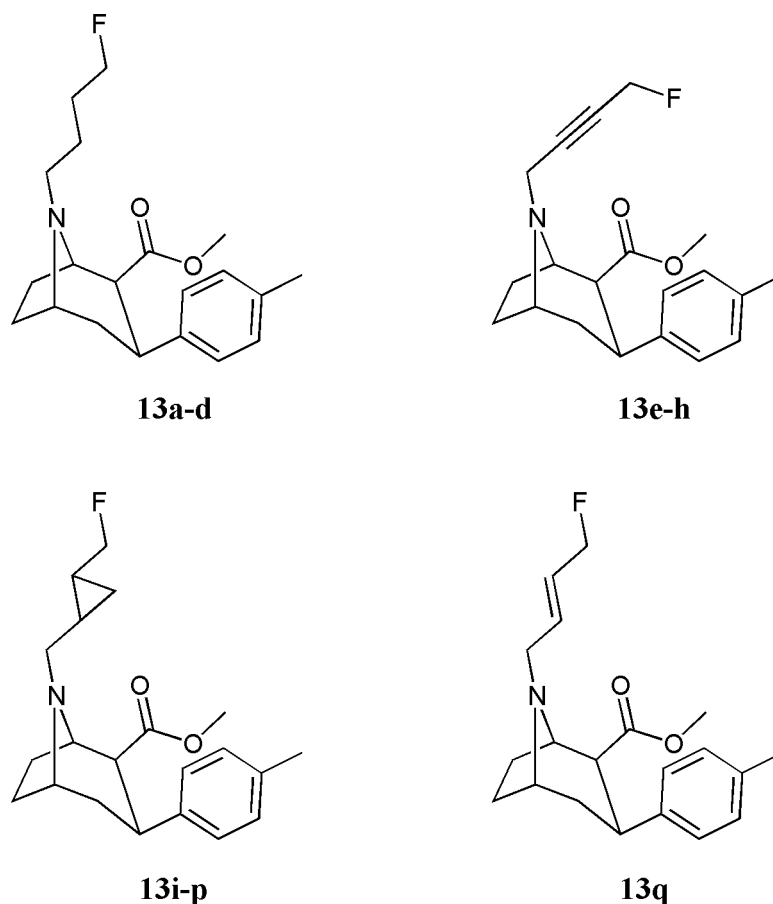


Figure 8: Target compounds for carbon-11 and fluorine-18 labelling: SAR

Based on these prerequisites, a set of 16 novel, fluorinated close structural analogues of the most promising references were designed, prepared and assayed for monoamine transporter selectivity (Figure 8). These were obtained by the introduction of conformationally restricted C₄-chains as N-substituents in 4'-substituted tropanes. To benefit a fast kinetic profile, the maximum weight was kept as low as reasonable achievable via the exclusion of heavy substituents. To elucidate the effect of conformationally restricted substituents, flexible analogues, retaining all degrees of freedom were included for comparison. The most promising candidates had to be selected, labelled and entered into autoradiographic evaluation. Finally, the novel tracer had to be labelled with carbon-11 and fluorine-18, ideally via direct nucleophilic substitution pathways, and should offer options to covalently attach bifunctional chelators for ⁶⁸Ga-labelling. Systematic small animal and an initial primate PET study had to be conducted to evaluate the visualisation of the striatal and extra-striatal DAT and to access the test-retest reliability of the compounds in a multi-injection protocol.

The following chapters contain published or submitted results from the projects outlined in the introduction. Publication manuscripts are provided as submitted to scientific journals. A patent, concerning the novel DAT-ligands and their application is also included.

The documents cover:

- 1) The development of a novel methodology for the enantioselective synthesis of terminally fluorinated cyclopropane building blocks and subsequent radiosynthesis of the fluorine-18 labelled analogues
- 2) The structure-activity relationship study on 16 novel tropane derivatives.
- 3) The initial radio-labelling and pharmacological characterisation of the promising high affinity candidate [^{18}F]PR04.MZ by autoradiography and PET in rodents.
- 4) An efficient method for the introduction of the [^{11}C]CH₃-label from readily available [^{11}C]MeI into carboxylate functions
- 5) A comparative primate study of [^{11}C]PR04.MZ and [^{18}F]PR04.MZ in papio anubis baboons, wherein the test retest reliability of [^{11}C]PR04.MZ and the long-term kinetics of [^{18}F]PR04.MZ were assessed
- 6) A microwave enhanced, efficient method for the time-effective production of [^{18}F]PR04.MZ and [^{18}F]LBT-999 from [^{18}F]F⁻ in high yield
- 7) The synthesis, gallium-68 radiolabelling and stability determination of novel polyamino-polycarboxylate bifunctional chelators and some model conjugates
- 8) Initial studies towards the development of a lipophilic bifunctional chelator based on 1,4,7-triazacyclononane, radiolabelling of a model compound and determination of the chelates octanol-water partition coefficient.

4 Manuscripts

The present thesis is based on the following nine manuscripts:

- i. P. J. Riss, F. Roesch,
A convenient chemo-enzymatic synthesis and ^{18}F -labelling of both enantiomers of *trans*-1-toluenesulfonyloxymethyl-2-fluoromethyl-cyclopropane
Org. Biomol. Chem. 2008, 6, 4567-4574
- ii. P. J. Riss, R. Hummerich, P. Schloss,
Synthesis and monoamine uptake inhibition of conformationally restricted 2 β -carbomethoxy-3 β -phenyl tropanes,
Org. Biomol. Chem 2009, in press
- iii. P. J. Riss, F. Debus, R. Hummerich, U. Schmidt, H. Lueddens, P. Schloss, F. Roesch,
In vitro, *ex vivo* and *in vivo* characterisation of [^{18}F]PR04.MZ in rodents: A selective dopamine transporter ligand for low concentration imaging.
Nucl. Med. Biol. 2008, submitted
- iv. P. J. Riss, J. M. Hooker, D. Alexoff, S.-W. Kim, J. S. Fowler, F. Roesch,
Efficient [^{11}C]MeI methylation of PR04.MZ: A DAT-ligand for low concentration imaging. Bioorg. Med. Chem. Letters 2009, in press
- v. P. J. Riss, J. M. Hooker, C. Shea, Y. Xu, P. Carter, D. Warner, S.-W. Kim, J. S. Fowler, F. Roesch,
Comparison of [^{11}C]PR04.MZ and [^{18}F]PR04.MZ in *anubis papio* baboons: A selective high-affinity DAT-ligand for low concentration imaging of the extrastriatal dopamine transporter, Synapse 2008, submitted
- vi. P. J. Riss, F. Roesch,
Efficient microwave-assisted direct fluorination of [^{18}F]PRD04 and [^{18}F]LBT999: Highly selective dopamine transporter ligands for PET,
J. Labelled Compd. Radiopharm. 2008, submitted
- vii. P. J. Riss, C. Kroll, V. Nagel, F. Roesch,
NODAPA-OH and NODAPA-(NCS)_n: Synthesis, ^{68}Ga -radiolabelling and *in vitro* characterisation of novel versatile bifunctional chelators for molecular imaging,
Bioorg. Med. Chem. Letters 2008, 18, 5364-5367
- viii. P. J. Riss, N. Hanik, F. Roesch,
Studies towards the synthesis of lipophilic bifunctional chelators for ^{68}Ga ,
Nucl. Med. Commun. 2008, submitted
- ix. P. J. Riss, F. Roesch,
Radioaktiv-markierte Cyclopropan-Derivate DAT-affiner Tropane,
patent submitted to DPMA

4.1 A convenient chemo-enzymatic synthesis and ^{18}F -labelling of both enantiomers of trans-1-toluenesulfonyloxymethyl-2-fluoromethyl-cyclopropane

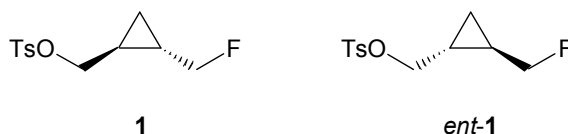
A convenient chemo-enzymatic synthesis and ^{18}F -labelling of both enantiomers of trans-1-toluenesulfonyloxymethyl-2-fluoromethyl-cyclopropane

Patrick Johannes Riss*, Frank Roesch

Institute of Nuclear Chemistry, Mainz University, Fritz Strassmann-Weg 2, 55128 Mainz; Germany

Abstract: The present report is concerned with a stereoselective, reliable route to trans-1,2-disubstituted cyclopropanes and in particular to (S,S)-1-tosyloxymethyl-2-fluoromethyl-cyclopropane (**1**) and (R,R)-1-tosyloxymethyl-2-fluoromethyl-cyclopropane (*ent-1*) as conformationally restricted, terminally fluorinated C₄-building blocks for medicinal chemistry. The enzymatic kinetic resolution based synthesis of **1** and *ent-1* utilises inexpensive, commercially available starting materials. It is based on enantiomeric resolution of rac-cyclopropane carboxylic esters using esterase from *Streptomyces diastatochromogenes*. Both enantiomers of **1** were prepared selectively in high overall yield over nine steps, starting from ethyl acrylate. The successful radiosynthesis of [^{18}F]-**1** and [^{18}F]-*ent-1* is also reported.

Introduction: Fluorine is increasingly included in substitution patterns during the systematic development of potential pharmaceuticals. The C-F bond is an isosteric substitution for C-H and an isoelectronic substitution for the hydroxyl group (van der Waals radii: H: 1.2 Å, F: 1.35 Å, OH: 1.43 Å). Therefore, carbon-bound fluorine can be introduced as a hydrogen mimic or a hydroxyl replacement. Its introduction can affect adsorption, distribution and metabolic properties of a pharmaceutically relevant lead structure.¹ Recent studies have elucidated specific contributions of fluorine in ligand-protein binding interactions.² In addition, fluorine-18 provides unique properties as a radiolabel for positron emission tomography (PET), a mode of non-invasive imaging and quantification of biochemical conversions and metabolic rates in living systems. Among the best suited and most frequently used PET-radionuclides, fluorine-18 presents outstanding nuclear and chemical properties.³ For these reasons, fluorinated building blocks remain of significant interest for the incorporation of fluorine in defined positions of potential radioligands.



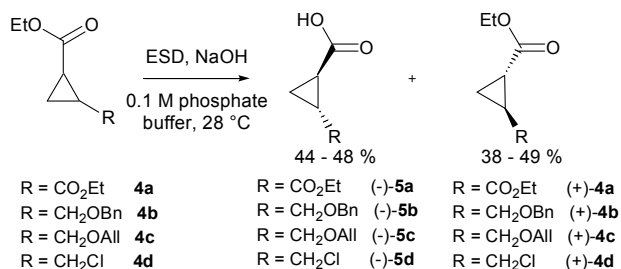
Scheme 1: (S,S)-(+)-Toluene-4-sulfonic acid 2-fluoromethyl-cyclopropylmethyl ester **1** and (R,R)-(-)-toluene-4-sulfonic acid 2-fluoromethyl-cyclopropylmethyl ester *ent-1*

We were interested in (S,S)-**1** and (R,R)-*ent-1* as C₄-synthons for the introduction of a terminally fluorinated, conformationally restricted cyclopropane ring constraint in suitable (radio-) pharmaceutical precursors.^{4a} In addition, trans-1,2-disubstituted cyclopropanes are versatile (E)-alkene mimics, which can be employed as isosteric double bond replacements.⁴ They are less sensitive to cytochrome p450 affected metabolism in general and to epoxidation in particular, thus eliminating a potential source of toxic metabolites.^{5a,b}

The synthesis of **1** and *ent*-**1** required an inexpensive, preparative scale access to a desymmetrised cyclopropane precursor in high enantiomeric excess. Considerable effort has been spent on the development and optimisation of (stereoselective) cyclopropanation methods, as cyclopropane units can be found in various natural products and pharmaceuticals.⁶ Previously published techniques for the resolution and synthesis of (S,S)- or (R,R)-1,2-disubstituted cyclopropanes have included: a) fractional crystallisation of the corresponding trans-1,2-cyclopropane dicarboxylates followed by reduction, b) chiral auxiliary-mediated,⁷ stereoselective Simmons-Smith-cyclopropanation of olefins (Charette-Denmark method),⁸ c) the former combined with enzymes,^{9a} d) transition metal-complex catalysed carbenoid additions,^{6d-f,9b} and e) multi-step synthesis from enantiomerically enriched starting materials.¹⁰ However, yields and enantiomeric excess vary widely. In addition, the Simmons-Smith-reaction provides only limited access to cyclopropanes from α,β -unsaturated carbonyl compounds.^{6g}

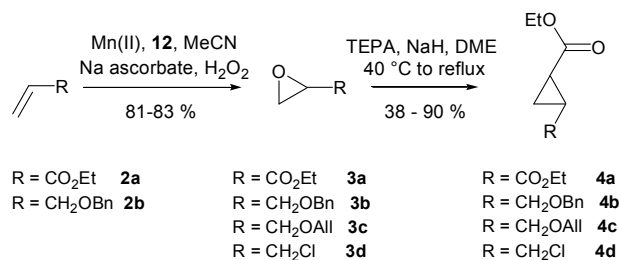
Herein we would like to report a convenient route to 2-substituted cyclopropanecarboxylic acid esters as well as an enzymatic method for the synthesis of diethyl (S,S)-(+)-cyclopropanedicarboxylate ((+)-**4a**) and ethyl (R,R)-(-)-cyclopropanedicarboxylate ((-)-**5a**) in high enantiomeric excess. ee-values of 99 % for the (S,S)-(+)-enantiomer and 97 % for the corresponding (R,R)-(-)-analogue were achieved, respectively, after half conversion ($E > 200$).¹¹ As a complement to the previously published chemical and enzymatic methods for the synthesis of 1,2-disubstituted cyclopropanes, the route presented herein readily affords versatile cyclopropane building blocks **7a** and **7b** in very high enantiomeric excess, avoiding sensitive or expensive reagents. **7a** was subsequently employed in the synthesis of **1** and *ent*-**1**. The labelling synthons [¹⁸F]-**1** and [¹⁸F]-*ent*-**1** were successfully synthesised from [¹⁸F]F⁻ and precursors **11a** and *ent*-**11a** in a radiochemical yield of 50 ± 6 %.

Results and Discussion



Scheme 2: Enantiomeric resolution of substrate esters **4a-d**

Our approach is based on the enantiomeric resolution of racemic mixtures of esters **4a-d**, (Scheme 2) employing an esterase from *Streptomyces diastatochromogenes* (ESD; E.C.3.1.1.1.), which we have found to show useful selectivity for the hydrolysis of cyclopropane carboxylic esters in the past.¹²



Scheme 3: Epoxidation of terminal olefins using the 1,4,7-trimethyl-1,4,7-triazacyclononane (12) (TMTACN) Mn(II) ascorbate system,¹⁴ followed by cyclopropane synthesis via Wadsworth-Emmons cyclopropanation on **3a-d**.

The Wadsworth-Emmons cyclopropanation was chosen for the preparation of racemic mixtures **4a-d** (Scheme 3), as it provides straightforward access to the desired trans-configured 1,2-disubstituted cyclopropanes in good yields at low cost.^{13,15} Therefore, triethyl phosphonoacetate (TEPA) was converted into the P-ylide with potassium tert.-butoxide and subsequently reacted with epoxides **3a-d**. The substrate epoxides **3a-d** were either prepared from parent olefins in >85 % yield or obtained from commercial suppliers. Starting from olefinic precursors, trans-cyclopropanes were isolated in 56 to 75 % yield employing a two-step procedure via Mn(II) catalysed epoxidation to afford compounds **3a-b** followed by trans-selective cyclopropanation under Horner-Wadsworth-Emmons conditions (Scheme 3).^{13,14} In contrast to most copper/rhodium catalysed or non-catalysed additions of carbenoids which were examined by us, this route afforded the desired trans-configured cyclopropanes as single products. Thereby, the elaborate separation of (Z)- or open chain by-products was made obsolete.¹⁶ During initial screening, racemates **4a-d** were hydrolysed employing ESD in phosphate buffer at pH 7.0. The pH was maintained via the controlled addition of 2 M NaOH solution. In the case of substrate **4a**, ESD showed a remarkably high selectivity. Only the (R,R)-configured enantiomer was recognised by the biocatalyst and both, the remaining diester (+)-**4a** and the acid (-)-**5a**, were isolated in high yield (49 % and 46 %, 99 % and 97 % ee, respectively). Unfortunately, only low enantioselectivity was observed after half conversion in all other cases. Neither esters **4b-d** nor acids **5b-d** were obtained in good enantiomeric excess. The addition of water miscible solvents, e.g. dioxane, decreased selectivity. In a multigram scale-up run (15.0 g substrate), ester **4a** was isolated in 49 % (99 % ee) yield, employing an enzyme concentration of 400 mg/l. Using diethyl ether for extraction of the non-hydrolysed (S,S)-ester, the residual enzyme in the buffer solution (containing acid **5a**) remained active for further hydrolysis of substrate **4a**. The latter facilitates fast, multi-batch syntheses of optically active ester (+)-**4a** without wasting the biocatalyst. In addition, the enzyme showed sufficient stability in solution at 28 °C to employ even lower concentrations in exchange for prolonged reaction times, without any significant loss in hydrolytic activity and yield.

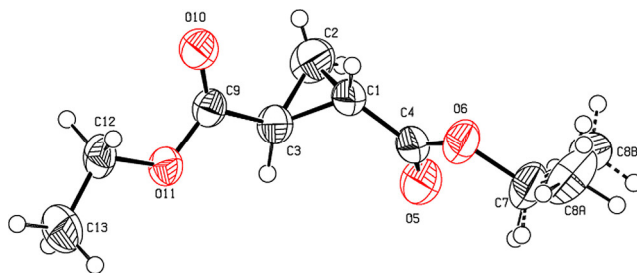
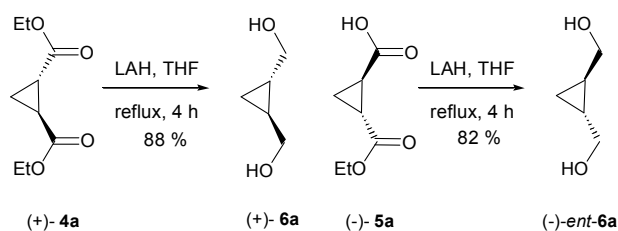


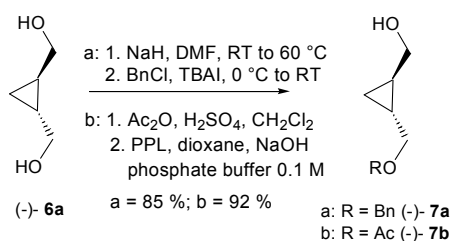
Figure 1: X-ray diffraction crystal structure of enantiopure (+)-**4a**.²⁷ A probability of 50% was chosen for the ellipsoids. One ethyl group (C7 and C8) is disordered unequally over two sites (C8A and C8B).

In contrast to the racemic mixture **4a** which remains liquid at r.t., neat (+)-**4a** crystallised in colourless platelets (mp = 38 °C) displaying an optical purity of 99 % ee. Acid (-)-**5a** was obtained via lyophilisation of the residual buffer solution, followed by acidic work-up to give carboxylic acid (-)-**5a** in 46 % yield (97 % ee). The relative configuration of compound **4a** was verified using X-ray crystallography. (Figure 1) The absolute configuration of (+)-**4a** and (-)-**5a** was assigned by comparison of the rotational directions with literature references. Therefore, a reference sample of ester (+)-**4a** and acid (-)-**5a** was hydrolysed to the diacid and the optical rotations were measured.^{27b} Compound (+)-**4a** was assigned diethyl (+)-(S,S)-trans-cyclopropane-1,2-dicarboxylate, after the hydrolysed product showed the same angle of rotation as (+)-(S,S)-trans-cyclopropane-1,2-dicarboxylic acid. The (R,R)-configuration was analogously assigned to (-)-**5a**.^{7, 26}



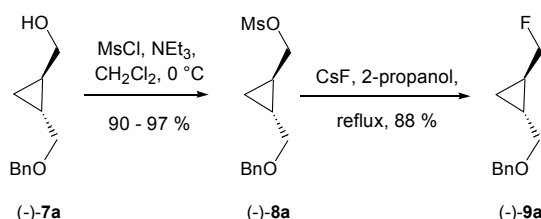
Scheme 4: Reductions of diester (S,S)-(+)-**4a** or acid (R,R)-(-)-**5a** to diol (+)-**6a** and (-)-*ent*-**6a**

Diols **6a** and *ent*-**6a** were conveniently obtained in 82 to 88 % yield via LiAlH₄ (LAH) reduction of **4** and **5** in THF using a modified procedure involving equimolar aqueous hydrolysis and quick short-path distillation in a Kugelrohr apparatus.^{7,17} (Scheme 4) The optical rotations of both product diols were in accordance with the assigned absolute configurations.⁷



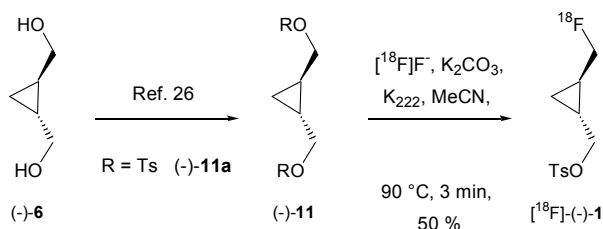
Scheme 5: De-symmetrisation of diol (-)-**6a**, via benzylation of the anion (a) or selective hydrolysis of the diacetate (b)

Compounds (+)-**6a** and (-)-**ent-6a** were desymmetrised using NaH in DMF followed by addition of benzyl chloride and catalytic amounts of TBAI. (Scheme 5) A two-step procedure involving diacetylation followed by selective removal of one acetyl group using porcine pancreatic lipase (PPL) in phosphate buffer/dioxane at pH 7 resulted in de-symmetrised diols **7b** in even higher yield.^{11,21} In addition, this double-enzymatic approach avoided preparative column chromatography as the products were substantially pure after complete hydrolysis to the monoacetate. (Scheme 5)



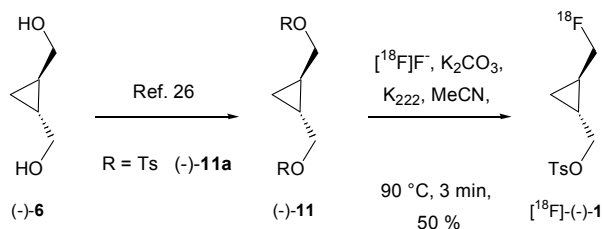
Scheme 6: Two-step fluorination via mesylation and Finkelstein exchange with CsF dissolved in 2-propanol

Product alcohols **7a** and *ent-7a* were preferably fluorinated via sulfonylation followed by a Finkelstein-analogue nucleophilic exchange using CsF in 2-propanol to obtain fluorides **9a** and *ent-9a*. (Scheme 6) CsF displays a remarkable solubility (12.6 mole in 1000 g MeOH), while CsBr is the least soluble in alcohols among all caesium halogenides. Nevertheless, as leaving group the mesylate gave even better results.¹⁹ Fluoro-dehydroxylation employing diethylamino sulphur trifluoride (DAST) in dichloromethane at -80 °C to r.t. was also examined.²⁰ Although freshly obtained DAST produced fluorides **9a** and *ent-9a* in good yields (>90 %), reagent stability issues led to poor reproducibility of fluorination outcomes after a few weeks.



Scheme 7: Debonylation of ether (-)-**9a** and subsequent tosylation to final product (-)-**1**²⁴

Hydrogenolytic cleavage of the fluorides in 2-methoxy-2-methyl-propane (MTBE) followed by concentration and tosylation in one pot finally afforded target compounds (S,S)-(+)-**1** and (R,R)-(-)-*ent-1* in 87 % yield over two steps. (Scheme 7)



Scheme 8: Preparation of labelling precursors, exemplified for (-)-11a and subsequent radio-fluorination

The radiosynthesis of [^{18}F]-**1** and [^{18}F]-*ent*-**1** was performed as illustrated for [^{18}F]-*ent*-**1** in Scheme 8. **6a** and *ent*-**6a** were converted to the labelling precursor **11a**²⁶ and *ent*-**11a** followed by exposure to pre-dried, cyclotron produced, no carrier added (n.c.a) [^{18}F]fluoride. The labelling synthons [^{18}F]-**1** and [^{18}F]-*ent*-**1**, were obtained in a non-decay-corrected radiochemical yield of $50 \pm 6\%$ after a reaction time of 3 min in MeCN at $90\text{ }^\circ\text{C}$ followed by HPLC-purification and solid phase extraction. Although the convenient half-life of fluorine-18 facilitates multi-step procedures and the production of ^{18}F -fluorinated **1** can be automated, direct nucleophilic labelling of a suitable precursor is even more efficient in some cases. In this regard, **7a** and **7b** can serve as versatile building-blocks for precursor synthesis.

Conclusions

In conclusion, both enantiomers of **1** were prepared selectively in 18.7 % and 16.4 % overall yield, respectively, over eight to ten steps, starting from ethyl acrylate. The more versatile intermediates (S,S)-(+)-**7a** and (S,S)-(+)-**7b** were obtained in 20.5 % and 22.2 % yield, respectively, over 5 steps. Again, cyclopropanation using epoxide precursors and TEPA-anion in DME proved to be a useful route to 2-substituted cyclopropane-1-carboxylic acid esters in trans-configuration. Although enzymatic resolution of substrates **4b-d** failed due to the lack of selectivity in the hydrolytic cleavage of the ethyl esters, both (+)-**4a** and (-)-**5a** were separated and isolated in high yields and high enantiomeric excess. Furthermore, [^{18}F]-**1** and [^{18}F]-*ent*-**1** were successfully synthesised for the first time and isolated in a non-decay corrected radiochemical yield of $50 \pm 6\%$.

Compounds (+)-**4a**, (-)-**5a**, along with de-symmetrised diols **7a**, *ent*-**7a**, **7b** and *ent*-**7b** provide broad access to enantiomerically enriched 1,2-disubstituted trans-cyclopropanes. Utilising the route presented herein, these can be prepared in a synthetically useful multigram scale, thereby providing the means for the synthesis of a broad range of 1,2-disubstituted cyclopropane building blocks.

Experimental

NMR-spectra were recorded with a Bruker AC 200 FT-NMR-spectrometer, J values are given in Hertz, chemical shifts are reported downfield from TMS ($\delta = 0$ ppm) referred to the solvent residual signal ^1H NMR (300 MHz, CHCl_3 7.224 ppm) and ^{13}C NMR (100 MHz, CDCl_3 77.0 ppm). Field desorption (FD) mass spectra were recorded on a Finnigan MAT90 FD spectrometer. HRMS-spectra were measured on a Micromass QTOF Ultima 3 spectrometer. IR-spectra were obtained from a Nicolet 6700 FTIR spectrometer. Boiling points are uncorrected. Enantiomeric excesses of volatile cyclopropanes were determined by gas-chromatography using hydrogen as carrier gas on a Macherey-Nagel Lipodex E capillary column. All chemicals were obtained in commercial quality from Acros Organics, Sigma Aldrich, VWR, TCI or STREAM and used without further purification. Enzymes were obtained

from Julich Chiral Solutions (Codexis®) (ESD, recombinant from *E. coli*) and Sigma-Aldrich (PPL, from hog pancreas). Optical rotations were determined using a Perkin-Elmer polarimeter 241 running at 546 and 578 nm (Hg-lamp) at 17 to 25 °C and were extrapolated to the sodium D line. $[\alpha]_D$ values are given in 10^{-1} deg $\text{cm}^2 \text{g}^{-1}$. TLC was conducted on self-cut Merck silica gel 60 covered aluminium plates. Detection and staining was performed either using iodine on silica gel, potassium permanganate solution, UV fluorescence, vanillin/sulphuric acid, Seebach-reagent (phosphomolybdic acid, cerium sulphate, H_2SO_4) or Dragendorff-reagent (basic bismuth nitrate, potassium iodide and tartaric acid). Column chromatography was performed on Acros silica gel 60, 0.063-0.200 mesh, p. a. solvents for chromatography were washed with aqueous acid and base and distilled once, prior to use. Anhydrous solvents were used for reactions.

General procedure for the synthesis of epoxides 3a-b: To a solution of olefin (1 mol) in MeCN (50 ml) were added, 1 ml of an 0.4 M TMTACN stock solution in MeCN, 2 ml of an 150 mM stock solution of Mn(II)acetate-tetrahydrate in water and 30 ml of a 80 mM stock solution of sodium ascorbate in water. The mixture was cooled to 0 °C, and approximately 1.8 equiv. of 30 % H_2O_2 -solution (stabilised with 1 ppm of Sn) was added in portions until all olefin had been consumed (monitored by TLC). The organic phase was separated and the aqueous layer was extracted with EtOAc (75 ml). The combined organic layers were dried, concentrated and distilled in vacuo to afford epoxides **3** in >80 % yield.

Ethyl 2,3-epoxypropanoate, compound 3a:¹⁴ From ethyl acrylate (1 mol) 94.3 g (812 mmol, 81 %), distilled at 4 mbar, bp = 42-44 °C (lit.,^{22a} 60-62 °C (17 mm)). Found: C, 51.78 H, 6.95 $\text{C}_5\text{H}_8\text{O}_3$ requires C, 51.72 H, 6.94%. $\nu_{\text{max}}/\text{cm}^{-1}$ (neat) 2986(CH), 1735(CO), 1468(CH_2), 1387(CH_3), 1291(C(O)-O-C), 1251(epoxide), 1200(C(O)-O-C), 1029(C(O)-O-C), 915(epoxide), 819(epoxide), 720(CH_2). (lit.,^{22b} 1750) δ_{H} (300 MHz, CDCl_3): 1.25 (t, J = 7.0 Hz, 3 H, CH_3), 2.90 (dd, J = 4 Hz, J = 6 Hz, 1 H, = CH), 2.93 (dd, J = 2.5 Hz, J = 6 Hz, 1 H, = CH) 3.39 (dd, J = 2.5 Hz, J = 4 Hz, 1 H, = CH_2), 4.20 (q, J = 7.0 Hz, 2 H, OCH_2) 4.21 (q, J = 7.4 Hz, 1 H, OCH_2). δ_{C} (100 MHz, CDCl_3): 14.07, 46.18, 47.33, 61.75, 169.45. m/z (FD) 117.05 ($[\text{M}+\text{H}]^+$ $\text{C}_5\text{H}_8\text{O}_3$ requires 116.0473).

3-Benzyloxymethylene-1,2-epoxypropane, compound 3b:²³ From allyl benzyl ether (0.1 mol), yield: 13.6 g (83 mmol, 83%). Found: C, 73.45 H, 7.7 $\text{C}_{10}\text{H}_{12}\text{O}_2$ requires C, 73.15; H, 7.4%. $\nu_{\text{max}} / \text{cm}^{-1}$ (neat) 3071(CH), 3057(CH), 3030(ArH), 2859(CH), 1496, 1453(CH_2), 1383(CH_3), 1252(epoxide), 1200(C(O)-O-C), 1029(C(O)-O-C), 898(epoxide), 845(epoxide), 736(ArH), 697(ArH). δ_{H} (300 MHz, CDCl_3): 2.20 (dd, J = 2.6 Hz, J = 4.8 Hz, 1 H, OCH_2), 2.79 (t, J = 4.4 Hz, 1 H, OCH_2), 3.14 – 3.21 (m, 1 H, CHO), 3.42 (dd, J = 5.9, J = 11.4 Hz, 1 H, OCH_2), 3.75 (dd, J = 3.0 Hz, J = 11.4 Hz, 1 H, OCH_2), 4.54 (d, J = 12.1 Hz, 1 H, ArCH_2), 4.60 (d, J = 11.8 Hz, 1 H, ArCH_2), 7.28 – 7.38 (m, 5 H, ArH). δ_{C} (100 MHz, CDCl_3): 44.3, 50.9, 70.8, 73.3, 127.8, 128.4, 137.9. m/z (FD) 164.1 (100) $[\text{M}+\text{H}]^+$ $\text{C}_{10}\text{H}_{12}\text{O}_2$ requires 164.0837.

General procedure for cyclopropane synthesis, compounds 4a-d: At 0 °C, potassium tert-butoxide (11.22 g, 0.1 mol) was dissolved in 1,2-dimethoxyethane (100 ml) under nitrogen. To this solution, triethyl phosphonoacetate (29.27 g, 0.13 mol) was added dropwise over 30 min. After effervescence ceased, the slightly turbid solution was slowly heated to 40 °C while epoxide **3a-d** (75 mmol) was added dropwise. The temperature was raised to 60 °C until all of the epoxide had been consumed (monitored by TLC), followed by reflux for 8 to 12 h to

complete the cyclopropane formation. The reaction was quenched using saturated ammonium chloride solution (25 ml). In all cases except **3b**, prolonged reaction times lead to product degradation. Ethyl acetate (50 ml) was added and phases were separated. The aqueous phase was extracted once with ethyl acetate (50 ml), the combined organic phase was washed with brine, dried and concentrated in vacuo. The residue was purified via flash chromatography on silica gel to afford 38 to 90 % of **4a-d** as colourless oils.

trans-Cyclopropane-1,2-dicarboxylic acid diethyl ester, compound 4a:^{6g, 9c,d, 16b,c, 26a} From ethyl 2,3-epoxypropanoate **3a** yield 9.63 g (52 mmol, 69 %). Found: C, 57.95 ; H 7.6, C₉H₁₄O₄ requires C, 58.05; H, 7.6%. $\nu_{\max}/\text{cm}^{-1}$ (neat): 2993(CH), 1716(CO), 1447(CH₂), 1407, 1367(CH₃), 1322, 1172(C(O)-O-C), 1033, 743. δ_{H} (300 MHz, CDCl₃): 1.22 (t, J = 7 Hz, 3 H, CH₃), 1.38 (p, J = 1.5 Hz, J = 7.4 Hz, 2 H, CH₂), 2.11 (p, J = 1.5 Hz, J = 7.4 Hz, 2 H, CH), 4.10 (q, J = 7 Hz, 2 H, OCH₂). δ_{C} (100 MHz, CDCl₃): 14.2, 15.2, 22.4, 31.0, 171.7. m/z (FD) 186.1 (100) [M+H]⁺ C₉H₁₅O₄ requires 186.0892

trans-2-Benzyloxymethylenecyclopropane-1-carboxylic acid ethyl ester, compound 4b:^{15a} From 3-benzyloxymethylene-1,2-epoxypropane **3b**, yield: 15.7 g (68 mmol, 90 %), chromatographed on silica gel, R_f = 0.6 (light petroleum–Et₂O, 7:3). Found: C, 71.8; H, 7.75 C₁₄H₁₈O₃ requires C, 71.8; H, 7.7. $\nu_{\max}/\text{cm}^{-1}$ (neat): 3028(ArH), 2977(CH), 2859(CH), 1720(CO), 1647, 1496, 1453(CH₂), 1367(CH₃), 1202(C(O)-O-C), 1177(C(O)-O-C), 1085(OCH₂), 735(ArH), 697(ArH). δ_{H} (300 MHz, CDCl₃): 0.80 – 0.89 (m, 1 H, CH₂), 1.22 (p, J = 4.4 Hz, 1 H, CH₂), 1.23 (t, J = 7 Hz, 3 H, CH₃), 1.54 (p, J = 4.4 Hz, 1 H, CHC(O)), 1.67 – 1.78 (m, 1 H, CH), 3.38 (dq, J = 10.3 Hz, J = 14.0 Hz, 2 H, CH₂O), 4.10 (q, J = 7 Hz, 2 H, OCH₂), 4.50 (s, 2 H, ArCH₂), 7.31 (m, 5 H, ArH). δ_{C} (100 MHz, CDCl₃): 12.9, 14.2, 18.6, 21.6, 60.6, 71.6, 72.7, 127.7, 128.4, 138.8, 173.8. m/z (FD) 234.2 (100) [M+H]⁺ C₁₄H₁₈O₃ requires 234.1256

trans-2-Allyloxymethylenecyclopropane-1-carboxylic acid ethyl ester, compound 4c:^{16e} From allyl-glycidyl ether **3c**, yield 9.8 g (53 mmol, 71 %), chromatographed on silica gel, R_f = 0.55 (light petroleum–Et₂O, 3:2). Found C, 65.0 H, 8.9. C₁₀H₁₆O₃ requires C, 65.2; H, 8.8%; $\nu_{\max}/\text{cm}^{-1}$ (neat): 2983(CH), 1720(CO), 1448(CH₂), 1366(CH₃), 1269(C(O)-O-C), 1175(C(O)-O-C), 1085(OCH₂), 996(C=C), 943(C=C). δ_{H} (300 MHz, CDCl₃): δ = 0.81 – 0.93 (m, 1 H, CH₂), 1.24 (t, J = 7 Hz, 3 H, CH₃), 1.26 – 1.34 (m, 1 H, CH₂), 1.58 (p, J = 4 Hz, 1 H, CH), 1.74 – 1.84 (m, 1 H, CHC(O)), 3.46 (dd, J = 8.5 Hz, J = 9.9 Hz, 1 H, OCH₂), 3.72 (dd, J = 5.8 Hz, J = 10.3 Hz, 1 H, OCH₂), 3.92 (dq, J = 1.5 Hz, J = 5.5 Hz, 2 H, CH₂O), 4.12 (q, J = 7.0 Hz, 2 H, OCH₂), 5.17 (d, J = 10.3 Hz, 1 H, =CH₂), 5.26 (d, J = 17.3 Hz, 1 H, =CH₂), 5.80 – 5.93 (m, 1 H). δ_{C} (100 MHz, CDCl₃): δ = 13.1, 14.2, 18.5, 22.0, 71.2, 71.7, 117.2, 134.4, 173.0. m/z (FD) 185.2 (100) [M+H]⁺ C₁₀H₁₆O₃ requires 184.1099

trans-2-Chloromethylenecyclopropane-1-carboxylic acid ethyl ester, compound 4d:^{16c,d,f} From epichlorohydrine **3d**, yield 3.72 g (28.5 mmol, 38 %), chromatographed on silica gel, R_f = 0.7 (light petroleum–Et₂O, 4:1). As a neat compound, **4d** will decompose albeit slowly at 4 °C. Found: C, 51.8; H, 6.85 C₇H₁₁ClO₂ requires C, 51.7; H, 6.8; Cl, 21.80%; δ_{H} (300 MHz, CDCl₃): 0.87 – 0.98 (m, 1 H), 1.23 (t, J = 7 Hz, 3 H, CH₃), 1.29 (p, J = 4.4 Hz, 1 H, CH₂), 1.62 (p, J = 4.4 Hz, 1 H, CH), 1.77 – 1.87 (m, 1 H, CHC(O)), 3.46 (dd, J = 1.1 Hz, = 7.0 Hz, 2 H, ClCH₂), 4.10 (q, J = 7 Hz, 2 H, OCH₂). δ_{C} (100 MHz, CDCl₃): δ = 11.4, 14.2, 14.9, 20.5, 46.8, 60.7, 172.9. m/z (FD) 162,1 (100) C₇H₁₁ClO₂ requires 162,0448

General procedure for enzymatic hydrolysis employing ESD, compounds (S,S)-4 and (R,R)-5: Racemic esters **4a-d** (5 mmol) were suspended in phosphate buffer (5 ml) at pH 7.0. Temperature was adjusted to 28 °C and the reaction was initiated via the addition of 5 mg of ESD. pH was kept at 7.0 via the automated, controlled addition of 2 M NaOH. After 1.25 ml (2.5 mmol) of NaOH had been added (14-28 h depending on substrate and the ratio of enzyme to substrate), the reaction buffer was extracted with diethyl ether (2 x 10 ml) followed by CH₂Cl₂ (2 x 10 ml). The organic phases were combined, dried over Na₂SO₄ and concentrated in vacuo, to afford **4a-d** as colourless oils. The remaining phosphate buffer was lyophilised over night and **5a-d** were isolated from the residue via acidic work-up. An aliquot of both, ester and acid fraction was dissolved in alcohol (1 ml) and the optical rotary power was measured as an indicator for enantioselectivity of the reaction.

(+)-(S,S)-Cyclopropane-1,2-dicarboxylic acid diethyl ester, compound (+)-4a: From trans-cyclopropane-1,2-dicarboxylic acid diethyl ester **4a**, yield: 0.456 g (2.45 mmol, 49 %), $[\alpha]_D^{20} = +168.8$; (c 1.15, EtOH) (lit.,12b-c $[\alpha]_D^{22} = +150.6$; (c 6.8, EtOH; ee = 100 %) . See **4a** for spectral data.

(+)-(S,S)-2-Benzyloxymethylenecyclopropane-1-carboxylic acid ethyl ester, compound (+)-4b: From trans-2-benzyloxymethylenecyclopropane-1-carboxylic acid ethyl ester **4b**, yield: 510 mg (2.2 mmol, 44 %), $[\alpha]_D^{20} = +9.8$; (c 1, MeOH). (lit.,15a $[\alpha]_D^{22}$ (R,R) = -77 (c 0.44, CHCl₃) ee >95%) See **4b** for spectral data.

(+)-(S,S)-2-Allyloxymethylenecyclopropane-1-carboxylic acid ethyl ester, compound (+)-4c: From trans-2-allyloxymethylenecyclopropane-1-carboxylic acid ethyl ester **4c**, yield: 414 mg (2.25 mmol, 45 %), $[\alpha]_D^{20} = +1.7$; (c 1.00, MeOH). See **4c** for spectral data.

(+)-(S,S)-2-Chloromethylenecyclopropane-1-carboxylic acid ethyl ester, compound (+)-4d: From trans-2-chloromethylenecyclopropane-1-carboxylic acid ethyl ester **4d**, crude yield: 249 mg (1.9 mmol, 38 %), $[\alpha]_D^{20} = +4.1$; (c 1.00, MeOH). See **4d** for spectral data.

(-)-(R,R)-Cyclopropane-1,2-dicarboxylic acid ethyl ester, compound (-)-5a:^{9b-c} From *trans*-cyclopropane-1,2-dicarboxylic acid diethyl ester **4a**, yield: 363 mg (2.3 mmol, 46 %), $[\alpha]_D^{23} = -203.4$; (c 1.00, EtOH) (lit.,12b-c $[\alpha]_D^{20} = +148.5$; (c 6.7, EtOH, ee = 90.4%). Found C, 53.4 H, 6.4 C₇H₁₀O₄ requires C, 53.16; H, 6.4%. $\nu_{\max}/\text{cm}^{-1}$ (neat): 2985(CH), 1692(CO), 1460(CH₂), 1379(CH₃), 1180(C(O)-O-C). δ_{H} (300 MHz, CDCl₃): 1.22 (t, J = 7.0 Hz, 3 H, CH₃), 1.38 – 1.51 (m, 2 H, CH₂), 2.08 – 2.22 (m, 2 H, CH(O)), 4.10 (q, J = 7.0 Hz, 2 H, CH₂), 11.5 (brs, 1H, COOH). δ_{C} (100 MHz, CDCl₃): 14.1, 15.8, 22.0, 23.0, 61.3, 171.4, 178.1. m/z (FD) 159.1 (100) [M+H]⁺ C₇H₁₀O₄ requires 158,0579

(-)-(R,R)-2-Benzyloxymethylenecyclopropane-1-carboxylic acid, compound (-)-5b: From ethyl trans-2-benzyloxymethylenecyclopropane-1-carboxylate **4b** yield: 459 mg (2.25 mmol, 45 %), $[\alpha]_D^{23} = -14.6$; (c 1.00, EtOH) (lit.,^{15a} $[\alpha]_D^{22} = -152$ (c 0.51, CHCl₃) ee >95%). Found C, 69; H, 7.0% C₁₂H₁₄O₃ requires C, 69,9; H, 6,8%. $\nu_{\max}/\text{cm}^{-1}$ (neat) 3028(Ar-H), 2858(CH), 1690(CO), 1454(CH₂), 1075(OCH₂), 735(Ar-H), 696(Ar-H). δ_{H} (300 MHz, CDCl₃): 0.9 – 0.96 (m, 1 H, CH), 1.26 (p, J = 4.4 Hz, 1 H, CH₂), 1.56 (p, J = 4.4 Hz, 1 H, CH₂), 1.75 – 1.82 (m, 1 H, CH(O)), 3.34 (dd, J = 6.6 Hz, J = 10.3 Hz, 1H) 3.46 (dd, J = 5.9 Hz, J = 10,3 Hz, 1 H), 4.51 (s, 2 H), 7.25 – 7.38 (m, 5 H, ArH), 11.2 (brs, 1H, COOH). δ_{C} (100 MHz, CDCl₃):

13.7, 18.4, 22.5, 71.2, 72.6, 127.7, 128.4, 138.0, 180.2. m/z (FD) 206.2 (100) C₁₂H₁₄O₃ requires 206.0943

(-)-(R,R)-2-Allyloxymethylenecyclopropane-1-carboxylic acid, compound (-)-5c: From trans-2-allyloxymethylenecyclopropane-1-carboxylic acid ethyl ester **4c**, yield: 343 mg (2.2 mmol, 44 %), $[\alpha]_D^{23} = -0.7$; (c 3.33, EtOH). Found C, 61.8; H, 7.9 C₈H₁₂O₃ requires C, 61.5; H, 7.7%. $\nu_{\max}/\text{cm}^{-1}$ (neat) 2930(CH), 1675(CO), 1464(CH₂), 1087(O-CH₂), 1007, 928(C=C). δ_{H} (300 MHz, CDCl₃): 0.87 – 0.97 (m, 1 H, CH), 1.24 (p, J = 4.4 Hz, 1 H, CH₂), 1.55 (p, J = 4.4 Hz, 1 H, CH₂), 1.69 – 1.81 (m, 1 H, CHC(O)), 3.31 (dd, J = 6.6 Hz, J = 10.7 Hz, 1 H) 3.41 (dd, J = 6.3 Hz, J = 10.7 Hz, 1H), 3.94 (d, J = 5.9 Hz, 2 H), 5.13 (d, J = 10.3 Hz, 1 H), 5.24 (d, J = 17.3 Hz, J = 1.1 Hz, 1 H), 5.79 – 5.95 (m, 1 H), 11.28 (brs, 1 H, COOH). δ_{C} (100 MHz, CDCl₃): 13.6, 18.4, 22.5, 71.2, 71.6, 117.2, 134.5, 180.1. m/z (FD) 156.1 (100) C₈H₁₂O₃ requires 156.0786

(-)-(R,R)-2-Chloromethylenecyclopropane-1-carboxylic acid, compound (-)-5d:^{16g} From trans-2-chloromethylenecyclopropane-1-carboxylic acid ethyl ester **4d**, yield: 246 mg (2.4 mmol, 48 %), $[\alpha]_D^{23} = -3.8$; (c 1.00, EtOH). $\nu_{\max}/\text{cm}^{-1}$ (neat) 3001(CH), 2945(CH), 2870(CH), 1675(CO), 1464(CH₂), 1190(C(O)-O-C), 928, 705, 659 δ_{H} (300 MHz, CDCl₃): 1.00 – 1.07 (m, 1 H, CH), 1.37 (p, J = 4.4 Hz, 1 H, CH₂), 1.65 (p, J = 4.4 Hz, 1 H, CH₂), 1.85 – 1.92 (m, 1 H, CHC(O)), 3.43 (dd, J = 7.0 Hz, J = 11.0 Hz, 1H), 3.51 (dd, J = 6.6 Hz, J = 11.4 Hz, 1H) 11.39 (brs, 1 H, COOH). δ_{C} (100 MHz, CDCl₃): 15.7, 20.3, 24.5, 46.4, 179.5 m/z (FD) 134, 1 (100) C₅H₇ClO₂ requires 134.0135

Preparative scale procedure for the enzymatic resolution of compound 4a: In a setup for reactions at controlled pH, **4a** (15.1 g, 80 mmol) was suspended in phosphate buffer (50 ml) at pH 7.1. After the addition of 20 mg of ESD the reaction was initiated. The progress of hydrolysis was monitored via NaOH consumption of the pH-stat setup. After 18 to 24 hours of continuous stirring at 28 °C the NaOH consumption ended. The reaction was terminated and filtered through a pad of celite®. The non hydrolysed (S,S)-ester was extracted with diethyl ether (2 x 50 ml) and methylene chloride (2 x 50 ml). After subsequent combination, drying and concentration of the organic phases (S,S)-**4** was obtained in 49 % yield of (+)-**4a** as colourless crystals displaying an optical purity 99 % ee (figure 1, crystal structure). $[\alpha]_D^{24} = 168.8$ (c 1.15, EtOH)

The remaining reaction mixture was lyophilised to leave a residue that was re-dissolved in a small amount of ice-cooled HCl (10 ml) with cooling. Subsequent exhaustive extraction with portions of diethyl ether (30 ml) at pH 1.8 afforded acid **5a** in 46 % yield and 97 % ee.²⁷

(R,R)-diol and (S,S)-diol, compound 6 and ent-6:^{7, 10, 17, 26} A solution of **4a** or **5a** (5.58 g, 30 mmol) in dry THF (10 ml) was added dropwise to a stirred solution of LiAlH₄ powder (95 %) 1.0 equiv. (1.2 g, 30 mmol) and 1.25 equiv. (1.5 g, 37.5 mmol), respectively, in THF (90 ml) at 0 °C. The reaction mixture was heated to reflux for 4 h. After 4 h a solution of 4.1 (2.22 ml, 123 mmol) and 5.1 equiv. (2.76 ml, 153 mmol) of water in THF (8 ml) was added dropwise with stirring under reflux, to obtain a fine suspension of LiOH and Al(OH)₃ in THF. The reaction mixture was filtered through a pad of celite, and the filter cake was washed twice with warm THF (15 ml) and once with dry acetone (15 ml). The filtrate was dried and concentrated in vacuo. Purification via bulb-to-bulb distillation in a Kugelrohr apparatus (1 mbar bp = 141 °C) (lit.,⁷ bp = 96-98 °C 2mm) gave products (R,R)-**6** and (S,S)-**6** in 88 % (2.69 g, 26.4 mmol) and 82 % (2.51 g, 24.6 mmol) yield, respectively, as colourless, viscous

oil. (bp 141 °C at 0.79 mbar). $[\alpha]_D^{21} = -22.6$; (c 1.31, EtOH) (lit.,⁷ $[\alpha]_D^{20} = -26.5$ (neat) ee >99%). $[\alpha]_D^{24} = +24.5$; (c 0.81, EtOH). Found: C, 58.7; H, 9.8%; C₅H₁₀O₂ requires C, 58.8; H, 9.9%. $\nu_{\max}/\text{cm}^{-1}$ (neat) 3353(OH), 2870(CH), 1430(CH₂), 1266, 1056(OCH₂). δ_{H} (300 MHz, CDCl₃): 0.42 (t, J = 6.6 Hz, 2 H, CH₂), 0.95 – 1.06 (m, 2 H, CH), 3.05 (dd, J = 2.9 Hz, J = 11.4 Hz, 2 H, CH₂), 3.80 (dd, J = 7.0 Hz, J = 11.4, 2 H, CH₂), 4.09 (brs, 2H, OH). δ_{C} (100 MHz, CDCl₃): 7.07, 19.80, 65.87. m/z (ESI) C₅H₁₀O₂ requires 102,0681

Desymmetrisation of diols 6 to 7a benzyloxymethylene-cyclopropylmethanol:^{8c,d, 10b} Diol **6** (2.04 g, 20 mmol) was added dropwise to a stirred suspension of 0.75 equiv. NaH 60 % dispersion in mineral oil (600 mg, 15 mmol) in dry DMF (25 ml) under N₂ and heated to 60 °C. After cooling to 0 °C, 0.75 equiv. benzyl chloride (1.89 g, 15 mmol) and 0.1 mol% of TBAI were added all at once. Stirring was continued for 45 min during which the reaction mixture was allowed to warm to RT. Saturated ammonium chloride solution (5 ml) was added and the resultant mixture was concentrated in vacuo to leave a residue that was taken up in water (20 ml) and extracted with dichloromethane (3 x 25 ml). The organic layer was separated, dried and concentrated in vacuo. The residual oil was purified via column chromatography on silica gel, to afford compounds **7a** and *ent-7a* as colourless viscous liquids in 85 % (3.45 g, 12.8 mmol) yield. R_f = 0.7 (EtOAc-light petroleum, 3:7) $[\alpha]_D^{21} = +17.7$, (c 2.15, CHCl₃) (lit.,^{8c} $[\alpha]_D^{23} = 13.8$ (c 2.25, CHCl₃ ee = 94%), $[\alpha]_D^{23} = 23.0$ (c 1.23, EtOH), $[\alpha]_D^{20} = -21.7$; (c 1.31, EtOH). Found: C, 75.35; H, 8.45; C₁₂H₁₆O₂ requires C, 75.0; H, 8.4%. $\nu_{\max}/\text{cm}^{-1}$ (neat) 3379(OH), 3032(Ar-H), 2859(CH), 1453(CH₂), 1363(CH₃), 1070(OCH₂), 1049, 734(Ar-H), 696(Ar-H). δ_{H} (300 MHz, CDCl₃): 0.38 – 0.47 (m, 2 H, CH₂), 0.91 – 1.03 (m, 2 H, CH), 3.15 – 3.32 (m, 2 H, CH₂O), 3.39 – 3.51 (m, 2 H, OCH₂), 4.5 (s, 2 H, ArCH₂O), 7.22 – 7.37 (m, 5 H, ArH). δ_{C} (100 MHz, CDCl₃): 8.0, 16.8, 19.8, 66.3, 72.6, 73.5, 127.6, 127.7, 128.4, 138.3. m/z (FD) 192.2 (100) C₁₂H₁₆O₂ requires 192,1150

Desymmetrisation of diols 6 to compounds 7b and ent-7b:^{24, 26a, 29, 30} Diol **6** (1.53 g, 15 mmol) was dissolved in methylene chloride (30 ml), cooled to 0 °C and acetic anhydride (5 ml) was added. The reaction was initiated via the addition of one drop of 97 % H₂SO₄. After stirring at RT for 14 h the reaction mixture was extracted with water (15 ml), dried and concentrated in vacuo. The residue was purified via bulb-to-bulb distillation in a Kugelrohr apparatus to obtain a colourless liquid. $[\alpha]_D^{21} = +17.5$; (c 1.00, EtOH), $[\alpha]_D^{25} = -17.3$; (c 1.00, EtOH) (lit.,²⁹ $[\alpha]_D^{23} = -14.1^\circ$ (c 2.1, EtOH). Found: C, H, C₉H₁₄O₄ requires C, 58,05; H, 7,58; $\nu_{\max} / \text{cm}^{-1}$ (neat) 2915(CH), 1732(CO), 1449(CH₂), 1366(CH₃), 1225(C(O)-O-C), 1072(OCH₂), 1029. δ_{H} (300 MHz, CDCl₃): 0.56 (t, J = 6.8 Hz, 2 H, CH₂), 1.03 – 1.15 (m, 2 H, CH), 2.02 (s, 6 H, CH₃), 3.89 (d, J = 7.0 Hz, 4 H, CH₂O).²³ m/z (FD) 186.1 (100) C₉H₁₄O₄ requires 186,0892

The product was added to a suspension of 1 g PPL in 20 ml of 0.1 M phosphate buffer at pH 7.1. The pH was maintained stable during the hydrolytic de-symmetrisation via the addition of 1.3 M NaOH when necessary. After 19 h, the reaction mixture was filtered through a pad of Celite®. The filter cake was washed with Et₂O (2 x 10 ml) and the organic layer was separated. The remaining buffer solution was extracted with diethyl ether (20 ml), followed by dichloromethane (20 ml) and again diethyl ether (20 ml). Subsequent combination, drying and concentration of the organic layers afforded **7b** (1.99 g, 13.8 mmol, 92 %) as colourless liquid. $[\alpha]_D^{25} = +21.9$; (c 1.00, EtOH) (lit.,³⁰ $[\alpha]_D^{25} = +7.8^\circ$ (c 0.35, CH₂Cl₂ ee ~ 20%). Found: C, 58.5; H, 8.3; C₇H₁₂O₃ requires C, 58.3; H, 8.4%. $\nu_{\max}/\text{cm}^{-1}$ (neat) 3004, 2948(CH), 2876(CH), 1717(CO), 1424(CH₂), 1369(CH₃), 1232(C(O)-O-C), 1067(OCH₂), δ_{H} (300

MHz, CDCl₃): δ = 0.51 (t, J = 7.0 Hz, 2 H, $\tilde{\text{C}}\text{H}_2$), 0.96 - 1.11 (m, 2 H, $\tilde{\text{C}}\text{H}$), 2.03 (s, 3 H, CH₃), 3.40 (dd, J = 6.5 Hz, J = 11.4 Hz, 1 H, $\tilde{\text{C}}\text{H}_2\text{OAc}$), 3.89 (dd, J = 6.5 Hz, J = 11.4 Hz, 1 H, $\tilde{\text{C}}\text{H}_2\text{OAc}$), 3.89 (d, J = 6.5, 2 H, $\tilde{\text{O}}\text{C}\tilde{\text{H}}_2$). δ_{C} (100 MHz, CDCl₃): 8.4, 15.6, 19.8, 21.0, 65.9, 67.8, 171.3 m/z (FD) 144.1 (100) C₇H₁₂O₃ requires 144,0786

2-Methylsulfonyloxymethylene cyclopropylmethyl benzyl ether, compounds 8a and ent-8a: Alcohols **7a** and ent-**7a** (1.92 g, 10 mmol) were added to 1 equiv. of triethylamine dissolved in CH₂Cl₂ (10 ml) and stirred at 0° C for 30 min. Subsequently, methanesulfonyl chloride was added dropwise to this mixture. The reaction was quenched via the addition of cold water (15 ml) with stirring and the mixture was diluted with CH₂Cl₂ (10 ml). The organic phase was washed with 5 % sodium carbonate solution (10 ml), dried over anhydrous sodium sulphate and concentrated in vacuo to afford **8a** and ent-**8a** in 90 % (2.4 g, 9 mmol) to 97 % (2.62 g, 9.7 mmol) yield. $[\alpha]_{\text{D}}^{24}$, = +19.1; (c 1.08, EtOH). Found: C, 57.5; H, 7.1, S, 11.5 ; C₁₃H₁₈O₄S requires C, 57.8; H, 6.7; S, 11.86%. $\nu_{\text{max}}/\text{cm}^{-1}$ (neat) 3023(Ar-H), 2937(CH), 2860(CH), 1454(CH₂), 1347(CH₃), 1168($\tilde{\text{S}}\text{O}_2$), 1075(OCH₂), 738(Ar-H), 698(Ar-H) δ_{H} (300 MHz, CDCl₃): 0.6 – 0.67 (m, 2 H, $\tilde{\text{C}}\text{H}_2$), 1.11 – 1.24 (m, 2 H, $\tilde{\text{C}}\text{H}$), 2.99 (s, 3 H, CH₃), 3.30 (dd, J = 6.3 Hz, J = 9.9 Hz, 1 H, $\tilde{\text{O}}\text{C}\tilde{\text{H}}_2$), 3.42 (dd, J = 5.9 Hz, J = 10.3 Hz, 1 H, $\tilde{\text{O}}\text{C}\tilde{\text{H}}_2$), 4.1 (d, J = 6.6 Hz, 2 H, $\tilde{\text{C}}\text{H}_2\text{O}$), 4.49 (s, 2 H, Ar $\tilde{\text{C}}\text{H}_2\text{O}$), 7.25 – 7.37 (m, 5 H, ArH). δ_{C} (100 MHz, CDCl₃): 9.0, 16.0, 17.7, 38.1, 66.3, 72.5, 74.0, 127.7, 128.4, 138.2. m/z (FD) 270,2 (100) C₁₃H₁₈O₄S requires 270,0926

2-Fluoromethylene cyclopropylmethyl benzyl ether, compounds 9a and ent-9a, two-step procedure: A solution of mesylate **8a** or ent-**8a** (901 mg, 3.3 mmol) was added dropwise to a stirred solution of dry CsF (750 mg, 5 mmol) in 2-propanol (4.5 ml) at reflux in a Supelco reactivial® with stirring. After 90 minutes a colourless caesium methane sulfonate precipitate was observed and all of **8** had been consumed. The slightly-brown reaction mixture was filtered and the filter cake was washed with Et₂O (2 x 5 ml). The organic phases were combined, concentrated in vacuo and chromatographed on silica gel to obtain **9a** and ent-**9a** (560 mg, 2.9 mmol, 88 %) as a colourless oil. $[\alpha]_{\text{D}}^{24}$ = - 29.3; (c 1.00 in EtOH); $[\alpha]_{\text{D}}^{21}$ = + 29.9; (c 1.00, EtOH), R_f = 0.6 (hexanes-Et₂O, 9:1). Found: C, 74.2; H, 8.0 ; C₁₂H₁₅FO requires C, 74.2; H, 7.8%. $\nu_{\text{max}}/\text{cm}^{-1}$ (neat) 3065(CH), 3010(ArH) 2922(CH), 2861(CH), 1453(CH₂), 1123($\tilde{\text{C}}\text{F}$), 1091(OCH₂), 735(ArH), 697(ArH), 613($\tilde{\text{C}}\text{F}$). δ_{H} (300 MHz, CDCl₃): δ = 0.54 – 0.64 (m, 2 H, $\tilde{\text{C}}\text{H}_2$), 1.06 – 1.18 (m, 2 H, $\tilde{\text{C}}\text{H}$), 3.25 – 3.46 (m, 2 H, $\tilde{\text{O}}\text{C}\tilde{\text{H}}_2$), 4.17 (ddd, J = 7 Hz, J = 12.5 Hz, J_{H-F} = 48.6 Hz, 1 H, $\tilde{\text{C}}\text{H}_2\text{F}$), 4.52 (s, 2 H, Ar $\tilde{\text{C}}\text{H}_2\text{O}$), 7.25 – 7.36 (m, 5 H, ArH). δ_{C} (100 MHz, CDCl₃): 8.2 (d, J_{C-F} = 6.8 Hz), 16.6 (d, J_{C-F} = 6.8 Hz), 16.8 (d, J_{C-F} = 22 Hz), 72.5, 72.8, 86.9 (d, J_{C-F} = 161.2 Hz), 127.7, 128.4, 138.4. δ_{F} (376 MHz, CDCl₃) -209.6 (t, J = 48.7 Hz) m/z (FD) 194.2 (100) C₁₂H₁₅FO requires 194.1107

2-Fluoromethylene cyclopropylmethyl benzyl ether, compounds 9a and ent-9a, one-step procedure: In an oven dried flask diethylamino sulphur trifluoride (DAST) (421 mg, 2.3 mmol) was added to dry dichloromethane (5 ml) via a septum inlet under dry argon. The flask was cooled to -80 °C and dry **7a** and ent-**7a** (385 mg, 2 mmol) dissolved in dry dichloromethane (5 ml) was added drop wise via a syringe. After several minutes of stirring, the flask was warmed to -43 °C (MeCN/dry ice) and the reaction mixture was stirred for 1 h after which the flask was warmed to 0 °C. Stirring was continued for an additional hour at 0 °C and then for 1 h at room temperature. The flask was cooled back to 0 °C prior to the careful, drop wise addition of 5 % sodium carbonate solution (intense foaming), followed by

pentane (5 ml). At this point the organic phase was separated, quickly dried and passed through a short silica column to remove the polar DAST-products. The addition of chloroform (15 ml) instead of hexane followed by further extraction of the organic phase using sodium carbonate solution (2 x 10 ml), drying and evaporation of the organic phase gave comparable results. The product was purified via flash column chromatography to obtain products **9a** and *ent-9a* in up to 92 % (360 mg, 18.5 mmol) yield. It was found that the presence of water during the reaction lead to the formation of sulphurous acid dialkyl esters as significant by-products. See above for spectral data.

2-Tosyloxymethylene cyclopropylmethyl fluoride, compounds **1 and *ent-1*:** Pd (5 mol%) on activated carbon was suspended in MTBE (20 ml), containing **9a** or *ent-9a* (388 mg, 2 mmol) and 2 % (v/v) of glacial acetic acid. Hydrogen was passed through this suspension until all **9** had been consumed. The reaction mixture was filtered through a pad of celite® to remove the catalyst, and concentrated to approximately 1 M alcohol per litre. 1.3 equivalents of NEt₃ were added and the reaction mixture was cooled to 0 °C. After the mixture was stirred for 15 min at 0° C, 1.25 equiv p-toluenesulfonyl chloride (476 mg, 2 mmol) was added in portions. The reaction was quenched after four to eight hours via the addition of cold, saturated ammonium chloride solution (15 ml) with stirring. The organic layer was diluted with dichloromethane (15 ml) and the organic phase was washed with 5 % sodium carbonate solution (10 ml) followed by water (10 ml). Subsequent drying over anhydrous sodium sulphate and concentration in vacuo afforded an oily residue that was purified via flash column chromatography (AcOEt-light petroleum, 1:4) to obtain (S,S)-(+)-**1** and *ent-1* as colourless crystals in 87 % (450 mg, 1.74 mmol) yield. $[\alpha]_D^{21} = -18.9$; (c 1.00, EtOH), $[\alpha]_D^{25} = +20.4$; (c 2.10, EtOH). Found: C, 55.7; H, 5.9; C₁₂H₁₅FO₃S requires C, 55.8; H, 5.85%. $\nu_{\max}/\text{cm}^{-1}$ (neat) 3025(ArH), 2959(CH), 2915(CH), 2870(CH), 1597, 1495, 1465(CH₂), 1380(CH₃), 1352(SO₂), 1307(CH₂), 1247(CH₃), 1188(CF), 1170(SO₂), 1096, 932(ArH), 776(ArH), 571(CF), 663, 553. δ_{H} (300 MHz, CDCl₃): 0.55 – 0.68 (m, 2 H, CH₂), 1.06 – 1.19 (m, 2 H, CH), 2.42 (s, 3 H, CH₃), 3.91 (d, J = 7.0 Hz, 2 H, CH₂OTs), 4.20 (dd, J = 6.6 Hz, J_{H-F} = 48.8 Hz, 1 H, CH₂F), 7.32 (d, J = 7.7 Hz, 2 H, ArH), 7.76 (d, J = 8.1 Hz, 2 H, ArH). δ_{C} (100 MHz, CDCl₃): 8.5 (d, J_{C-F} = 6.8 Hz) 15.6 (d, J_{C-F} = 6.8 Hz), 17.4 (d, J_{C-F} = 24.9 Hz), 21.6, 73.5, 85.7 (d, J_{C-F} = 167.3 Hz), 127.8, 129.9, 133.2, 144.8. δ_{F} (376 MHz, CDCl₃): -211.92 (1 F, t, J_{H-F} = 48.79 Hz). m/z (FD) 258.1 C₁₂H₁₅FO₃S requires 258.0726. HRMS (ESI) 281.0634 (100) ([M+Na]⁺ C₁₂H₁₅FNaO₃S requires 281.0624).

2-[¹⁸F]Fluoromethylene cyclopropylmethyl tosylate, compounds [¹⁸F]-1** and [¹⁸F]-*ent-1*:** [¹⁸F]fluoride was produced by proton bombardment of an isotopically enriched [¹⁸O]H₂O-target, using the ¹⁸O[p,n]¹⁸F nuclear reaction. The [¹⁸F]HF containing [¹⁸O]H₂O was passed through a Waters Accell plus light QMA strong anion exchanger cartridge, preconditioned with 1 M K₂CO₃-solution (10 ml) followed by water (20 ml). The trapped [¹⁸F]fluoride was eluted with a solution of cryptand Kryptofix® K222 (15 mg, 0.04 mmol) and K₂CO₃ (2 mg, 0.015 mmol) in MeCN (1 ml). The MeCN was evaporated at 88 °C under a stream of nitrogen (300 ml/min) in vacuo (102 mbar) to remove the remaining water. Additional MeCN was added (2 x 1 ml) and evaporated. The dried [¹⁸F]fluoride complex was redissolved in 1 ml of MeCN containing precursor **11a** (4.5 mg) or *ent-11a*, respectively, and heated to 90 °C for three minutes. The reaction was quenched via the addition of HPLC-eluent (MeCN-H₂O, 1:1; 1 ml) and the reaction mixture was purified by semipreparative HPLC (10 x 250 mm VWR Lichrosorb® RP-18 5 μ). The product fraction was collected after a retention time of 12-15 min. The collected HPLC-solvent was diluted with water (4:1) and the obtained solution was

passed through a VWR EN cartridge. The resin was washed once with water (3 ml) and dried in a gentle stream of nitrogen (200 ml/min). [¹⁸F]-**1** or [¹⁸F]-*ent-1* was isolated in a radiochemical purity of >98 % and a non decay corrected radiochemical yield of 50 ± 6 % via elution of the cartridge with Et₂O followed by careful evaporation of the solvent.

Acknowledgment

The authors are grateful to Prof. Dr. G. E. Jeromin for his kind donation of authentic (-)-(R,R)-cyclopropane-1,2-dicarboxylic acid as reference, to Prof. Dr. U. Nubbemeyer and to Jacob Hooker, PhD for proofreading the manuscript together with helpful discussions. The authors would like to thank Dr. D. Schollmeyer for X-ray-diffraction measurement. This study was financially supported by the DFG grant Ro985/21.

Notes and references

Institute of Nuclear Chemistry, Johannes Gutenberg-University Mainz, Fritz Strassmann-Weg 2, 55128 Mainz, Germany, Fax: +4961313924692, Tel: +49 6131 3925302, E-mail: riss@uni-mainz.de.

- (1) (a) K. L. Kirk, *Current Topics in Medicinal Chemistry* 2006, 1445 (b) J.-P. Bégué, D. Bonnet-Delpon, *J. Fluorine Chem.* 2006, 127, 992 (c) K. L. Kirk, *J. Fluorine Chem.* 2006, 127, 1013 (d) C. Isanbor, D. J. O'Hagan, *J. Fluorine Chem.* 2006, 127, 297 (e) S. Purser, P. R. Moore, S. Swallow, V. Gouverneur, *Chem. Soc. Rev.* 2008, 37, 320
- (2) H. J. Böhm, D. Banner, S. Bendels, M. Kansy, B. Kuhn, K. Müller, U. Obst-Sander, M. Stahl, *ChemBioChem* 2004, 5, 637 (b) K. Müller, C. Faeh, F. Diederich, *Science* 2007, 317, 1881 (c) E. Schweizer, A. Hoffmann-Roeder, K. Schärer, J. A. Olsen, C. Fäh, P. Seiler, U. Obst-Sander, B. Wagner, M. Kansy, F. Diederich, *ChemMedChem* 2006, 1, 611
- (3) (a) M.-C. Lasne, C. Perrio, J. Rouden, L. Barré, D. Roeda, F. Dolle, C. Crouzel, *Topics in Current Chemistry* 2002, 222, 201 (b) L. Cai, S. Lu, V. W. Pike, *Eur. J. Org. Chem.* 2008, 2853 (c) H.J. Wester, *Handbook of Nuclear Chemistry* 4, 119-202, Kluwer Academic Publishers: Dordrecht 2003
- (4) (a) M. Watanabe, Y. Kazuta, H. Hayashi, S. Yamada, A. Matsuda, S. Shuto, *J. Med. Chem.* 2006, 49, 5587 (b) A. De Meijere, *Angew. Chem.* 1979, 18, 909 (c) B. Perly, I. C. P. Smith, H. C. Jarrell, *Biochemistry* 1985, 24, 1055
- (5) (a) M. A. Carroll, M. Schwartzman, J. Capdevila, J. R. Falok, J. C. McGiff, *Eur. J. Pharmacol.* 1987, 138, 281 (b) S.K. Yang, D. W. McCourt, P. P. Roller, H. V. Gelboin, *Proc. Natl. Acad. Sci. USA* 1976, 73, 2594
- (6) For reviews and collections see: (a) H.-U. Reissig, R. Zimmer, *Chem. Rev.* 2003, 103, 1151; (b) H. Lebel, J.-F. Marcoux, C. Molinaro, A. B. Charette, *Chem. Rev.* 2003, 103, 977 (c) J. Pietruszka, *Chem. Rev.* 2003, 103, 1051 (d) G. Maas, *Chem. Soc. Rev.* 2004, 33, 183 (e) Houben-Weyl, Vol. E17a-c; A. de Meijere., Ed.; Thieme: Stuttgart, 1996 (f) H.-U. Reissig, Houben-Weyl, Vol. E 21, G. Helmchen, R. W. Hoffmann, J. Mulzer, E. Schaumann, Eds.; Thieme: Stuttgart, 1995 (g) H. E. Simmons, T. L. Cairns, S. A. Vladuchick, C. M. Hoiness, *Organic Reactions*, Vol. 20, pp 3 – 131, Wiley: New York, 1973

- (7) M. Schlosser, G. Fouquet, Chem. Ber. 1974, 1162 and references cited therein.
- (8) (a) A. B. Charette, H. Juteau, J. Am. Chem. Soc. 1994, 116, 2651; (b) S. E. Denmark, J. P. Edwards, Synlett 1992, 229 (c) A. B. Charette, H. Juteau, H. Lebel, C. Molinaro, J. Am. Chem. Soc. 1998, 120; 11943 (d) J. Balsells, P. J. Walsh, J. Org. Chem. 2000, 65, 5005 (e) S. E. Denmark, S. P. O'Connor, S. R. Wilson, Angew. Chem. Int. Ed. Engl. 1998, 37, 1149, (f) A. B. Charette, C. Molinaro, C. Brochu, J. Am. Chem. Soc. 2001, 123, 12168
- (9) (a) J. Pietruszka, A. C. M. Rieche, T. Wilhelm, A. Witt, Adv. Synth.Catal. 2003, 345, 1273 (b) J. A. Miller, E. J. Hennessy, W. J. Marshall, M. A. Scialdone, S. T. Nguyen, J. Org. Chem. 2003, 68, 7884 (c) R. Csuk, Y. von Scholz Tetrahedron 1994 50, 10431 and references cited therein. (d) V. K. Aggarwal, H. W. Smith, G. Hynd, R. V. H. Jones, R. Fieldhouse, S. E. Spey, Perkin Trans 1 2000, 19, 3267
- (10) (a) R. E. Taylor, F. C. Engelhardt, M. J. Schmitt, H. Yuan, J. Am. Chem. Soc. 2001, 123, 2964 (b) Y. Kazuta, H. Abe, T. Yamamoto, A. Matsuda, S. Shuto, J. Org. Chem. 2003, 68, 3511
- (11) K. Faber, Biotransformations in Organic Chemistry, 5th ed., Springer: Heidelberg 2004
- (12) (a) C. Tesch, K. Nikoleit, V. Gnau, F. Goetz, C. Bormann, Journal of Bacteriology 1996, 178; (b) G. E. Jeromin, T. Dausmann, H. Hippchen, P. Riss, Ger. Offen. DE 102004059469 2006; Chem. Abstr. 2006, 143, 26701 (c) G. E. Jeromin, M. Bertau, Bioorganikum, Wiley-VCH: Weinheim, 2005
- (13) W. S. Whadsworth, W. D. Emmons, J. Am Chem.Soc. 1961, 79, 1733
- (14) (a) A. Berkessel, C. A. Sklorz, Tetrahedron Lett. 1999, 7965. (b) A. Grenz, S. Ceccarelli, C. Bolm, Chem. Commun. 2001, 1726 and references cited therein.
- (15) (a) A. Armstrong, J. N. Scutt, Org. Lett. 2003, 5, 2331; (b) A. K. Singh, M. N. Rao, J. H. Simpson, W.-S. Li, J. E. Thornton, D. E. Kuehner, D. J. Kacsur, Org. Process Res. Dev. 2002, 618
- (16) (a) T. Rasmussen, J. F. Jensen, N. Èstergaard, D. Tanner, T. Ziegler, P.-O. Norrby, Chem. Eur. J. 2002, 8, 177 and references cited therein, (b) K. B. Wiberg, R. K. Barnes, J. Albin, J. Am. Chem. Soc. 1975, 79, 4994 (c) M. P. Doyle, W. H. Tamblin, V. Bagheri, J. Org. Chem. 1981, 46, 5094 (d) I. A. D'yakonov, T. V. Domareva, Zh. Obshch. Khim. 1955, 25, 934, 1486 (e) T. Saegusa, Y. Ito, S. Kobayashi, K. Hirota, T. Shimizu, J. Org. Chem. 1968, 33, 544 (f) B. T. Golding, S. Mwesigye-Kibende J. Chem. Soc. Chem. Commun. 1983, 1103. (g) I. A. D'yakonov, O. V. Guseva, Sbornik Statei Obsheei Khim., Akad. Nauk S.S.S.R.1953, 1, 425
- (17) Most published Methods make use of continuous liquid-liquid extraction, e.g.: K. Ruhland, E. Herdtweck, Adv. Synth.Catal. 2005, 347, 398
- (18) O. Houille, T. Schmittberger, D. Uguen, Tetrahedron Lett. 1996, 37, 625
- (19) Gmelins Handbuch der Anorganischen Chemie, 8th ed., Verlag Chemie: Weinheim 1938, reprint 1955
- (20) (a) M. Hudlicky, Organic Reactions, Vol.35; Wiley: Hoboken, 1988 (b) R. P. Singh, J. M. Shreeve, Synthesis 2002, 2561 (c) R. P. Singh, D. T. Meshri, J. M. Shreeve, Adv. Org. Synth. 2006, 2, 291

- (21) T. W. Greene, P. G. M. Wuts, *Protective Groups in organic Synthesis*, 3rd ed., Wiley: Hoboken
- (22) (a) H.-D. Becker, B. Ruge, *J. Org. Chem.* 1980, 45, 2189 (b) R. W. White, W. D. Emmons, *Tetrahedron* 1962, 17, 31
- (23) (a) S. Krompiec, N. Kuznik, M. Urbala, J. Rzepa, *J. Mol.Cat. A* 2006, 248, 198 (b) M. Muehlbacher, C. D. Poulter, *J. Org. Chem.* 1988, 53, 1026
- (24) C. D. Poulter, J. Muscio, and R. J. Goodfellow, *J. Org. Chem.* 1975, 40, 139
- (25) Please note that fluoroalcohols 10 may be strong skin irritants.
- (26) (a) A. T. Blomquist, D. T. Longone, *J. Am. Chem. Soc.* 1959, 81, 2012 (b) Y. Inouye, T. Sugita, H. M. Walborsky, *Tetrahedron* 1964, 20, 1695. (c) Y. Inouye, S. Sawada, M. Ohno, H. M. Walborsky, *Tetrahedron* 1967, 23, 3237. (d) V. J. Heintz, T. A. Keiderling, *J. Am. Chem. Soc.* 1981, 103, 2395
- (27) (a) An ether solution of acid 5a was dried over sodium sulphate and exposed to excess diazomethane in ether in a standard 2 ml screw-cap vial for 20 minutes. The obtained solution can be used for GC-determination of ee-values. (b) S. R. Landor, P. D. Landor, M. Kalli, *J. Chem. Soc. Perkin Trans. 1* 1983, 12, 2921 (m.p. acid = 172-174 °C; (R,R): $[\alpha]_{D20} = -218$. (c 1, EtOH); (lit.,7 $[\alpha]_{D20} = -238.8$ (c 2.036, H₂O). (S,S) $[\alpha]_{D20} = +232.4$ (c 1, EtOH) (lit.,26d $[\alpha]_{D20} = +228$, (c 1.75, EtOH)
- (28) Deposited at the Cambridge Structural Database: CCDC 691513
- (29) (a) B. S. J. Blagg, M. B. Jarstfer, D. H. Rogers, and C. D. Poulter, *J. Am. Chem. Soc.* 2002, 124, 8846, (b) A. G. M. Barrett, D. Hamprecht, J. P. White, D. J. Williams, *J. Am. Chem. Soc.* 1997, 119, 8608
- (30) S. Hu and J. S. Dordick, *J. Org. Chem.* 2002, 67, 314

4.2 Synthesis and monoamine uptake inhibition of conformationally constrained 2 β -carbomethoxy-3 β -phenyl tropanes

Synthesis and monoamine uptake inhibition of conformationally constrained 2 β -carbomethoxy-3 β -phenyl tropanes

Patrick Johannes Riss, René Hummerich, Patrick Schloss

Institute of Nuclear Chemistry, Mainz University, Fritz Strassmann-Weg 2, 55128 Mainz; Germany

A series of 2 β -carbomethoxy-3 β -phenyl tropanes with conformationally constrained nitrogen substituents were synthesized as potential selective dopamine transporter ligands. These novel compounds were examined for their monoamine uptake inhibition potency at the human dopamine transporter (hDAT), the human serotonin transporter (hSERT) and the human noradrenalin transporter (hNET), stably expressed in human embryonic kidney cells (HEK). A SAR-study was conducted to determine the contribution of extended, 4-fluorinated, conformationally constrained C₄ chains at the tropane nitrogen to human monoamine transporter affinity and selectivity.

Introduction

The dopaminergic system remains an important molecular target for basic research, drug development and diagnostic imaging.¹ This is due to its relevance to addiction, psychiatric and neurodegenerative diseases.² The dopamine transporter (DAT) mediated dopamine reuptake, in particular, has been of significant interest.³ Quantification of the availability of neuronal DAT-binding sites with positron emission tomography (PET) is a sensitive measure of function and integrity of the dopaminergic system.⁴

Two different classes of compounds display high *in vitro* affinity and selectivity to the DAT. These are benzhydryl substituted piperazine derivatives and ligands based on the methyl 3 β -phenyltropane-2 β -carboxylate lead (Figure 1).⁵ Radiolabelled high affinity analogues of the latter proved to be the most promising candidates for DAT imaging.^{6,7}

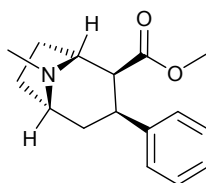


Figure 1: 2 β -carbomethoxy-3 β -phenyl tropane, lead structure for DAT-selective monoamine transporter ligands.

Considerable effort has already been spent on the modification of the available lead structure.⁸ However, the development of highly potent, selective DAT inhibitors was often complicated by the mixed binding profile of this class of compounds. Various highly potent cocaine-derived DAT inhibitors show a similar inhibition of norepinephrine or serotonin uptake.^{8,9} In fact, the hDAT is closely related to the human serotonin transporter (hSERT; 49%

amino acid homology) and the human norepinephrine transporter (hNET; 67% amino acid homology).¹⁰

Nevertheless, modifications of the phenyltropane carboxylate lead have already generated promising examples of hDAT or hSERT selective radio-ligands. These successful molecular modifications indicate that the selectivity for the DAT can be affected by substitutions at the ester function, at the phenyl ring as well as at the nitrogen.^{8-9,11-12} With regard to a potential application as fluorinated DAT radio-ligands for PET, variation of ω -fluorohydrocarbon chains at the tropane nitrogen showed the most promising results.^{7,11} A trend in selectivity as well as affinity was found in the ω -fluoroalkyl series.^{9,11} While nortropans are more potent at the SERT, DAT affinity, SERT/DAT and NET/DAT ratios correlate with increasing chain lengths.^{8,9,11-12} The 4-fluorobutyl moiety has rarely been investigated in this relationship. Instead, (*E*)-configured 3-iodoallyl substituted nortropans showed encouraging improvements.^{13a} Isosteric substitution of the (*E*)-iodoallyl moiety by an (*E*)-4-fluorobut-2-ene-1-yl residue led to the development of (*E*)-fluorobutenyl substituted 4'-halophenyl (FBCFT) and 4'-methylphenyl (LBT999, **7q**) derivatives. Most of these displayed remarkable selectivity and affinity (Figure 2).^{13,14}

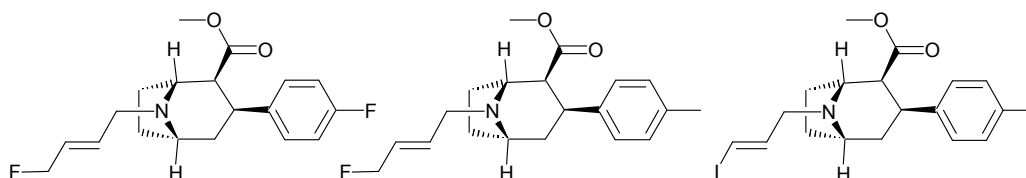


Figure 2: FBCFT, LBT-999 and PE21

It has been proposed that this improvement might be particularly effected by an olefinic residue in the vicinity of the nitrogen. These findings may also indicate preferred binding of extended conformations of the *N*-C₄ substituted derivatives to the DAT. This is presumably due to their reduced flexibility in the slow isomerisation step upon binding to the DAT.¹⁵ Although the concept of conformational restriction based monoamine transporter ligand design has been studied previously,¹⁶ no further systematic elucidation of the contribution of conformational restriction at the *N*-substituent has been reported so far.¹⁷

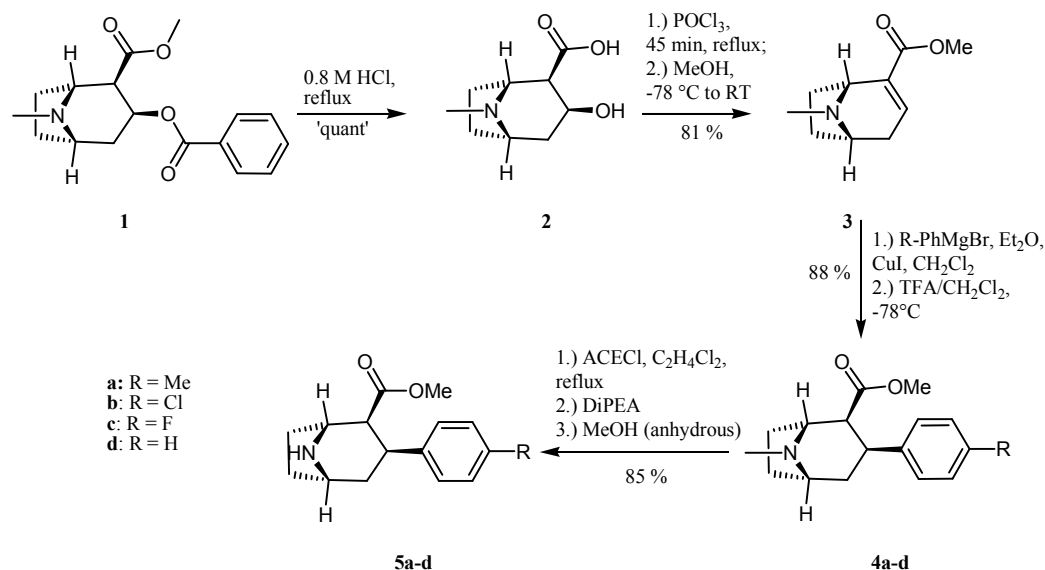
Para-substitution at the phenyl ring is known to have a significant effect on potency and selectivity of cocaine-analogue tropanes. Bulky groups may increase SERT affinity, and even 4-iodo and 4-bromo derivatives exhibit a remarkable increase in SERT and NET affinity. In contrast, their DAT-inhibition-potencies and binding affinities are in a similar range as the ones of the methyl analogues.¹⁸

Herein, the influence of conformationally constrained, extended C₄-chains in rigid tropane-based monoamine transporter ligands to hDAT, hSERT and hNET selectivity and inhibition potency is examined. The 4-position at the phenyl ring was varied from hydrogen via fluoride and chloride to methyl. For comparison, the non-restricted 4-fluorobutyl derivatives have also been prepared.

Results and Discussion

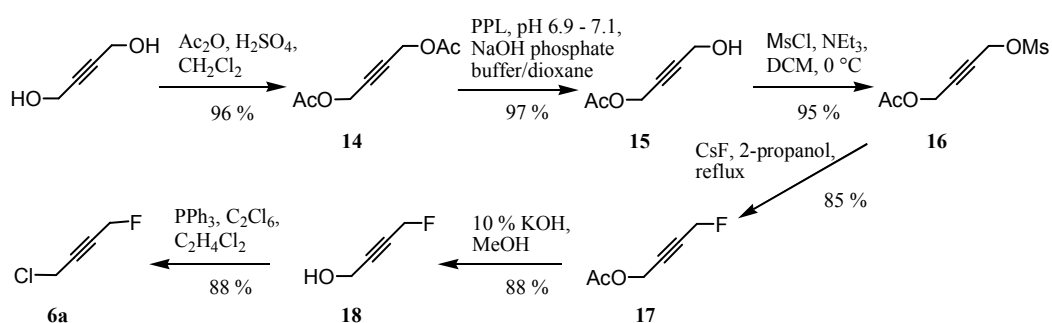
The synthesis of Michael-acceptor **3** was performed as published elsewhere (Scheme 1).^{19a,b} Stereoselective 1,4-addition of the corresponding Normant-cuprates furnished phenyltropanes **4a-d** in high yield (88%) and high diastereomeric excess (*de* >95%).²⁰ Demethylation to

nortropanes **5a-d** was achieved via a modified procedure,^{19c} providing up to 97 % nortropane. More than 85 % of demethylated product was isolated after flash chromatography in a preparative scale run.



Scheme 1: Synthesis of nortropanes **5a-d**; see Table 1 for compound numbers and structures.

Compound **6a** (Figure 3) was obtained from but-2-yne-1,4-diol via acetylation of both alcohol functions (**14**) followed by enzyme catalysed selective hydrolysis of one acetyl group using porcine pancreatic lipase (PPL, E.C. 3.1.1.1.; 96 and 97 % respectively). Product alcohol **15** was mesylated in dichloromethane at 0 °C. Subsequent fluorination with CsF in 2-propanol furnished fluoride **17** in 81 % yield. Fluoride (**17**) was deprotected in methanol containing KOH (10 %) at room temperature to afford alcohol (**18**) in 88 % yield. Appel halogenation using hexachloroethane in 1,2-dichloroethane followed by bulb-to-bulb distillation afforded 4-fluorobut-2-yne-1-yl chloride (**6a**) in 88 % yield, resulting in an overall yield of 60 % over six steps (Scheme 2).



Scheme 2: Synthesis route to 4-fluorobut-2-yne-1-yl chloride

Cyclopropane **6b** and the opposite enantiomer **6c** (Figure 3) were synthesised stereoselectively as reported recently.²¹

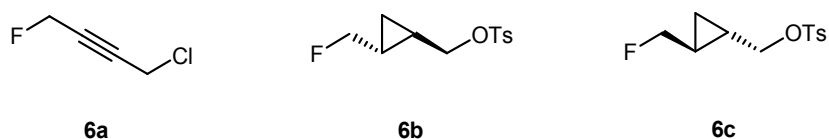
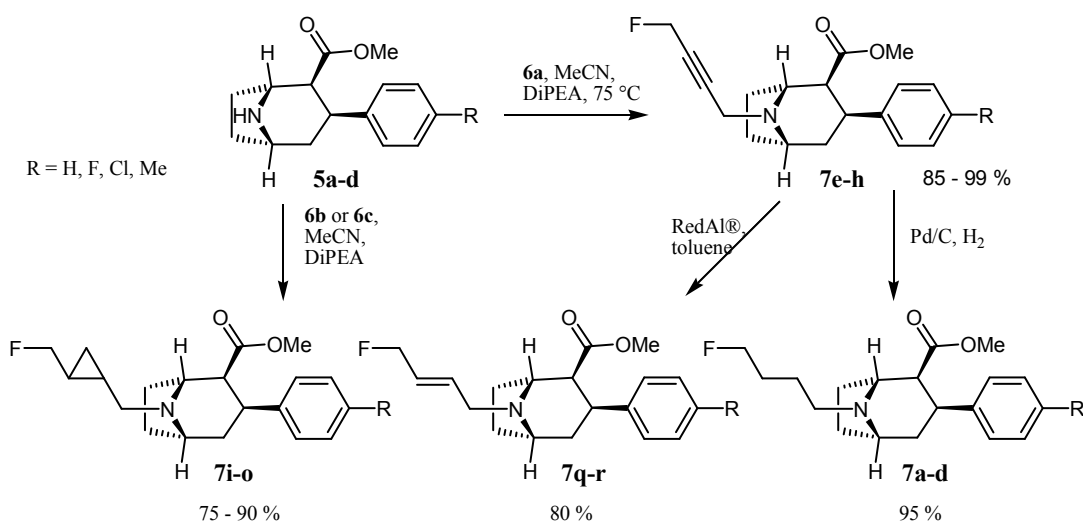


Figure 3: Electrophilic building blocks for the introduction of terminally fluorinated C₄-residues

Nortropanes **5a-d** were alkylated using electrophiles **6a-c** (Scheme 3) with acetonitrile as solvent and diisopropylethylamine as base in 75-97 % yield. Compounds **7a-d** were obtained directly from **7e-h** via catalytic hydrogenation with Pd⁰ on activated carbon. Compounds **7q** and **7r** were obtained via reduction of alkynes **7e** and **7h**, respectively, with sodium (bismethoxyethoxy)aluminium hydride (RedAl[®]).



Scheme 3: Synthesis of compounds **7a-r**; see Table 1 for compound numbers and structures

The final compounds were purified by semi-preparative HPLC and converted into water soluble hydrochlorides for cell studies. The purity of all assayed compounds exceeded 99 % (by HPLC peak-area at UV₂₅₄).

Saturation analyses of [³H]dopamine ([³H]DA), [³H]serotonin ([³H]5HT) and [³H]noradrenalin ([³H]NE) uptake into HEK293 cells stably expressing the human monoamine transporters hDAT, hNET and hSERT, respectively, were performed. The resulting IC₅₀ values are summarized in Table 2. A representative experiment is shown in Figure 4.⁹ The selectivity was expressed as IC₅₀-ratios between the hSERT and the hDAT as well as the hNET and the hDAT, respectively.

To elucidate the effect of non-constrained C₄-chains, compounds **7a-d** were synthesised. Among these, the degree of inhibition of DA reuptake increases in the sequence H < Cl ≈ F < Me. This relation is even more pronounced at the hSERT. Inhibition potency significantly increases with the size of the *para*-substituent: H (4 μM) < F (2.6 μM) < Cl (1.4 μM) < Me

(0.8 μM). At the hNET, both electron withdrawing substituents show a similar potency, comparable to the hDAT. Potency decreases from chlorine to hydrogen ($\text{Cl} \approx \text{F} > \text{Me} > \text{H}$). Both compounds with an electron donating substituent (**7a** and **7d**) show a remarkable selectivity over the hSERT (>100). They also show a reasonable selectivity over the hNET (4-5). However, hydrogen derivative **7d** is ~ 4 -fold less potent at the hDAT ($\text{IC}_{50} = 33$ nM), compared to **7a** (8 nM). On the other hand, both compounds with electron withdrawing substituents show a similar potency at hDAT and hNET. As a result, **7b** and **7c** display a threefold lower selectivity over the hNET. Selectivity over the hSERT is retained (60 - 140).

To examine the contribution of both a linear C_4 -segment as well as the necessity of an olefinic nitrogen-residue, alkynes **7e-h** were prepared. Both compounds containing an electron donating substituent **7e** and **7h** display a low nanomolar potency of 3 nM and 6 nM at the hDAT, respectively. Compared to the flexible analogues **7a** and **7d**, a twofold to six fold increase in potency is achieved. However, the results at the hSERT are even more significant. The introduction of a 4-fluorobut-2-yne-1-yl chain strikingly increases hSERT potency for **7e-h**. The size dependency of potency and selectivity, observed for the flexible analogues **7a-d**, is absent within the alkyne series. Interestingly, methyl derivative **7e** displays outstanding characteristics. This is consistent with the known restricted methyl analogues e.g. PE2I and LBT999 (**7q**). Its high potency is combined with good selectivity over the hSERT (73-fold) and the NET (10-fold). A significant increase in hDAT potency is observed for **7h**. This is accompanied by even higher increases at both, the hSERT (16 fold) and the hNET (11-fold). The 4-fluorophenyl and 4-chlorophenyl derivatives **7f** and **7g** show a moderate potency (~ 16 nM) at the hDAT. This is comparable to their flexible analogues. Nonetheless, their hSERT-

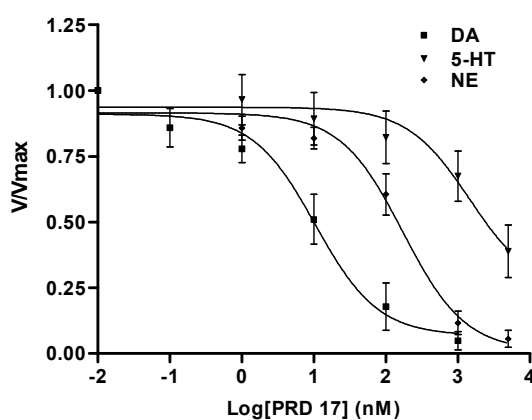


Figure 4: Inhibition of $[^3\text{H}]\text{DA}$, $[^3\text{H}]\text{NE}$ and $[^3\text{H}]\text{5-HT}$ uptake into HEK293 cells stably expressing human DAT, NET or SERT, respectively. HEKhDAT, HEKhNET and HEKhSERT cells were incubated with transporter buffer containing 250 nM $[^3\text{H}]\text{DA}$ (\blacksquare), $[^3\text{H}]\text{NE}$ (\blacklozenge) and $[^3\text{H}]\text{5-HT}$ (\blacktriangledown), respectively, and increasing concentrations of **7l**. The IC_{50} values for the inhibition of the single monoamines obtained in these representative experiments were as follows: 10.5 ± 0.2 nM for $[^3\text{H}]\text{DA}$, 172.5 ± 0.3 nM for $[^3\text{H}]\text{NE}$ and 1456 ± 0.2 nM for $[^3\text{H}]\text{5-HT}$.

Table 1: Ligand structures of new compounds and references

compound ^a	structure ^b	R ^c	name ^d
7a		Me	PRD01
7b		Cl	PRD07
7c		F	PRD11
7d		H	PRD15
7e		Me	PRD04
7f		Cl	PRD08
7g		F	PRD12
7h		H	PRD16
7i		Me	PRD05
7j		Cl	PRD09
7k		F	PRD13
7l		H	PRD17
7m		Me	PRD06
7n		Cl	PRD10
7o		F	PRD14
7p		H	PRD18
7q		Me	LBT999
7r		H	PRD19
8		F	β-CFT
9		I	β-CIT
10		Cl	FECNT
11		I	FE-β-CIT
12		I	FP-β-CIT
13			cocaine

[a] compound number [b] general structure [c] phenyl substituent [d] project tag or common name of compound

potency is partially augmented. In particular **7f** displays a 4-fold loss in hSERT selectivity. Also, **7f** has a twofold lower potency at the hNET, resulting in a higher hNET selectivity. To investigate the effect of (*E*)-configuration, *trans*-cyclopropanes **7i-p** were examined. These derivatives facilitate the evaluation of particular effects of olefinic double bonds in the same position. Both diastereoisomeric forms lead to clearly distinguishable characteristics. Within the (*S,S*)-configured cyclopropanes, the hDAT activity increases in the sequence F < Me < H < Cl. In contrast, the hDAT potency within the (*R,R*)-analogues increases in the sequence H < F < Cl < Me. The hSERT and the hNET potencies follow the order H < F < Me < Cl, completely independent of the absolute configuration. Compared to the 4-fluorobutyl- and 4-fluorobutynyl-residues, profound changes can be observed for the compounds containing an electron withdrawing phenyl substituent. Chloro derivatives **7j** and **7n** display a remarkably high hDAT potency of 4 and 9 nM, respectively. However, the (*S,S*)-analogue **7j** is 2.5-fold more selective to the hSERT (SERT/DAT ~ 50) and 1.3-fold more selective to the hNET (NET/DAT ~ 3.6). In contrast, the overall activities of fluoro-analogues **7k** and **7n** are significantly lower (31 nM and 12 nM, respectively). In this case the (*R,R*) analogue **7o** exhibits a 1.5-fold higher hSERT selectivity and a 1.25-fold higher selectivity over the hNET. Among the compounds containing an electron donating phenyl substituent, the hSERT and hNET potencies of the (*S,S*)-derivatives are slightly (at least twofold) lower than the corresponding (*R,R*)-analogues. Conversely, (*R,R*)-analogue **7p** shows the lowest hDAT potency (34 nM) of all novel compounds. Methyl derivative **7i** has a lower hDAT-potency (14 nM) than its (*R,R*)-counterpart **7m** (6 nM). Both display similar selectivity over the hNET. However, the (*S,S*)-diastereoisomer **7i** is more selective over the hSERT. Finally, the introduction of the (*S,S*)-2-fluoromethylcyclopropylmethyl-residue led to the discovery of a potent hDAT inhibitor **7l** (11 nM) which provides remarkable selectivity over the hSERT (134-fold) and the hNET (17-fold). Interestingly, the correlation between activity and the characteristics of the phenyl substituent is absent between **7i-l**.

Table 2^b: IC₅₀ values and monoamine transporter selectivity of novel phenyl tropanes, as determined in human embryonic kidney cells (HEK 293) stably transfected with hDAT, hSERT and hNET-RNA.

compound	hDAT _{IC50} ^c	hSERT _{IC50} ^c	hNET _{IC50} ^c	hSERT	hNET
	(hDAT _{Ki}) / nM	(hSERT _{Ki}) / nM	(hNET _{Ki}) / nM	/hDAT	/hDAT
7a	7.8±0.3	810±5	37±1	104	5
7b	22±1	1400±0.3	29±1.2	64	1.5
7c	19±1	2600±0.4	31±1	137	1.5
7d	33±1	4000±0.5	136±1	121	4
7e	3.3±0.5	240±4	31±1	74	10
7f	17±1	270±0.2	41±1	17	2.5
7g	16±1	1400±0.2	21±1.3	89	1.5
7h	5.8±0.6	250±0.1	13±0.5	44	2
7i	14±0.5	950±3	56±0.4	70	4
7j	4.3±0.5	220±0.4	16±0.4	50	3.5
7k	31±1	690±5	76±1	22	2.5
7l	11±0.5	1400±3	175±1	134	17
7m	5.7±0.3	290±4	25±0.5	51	4.5
7n	8.9±0.3	160±2	24±1	18	3
7o	12±0.6	420±2	37±1	34	3
7p	34 ±1	560±3	84±1	16	2.5
7q	26±1	700±2	150±2	27	6
7r	53.3±0.8	2650±200	210±0.6	50	4
8	40±1	2300±0.3	120±2	57	3
9^a	(6.3±1.7)	(29±6.4)	(33±13)	4.5	5
10^a	2.5±0.2	530±1.5	10.6±0.5	210	4.2
11^a	(91±5)	(130±31)	(130±50)	1.5	1.5
12^a	(28±7)	(110±64)	(70±15)	4	2.5
13	(320±130)	(580±110)	(180±25)	2	0.6

a) Taken from Ref. 9: IC₅₀ values were converted to K_i values using the Cheng and Prusoff equation by the authors, $K_i = IC_{50} / (1 + [L]/K_m)$ (where [L] is concentration of [³H]DA, [³H]5-HT or [³H]NE; K_m values from Eadie-Hofstee-plots. b) Values are mean ± SD (nM). c) compounds **7a-7r** did not exhibit competitive inhibition of substrate transport.

Conclusion

In summary, overall potency within the 4-fluorobutyl series is dependent on the size of the phenyl-substituent. In comparison, the introduction of a linear alkyne strongly increases activity at all transporters. Among the cyclopropane containing ligands, both diastereoisomeric isomers lead to clearly distinguishable characteristics.

The above findings indicate a strong influence of inflexible nitrogen substituents. In particular, the extended (*S,S*)-configured side chain. The *N*-substituent might influence the overall orientation of the molecule, which leads to a different arrangement of the phenyl substituent in the proximity of the aromatic binding site. This preset orientation might furthermore limit the beneficial effect of aromatic interactions on binding and thereby inhibition potency.

In all other cases, the overall effect of the phenyl-substituents remains similar as described for the *N*-methyl analogues. More or less the same order of affinity is found within the present study. This could give rise to the conclusion that the derivatives presented herein still bind in the same environment as the non-*N*- modified tropanes.

Most novel derivatives provide low to moderate nanomolar IC₅₀ at the hDAT (**7a,c,e-j,l-o**) and selectivity over the hSERT (**7a-p**) and also over the hNET (**7a,d-f,h-p**). Two potent compounds, **7e** and **7l**, emerge as outstandingly selective over the hNET (10 and 17-fold, respectively), while maintaining significant selectivity over the hSERT (74 and 134-fold, respectively). In both cases, the inhibition potencies remain in a range comparable to the reference compounds (**7q**, **8-9**, **11-12**), whereas their selectivity ratios exceed the values for these reference compounds.

The only exception in terms of a superior hSERT/hDAT-ratio is the clinically established imaging-agent FECNT (**10**) which, on the other hand, provides only moderate selectivity over the hNET. Furthermore, LBT-999 (**7q**) has recently been validated as appropriate radio-ligand for PET-studies of the striatal and extra-striatal DAT. Based on these findings we conclude that two potent DAT-inhibitors (**7e** and **7l**) of improved in vitro selectivity have been discovered.

Compounds **7e** and **7l** are currently under investigation regarding their potential as ¹¹C and ¹⁸F-labelled radio-probes for the non-invasive quantification of DAT availability in living subjects.

Experimental Section

Melting points were determined on an Electrothermal[®] 9100 melting point apparatus and reported uncorrected. NMR-spectra were recorded with a Bruker AC 300 FT-NMR-spectrometer, *J* values are given in Hertz, chemical shifts are reported downfield from TMS ($\delta = 0$ ppm), referred to the solvent residual signal ¹H NMR (CHCl₃ 7.24 ppm) and ¹³C NMR (CDCl₃ 77.0 ppm). Field desorption (FD) mass spectra were recorded on a Finnigan MAT90 FD spectrometer. HRMS-spectra were measured on a Micromass QTOF Ultima 3 spectrometer. IR-spectra were obtained from a Nicolet 6700 FTIR spectrometer. Optical rotations were determined using a Perkin-Elmer polarimeter 241 at 546 and 578 nm (Hg-lamp) and were extrapolated to the sodium D line. $[\alpha]_D$ -values are given in 10⁻¹ deg cm² g⁻¹. Boiling points are uncorrected. All chemicals were obtained in commercial quality from Acros Organics, Sigma Aldrich, VWR, TCI or STREM and used without further purification. Enzymes were obtained from Sigma-Aldrich. TLC was conducted on self-cut Merck silica gel 60 covered aluminium plates. Detection and staining was performed either using iodine on

silica gel, potassium permanganate solution, UV fluorescence, vanillin/sulphuric acid, Seebach-reagent (phosphomolybdic acid, cerium sulphate, H₂SO₄) or Dragendorff-reagent (basic bismuth nitrate, potassium iodide and tartaric acid). Column chromatography was performed on Acros silica gel 60, 0.063-0.200 mesh, p. a. solvents for chromatography were washed with aqueous acid and base and distilled once, prior to use. Anhydrous solvents were used for reactions.

2 β -carbomethoxy-3 β -phenyltropanes (4a-d): A solution of p-substituted phenylmagnesium bromide (40 mmol, 40 ml) 1 M in THF was added to a suspension of CuI (40 mmol, g) in THF (50 ml) under nitrogen and stirred at 0 °C for 30 min. The mixture was cooled to -43 °C and ecgonidine methyl ester (3.6 g, 20 mmol) in THF (6:4, 75 ml) was added dropwise, so that the temperature inside the flask did not exceed -40°C. Stirring was continued for 5 h after which the reaction mixture was cooled to -78 °C and TFA (g, 40 mmol) in CH₂Cl₂ was added dropwise over 30 min. The solvents were removed in vacuo to leave a semisolid residue that was partitioned between CH₂Cl₂ and cold 28 % ammonium hydroxide solution (25 ml). The aqueous phase was extracted with CH₂Cl₂ (2 x 40 ml) followed by Et₂O (40 ml) purified via flash column chromatography (Et₂O-Hexanes, 1:9, 10 % NEt₃). **4a-d** were obtained as colourless to slightly yellow solids in 88-90 % yield (4.78 g, 35 mmol). NMR-spectra and FD-mass were in accordance with those published elsewhere.^{19a,b}

Procedure A: General procedure for N-alkylation: Nortropine **5a-d** (100 mg, 0.35-0.45 mmol) was added to a stirred solution of Hünig's base (1.01 equiv.) in 10 ml of acetonitrile. Electrophile **6a-c** (1 equiv.) was added and the mixture was stirred at 70 °C for 12 h. The mixture was carefully concentrated in vacuo to leave a mobile residue that was chromatographed on silica gel (20 g, ether-hexanes, 1:9, 10 % NEt₃) to afford products **7e-p** in 75-97 % yield.

Procedure B: General procedure for N-demethylation: Tropanes **4a-d** (1.5 g, 5.4 – 6.1 mmol) were dissolved in dichloroethane (30 ml) and refluxed with 1-chloroethyl chloroformate (7 equiv.) for one hour. One equiv. of N,N-diisopropyl-N-ethylamine (700 – 790 mg) was added and the mixture was refluxed for one additional hour. Subsequently, the reaction mixture was concentrated in vacuo to leave a colourless, viscous residue that was taken up in MeOH (30 ml) with cooling and stirring. After refluxing for 2 additional hours, the resultant, pale yellow solution was concentrated, and the residue was taken up in cold ammonium hydroxide solution (28 %, 15 ml) with intense cooling and extracted with Et₂O (2 x 25 ml), followed by dichloromethane (2 x 25 ml) and again Et₂O (25 ml). Combination, drying (anhydrous K₂CO₃) and concentration of the organic layers afforded crude nortropines **5a-d**. Purification was performed on silica gel 60 (AcOEt-hexanes, 3:7, 10 % NEt₃) to obtain products **5a-d** in 85-88 % yield. NMR spectra were in accordance with those published previously.^{13a,19a,b}

1,4-Diactyl but-2-yne-1,4-diol (14): But-2-yne-1,4-diol (8.61 g, 0.1 mol) was dissolved in methylene chloride (75 ml) and cooled to 0 °C. Acetic anhydride (25 ml) was added with efficient stirring and the reaction was initiated via the addition of 1-2 drops of 97 % sulphuric acid. The reaction mixture rapidly heated to reflux and darkened. Stirring was continued overnight at RT. The reaction mixture was washed with 1 M potassium carbonate solution (35 ml), followed by water (35 ml), dried over Na₂SO₄ and concentrated. Distillation afforded 94 % (15.9 g, 0.094 mol) of a colourless liquid that crystallized upon standing: m. p. 30-31 °C;

$C_8H_{10}O_4$ requires C 56.5, H 5.9, found C 56.7, H 5.9; δ_H (300 MHz, $CDCl_3$): 4.11 (s, 2H), 2.06 (s, 3 H); δ_C (100 MHz, $CDCl_3$): 170.1, 80.7, 52.0, 20.6; ν_{max}/cm^{-1} (neat): 2944, 2359, 1739, 1433, 1377, 1360, 1210, 1153, 1021, 964, 604; m/z (FD) 170.1 (100) $C_8H_{10}O_4$ requires 170.0579.

4-Acetoxy-but-2-yne-1-ol (15): A solution of 1,4-diacetyl but-2-yne-1,4-diol (5.0 g, 0,03 mol) in dioxane (10 ml) was added at once to 500 mg of porcine pancreatic lipase in 0,1 M phosphate buffer (25 ml, pH 6,9) at 25 °C. The reaction mixture was stirred at 25 °C for 12 h while maintaining the pH stable via the controlled addition of 1,3 M NaOH solution. To determine progress of the reaction, 500 μ l samples were withdrawn from the mixture, extracted with Et_2O and the organic extracts were analyzed via TLC. After 12-14 h the reaction was interrupted leaving less than 10 % of 1,4-diacetyl but-2-yne-1,4-diol unaffected. Chromatography on silica gel (30g/g; 40 % ethyl acetate in hexanes, $r_f = 0,6$) afforded 3,31 g (0,029 mol) **15** as a colourless liquid (88 %). $C_6H_8O_3$ requires C 56.2, H 6.3, found C 56.4, H 6.4; ν_{max}/cm^{-1} (neat): 3437, 2940, 2860, 2359, 1736, 1436, 1378, 1359, 1219, 1136, 1015, 965, 606; δ_H (300 MHz, $CDCl_3$): 4.69 (t, $J = 1.8$ Hz, 2 H), 4.26 (t, $J = 1.8$ Hz, 2 H), 2.28 (brs, 1 H, OH), 2.07 (s, 3 H); δ_C (100 MHz, $CDCl_3$): 170.5, 85.1, 79.5, 52.3, 50.8, 20.7; m/z (FD) 128.1 (100) $C_6H_8O_3$ requires 128.0473.

4-Acetoxy-but-2-yne-1-yl mesylate (16): 4-acetoxy-but-2-yne-1-ol (1.28 g, 10 mmol) was dissolved in methylene chloride (10 ml) and triethylamine (1.02 g, 10 mmol) was added. After stirring at 0 °C for 30 min, methanesulfonyl chloride (1.146 g, 10 mmol) was added dropwise with stirring. After all mesyl chloride had been added (~10 min), TLC indicated complete conversion of **15**. The reaction mixture was filtered and the filter cake was washed with cold CH_2Cl_2 (2 x 10 ml). The filtrate was washed with 1 M K_2CO_3 (15 ml), followed by water (15 ml). Subsequent drying and concentration *in vacuo* afforded **16** (1.95 g, 9.5 mmol; 95 %) as a slightly turbid, colourless oil. $C_7H_{10}O_5S$ requires C 40.77, H 4.89, S 15.55, found C, 40.7 H, 4.95, S 15.6. ν_{max}/cm^{-1} (neat): 3028, 2942, 2362, 1739, 1435, 1350, 1220, 1171, 1029, 936, 803, 526; δ_H (300 MHz, $CDCl_3$): 4.86 (t, $J = 2$ Hz, 2 H), 4.71 (t, $J = 2$ Hz, 2 H), 3.10 (s, 3 H), 2.07 (s, 3 H). δ_C (100 MHz, $CDCl_3$): 170.1, 83.9, 78.7, 57.3, 51.7, 39.0, 20.6; m/z (FD) 206.1 (100) $C_7H_{10}O_5S$ requires 206.0249.

4-Acetoxy-but-2-yne-1-yl fluoride (17): Caesium fluoride (1.51 g, 10 mmol) was suspended in 2-propanol (15 ml) and heated to reflux. After the inorganic material had dissolved, 4-acetoxy-but-2-yne-1-yl mesylate (1.35 g, 6.6 mmol) was added drop wise with stirring. The reaction mixture was refluxed for further 90 min. A waxy Caesium mesylate precipitate indicated reaction progress. After all mesylate had been consumed (TLC-monitoring) the reaction mixture was cooled to RT, filtered and the filter cake was washed with cold Et_2O and concentrated. The oily brown residue was chromatographed on silica gel (Et_2O -hexanes) to obtain **17** (730 mg, 85 %, 5.6 mmol) as a slightly yellow liquid: $C_6H_7FO_2$ requires C 55.4, H 5.4, found: C 55.3, H 5.4; ν_{max}/cm^{-1} (neat): 2943, 2850, 1742, 1434, 1376, 1360, 1216, 1150, 1025, 988, 969; δ_H (300 MHz, $CDCl_3$): 5.01 (t, $J = 1.8$ Hz, $J_{H-F} = 47.7$ Hz, 1 H), 4.85 (t, $J = 1.8$ Hz, $J_{H-F} = 47.7$ Hz, 1 H), 4.05 (t, $J = 1.8$ Hz, 2 H), 2.04 (s, 3 H); δ_C (100 MHz, $CDCl_3$): 170.1, 83.9, 81.3, 70.4 (d, $J_{C-F} = 161.5$ Hz), 52.1, 20.6; m/z (FD) 130.1 (100) $C_6H_7FO_2$ requires 130.0430.

4-Fluorobut-2-yne-1-ol (18): 4-acetoxy-but-2-yne-1-yl fluoride (1.3 g, 10 mmol) was dissolved in methanol (10 ml) containing KOH (560 mg, 10 mmol) and stirred at RT for 30 min after which all acetate **17** had been consumed. The reaction mixture was concentrated in vacuo to leave a waxy, solid residue that was taken up in Et₂O (20 ml). The solids were filtered off and the ethereal solution was washed with water (10 ml), followed by brine (5 ml). The organic layer was dried and concentrated to afford **18** in 88 % yield: C₄H₅FO requires C 54.5, H 5.7, found C 54.1, H 5.8; $\nu_{\max}/\text{cm}^{-1}$ (neat): 3358, 2872, 2855, 1454, 1295, 1138, 1025, 982, 907, 731; δ_{H} (300 MHz, CDCl₃): 5.00 (t, $J = 1.8$ Hz, $J_{\text{H-F}} = 47.4$ Hz, 1 H), 4.84 (t, $J = 1.8$ Hz, $J_{\text{H-F}} = 47.4$ Hz, 1 H), 4.05 (t, $J = 1.8$ Hz, 2 H), 2.04 (s, 3 H); δ_{C} (100 MHz, CDCl₃): 89.0 (d, $J_{\text{C-F}} = 22$ Hz), 85.1 (d, $J_{\text{C-F}} = 22$ Hz), 70.6 (d, $J_{\text{C-F}} = 163.9$ Hz), 50.4; m/z (FD) 88.1 (100) C₄H₅FO requires 88.0324.

4-Fluorobut-2-yne-1-yl chloride (6a): 4-fluorobut-2-yne-1-ol (1.0 g, 11 mmol) was dissolved in dry C₂H₄Cl₂ (10 ml) containing triphenylphosphine (1.00 equiv.). The mixture was cooled to 0 °C with stirring over 30 min. Then C₂Cl₆ (2.6 g, 11 mmol) was added in portions. The mixture was stirred for one additional hour. Hexane was added until the mixture turned slightly turbid. The mixture was passed through a short silica column to remove the triphenylphosphine oxide and the solvent was evaporated. The volatile residue was purified via bulb to bulb distillation to obtain **6a** as colourless, mobile oil. C₄H₄ClF requires C 45.10, H 3.78, found: C 45.3, H 3.7; $\nu_{\max}/\text{cm}^{-1}$ (neat): 2955, 1454, 1430, 1373, 1264, 1155, 987, 787, 699, 524; δ_{H} (300 MHz, CDCl₃): 4.99 (dt, $J = 1.8$ Hz, $J_{\text{H-F}} = 47.4$ Hz, 2 H), 4.19 (dt, $J = 1.8$ Hz, $J = 7.0$ Hz, 1 H), 4.17 (dt, $J = 1.8$ Hz, $J = 7.0$ Hz, 1 H); δ_{C} (100 MHz, CDCl₃): 84.6, 79.8, 70.4 (d, $J_{\text{C-F}} = 166.2$ Hz), 29.8; m/z (FD) 106.0 (100) C₄H₄ClF requires 106.0.

Methyl 8-(4-fluorobutyl)-3-p-tolyl-8-aza-bicyclo[3.2.1]octane-2-carboxylate (7a, PRD01): **7e** (100 mg, 0.3 mmol), was dissolved in EtOH (5 ml) and Pd⁰ (5 %) on activated carbon was added (10 mg). H₂ was passed through this solution until all olefin had been consumed (monitored by TLC). The reaction mixture was filtered through a pad of celite[®], the filter cake was washed with EtOH (5 ml) followed by CH₂Cl₂ (10 ml). The organic phases were combined and concentrated *in vacuo*. The residue was purified via chromatography on silica gel (Et₂O-hexanes, 1:4, 10 % NEt₃) to obtain **7a** as colourless crystals (90 mg, 89 %): m. p. 66 - 77 °C; $[\alpha]_{\text{D}}^{23} -39.2$ (c 1.25 in MeOH). C₂₀H₂₈FNO₂ requires C 72.04, H 8.46, N 4.20, found: C 72.16, H 8.47, N, 4.22; δ_{H} (300 MHz, CDCl₃): 7.13 (d, $J = 8.5$ Hz, 2 H, ArH), 7.05 (d, $J = 8.5$ Hz, 2 H, ArH), 4.42 (dt, $J = 6$ Hz, $J_{\text{HF}} = 47.4$ Hz, 2 H), 3.65 (brs, 1H), 3.45 (s, 3 H, OCH₃), 3.36 (brs, 1 H), 2.97 (dt, $J = 4.8$ Hz, $J = 13.2$ Hz, 1 H), 2.88 (t, $J = 4$ Hz, 1 H), 2.54 ($J = 2.9$ Hz, $J = 12.5$ Hz, 1 H), 2.32 - 2.20 (m, 2H), 2.27 (s, 3H, ArCH₃), 2.10 - 1.90 (m, 2 H), 1.82 - 1.53 (m, 5 H), 1.52 - 1.38 (m 2 H); δ_{C} (100 MHz, CDCl₃): 172.2, 138.1, 127.9, 127.3, 125.7, 84.0 (d, $J_{\text{C-F}} = 161.4$ Hz), 62.8, 61.4, 56.8, 52.9, 50.9, 34.3, 33.9, 28.2, 27.9, 26.0, 25.9, 24.7, 24.6, 21.0; m/z (FD) 334.2 (100) C₂₀H₂₉FNO₂ requires 334.2; HRMS(ESI): exact mass calcd for C₂₀H₂₉FNO₂: 334.2182, found: 334.2180.

Methyl 8-(4-fluorobut-2-en-1-yl)-3-p-tolyl-8-aza-bicyclo[3.2.1]octane-2-carboxylate (7q, LBT999): **7e** (100 mg) was dissolved in dry THF (5 ml) and cooled to 0 °C. RedAl[®] (0.2 mL, 0.36 mmol; 70% in toluene) was added dropwise under nitrogen. The reaction mixture was stirred at RT for 1h. The reaction was terminated by the drop wise addition of saturated ammonium chloride solution. The mixture was further stirred and allowed to warm to RT. The reaction mixture was filtered through a pad of celite[®] and the filter cake was washed with THF (5 ml) and acetone (2 x 5 ml). The filtrate was dried (MgSO₄) and concentrated in

vacuo. The residue was purified via column chromatography (Et₂O-hexanes, 1:4, 10 % NEt₃) to obtain **7q** as colourless crystals (86 mg, 85%): m. p. 113.5 °C; $[\alpha]_D^{23}$ -16.9 (c 1.42 in MeOH). C₂₀H₂₆FNO₂ requires C 72.48, H 7.91, N 4.23, found: C 72.20, H 8.09, N 4.41; δ_H (300 MHz, CDCl₃): 7.14 (d, $J = 8$ Hz, 2 H, ArH), 7.06 (d, $J = 8$ Hz, 2 H, ArH), 5.82 - 5.74 (m, 2 H), 4.89 (d, $J = 5$ Hz, $J_{H-F} = 47.4$ Hz, 1 H), 4.73 (d, $J = 3$ Hz, $J_{H-F} = 47.4$ Hz, 1 H), 3.69 (brs, 1H), 3.48 (s, 1H, OCH₃), 3.40 (brs, 1 H), 3.06 - 2.92 (m, 2 H), 2.91 - 2.81 (m, 2 H), 2.59 (dt, $J = 12.5$ Hz, $J = 2.7$ Hz, 1 H), 2.28 (s, 3 H), 2.13 - 1.92 (m, 2 H), 1.78 - 1.57 (m, 3 H); δ_C (100 MHz, CDCl₃): 172.0, 139.9, 135.2, 134.4 (d, $J_{C-F} = 12$ Hz), 128.6, 127.2, 126.2 (d, $J_{C-F} = 17$ Hz), 83.1 (d, $J_{C-F} = 161$ Hz), 62.3, 61.3, 54.9, 52.7, 50.9, 34.1, 33.8, 26.1, 25.9, 21.0; m/z (FD) 332.2 (100) C₂₀H₂₇FNO₂ requires 332.2; HRMS(ESI): exact mass calcd for C₂₀H₂₇FNO₂: 332.2026, found: 332.2024.

Methyl 8-(4-fluorobut-2-yn-1-yl)-3-p-tolyl-8-aza-bicyclo[3.2.1] octane-2-carboxylate (7e, PRD04): Synthesised according to procedure A, 97 % yield. Yellowish crystals, m. p. 73.5 °C; $[\alpha]_D^{23}$ -14.7 (c 1.46 in MeOH). C₂₀H₂₄FNO₂ requires C 72.92, H 7.34, N 4.25, found: C 72.79, H 7.03, N 4.53. δ_H (300 MHz, CDCl₃): 7.14 (d, $J = 8.5$ Hz, 2 H, ArH), 7.06 (d, $J = 8.5$ Hz, 2 H, ArH), 5.02 (t, $J = 1.5$ Hz, $J_{H-F} = 47.8$ Hz, 1 H), 4.86 (t, $J = 1.5$ Hz, $J_{H-F} = 47.8$ Hz, 1 H), 3.89 (brs, 1 H), 3.51 (s, 3 H, OCH₃), 3.47 (brs, 1 H), 3.25 (ddt, $J = 1.5$ Hz, $J = 7.5$ Hz, $J = 16.5$ Hz, 1 H), 3.10 (ddt, $J = 1.5$ Hz, $J = 7.5$ Hz, $J = 16.5$ Hz, 1 H), 2.98 (dt, $J = 5$ Hz, $J = 12.9$ Hz, 1 H), 2.94 - 2.89 (m, 1 H), 2.62 (dt, $J = 2.9$ Hz, $J = 12.5$ Hz, 1 H), 2.27 (s, 3 H, ArCH₃), 2.16 - 1.92 (m, 2 H), 1.82 - 1.61 (m, 3 H); δ_C (100 MHz, CDCl₃): 171.7, 139.6, 135.3, 128.7, 127.2, 127.1, 87.7, 87.5, 70.8 (d, $J_{C-F} = 163.5$ Hz), 62.6, 61.2, 52.8, 52.6, 51.1, 42.9, 34.1, 33.7, 25.9, 25.7, 21.0; m/z (FD) 330.2 (100) C₂₀H₂₅FNO₂ requires 330.2; HRMS(ESI): exact mass calcd for C₂₀H₂₅FNO₂: 330.1869, found: 330.1885.

Methyl 8-(((1S,2S)-2-(fluoromethyl)cyclopropyl)methyl)-3-p-tolyl-8-aza-bicyclo[3.2.1] octane-2-carboxylate (7i, PRD05): Synthesised according to procedure A, 87 % yield. Colourless crystals, m. p. 79 °C; $[\alpha]_D^{23}$ -26.0 (c 1.38 in MeOH). C₂₁H₂₈FNO₂ requires C 73.01, H 8.17, N 4.05, found C 72.9, H 8.2, N 4.0. δ_H (300 MHz, CDCl₃): 7.14 (d, $J = 8$ Hz, 2 H, ArH), 7.06 (d, $J = 8$ Hz, 2 H, ArH), 4.23 (dm, $J_{H-F} = 48.5$ Hz, 2 H), 3.81 (brs, 1H), 3.48 (s, 1H, OCH₃), 3.45 (brs, 1 H), 2.98 (dt, $J = 12.5$ Hz, $J = 5$ Hz, 1 H), 2.89 (t, $J = 4$ Hz, 1 H), 2.57 (td, $J = 12.5$ Hz, $J = 2.6$ Hz, 1 H), 2.42 (dd, $J = 12.5$ Hz, $J = 5$ Hz, 1 H), 2.28 Hz (s, 3 H), 2.07 (dd, $J = 12.5$ Hz, $J = 7$ Hz, 1 H), 1.98 (m, 2 H), 1.76 - 1.54 (m, 3 H), 1.01 (m, 1 H), 0.82 (m, 1 H), 0.52 (m, 2 H); δ_C (100 MHz, CDCl₃): 172.2, 140.1, 135.1, 128.6, 127.2, 87.4 (d, $J_{C-F} = 161.5$ Hz), 62.9, 61.3, 56.5, 52.9, 50.9, 34.1, 33.8, 26.0, 25.9, 21.0, 16.6, 16.5, 16.2, 15.9, 9.5, 9.4; m/z (FD) 346.2 (100) C₂₁H₂₉FNO₂ requires 346.2; HRMS(ESI): exact mass calcd for C₂₁H₂₉FNO₂: 346.2182, found: 346.2181.

Methyl 8-(((1R,2R)-2-(fluoromethyl)cyclopropyl)methyl)-3-p-tolyl-8-aza-bicyclo[3.2.1] octane-2-carboxylate (7m, PRD06): Synthesised according to procedure A, 86 % yield. Colourless crystals: m. p. 77 °C; $[\alpha]_D^{23}$ -27.7 (c 1.21 in MeOH). C₂₁H₂₈FNO₂ requires C 73.01, H 8.17, N 4.05, found C 73.4, H 8.1, N 3.95. δ_H (300 MHz, CDCl₃): 7.14 (d, $J = 8$ Hz, 2 H, ArH), 7.06 (d, $J = 8$ Hz, 2 H, ArH), 4.33 (m, $J_{H-F} = 48.9$ Hz, 1 H), 4.17 (m, $J_{H-F} = 48.9$ Hz, 1 H), 3.91 (brs, 1H), 3.48 (s, 1H, OCH₃), 3.40 (brs, 1 H), 2.98 (dt, $J = 12.9$ Hz, $J = 4.4$ Hz, 1 H), 2.91 (t, $J = 4.4$ Hz, 1 H), 2.58 (td, $J = 12.5$ Hz, $J = 2.9$ Hz, 1 H), 2.47 (dd, $J = 12.5$ Hz, $J = 3.7$ Hz, 1 H), 2.28 Hz (s, 3 H), 2.1 (m, 3H), 1.83 - 1.53 (m, 3 H), 1.03 (m, 1 H), 0.81 (m, 1 H), 0.45 (m, 2 H); δ_C (100 MHz, CDCl₃): 172.1, 140.0, 135.1, 128.6, 127.2, 87.3 (d, J_{C-F}

= 161.5 Hz), 62.0, 61.8, 56.4, 52.7, 50.9, 34.0, 33.9, 26.0, 25.8, 21.0, 18.5, 18.2, 16.6, 16.5, 7.3, 7.2; m/z (FD) 346.2 C₂₁H₂₉FNO₂ 346.2; HRMS(ESI): exact mass calcd for C₂₁H₂₉FNO₂: 346.2182, found: 346.2188.

Methyl 8-(4-fluorobutyl)-3-(4-chlorophenyl)-8-aza-bicyclo [3.2.1]octane-2-carboxylate (7b, PRD07): For preparative details see **7a**, 75% yield. Colourless crystals: m. p. 70 °C; [α]_D²³ -44.1 (c 0.33 in MeOH). C₁₉H₂₅ClFNO₂ requires C 64.49, H 7.12, N 3.96, found C 64.6, H 6.9, N 3.9. δ_{H} (300 MHz, CDCl₃): 7.22 (d, *J* = 8.8 Hz, 2 H, ArH), 7.15 (d, *J* = 8.8, 2 H, ArH), 4.50 (t, *J* = 6.2 Hz, *J*_{H-F} = 47.4 Hz, 1 H) 4.34 (t *J* = 6.2 Hz, *J*_{H-F} = 47.4 Hz, 1 H), 3.66 (brs, 1 H), 3.46 (s, 3H, CH₃), 3.37 (brs, 1 H), 2.95 (dt, *J* = 4.8 Hz, *J* = 12.9 Hz, 1 H), 2.86 (m, 1 H), 2.52 (dt, *J* = 2.9 Hz, *J* = 12.5 Hz, 1 H), 2.26 (m, 2 H), 2.02 (m, 2 H), 1.65 (m, 5 H), 1.46 (m, 2 H); δ_{C} (100 MHz, CDCl₃): 171.8, 141.8, 131.4, 128.7, 128.0, 84.2 (d, *J*_{C-F} = 161.5 Hz), 62.9, 61.3, 52.9, 50.9, 38.7, 34.0, 33.8, 28.2, 27.9, 26.0, 25.9, 24.7, 24.6; m/z (FD) 353.2 C₂₁H₂₉FNO₂ requires 353.2; HRMS(ESI): exact mass calcd for C₁₉H₂₅ClFNO₂: 353.1558, found: 353.1560.

Methyl 8-(4-fluorobut-2-yn-1-yl)-3-(4-chlorophenyl)-8-aza-bicyclo[3.2.1]octane-2-carboxylate (7f, PRD08): Synthesised according to procedure A, 95 % yield. Yellowish crystals. m. p. 76 °C; [α]_D²³ -13.2 (c 1.58 in MeOH). C₁₉H₂₁ClFNO₂ requires C 65.23, H 6.05, N 4.00, found C 65.5, H 6.15, N 3.8; δ_{H} (300 MHz, CDCl₃): 7.23 (d, *J* = 8.5 Hz, 2 H, ArH), 7.16 (d, *J* = 8.5, 2 H, ArH), 5.01 (t, *J* = 2.2 Hz, *J*_{H-F} = 47.4 Hz, 1 H) 4.85 (t *J* = 2.2 Hz, *J*_{H-F} = 47.4 Hz, 1 H), 3.90 (brs, 1 H), 3.51 (s, 3H, OCH₃), 3.47 (brs, 1 H), 3.25 (ddt, *J* = 1.5 Hz, *J* = 7.5 Hz, *J* = 16.5 Hz, 1 H), 3.10 (ddt, *J* = 1.5 Hz, *J* = 7.5 Hz, *J* = 16.5 Hz, 1 H) 2.97 (dt, *J* = 5.1 Hz, *J* = 12.5 Hz, 1 H), 2.90 (m, 1 H), 2.59 (dt, *J* = 2.9 Hz, *J* = 12.5 Hz, 1 H), 2.05 (m, 2 H), 1.70 (m, 4 H); δ_{C} (100 MHz, CDCl₃): 171.5, 141.3, 131.6, 128.7, 128.0, 87.4, 70.8 (d, *J*_{C-F} = 163.5 Hz), 62.5, 61.0, 52.5, 51.2, 42.9, 42.8, 34.0, 33.7, 25.8, 25.6; m/z (FD) 350.1 (100) C₁₉H₂₂ClFNO₂ 350.1; HRMS(ESI): exact mass calcd for C₁₉H₂₂ClFNO₂: 350.1323, found: 350.1331.

Methyl 8-(((1S,2S)-2-(fluoromethyl)cyclopropyl)methyl)-3-(4-chlorophenyl)-8-aza-bicyclo[3.2.1]octane-2-carboxylate (7j, PRD09): Synthesised according to procedure A, 85 % yield. Yellowish crystals: m. p. 76-77 °C; [α]_D²³ -90.6 (hydrochloride) (c 0.96 in MeOH). δ_{H} (300 MHz, CDCl₃): 7.21 (d, *J* = 8.8 Hz, 2 H, ArH), 7.16 (d, *J* = 8.5, 2 H, ArH), 4.30 (dq, *J* = 7.3 Hz, *J* = 9.56 Hz, *J*_{H-F} = 48.5 Hz, 1 H), 4.14 (dq, *J* = 7.3 Hz, *J* = 9.56 Hz, *J*_{H-F} = 48.5 Hz, 1 H), 3.81 (brs, 1 H), 3.48 (s, 3 H, CH₃) 3.45 (brs, 1H), 2.95 (dt, *J* = 5 Hz, *J* = 12.5 Hz, 1 H), 2.86 (dt, *J* = 4.4 Hz, 1 H), 2.53 (dt, *J* = 2.9 Hz, *J* = 12.5 Hz, 1 H), 2.40 (dd, *J* = 6 Hz, *J* = 12.5 Hz, 1 H), 2.07 (dd, *J* = 6 Hz, *J* = 12.5 Hz, 1 H), 2.05 – 1.85 (m, 2 H), 1.75 – 1.55 (m, 3 H), 0.99 (m, 1 H), 0.80 (m, 1 H), 0.50 (m, 2 H); δ_{C} (100 MHz, CDCl₃): 171.9, 141.7, 131.4, 129.8, 128.7, 128.0, 87.4 (d, *J*_{C-F} = 161.5 Hz), 62.9, 61.1, 56.6, 52.8, 51.0, 34.0, 33.8, 26.0, 25.9, 16.6, 16.5, 16.3, 16.0, 9.3, 9.2; m/z (FD) 366.2 (100) C₂₀H₂₆ClFNO₂ 366.2; HRMS(ESI): exact mass calcd for C₂₀H₂₆ClFNO₂: 366.1636, found 366.1631.

Methyl 8-(((1R,2R)-2-(fluoromethyl)cyclopropyl)methyl)-3-(4-chlorophenyl)-8-aza-bicyclo[3.2.1]octane-2-carboxylate (7n, PRD10): Synthesised according to procedure A, 88 % yield. Off white crystals: m. p. 75 °C; [α]_D²³ -25.5 (c 0.42 in MeOH). C₂₀H₂₅ClFNO₂ requires C 65.66, H 6.89, N 3.83, found C 65.95, H 7.16, N 3.81. δ_{H} (300 MHz, CDCl₃): 7.21 (d, *J* = 8.5 Hz, 2 H, ArH), 7.16 (d, *J* = 8.5, 2 H, ArH), 4.32 (d, *J* = 7.4 Hz, *J*_{H-F} = 48.5 Hz, 1

H), 4.17 (dq, $J = 7.4$ Hz, $J_{\text{H-F}} = 48.5$ Hz, 1 H), 3.91 (brs, 1 H), 3.47 (s, 3 H, CH₃) 3.40 (brs, 1H), 2.96 (dt, $J = 5$ Hz, $J = 12.5$ Hz, 1 H), 2.88 (t, $J = 4.4$ Hz, 1 H), 2.55 (dt, $J = 12.5$ Hz, $J = 2.9$ Hz, 1 H), 2.38 (dd, $J = 12.5$ Hz, $J = 5$ Hz, 1 H), 2.11 – 1.87 (m, 3 H), 1.79 – 1.52 (m, 3 H), 1.01 (m, 1 H), 0.80 (m, 1 H), 0.44 (m, 2 H); δ_{C} (100 MHz, CDCl₃): 171.9, 141.8, 131.5, 128.7, 128.0, 87.2 (d, $J_{\text{C-F}} = 160.5$ Hz), 62.0, 61.6, 56.4, 52.7, 51.0, 34.0, 33.8, 26.0, 25.8, 18.5, 18.2, 16.6, 16.5, 7.4, 7.3; m/z (FD) 366.2 (100) C₂₀H₂₆ClFNO₂ 366.2; HRMS(ESI): exact mass calcd for C₂₀H₂₆ClFNO₂: 366.1636, found: 366.1620.

Methyl 8-(4-fluorobutyl)-3-(4-fluorophenyl)-8-aza-bicyclo [3.2.1]octane-2-carboxylate (7c, PRD11): For experimental details see **7a**, 92 % yield. **7c** was obtained as colourless oil that solidified upon standing: m. p. 65 °C; $[\alpha]_{\text{D}}^{23}$ -90.6 (hydrochloride) (**c** 1.75 in MeOH). C₁₉H₂₅F₂NO₂ requires C 67.64, H 7.47, N 4.15, found C 67.5, H 7.6, N 4.05. δ_{H} (300 MHz, CDCl₃): 7.20 (dd, $J = 5.5$ Hz, $J = 2.9$ Hz, 2 H, ArH), 6.93 (t, $J = 8.8$ Hz, 2 H, ArH), 4.49 (t, $J = 5.9$ Hz, $J_{\text{H-F}} = 47.4$ Hz, 1 H) 4.33 (t, $J = 5.9$ Hz, $J_{\text{H-F}} = 47.4$ Hz, 1 H), 3.67 (brs, 1 H), 3.46 (s, 3H, CH₃), 3.36 (brs, 1 H), 2.96 (dt, $J = 5.1$ Hz, $J = 12.5$ Hz, 1 H), 2.85 (t, $J = 3.7$ Hz, 1 H), 2.53 (dt, $J = 2.9$ Hz, $J = 12.5$ Hz, 1 H), 2.26 (m, 2 H), 2.02 (m, 2 H), 1.67 (m, 6 H), 1.47 (m, 2 H); δ_{C} (100 MHz, CDCl₃): 171.9, 161.2 (d, $J_{\text{C-F}} = 243$ Hz), 138.8, 128.8, 128.7, 114.7, 114.4, 84.2 (d, $J_{\text{C-F}} = 162$ Hz), 62.9, 61.4, 52.946, 50.893, 34.2, 33.7, 28.2, 27.9, 26.0, 25.9, 24.7, 24.6; m/z (FD) 338.3 (100) C₁₉H₂₆F₂NO₂ requires 338.2; HRMS(ESI): exact mass calcd for C₁₉H₂₆F₂NO₂: 338.1933 found: 338.1932.

Methyl 8-(4-fluorobut-2-yn-1-yl)-3-(4-fluorophenyl)-8-aza-bicyclo[3.2.1]octane-2-carboxylate (7g, PRD12): Synthesised according to procedure A, 96 % yield. Colourless crystals: m. p. 72 °C; $[\alpha]_{\text{D}}^{23}$ -60.2 (**c** 1.17 in MeOH). C₁₉H₂₁F₂NO₂ requires C 68.45, H 6.35, N 4.20, found: C 68.7, H 6.6, N 4.40; δ_{H} (300 MHz, CDCl₃): 7.20 (dd, $J = 8.1$ Hz, $J = 5.5$ Hz, 2 H, ArH), 6.93 (dd, $J = 8.8$ Hz, 2 H, ArH), 5.02 (t, $J = 2.0$ Hz, $J_{\text{H-F}} = 49.6$ Hz, 1 H) 4.85 (t, $J = 2.0$ Hz, $J_{\text{H-F}} = 49.6$ Hz, 1 H), 3.89 (brs, 1 H), 3.51 (s, 3H, CH₃), 3.48 (brs, 1 H), 3.26 (ddt, $J = 1.5$ Hz, $J = 7.4$ Hz, $J = 16.5$ Hz, 1 H), 3.11 (ddt, $J = 1.5$ Hz, $J = 7.4$ Hz, $J = 16.5$ Hz, 1 H), 2.98 (dt, $J = 5.1$ Hz, $J = 12.5$ Hz, 1 H), 2.82 (m, 1 H), 2.61 (dt, $J = 2.9$ Hz, $J = 12.5$ Hz, 1 H), 2.05 (m, 2 H), 1.70 (m, 4 H); δ_{C} (100 MHz, CDCl₃): 171.5, 161.4 (d, $J_{\text{C-F}} = 253$ Hz), 138.3, 128.9, 128.8, 114.8, 114.5, 87.5, 70.7 (d, $J_{\text{C-F}} = 163.5$ Hz), 62.5, 61.1, 52.7, 51.1, 42.9, 34.2, 33.6, 25.8, 25.7; m/z (FD) 334.2 (100) C₁₉H₂₂F₂NO₂ requires 334.2; HRMS(ESI): exact mass calcd for C₁₉H₂₂F₂NO₂: 334.1619 found: 334.1627.

Methyl 8-(((1R,2R)-2-(fluoromethyl)cyclopropyl)methyl)-3-(4-fluorophenyl)-8-aza-bicyclo[3.2.1]octane-2-carboxylate (7k, PRD13): Synthesised according to procedure A, 89 % yield. Colourless to off white crystals: m. p. 74 °C; $[\alpha]_{\text{D}}^{23}$ -22.5 (**c** 0.58 in MeOH). C₂₀H₂₅F₂NO₂ requires C 68.75, H 7.21, N 4.01, found: C 68.9, H 7.1, N 3.9. δ_{H} (300 MHz, CDCl₃): 7.19 (dd, $J = 8.5$ Hz, $J = 5.5$ Hz, 2H, ArH), 6.93 (t, $J = 8.8$ Hz, 2 H), 4.30 (dq, $J = 4.4$ Hz, $J = 7.4$ Hz, $J = 9.6$ Hz, $J_{\text{H-F}} = 48.9$ Hz, 1 H), 4.14 (dq, $J = 4.4$ Hz, $J = 7.5$ Hz, $J = 9.5$ Hz, $J_{\text{H-F}} = 48.9$ Hz, 1 H), 3.79 (brs, 1 H), 3.49 (s, 3 H, CH₃) 3.43 (brs, 1H), 2.97 (dt, $J = 5$ Hz, $J = 12.5$ Hz, 1 H), 2.86 (dt, $J = 4.4$ Hz, 1 H), 2.53 (dt, $J = 2.9$ Hz, $J = 12.5$ Hz, 1 H), 2.41 (dd, $J = 12.8$ Hz, $J = 5.5$ Hz, 1 H), 2.17 (dd, $J = 12.1$ Hz, $J = 6.6$ Hz, 1 H) 2.03 – 1.85 (m, 2 H), 1.76 – 1.53 (m, 3 H), 1.00 (m, 1 H), 0.82 (m, 1 H), 0.50 (m, 2 H); δ_{C} (100 MHz, CDCl₃): 172.0, 161.0 (d, $J_{\text{C-F}} = 248$ Hz), 138.8, 128.8, 128.6, 114.7, 114.5, 87.5 (d, $J_{\text{C-F}} = 160.5$ Hz), 86.6, 62.9, 61.2, 56.5, 53.0, 51.0, 34.2, 33.8, 26.0, 25.9, 16.6, 16.5, 16.3, 16.0, 9.4, 9.3; m/z (FD) 350.0 (100) C₂₀H₂₆F₂NO₂ requires 350.2; HRMS(ESI): exact mass calcd for C₂₀H₂₆F₂NO₂: 350.1932 found: 350.1940.

Methyl 8-(((1S,2S)-2-(fluoromethyl)cyclopropyl)methyl)-3-(4-fluorophenyl)-8-aza-bicyclo[3.2.1]octane-2-carboxylate (7o, PRD14): Synthesised according to procedure A, 83 % yield. Colourless crystals: m. p. 72 °C; $[\alpha]_D^{23}$ -75.9 (hydrochloride) (c 1.13 in MeOH). $C_{20}H_{25}F_2NO_2$ requires C 68.75, H 7.21, N 4.01, found: C 68.69, H 7.0, N 4.3. δ_H (300 MHz, $CDCl_3$): 7.21 (dd, $J = 8.5$ Hz, $J = 5.5$ Hz, 2H, ArH), 6.93 (t, $J = 8.8$ Hz, 2 H), 4.30 (dq, $J = 7.5$ Hz, $J = 9.5$ Hz, $J_{H-F} = 48.5$ Hz, 1 H), 4.16 (dq, $J = 7.5$ Hz, $J = 9.5$ Hz, $J_{H-F} = 48.5$ Hz, 1 H), 3.79 (brs, 1 H), 3.49 (s, 3 H, CH_3) 3.43 (brs, 1H), 2.97 (dt, $J = 5$ Hz, $J = 12.5$ Hz, 1 H), 2.89 (dt, $J = 4.4$ Hz, $J = 1.1$ Hz, 1 H), 2.53 (dt, $J = 2.9$ Hz, $J = 12.5$ Hz, 1 H), 2.41 (dd, 1 H), 2.00 (m, 3 H), 1.63 (m, 4 H), 1.00 (m, 1 H), 0.80 (m, 1 H), 0.50 (m, 2 H); δ_C (100 MHz, $CDCl_3$): 172.1, 161.2 (d, $J_{C-F} = 248$ Hz), 138.6, 128.9, 128.4, 114.7, 114.5, 87.4 (d, $J_{C-F} = 160.0$ Hz), 62.5, 61.5, 56.4, 52.9, 51.0, 34.2, 33.9, 26.0, 25.9, 18.5, 18.2, 16.6, 16.5, 7.4, 7.3; m/z (FD) 350.2 (100) $C_{20}H_{26}F_2NO_2$ requires 350.2; HRMS(ESI): exact mass calcd for $C_{20}H_{26}F_2NO_2$: 350.1932, found: 350.1926.

Methyl 8-(4-fluorobutyl)-3-phenyl-8-aza-bicyclo[3.2.1]octane-2-carboxylate (7d, PRD15): For experimental details see 7a, 89 % yield. Colourless oil that solidified upon standing: m. p. 61-62 °C; $[\alpha]_D^{23}$ -96.5 (hydrochloride) (c 1.75 in MeOH). $C_{19}H_{26}FNO_2$ requires C 71.44, H 8.20, N 4.39, found: C 71.7, H 8.0, N, 4.5; δ_H (300 MHz, $CDCl_3$): 7.23 (m, 4 H, ArH), 7.14 (m, 1 H, ArH), 4.51 (t, $J = 5.9$ Hz, $J_{H-F} = 47.4$ Hz, 1 H) 4.34 (t, $J = 5.9$ Hz, $J_{H-F} = 47.4$ Hz, 1 H), 3.66 (brs, 1 H), 3.45 (s, 3H, CH_3), 3.37 (brs, 1 H), 3.01 (dt, $J = 5.2$ Hz, $J = 12.5$ Hz, 1 H), 2.92 (t, $J = 4.0$ Hz, 1 H), 2.57 (dt, $J = 2.6$ Hz, $J = 12.5$ Hz, 1 H), 2.27 (m, 2 H), 2.02 (m, 2 H), 1.69 (m, 6 H), 1.47 (m, 2 H); δ_C (100 MHz, $CDCl_3$): 172.0, 143.2, 127.9, 127.3, 125.8, 84.2 (d, $J_{C-F} = 161.4$ Hz), 62.9, 61.4, 52.9, 50.9, 34.2, 34.0, 28.2, 26.0, 25.1, 24.6; m/z (FD) 320.2 (100) $C_{19}H_{27}FNO_2$ requires 320.2; HRMS(ESI): exact mass calcd for $C_{19}H_{27}FNO_2$: 320.2026, found: 320.2021.

Methyl 8-(4-fluorobut-2-yn-1-yl)-3-phenyl-8-aza-bicyclo[3.2.1]octane-2-carboxylate (7h, PRD16): Synthesised according to procedure A, 96 % yield. Colourless crystals, m. p. 70 °C; $[\alpha]_D^{23}$ -95.7 (hydrochloride) (c 1.75 in MeOH). $C_{19}H_{22}FNO_2$ requires C 72.4, H 7.0, N 4.4, found C 72.8, H 6.9, N 4.2; δ_H (300 MHz, $CDCl_3$): 7.24 (m, 4 H, ArH), 7.14 (m, 1 H, ArH), 5.02 (t, $J = 2$ Hz, $J_{H-F} = 47.8$ Hz, 1 H) 4.86 (t, $J = 2$ Hz, $J_{H-F} = 47.8$ Hz, 1 H), 3.90 (brs, 1 H), 3.50 (s, 3H, CH_3), 3.40 (brs, 1 H), 3.25 (ddt, $J = 1.5$ Hz, $J = 7.5$ Hz, $J = 16.5$ Hz, 1 H), 3.12 (ddt, $J = 1.5$ Hz, $J = 7.5$ Hz, $J = 16.5$ Hz, 1 H), 3.02 (dt, $J = 5.2$ Hz, $J = 12.9$ Hz, 1 H), 2.94 (t, $J = 3.3$ Hz, 1 H), 2.69 (dt, $J = 2.6$ Hz, $J = 12.9$ Hz, 1 H), 2.05 (m, 2 H), 1.68 (m, 4 H); δ_C (100 MHz, $CDCl_3$): 171.6, 142.7, 127.9, 127.4, 127.3, 125.9, 87.5, 70.8 (d, $J_{C-F} = 163.5$ Hz), 62.6, 61.1, 52.6, 51.1, 42.9, 42.8, 34.1, 34.0, 25.9, 25.9, 25.7; MS(FD) 316.2 (100) $C_{19}H_{23}FNO_2$ requires 316.2; HRMS(ESI): exact mass calcd for $C_{19}H_{23}FNO_2$: 316.1713, found: 316.1722.

Methyl 8-(((1S,2S)-2-(fluoromethyl)cyclopropyl)methyl)-3-phenyl-8-aza-bicyclo[3.2.1]octane-2-carboxylate (7l, PRD17): Synthesised according to procedure A, 84 % yield. Colourless to yellowish crystals: m. p. 76 °C; $[\alpha]_D^{23}$ -27.0 (c 1.42 in MeOH). $C_{20}H_{26}FNO_2$ requires C 72.48, H 7.91, N 4.23, found: C 72.4, H 8.0, N 4.2; δ_H (300 MHz, $CDCl_3$): 7.25 (brs, 4H, ArH), 7.14 (m, 1H, ArH), 4.30 (dq, $J = 7$ Hz, $J = 9.6$ Hz, $J_{H-F} = 48.9$ Hz, 1 H), 4.13 (dq, $J = 7$ Hz, $J = 9.6$ Hz, $J_{H-F} = 48.9$ Hz, 1 H), 3.82 (brs, 1 H), 3.47 (s, 3 H, CH_3) 3.45 (brs, 1H), 3.00 (dt, $J = 5.2$ Hz, $J = 12.9$ Hz, 1 H), 2.91 (dt, $J = 4.4$ Hz, $J = 0.7$ Hz, 1 H), 2.59 (dt, $J = 2.9$ Hz, $J = 12.5$ Hz, 1 H), 2.52 (q, $J = 7$ Hz, 1 H), 2.0 (m, 3 H), 1.67 (m, 4 H), 1.02 (m, 1 H), 0.82 (m, 1 H), 0.52 (m, 2 H); δ_C (100 MHz, $CDCl_3$): 172.1, 143.2, 127.9, 127.3, 125.8,

87.4 (d, $J_{C-F} = 161.5$ Hz), 63.0, 61.2, 56.5, 52.9, 50.0, 34.2, 34.0, 26.0, 25.9, 16.6, 16.5, 16.3, 16.0, 9.4, 9.3; MS (FD) 332.2 (100) $C_{20}H_{27}FNO_2$ requires 323.2; HRMS(ESI): exact mass calcd for $C_{20}H_{27}FNO_2$: 332.2026, found: 332.2034.

Methyl 8-(((1R,2R)-2-(fluoromethyl)cyclopropyl)methyl)-3-phenyl-8-aza-bicyclo[3.2.1]octane-2-carboxylate (7p, PRD18): Synthesized according to procedure A, 84 % yield. Colourless crystals: m.p. 88 °C; $[\alpha]_D^{23} -30.0$ (c 1.17 in MeOH). $C_{20}H_{27}FNO_2$ requires C 72.48, H 7.91, N 4.23, found: C 72.2, H 8.1, N 4.4. δ_H (300 MHz, $CDCl_3$): 7.25 (brs, 4H, ArH), 7.14 (m, 1H, ArH), 4.33 (dq, $J = 7$ Hz, $J = 9.6$ Hz, $J_{H-F} = 48.9$ Hz, 1 H), 4.13 (dq, $J = 7$ Hz, $J = 9.6$ Hz, $J_{H-F} = 48.9$ Hz, 1 H), 3.92 (brs, 1 H), 3.46 (s, 3 H, OCH_3) 3.42 (brs, 1H), 3.01 (dt, $J = 5$ Hz, $J = 12.9$ Hz, 1 H), 2.93 (t, $J = 4.4$ Hz, 1 H), 2.6 (dt, $J = 2.9$ Hz, $J = 12.5$ Hz, 1 H), 2.47 (dd, $J = 12.5$ Hz, $J = 4.8$ Hz, 1 H), 2.11 – 1.87 (m, 2 H), 1.79 – 1.54 (m, 3 H), 1.03 (m, 1 H), 0.82 (m, 1 H), 0.45 (m, 2 H); δ_C (100 MHz, $CDCl_3$): 172.3, 143.1, 127.9, 127.4, 125.7, 87.3 (d, $J_{C-F} = 160.5$ Hz), 62.1, 61.8, 56.4, 52.8, 50.9, 34.3, 34.0, 26.0, 25.9, 18.5, 18.2, 16.6, 16.5, 7.4, 7.3; MS (FD) 332.2 (100) $C_{20}H_{27}FNO_2$ requires 323.2; HRMS(ESI): exact mass calcd for $C_{20}H_{27}FNO_2$: 332.2026, found: 332.2035.

Methyl 8-(4-fluorobut-2-en-1-yl)-3-phenyl-8-aza-bicyclo[3.2.1]octane-2-carboxylate (7r, PRD19): Synthesized from **7h** according to the procedure described for **7q**. Colourless crystals (90 mg, 91%): m. p. 107-109 °C; $[\alpha]_D^{23} -18.6$ (c 1.42 in MeOH). $C_{19}H_{24}FNO_2$ requires C 71.90, H 7.62, N 4.41, found C 72.15, H 8.0, N 4.25. δ_H (400 MHz, $CDCl_3$): 7.30-7.26 (m, 4H, ArH), 7.21-7.14 (m, 1H, ArH), 5.81 (brs, 2H), 4.85 (dd, $J = 2$ Hz, $J = 5$ Hz, $J_{H-F} = 48.5$ Hz, 2 H), 3.69 (brs, 1 H), 3.49 (s, 3 H, OCH_3) 3.45 (brs, 1H), 3.06 (dt, $J = 5$ Hz, $J = 12.5$ Hz, 1 H), 2.94 (t, $J = 4$ Hz, 1 H), 2.94-2.87 (m, 1 H), 2.65 (dt, $J = 3$ Hz, $J = 12.5$ Hz, 1 H), 2.17 – 1.97 (m, 2 H), 1.82 – 1.63 (m, 3 H); δ_C (100 MHz, $CDCl_3$): 171.9, 142.9, 134.3, 127.9, 127.4, 125.7, 83.2 (d, $J_{C-F} = 166.5$ Hz), 62.3, 61.4, 54.9, 52.7, 51.0, 34.2, 34.0, 26.0, 25.9; MS (FD) 318.2 (100) $C_{19}H_{25}FNO_2$ requires 318.2; HRMS(ESI): exact mass calcd for $C_{19}H_{25}FNO_2$: 318.1869, found: 318.1870.

Methyl 8-(2-fluoroethyl)-3-(4-chlorophenyl)-8-aza-bicyclo[3.2.1]octane-2-carboxylate (10, FECNT): Synthesized according to procedure A, 83 % yield. Colourless crystals: m.p. °C; $[\alpha]_D^{23} -43.5$ (c 1.25 in MeOH). $C_{17}H_{21}ClFNO_2$ requires C 62.67, H 6.50, N 4.30, found C 62.5, H 6.9, N 4.1. δ_H (400 MHz, $CDCl_3$): 7.24 (d, $J = 8.6$ Hz, 2H, ArH), 7.19 (d, $J = 8.6$ Hz, 2H, ArH), 4.57-4.33 (dm, $J_{H-F} = 47.5$ Hz, 2 H), 3.79 (brs, 1 H), 3.52 (s, 3 H, OCH_3) 3.44 (brs, 1H), 2.98 (dt, $J = 6$ Hz, $J = 12.5$ Hz, 1 H), 2.91 (t, $J = 4$ Hz, 1 H), 2.66-2.53 (m, 2 H), 2.65 (dt, $J = 3$ Hz, $J = 12.5$ Hz, 1 H), 2.2 – 2.08 (m, 1 H), 2.06-1.96 (m, 1H), 1.77 (dt, $J = 4$ Hz, $J = 12.5$ Hz, 1 H), 1.72 – 1.63 (m, 2 H); δ_C (100 MHz, $CDCl_3$): 171.8, 141.6, 131.5, 128.7, 128.0, 125.7, 83.9 (d, $J_{C-F} = 166.5$ Hz), 63.5, 62.3, 53.8, 53.6, 52.6, 51.1, 34.0, 33.6, 26.2, 25.7 ; MS (FD) 326.1 (100) $C_{17}H_{22}ClFNO_2$ requires 326.1; HRMS(ESI): exact mass calcd for $C_{17}H_{22}ClFNO_2$: 326.1323, found: 326.1328.

Formation of hydrochloride salts for cell assay: Compounds **7a-q** were purified by HPLC (Phenomenex Luna® RP-18 10 μ semi-preparative HPLC-column (250 x 40 mm) using 10-20 % 7 mM aqueous ammonia solution in MeCN. The product fractions were collected and the eluent was evaporated in vacuo. The residue was taken up in MilliQ®-water and the resultant solution was lyophilised over night. The lyophilised tropanes were re-dissolved in dry ether and 2 M ethereal HCl was added drop wise (2 equiv.). The mother liquor was removed and the hygroscopic hydrochlorides were dried in vacuo. 1 mg of the dried

hydrochloride was re-dissolved in 1 ml CH₃CN containing 20 % of 0.05 M ammonium acetate buffer and analysed by HPLC. The HPLC-purity of all compounds used for biological assays exceeded 99 % (by UV-area at 254 nm).

Generation of cell lines stably expressing the hSERT, hDAT and hNET: Selection of clonal lines stably expressing the human dopamine transporter, the human norepinephrine transporter and the human Serotonin transporter (HEKhDAT, HEKhNET and HEKhSERT), respectively, was performed as described previously.^[22]

Cell culture: HEKhSERT, HEKhNET and HEKhDAT cells were maintained in Dulbecco's modified Eagle's medium supplemented with 10% fetal bovine serum, penicillin (100 U/mL), streptomycin (100 lg/mL), and geneticin (G418, 200 lg/mL) at 37°C in 95% humidified air with 5% CO₂. Cells were split in a defined dilution to reach 80% confluency at the beginning of the experiment. [³H]5-HT, [³H]NE and [³H]DA transport measurement of monoamine uptake was performed as described previously and modified for IC₅₀-determination.^[8a,22b] Briefly, HEKhSERT, HEKhNET and HEKhDAT cells were plated into 24-well dishes (2 cm in diameter), which had previously been treated with poly-L-lysine (0.1 mg/mL) and allowed to grow to 80% confluency. Culture medium was replaced by TB1 buffer (200 IL: containing 120 mM NaCl, 2 mM KCl, 1 mM CaCl₂, 1 mM MgCl₂ and 10 mM HEPES, pH 7.5) containing 250 nM of [³H]5-HT, [³H]NE or [³H]DA with various concentrations (0.1 – 5000 nM) of each tracer ([³H]DA: K_M = 1.37 μM, [³H]5HT: K_M = 1.1 μM and [³H]NE: K_M = 0.61 μM). After 6 min at room temperature, the medium was removed quickly and cells were washed twice with ice-cold TB1 before lysing with 10% (w/v) sodium dodecyl sulfate. Radioactivity was determined by scintillation counting. Specific uptake is determined as the difference between HEKhSERT, HEKhNET and HEKhDAT-mediated and control HEK293 uptake in parallel culture dishes. All transport measurements were analysed by nonlinear regression analysis using the graphics program GraphPad Prism®.

Data analysis: All uptake data represent the means of quadruplicate determinations; each experiment was repeated at least three times. Data were analyzed by non-linear regression analysis program (GraphPad Prism®), which fitted sigmoidal uptake curves to the equations (1) and (2):

$$V = \frac{V_{\max}}{\left[1 + \left(\frac{K_M}{S}\right)^{n_H}\right]} \quad (1)$$

and

$$\frac{V}{V_{\max}} = \frac{IC_{50}^{n_H}}{(I^{n_H} + IC_{50}^{n_H})} \quad (2)$$

V represents transport rate; V_{max}, maximal transport rate; S, substrate concentration; I, inhibitor concentration; IC₅₀, inhibitor concentration for half maximal transport inhibition; K_M, the Michaelis-Menten constant; and n_H, the Hill-coefficient.

Acknowledgements

The authors are grateful to the Fonds der Chemischen Industrie. This study was financially supported by a DFG grant (Ro985/21). The authors wish to thank Dr. Alexander Hoepfing for helpful discussion and Prof. Dr. F. Roesch for scientific support.

Notes and references

Institute of Nuclear Chemistry, Johannes Gutenberg-University Mainz, Fritz Strassmann-Weg 2, 55128 Mainz, Germany, Fax: +4961313924692, Tel: +49 6131 3925302, E-mail: riss@uni-mainz.de.

- (1) a) N. D. Volkow, J. S. Fowler, G. J. Wang, R. Baler, F. Telang, *J. Neuropharm.* 2008, in press, doi: 10.1016/j.neuropharm.2008.05.022; b) P. H. Elsinga, K. Hatano, K. Ishiwata, *Curr. Med. Chem.* 2006, **13**, 2139-2153; c) G. Grunder, D. F. Wong, *Fortschr. Neurol. Psychiat.* 2003, **71**, 415-420; d) J. M. Swanson; *The Lancet* 2000, **355**, 1461-2, e) D. D. Dougherty, A. A. Bonab, T. J. Spencer, S. L. Rauch, B. K. Madras, A. J. Fischman. *The Lancet* 1999, **354**, 2132 - 2133. f) P. K. Morrish, *Movement Disorders* 2003, **18**, S63-S70.
- (2) a) V. Marshall, D. Grosset, *Mov. Disord.* 2003, **18**, 1415-23 ; b) K. A. Bergström, E. Tupala, J. Tiihonen, *Pharmacol. Toxicol.* 2001, **88**, 287 – 239; c) M. Laruelle, M. Slifstein, Y. Huang, *Methods* 2002, **27**, 287-299.
- (3) R. L. Clarke, S. J. Daum, A. J. Gambino, M. D. Aceto, J. Pearl, M. Levitt, W. R. Cuminsky, E. F. Bogado, *J. Med. Chem.* 1973, **16**, 1260 – 1267.
- (4) a) M.-C. Lasne, C. Perrio, J. Rouden, L. Barré, D. Roeda, F. Dollé, C. Crouzel, *Top. Curr. Chem.* 2002, **222**, 201; b) L. Cai, S. Lu, V. W. Pike, *Eur. J. Org. Chem.* 2008, 2853; c) H. J. Wester *Handbook of Nuclear Chemistry* 4, Kluwer Academic Publishers, Dordrecht, 2003, pp. 119-202.
- (5) L. Müller, C. Halldin, C. Lundquist, C.-G. Swahn, C. Foged, H. Hall, P. Karlsson, N. Ginovart, Y. Nakashima, T. Suhara, L. Farde, *J. Radioanal. Nucl. Chem.* 1996, **206**, 133-144.
- (6) a) I. Günther, H. Hall, C. Halldin, C.-G. Swahn, L. Farde, G. Sedvall, *Nucl. Med. Biol* 1997, **24**, 629-634. b) M. M. Goodman, C. D. Kilts, R. Keil, B. Shi, L. Martarello, D. Xing, J. Votaw, T. D. Ely, P. Lambert, M. J. Owens, V. M. Camp, E. Malveaux, J. M. Hoffman, *Nucl. Med. Biol* 2000, **27**, 1-12; c) S. S. Zoghbi, H. U. Shetty, M. Ichise, M. Fujita, M. Imaizumi, J.-S. Liow, J. Shah, J. L. Musachio, V. W. Pike, R. B. Innis, *J. Nucl. Med.* 2006, **47**, 3520-3527
- (7) M. Yaqub, R. Boellaard, B. N. M. van Berckel, M. M. Ponsen, M. Lubberink, A. D. Windhorst, H. W. Berendse, A. A. Lammertsma, *J. Cereb. Blood Flow Metab.* 2007, **27**, 1397–1406.
- (8) a) S. Singh, *Chem. Rev.* 2000, **100**, 925-1024; b) F. Dolle, P. Emond, S. Mavel, S. Demphel, F. Hinnen, Z. Mincheva, W. Saba, H. Valette, S. Chalon, C. Halldin, J. Helfenbein, J. Legailard, J.-C. Madelmont, J.-B. Deloye, M. Bottlaender, D. Guilloteau, *Bioorg. Med. Chem.* 2006, **14**, 1115-1125.
- (9) a) T. Okada, M. Fujita, S. Shimada, K. Sato, P. Schloss, Y. Watanabe, Y. Itoh, M. Tohyama, T. Nishimura; *Nucl. Med. Biol.* 1998, **25**, 53-58; b) P. Frankhauser, Y.

- Grimmer, P. Bugert, M. Deuschle, M. Schmidt, P. Schloss; *Neurosci. Lett.* 2006, **399**, 197-201.
- (10) a) U. Gether, P. H. Andersen, O. M. Larsson, A. Schousboe, *Trends Pharmacol. Sci.* 2006, **27**, 375-383; b) N. Chen, M. E. A. Reith, *Eur. J. Pharmacol.* 2000, 329-339.
- (11) R. M. Baldwin, Y. Zea-Ponce, M. S. Al-Tikriti, A. S. Zoghbi, J. P. Seibyl, D. S. Charney, P. B. Hoffer, S. Wang, R. A. Milius, J. L. Neumeyer, R. B. Innis, *Nucl. Med. Biol.* 1995, **22**, 211-219.
- (12) a) J. L. Neumeyer, S. Wang, Y. Gao, R. A. Milius, N. S. Kula, A. Campbell, R. S. Baldessarini, Y. Zea-Ponce, R. M. Baldwin, R. B. Innis, *J. Med. Chem.* 1994, **37**, 1558-1561; b) X.-H. Gu, R. Zong, N. S. Kula, R. J. Baldessarini, J. L. Neumeyer, *Bioorg. Med. Chem. Lett.* 2001, **11**, 3049-3053.
- (13) a) P. Emond, L. Garreau, S. Chalon, M. Boazi, M. Caillet, J. Bricard, Y. Frangin, L. Mauclaire, J.-C. Besnard, D. Guilloteau, *J. Med. Chem.* 1997, **40**, 1366-1372; b) S. Chalon, L. Garreau, P. Emond, L. Zimmer, M.-P. Vilar, J.-C. Besnard, D. Guilloteau, *J. Pharmacol. Exp. Ther.* 1999, **291**, 648-654; c) F. Dolle, M. Bottlaender, S. Demphel, P. Emond, C. Fuseau, C. Coulon, M. Ottaviani, H. Valette, C. Loc'h, C. Halldin, L. Mauclaire, D. Guilloteau, B. Maziere, C. Crouzel, *J. Label. Compd. Radiopharm.* 2000, **43**, 997-1004; d) S. Chalon, H. Hall, W. Saba, L. Garreau, F. Dolle, C. Halldin, P. Emond, M. Bottlaender, J.-B. Deloye, J. Helfenbein, J.-C. Madelmont, S. Bodard, Z. Mincheva, J.-C. Besnard, D. Guilloteau, *J. Pharmacol. Exp. Ther.* 2006, **317**, 147-152; e) W. Saba, H. Valette, M.-A. Schollhorn-Peyronneau, C. Coulon, M. Ottaviani, S. Chalon, F. Dolle, P. Emond, C. Halldin, J. Helfenbein, J.-C. Madelmont, J.-B. Deloye, D. Guilloteau, M. Bottlaender, *Synapse* 2006, **61**, 17-23.
- (14) a) M. M. Goodman, P. Chen, Fluoroalkenyl nortropanes. *PCT Int. Appl.* 2000, 37 pp. WO 2000064490 [*Chem. Abstr.* 2000,133, 331552]; b) P. Chen, C. Kilts, V. M. Camp, T. Ely, R. Keil, E. Malveaux, D. Votaw, J. M. Hoffman, M. M. Goodman, *J. Label. Compd. Radiopharm.* 1999, **42**, S400-S402; c) J. S. Stehouwer, P. Chen, R. J. Voll, L. Williams, J. R. Votaw, L. L. Howell, M. M. Goodman; *J. Label. Compd. Radiopharm.* 2007, **50**, S1, S335.
- (15) a) V. Stepanov, J. Järv, *Neurosci. Lett.* 2006, **410**, 218 - 221; b) V. Stepanov, J. Järv, *Neurochem. Int.* 2008, **53**, 370-373
- (16) a) M. P. Smith, K. M. Johnson, M. Zhang, J. L. Flippen-Anderson, A. P. Kozikowski, *J. Am. Chem. Soc.* 1998, **120**, 9072-9073; b) A. Hoepfing, K. M. Johnson, C. George, J. L. Flippen-Anderson, A. P. Kozikowski, *J. Med. Chem.* 2000, **43**, 2064-2071.
- (17) a) A. Yurek-George, A. R. L. Cecil, A. H. K. Mo, S. Wen, H. Rogers, F. Habens, S. Maeda, M. Yoshida, G. Packham, A. Ganesan, *J. Med. Chem.* 2007, **50**, 5720-5726; b) M. Watanabe, Y. Kazuta, M. Arisawa, A. Matsuda, S. Shuto, *Abstracts of Papers*, 234th ACS National Meeting, 2007; c) M. Watanabe, Y. Kazuta, H. Hayashi, S. Yamada, A. Matsuda, S. Shuto, *J. Med. Chem.* 2006, **49**, 5587-5596; d) A. Mann, H.-L. Le Chatelier, In: *Practice of Medicinal Chemistry*, (Ed. C. G. Wermuth) Elsevier, London, 2003, pp. 233-250; e) S. Ono, K. Ogawa, K. Yamashita, T. Yamamoto, Y. Kazuta, A. Matsuda, S. Shuto, *Chem. Pharm. Bull.* 2002, **50**, 966-968; f) A. Valasinas, A. Sarkar, V. K. Reddy, J. L. Marton, H. S. Basu, B. Frydman, *J. Med. Chem.* 2001, **44**, 390-403.

- (18) a) J. S. Stehouwer, N. Jarkas, F. Zeng, R. J. Voll, L. Williams, M. J. Owens, J. R. Votaw, M. M. Goodman, *J. Med. Chem.* 2006, **49**, 6760-6767; b) J. S. Stehouwer, C. Plisson, N. Jarkas, F. Zeng, R. J. Voll, L. Williams, L. Martarello, J. R. Votaw, G. Tamagnan, M. M. Goodman, *J. Med. Chem.* 2005, **48**, 7080-7083; c) F. I. Carrol, S. R. Runyon, P. Abraham, H. Navarro, M. J. Kuhar, G. T. Pollard, J. L. Howard, *J. Med. Chem.* 2004, **47**, 6401-6409.
- (19) a) P. C. Meltzer, A. Y. Liang, A. L. Brownell, D. R. Elmaleh, B. K. Madras, *J. Med. Chem.* 1993, **36**, 855; b) L. Xu, M. Trudell, *J. Heterocycl. Chem.* 1996, **33**, 2037-2039; c) R. A. Olofson, J. T. Martz, J.-P. Senet, M. Piteau. *J. Org. Chem.* 1984, **49**, 2081-2082.
- (20) a) H. Heaney, S. Christie, *Science of Synthesis* 3, Thieme: Stuttgart, 2003, p. 529; b) G. Posner, *Org. React.* 1972, **19**, 1-113.
- (21) P. J. Riss, F. Roesch, *Org. Biomol. Chem.* 2008, **6**, 4567-4574.
- (22) a) H. H. Sitte, S. Huck, H. Reither, S. Boehm, E. A. Singer, C. Pifl, *J. Neurochem.* 1998, **71**, 1289-1297; b) C. Sur, H. Betz, P. Schloss, *J. Neurochem.* 1998, **70**, 2545-2553.

4.3 *Ex vivo* and *in vivo* evaluation of [¹⁸F]PR04.MZ in rodents: A novel highly selective dopamine transporter ligand for PET

Ex vivo and in vivo evaluation of [¹⁸F]PR04.MZ in rodents: A novel highly selective dopamine transporter ligand for PET

**Riss, Patrick¹, Debus, Fabian², Hummerich, René³, Schmidt, Ulrich², Lueddens,
Hartmut², Schloss, Patrick³, Roesch, Frank¹**

¹*Institute of Nuclear Chemistry, Mainz University, Fritz Strassmann-Weg 2, 55128 Mainz; Germany*

²*Institute of Psychiatry, Psychiatry, Mainz-University Hospital, Mainz, Germany.*

³*Central Institute of Mental Health, Biochemical Laboratories, J5, Mannheim, Germany*

Abstract: N-4-fluorobut-2-yn-1-yl-2β-carbomethoxy-3β-phenyltropane (PR04.MZ) has been developed as a potential DAT-ligand for molecular imaging. It contains a terminally fluorinated, conformationally restricted nitrogen substituent which is well suited for introduction of fluorine-18. The present report is concerned with the pharmacological characterisation of PR04.MZ. The novel ligand shows an IC₅₀-value of 3 nM at the human dopamine transporter (hDAT), whereas the IC₅₀-value at the human serotonin transporter (hSERT) and the human noradrenaline transporter (hNET) is significantly lower (240 and 31 nM, respectively). Furthermore, its biodistribution, its binding profile in the rat brain and reversibility of binding are examined. A preliminary PET-study is also presented and finally the novel ligand is challenged by a selective DAT inhibitor in a PET-displacement study

Introduction: Dopamine (DA) is one of the most important neurotransmitters in the mammalian brain. It is crucial for the downstream transfer of electrical excitations of dopaminergic neurons. Briefly, DA is synthesised in two subsequent biotransformations from L-Tyrosine. After the latter is hydroxylated in position 3 by the neuronal enzyme tyrosine hydroxylase to form L-DOPA, the conversion into DA is catalysed by an aromatic aminoacid decarboxylase (AADC). Once synthesised, the DA is transported into vesicles, located at the presynaptic terminals of DA-neurons, by the vesicular dopamine transporter protein (VMAT). DA signal transduction is initiated by the depolarisation of the parent neuron, followed by Ca²⁺ influx into the cell. Thereby, the DA-containing vesicles are fused with the cellular membrane and the DA is released into the synaptic gap. Downstream transfer of the electrical signal is facilitated via diffusion of DA to postsynaptic G-protein coupled receptors such as the D₂-like receptor family. Internalisation of the DA-receptor complex followed by G-protein activation initiates the depolarisation of the downstream neuron. In parallel, the excreted dopamine can interact with two presynaptic membrane proteins, on the one hand D₁-like DA-receptors and on the other hand the DA-transporter (DAT). The DAT is a transmembrane protein which mediates the reuptake of excreted DA into the parent cell. Thereby the transmitter is recycled and basal DA-levels are restored. Furthermore, the neuronal excretion of DA is terminated. For this reason, the DAT is crucial for the regulation of DA neurotransmission. Similar transporters were found in various neurotransmitter systems, e.g. the GABA-transporter (GAT), the norepinephrine-transporter (NET) and the serotonin-transporter SERT. These transmembrane transporters belong to the family of neurotransmitter sodium symporters (NSS).² The mammalian DAT presents an amino acid homology of about 49 % with the SERT and about 67 % with the NET.² The dopaminergic system is relevant in a variety of pathologies e.g. in addiction,^{3,4} obesity,⁵

psychosis,⁶ major depression,⁷ Huntington's chorea,⁸ ADHD⁹ as well as Parkinson's disease,^{10,11} Alzheimer's disease and Tourette's syndrome.¹²

With respect to the non-invasive, quantitative exploration of the dopaminergic system, numerous compounds have been evaluated as potential radiotracers for molecular imaging using positron emission tomography (PET).¹³ Briefly, 6-[¹⁸F]fluoro-L-DOPA, a substrate for the AADC, is routinely employed for the visualisation of the DA-synthesis rate.¹⁴ Recent studies report on the experimental progress in visualising the VMAT.¹⁵

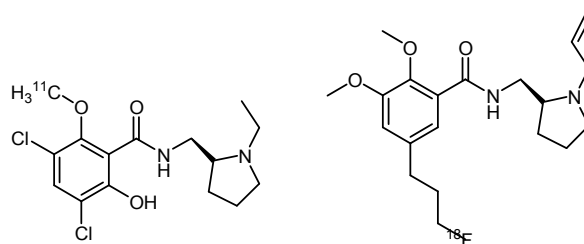


Figure 1: [¹¹C]raclopride and [¹⁸F]fallypride

Several butyrophenones and benzamides, e.g. [¹¹C]raclopride or [¹⁸F]fallypride are used for the examination of the availability of D₂-like receptors.¹⁶ It has been proposed that the DAT may serve as an indicator on the integrity of the DA-system in general, as its availability is sensitive to minor changes within the system.¹⁷ Unfortunately, studies of the DAT were often complicated by the absence of a suitable radiotracer. Considerable effort has already been spent on the development of DAT selective positron emitter labelled radioligands. The first attempts included [¹¹C]nomifensine, [¹⁸F]GBR13119 and [¹¹C]cocaine.^{3a,18a,b}

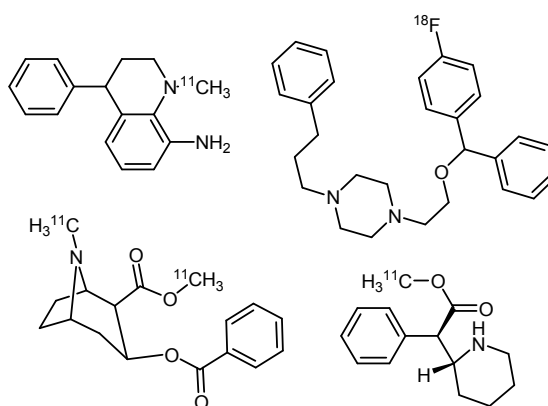


Figure 2: [¹¹C]nomifensine, [¹⁸F]GBR13119, [¹¹C]cocaine and d-*threo*-[¹¹C]methylphenidate

Later on, d-*threo*-[¹¹C]methylphenidate, known as the ADHD-therapeutic Ritalin[®] was examined.^{18c} However, these early candidates suffered from low striatum to cerebellum ratios (1.5 to 2.4) and in particular from low selectivity for the DAT. Cocaine analogue phenyltropanes, with the metabolically sensitive benzoyl ester moiety replaced by a carbon-bound phenyl ring, proved to be a more promising lead. Representative derivatives from this series include [¹⁸F]MCL-322,¹⁹ β-CFT,²⁰ β-CIT,²¹ FE-CNT,²² and FP-CIT.²³ These compounds almost generally provide higher affinity to the DAT, resulting in higher specific to non-

specific binding ratios. Although remarkable increases in striatum to cerebellum ratios were achieved, these candidates still suffer from low specificity, due to the inherent similarity of DAT, SERT and NET. Other drawbacks include the slow accumulation in the DAT rich brain regions, resulting in a slow binding equilibrium at the DAT (up to 120 min).

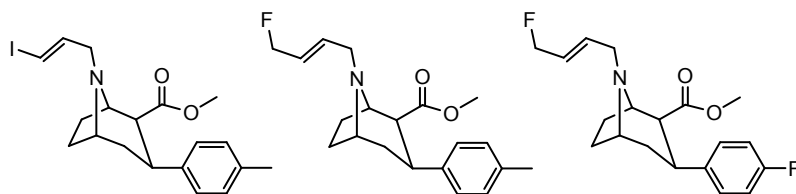


Figure 3: PE2I, LBT999 and FBCFT

Recent progress in this field was made in a modification of the highly suitable radioligand PE2I (cf. figure 4).²⁴ While the former facilitates labelling with iodine-123-125, the isosteric exchange of iodine for a fluoromethyl group in the novel candidates LBT999 and FBCFT enable fluorine-18 labelling.^{25,26} Its nuclide properties include one of the lowest β^+ energy of all PET nuclides, resulting in a high theoretical resolution and an increased availability. Furthermore, ^{18}F provides a convenient half-life of approximately 109 min, which facilitates satellite distribution of the radioprobe. Therefore, fluorine-18 labelled probes for non-invasive quantitative visualisation of DAT-availability are of significant clinical relevance.

We were interested in a high-selective and high affinity radiotracer, suitable for the visualisation of both, the dopamine rich brain regions in the basal ganglia, as well as the lower-density extrastriatal DAT populations. The DAT is located on DA-neurons, as well as in the surrounding glia cells and on blood platelets.²⁷ Highest DAT densities can be found in the caudate-putamen. The hDAT is present in lower densities in the amygdala, and in particular in the substantia nigra and the tegmental area, brain regions where the dopaminergic signal pathways originate.²⁸

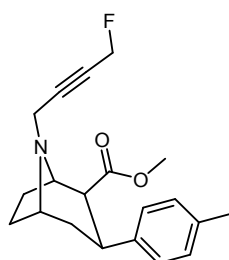
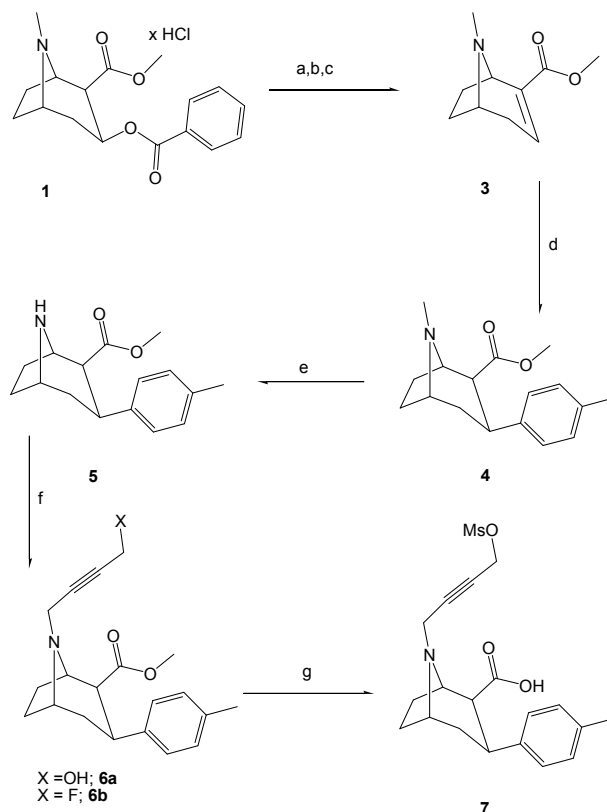


Figure 4: *N*-4-fluorobut-2-yn-1-yl-2β-carbomethoxy-3β-phenyltropane PR04.MZ (**6b**)

Therefore, we have designed, synthesised and evaluated a set of novel, structurally sophisticated cocaine derivatives based on the phenyltropane lead. All compounds contain fluorine in a position, readily available for direct nucleophilic aliphatic fluorination. Additionally, the methyl-ester function provides a site for the convenient introduction of an [^{11}C]CH₃-label. Among these novel compounds, the one we termed PR04.MZ displays the most favourable combination of monoamine transporter inhibition potency, lipophilic properties and DAT/SERT and DAT/NET-selectivity. The present report concerns the synthesis of the labelling precursor for direct nucleophilic aliphatic radio-fluorination, the

radiolabelling with [^{18}F] F^- , the characterisation of the ligand with binding studies in HEK-cell membranes stably transfected with hDAT, hSERT and hNET, *in vitro* and *ex vivo* autoradiography (AR), biodistribution and initial μPET -studies.

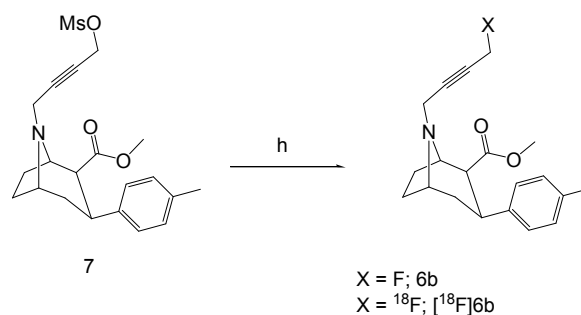
Results and Discussion



Scheme 1 Synthesis route to PR04.MZ (**6b**) and labelling precursor **7**; (a) 0.8 M HCl_{aq} , 14 h, reflux, 'quant'; (b) POCl_3 , reflux, 90 min 'quant' (c) MeOH/HCl , $-78\text{ }^\circ\text{C}$ to RT, 14 h, 85 %; (d) 1. *p*-tolylLi, THF, CuI (1 equiv.), THF, $-43\text{ }^\circ\text{C}$, 5 h; 2. TFA/ CH_2Cl_2 , $-78\text{ }^\circ\text{C}$, 30 min, 75 %; (e) 1. ACECl, DiPEA, $\text{C}_2\text{H}_4\text{Cl}_2$, reflux, 90 min; 2. MeOH (anhydrous), 85 % (f) 4-hydroxybut-2-ynyl chloride (\rightarrow **6a**) 4-Fluoro-but-2-ynyl chloride (\rightarrow **6b**); DiPEA, MeCN, $70\text{ }^\circ\text{C}$, 12 h, ~95 %; (g) MsCl , CH_2Cl_2 , NEt_3 , $0\text{ }^\circ\text{C}$, 15 min, 97 %.

Synthesis

Commercially available cocaine hydrochloride **1** was hydrolysed to ecgonine **2** in dilute hydrochloric acid. Subsequent elimination of water and re-esterification with methanol gave Michael-acceptor **3** in > 85% yield over 3 steps.²⁹ Compound **3** was converted to 4-methylphenyltropane **4** in 88 % yield (> 95 % *de*). Demethylation of **4** using (1-chloroethyl)chloroformate (ACECl) afforded nortropine **5** in 85 % yield which was subsequently converted to reference compound **6b** and alcohol **6a**. Finally, mesylation of alcohol **6a** under standard conditions afforded labelling precursor **7** in an overall yield of 50%.



Scheme 2 Direct nucleophilic radiofluorination of precursor **7**, conditions h) $[\text{K}^+\text{cK222}][^{18}\text{F}]\text{F}^-$ cryptate complex, K_2CO_3 , MeCN, 120 °C, 3 min, ~20 % radiochemical yield

Radiosynthesis

The radiosynthesis of $[^{18}\text{F}]\text{PR04.MZ}$ was straightforward from labelling precursor **7**. PR04MZ was labelled at its fluorobutynyl moiety via direct aliphatic nucleophilic radiofluorination.

Therefore, neat mesylate **7** was exposed to a solution of predried $[\text{K}^+\text{cK222}][^{18}\text{F}]\text{F}^-$ cryptate complex in acetonitrile at 120 °C in a pressure tight reaction vial. The product $[^{18}\text{F}]\text{PR04.MZ}$ was purified via high performance liquid chromatography (HPLC) and isolated via solid phase extraction on an acidic strong cation exchanger. The sterile formulation of $[^{18}\text{F}]\text{PR04.MZ}$ in PBS was obtained in 10 ± 3 % non-decay corrected radiochemical yield (RCY) after a total synthesis duration of 50 min. The radiochemical purity was 98 ± 2 %, and the specific activity was 18-95 GBq/ μmol .

Displacement studies in HEK293 cell membranes

The binding affinity for PR04.MZ to hDAT, hNAT and hSERT was determined in a cell assay, using human embryonic kidney cells (HEK293 cell line), stably transfected with hDAT, hSERT and hNET. β -CFT, citalopram and nisoxetine were used as radioligands. An IC_{50} value of 1.93 ± 0.2 nM was found for PR04.MZ at the hDAT. The corresponding values at the hNET and the hSERT were 108.4 ± 1.3 nM and 22.48 ± 0.83 nM, respectively.

Ex vivo autoradiography in wildtype mice

Three wildtype mice were injected with 5 ± 0.2 MBq of $[^{18}\text{F}]\text{PR04.MZ}$ under CO_2 -anaesthesia and sacrificed 35 min p.i.. The brains were taken out and rapidly frozen prior to the preparation of 14 μm coronal cryo sections. Some representative sections of each animal were washed to remove nonspecific binding prior to the detection.

Three wildtype mice were furthermore pretreated with GBR12909, 20 min prior to the i.p. injection of 6 ± 1 MBq of $[^{18}\text{F}]\text{PR04.MZ}$ and treated equally. The autoradiography is shown in figure 4.

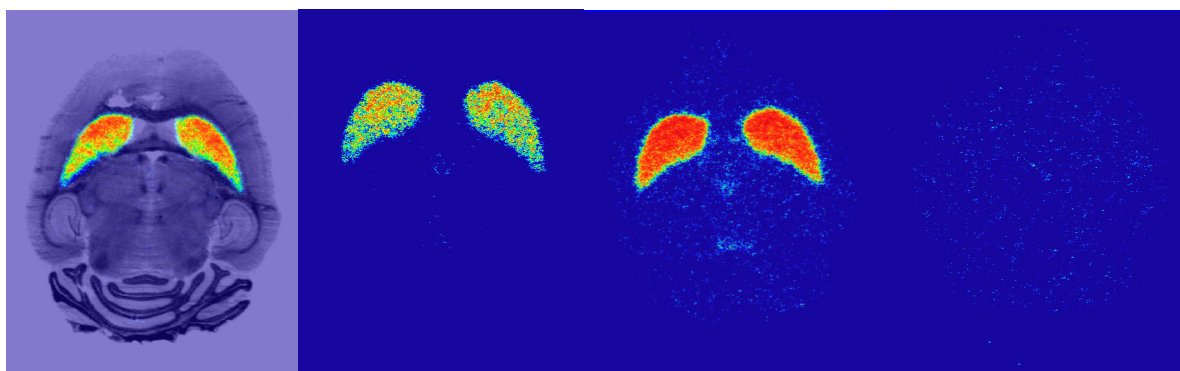


Figure 4: *In vivo* autoradiography on coronal sections of wild-type mice 35 min p.i., **outer left:** specific binding, coregistered with thionin coloured specimen; **inner left:** specific binding; **inner right:** total binding, **outer right:** displacement with GBR12909 (i.p. application of 1 mg/kg GBR12909, 20 min prior to the application of the radioligand)

The autoradiographies show a high accumulation of the radiotracer in the DAT rich caudate putamen, whereas the pretreated animals do not show any specific uptake of [¹⁸F]PR04.MZ into the DAT-containing brain regions (Table 1). Instead, the radioactivity accumulation in the blocked animals remains in the range of non-specific binding. Striatum to cerebellum ratios are shown in Table 1. Quantitative evaluation revealed an uptake of 123.8 ± 5.8 fmol of [¹⁸F]PR04.MZ per μ l of striatal tissue.

Table 1: Striatum to cerebellum ratios for washed and unwashed baseline animals and blocked animals

	Striatum / cerebellum	Thalamus / cerebellum	Cortex / cerebellum
non-washed	15.6	1.52	1.03
washed	23.5	1.09	0.7
blocked	1	1	1

***Ex vivo* biodistribution in Sprague Dawley rats and metabolism of [¹⁸F]PR04.MZ**

In order to gain some insights into the whole body biodistribution of [¹⁸F]PR04.MZ, an *ex vivo* biodistribution was conducted in Sprague Dawley rats. Furthermore, blood samples were analysed to determine the percentage of intact tracer present in the blood at each timepoint. The biodistribution is shown in Figure 5. Although the highest radioactivity concentration at the earliest time-point is found in the blood, the blood radioactivity concentration decreases over time. The initial value of 2.6 %ID/g at 5 min is reduced to 2.2 %ID/g after 15 min, 1.3 %ID/g after 30 min and finally to 0.7 %ID/g, 60 min p.i.. Furthermore, the metabolite analysis revealed that the tracer is moderately metabolised within the first 15 min p.i. whereas only traces of intact [¹⁸F]PR04.MZ were found in the blood 60 min p.i.. The highest whole brain uptake of 2.5 %ID/g was found 5 min p.i., followed by some washout during the following 55 min. The whole brain radioactivity is reduced to 1.8 %ID/g after 15 min, 1.05 %ID/g after 30 min and 0.55 %ID/g after 60 min. Interestingly, the heart shows peak radioactivity uptake 15 min (1.2 %ID/g) p.i. followed by slow washout (0.95 %ID/g after 30 min and 0.5 % ID/g after 60 min). Radioactivity uptake into the kidneys and the liver is shifted to intermediate time-points. The percentage of ¹⁸F radioactivity in the kidneys peaks at 15 min p.i. (3.95 %ID/g),

whereas the liver uptake is further increased, until the peak level of 7.2 % ID/g is reached after 30 min. At 60 min p.i. both organs show only moderate radioactivity doses of 1.8 %ID/g in the liver and 1.6 %ID/g in the kidneys, respectively. The bone radioactivity continuously increases from an initial value of less than 0.1 %ID/g after 5 min to 0.1 %ID/g after 15 min to a stable value of approximately 0.5 % ID/g at 30 and 60 minutes, respectively.

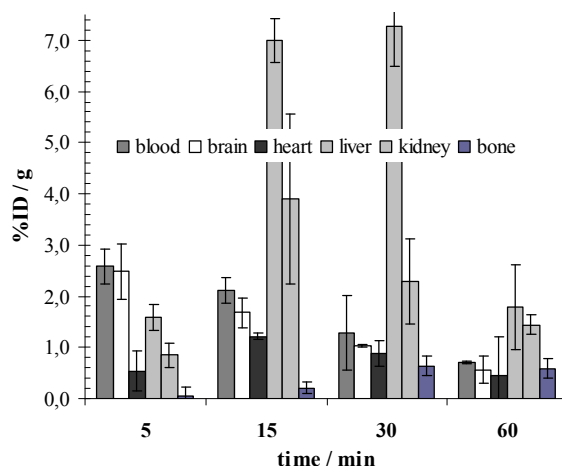


Figure 5: *Ex vivo* biodistribution of [¹⁸F]PR04.MZ

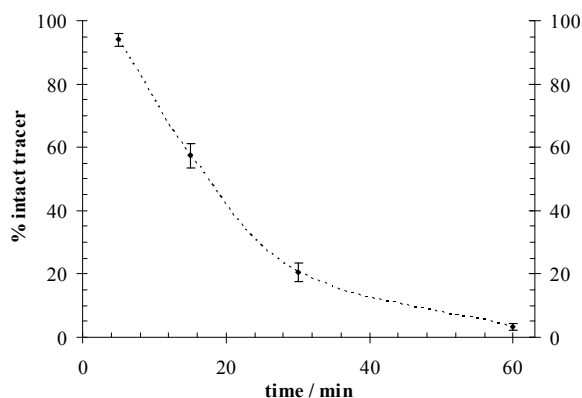


Figure 6: Metabolism of [¹⁸F]PR04.MZ in rat blood

Blood analysis and biodistribution revealed, that [¹⁸F]PR04.MZ is almost completely metabolised to polar metabolites within the first 60 minutes p.i.. Although liver and kidney contain some homologous monoamine transporters that might interact with the radioligand, these findings are underlined by the high accumulation of the injected dose into the liver and the increasing bone bound radioactivity which most likely represents [¹⁸F]fluoride. In contrast, no major metabolites were found in the homogenised brain. Instead, more than 94 % of the intact tracer was found in the central nervous system (CNS) after 60 min, whereas no major metabolite was found in the brain. However, the radioactivity in the bone remains stable within the two later time-points. The very high initial brain uptake at the earliest time-point is significantly reduced within the following 55 min. This result might hint on a reasonable time-dependency of the washout.

In vitro autoradiography and displacement with β -CFT

A quantitative *in vitro* autoradiography was conducted in 14 μm cryo sections of male, adult wistar rats. Therefore, coronal sections were incubated for 60 min with a 3 nM PBS-solution of [^{18}F]PR04.MZ. The sections were washed to remove the non-specific binding and the radioactivity distribution was measured on a Fuji phospho-screen (cf. Figure 7). To investigate the reversibility of binding of [^{18}F]PR04.MZ, some sections were challenged with a 1 mM β -CFT-solution and treated equally. The fluorine-18 labelled tracer specifically accumulated in the DAT-rich brain regions of the rat, whereas the sections challenged with the competing ligand showed a complete displacement of the bound radioactivity.

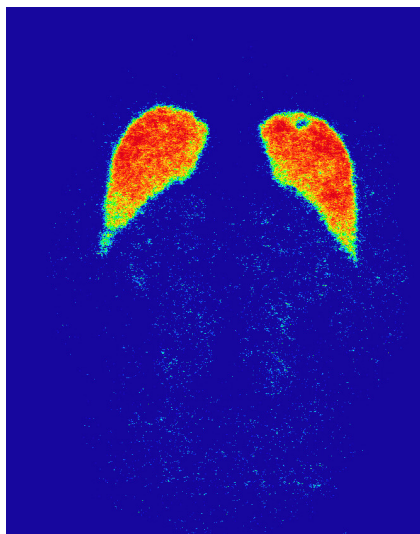


Figure 7: Whole brain distribution of [^{18}F]PR04.MZ in a rat brain section (approx. 4.5 mm downward from bregma)

[^{18}F]PR04.MZ shows a high specific uptake into the caudate putamen ($\text{fmol}/\mu\text{l}$) and a striatum-to-cerebellum ratio of 18.5 ± 2.7 . Neither in cortical regions (cortex-to-cerebellum 1 ± 0.12) nor in the thalamus (thalamus-to-cerebellum 1.87 ± 0.25), any significant specific binding could be detected. In opposite to these findings, the binding of [^{18}F]PR04.MZ was completely displaced to the level of non-specific binding by a 300-fold concentration of a structurally analogue. A result that further underlines the full reversibility of [^{18}F]PR04.MZ binding in rat dopamine transporters. Furthermore the high DAT-specificity is confirmed again.

Preliminary μPET -imaging study

A μPET -study was conducted in five male, healthy Wistar-rats. In addition, an *in vivo* displacement study was performed in each animal. In correlation with the earlier experiments, the radiotracer rapidly accumulates in the DAT-bearing brain regions (cf. Figure 8). The peak striatal uptake is reached at 20 min p.i.. Furthermore, the PET-images show a high striatum-to-cerebellum ratio of 7.3 already at 20 min, which is further increased to 17.2 at 40 min (cf. Figure 9). Besides the low background in the residual brain regions, the tracer is not taken up into the Harderian glands to the usual extend.

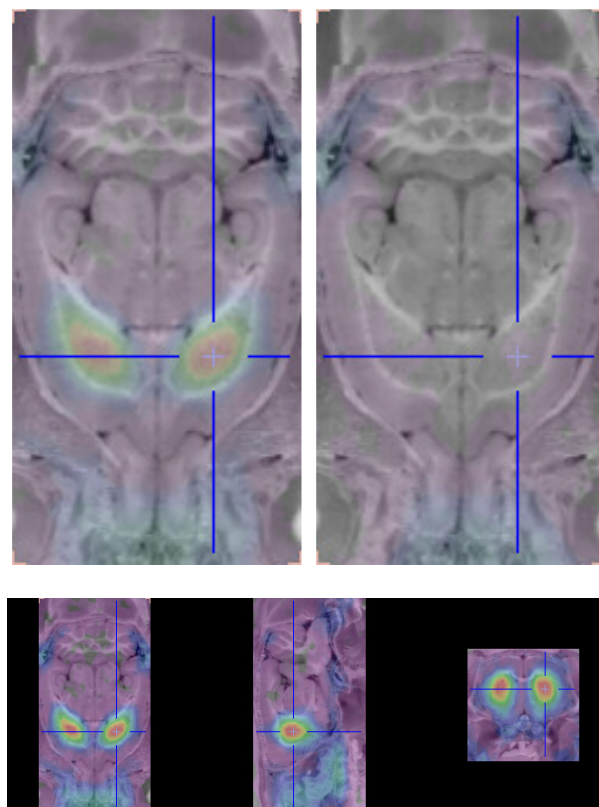


Figure 8: MR (LONI MR atlas of the rat brain)³¹ fused PET-images of [¹⁸F]PR04.MZ; **upper left:** control summed frames from 5 to 40 min; **upper right:** summed frames from 50 to 63 min; **bottom:** coronal, sagittal, and transversal view for orientation.

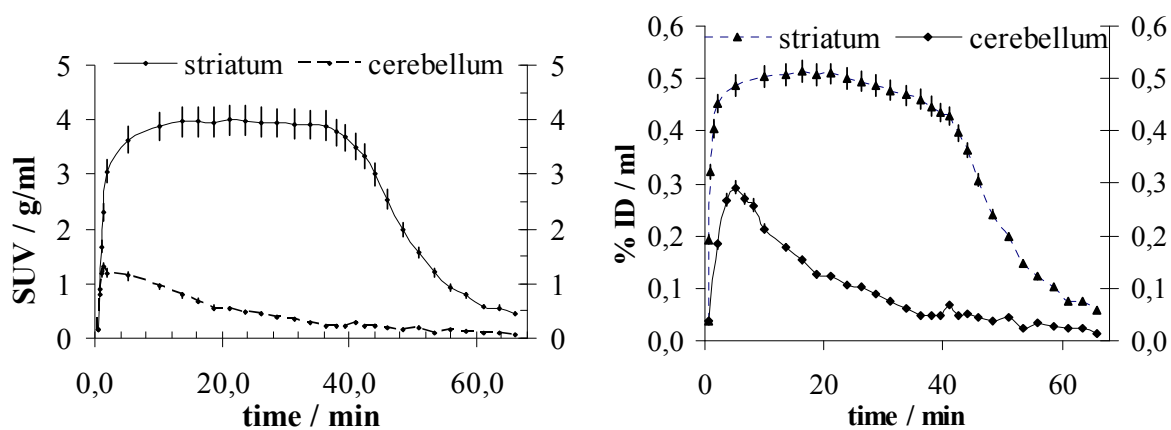


Figure 9: Time activity curve (TAC) for [¹⁸F]PR04.MZ in rat striatum and cerebellum. (Averaged after dose normalisation from 5 studies, values are mean \pm 1 S.D.). Displacement with 2 mg/kg β -CFT at 40 min p.i.

The *in vivo* displacement of [¹⁸F]PR04.MZ with β -CFT results in a significant decrease of the striatal radioactivity, whereas the injected dose per ml (%ID/ml) in the cerebellum remains almost constant. The striatum-to-cerebellum ratio at the time of injection of β -CFT was 17. It was reduced to 5, 20 min after the injection of β -CFT. These results display the good transporter specificity and the reversibility of binding of the novel candidate [¹⁸F]PR04.MZ

and its suitability as a radioprobe for the specific, non-invasive exploration of the DAT.

Conclusions

The labelling precursor of [^{18}F]PR04.MZ, a radio-fluorinated tropane derivative containing an inflexible C_4 chain at the bridge-nitrogen has been successfully synthesized. The former was labelled with [^{18}F]F $^-$ in a radiochemical yield of $13 \pm 3\%$ and formulated in a radiochemical purity of $98 \pm 2\%$ for *in vitro*, *ex vivo* and *in vivo* evaluation in rodents. The radioligand shows moderately fast kinetics, good selectivity and reversible binding characteristics in the DAT-rich brain regions of mice and rats. The distribution of [^{18}F]PR04.MZ in the rodent brain is in accordance with the distribution of the DAT as shown by immunochemical detection of the DAT-RNA.²⁸ The cerebellum can be used as a reference region. Neither in cortical regions nor in the thalamus any significant specific binding was detected. Furthermore, the accumulation of the radioligand proved to be highly sensitive to pretreatment with a structurally non-analogous selective DAT-ligand. Reversibility of binding was demonstrated using the established DAT-inhibitor β -CFT (WIN 35,428). These results exemplify the good dopamine transporter selectivity of the novel candidate [^{18}F]PR04.MZ. Furthermore, the high initial brain uptake within 5 min p.i. followed by moderate washout may hint on an improved kinetic behaviour compared to e.g. FP- β -CIT. This thesis is further strengthened by the somewhat fast uptake and equilibrium observed in the μ PET experiment provided in the present report. The observed kinetic behaviour facilitates comparative studies of dopaminergic signal pathways involving D_2/D_3 -selective radioligands, such as [^{18}F]Fallypride ([^{18}F]FP) and [^{18}F]Desmethoxyfallypride ([^{18}F]DMFP).

Experimental

NMR-spectra were recorded with a Bruker DRX 400 FT-NMR-spectrometer, J values are given in Hertz, chemical shifts are reported downfield from tetramethylsilane (TMS), referred to the solvent residual signal ^1H NMR (300 MHz, CHCl_3 7.24 ppm) and ^{13}C NMR (100 MHz, CDCl_3 77.0 ppm). Field desorption (FD) mass spectra were recorded on a Finnigan MAT90 FD spectrometer. HRMS-spectra were measured on a Micromass QTOF Ultima 3 spectrometer. All chemicals were obtained in commercial quality from Acros Organics, Sigma Aldrich, VWR, TCI or STREM and used without further purification. TLC was conducted on self-cut Merck silica gel 60 covered aluminium plates. Detection and staining was performed either using iodine on silica gel, potassium permanganate solution, UV fluorescence, vanillin/sulphuric acid, Seebach-reagent (phosphomolybdic acid, cerium sulphate, H_2SO_4) or Dragendorff-reagent (basic bismuth nitrate, potassium iodide and tartaric acid). Column chromatography was performed on Acros silica gel 60, 0.063-0.200 mesh, p. a. solvents for chromatography were washed with aqueous acid and base and distilled once, prior to use. Anhydrous solvents were used for reactions.

Ecgonidine methyl ester: Cocaine hydrochloride (25 g, 82.4 mmol) was dissolved in 0.8 M hydrochloric acid (150 ml) and refluxed over night. The reaction mixture was cooled to $4\text{ }^\circ\text{C}$ and the benzoic acid precipitate was filtered off. Subsequent extraction of the reaction mixture with Et_2O , followed by complete evaporation of the hydrochloric acid and drying *in vacuo* afforded ecgonine 2 in quantitative yield (g, mmol). The colourless solid residue was dissolved in POCl_3 (60 ml) and heated to reflux for 90 min after which the phosphoryl chloride was removed *in vacuo*. The colourless oily residue was cooled to $-43\text{ }^\circ\text{C}$ in an

MeCN/dry ice bath, covered with dry MeOH (60 ml) and warmed to room temperature with stirring. Stirring was continued over night, prior to the complete evaporation of the alcohol. The residue was partitioned between Et₂O (50 ml) and cold 28 % ammonium hydroxide solution (50 ml). The aqueous phase was further extracted with two portions of CH₂Cl₂ (50 ml) followed by Et₂O (50 ml). The organic layers were combined, dried (anhydrous K₂CO₃) and evaporated. Purification in a Kugelrohr apparatus afforded ecgonidine methyl ester (13.1 g, 85 %, 70 mmol) as a colourless oil. NMR-spectra and boiling point were in accordance with those published previously.

2β-carbomethoxy-3β-tolytropane (4): A solution of p-tolylmagnesium bromide (40 mmol, 40 ml) 1 M in THF was added to a suspension of CuI (40 mmol, g) in THF (50 ml) under nitrogen and stirred at 0 °C for 30 min. The mixture was cooled to -43 °C and ecgonidine methyl ester (3.6 g, 20 mmol) in THF (6:4, 75 ml) was added dropwise, so that the temperature inside the flask did not exceed -40°C. Stirring was continued for 5 h after which the reaction mixture was cooled to -78 °C and TFA (g, 40 mmol) in CH₂Cl₂ was added dropwise over 30 min. The solvents were removed in vacuo to leave a semisolid residue that was taken partitioned between CH₂Cl₂ and cold 28 % ammonium hydroxide solution (25 ml). The aqueous phase was extracted with CH₂Cl₂ (2 x 40 ml) followed by Et₂O (40 ml) purified via flash column chromatography (Et₂O-Hexanes, 1:9, 10 % NEt₃). 2β-carbomethoxy-3β-tolytropane (**4**) was obtained as a colourless to slightly yellow solid in 88 % yield (4.78 g, 35 mmol). NMR-spectra and FD-mass were in accordance with those published somewhere else.³⁰

2β-carbomethoxy-3β-tolynortropane (5): Tropane **4** (275 mg, 1 mmol) was dissolved in dichloroethane (5 ml) and refluxed with 1-chloroethyl chloroformate (7 equiv.) for one hour. One equiv. of N,N-diisopropyl-N-ethylamine was added and the mixture was refluxed for one additional hour. Subsequently, the reaction mixture was concentrated *in vacuo* to leave a colorless, viscous residue that was taken up in MeOH (10 ml) with cooling and stirring. After refluxing for two additional hours, the resultant, pale yellow solution was concentrated, and the residue was taken up in cold ammonium hydroxide solution (28 %, 5 ml) with intense cooling and extracted with Et₂O (2 x 15 ml), followed by dichloromethane (2 x 15 ml) and again Et₂O (15 ml). Combination, drying (K₂CO₃) and concentration of the organic layers afforded crude nortropane **2**. Purification was performed on silica gel 60 (AcOEt-hexanes, 3:7, 10 % NEt₃) to obtain products **2** in 85 % yield (0.223 g, 0.86 mmol). NMR spectra were in accordance with those published previously.^{29,30}

General procedure for N-alkylation: Nortropane **5** (100 mg, 0.39 mmol) was added to a stirred solution of Hünig's base (52 mg, 0.4 mmol) in acetonitrile (10 ml). Electrophile (1 equiv.) was added and the mixture was stirred at 70 °C for 12 h. The mixture was carefully concentrated *in vacuo* to leave a mobile residue that was chromatographed on silica gel (20 g, ether-hexanes, 2:8, 10 % NEt₃) to afford products **6a-b** in 75-97 % yield. **6a**: ¹H-NMR: (300 MHz, CDCl₃) δ (in ppm): 7.14 (d, *J* = 8.5 Hz, 2 H, ArH), 7.06 (d, *J* = 8.5 Hz, 2 H, ArH), 5.02 (t, *J* = 1.5 Hz, *J*_{H-F} = 47.8 Hz, 1 H), 4.86 (t, *J* = 1.5 Hz, *J*_{H-F} = 47.8 Hz, 1 H), 3.89 (brs, 1 H), 3.51 (s, 3 H, OCH₃), 3.47 (brs, 1 H), 3.25 (ddt, *J* = 1.5 Hz, *J* = 7.5 Hz, *J* = 16.5 Hz, 1 H), 3.10 (ddt, *J* = 1.5 Hz, *J* = 7.5 Hz, *J* = 16.5 Hz, 1 H), 2.98 (dt, *J* = 5 Hz, *J* = 12.9 Hz, 1 H), 2.94 – 2.89 (m, 1 H), 2.62 (td, *J* = 2.9 Hz, *J* = 12.5 Hz, 1 H), 2.27 (s, 3 H, ArCH₃), 2.16 – 1.92 (m, 2 H), 1.82 – 1.61 (m, 3 H). ¹³C-NMR: (100 MHz, CDCl₃) δ (in ppm): 171.7, 139.6, 135.3, 128.7, 127.2, 127.1, 87.7, 87.5, 69.7, 62.6, 61.2, 52.8, 52.6, 51.1, 42.9, 34.1, 33.7, 25.9, 25.7,

21.0. Anal. Calcd. C, 72.92; H, 7.34; F, 5.77; N, 4.25; O, 9.71. Found: C, 72.79; H, 8.03; N, 4.53. MS (FD) 327.2 (100) C₂₀H₂₆NO₃ requires 327.1834. **6b**: ¹H-NMR: (300 MHz, CDCl₃) δ (in ppm): 7.16 (d, *J* = 8 Hz, 2 H, ArH), 7.08 (d, *J* = 8 Hz, 2 H, ArH), 4.26 (t, *J* = 2 Hz, 2 H), 3.92 (brs, 1 H), 3.53 (s, 3 H, OCH₃), 3.51 (brs, 1 H), 3.21 (dt, *J* = 2 Hz, *J* = 16 Hz, 1 H), 3.09 (dt, *J* = 2 Hz, *J* = 16 Hz, 1 H), 3.02 (dt, *J* = 12.7 Hz, *J* = 5 Hz, 1 H), 2.94 ("t", *J* = 4 Hz, 1 H), 2.62 (td, *J* = 2.9 Hz, *J* = 12.5 Hz, 1 H), 2.30 (s, 3 H, CH₃), 2.20 - 2.09 (m, 1 H), 2.07 - 1.96 (m, 1 H), 1.83 - 1.60 (m, 3 H). ¹³C-NMR: (100 MHz, CDCl₃) δ (in ppm): 172.1, 139.7, 135.3, 129.0, 128.6, 127.2, 82.8, 81.7, 62.6, 60.9, 52.8, 51.2, 50.9, 42.9, 34.1, 33.7, 25.9, 25.8, 21.0. Anal. Calcd. C, 72.92; H, 7.34; F, 5.77; N, 4.25; O, 9.71. Found: C, 72.79; H, 8.03; N, 4.53. MS (FD) 330.2 (100) C₂₀H₂₅FNO₂ requires 330.1869.

Labelling precursor *N*-(4-methylsulfonyloxy but-2-yn-1-yl)-2β-carbomethoxy-3β-p-tolyl nortropine (7): *N*-(4-hydroxybut-2-yn-1-yl)-2β-carbomethoxy-3β-tolyl nortropine (**6a**) (109 mg, 0.3 mmol) was dissolved in CH₂Cl₂ (1 ml) containing NEt₃ (40 mg, 0.4 mmol) and cooled to 0 °C. After continuous stirring for 30 min, methanesulfonyl chloride (35 mg, 0.3 mmol) was added dropwise and the mixture was stirred for 15 min. 1 M HCl (1 ml) was added and the organic layer was diluted with CH₂Cl₂ (4 ml). The organic layer was separated and extracted with 1 M Na₂CO₃ solution (3 ml). The organic layer was dried and concentrated to afford **7** as a colourless oil (123 mg, 97 %) that solidified upon standing at 4 °C. Please note that **7** will degrade albeit slowly at 4 °C. ¹H-NMR: (300 MHz, CDCl₃) δ (in ppm): 7.15 (d, *J* = 8 Hz, 2 H, ArH), 7.08 (d, *J* = 8 Hz, 2 H, ArH), 4.23 (t, *J* = 2 Hz, 2 H), 3.91 (brs, 1 H), 3.52 (s, 3 H, OCH₃), 3.50 (brs, 1 H), 3.22 (dt, *J* = 2 Hz, *J* = 16 Hz, 1 H), 3.10 (dt, *J* = 2 Hz, *J* = 16 Hz, 1 H), 3.02 (dt, *J* = 12.5 Hz, *J* = 5 Hz, 1 H), 2.93 ("t", *J* = 4 Hz, 1 H), 2.89 (s, 3 H, SO₂CH₃), 2.61 (td, *J* = 2.9 Hz, *J* = 12.5 Hz, 1 H), 2.29 (s, 3 H, CH₃), 2.21 - 2.10 (m, 1 H), 2.07 - 1.95 (m, 1 H), 1.83 - 1.59 (m, 3 H). ¹³C-NMR: (100 MHz, CDCl₃) δ (in ppm): 172.1, 139.7, 135.3, 129.0, 128.6, 127.2, 82.7, 81.7, 62.5, 60.9, 52.8, 51.2, 50.9, 42.9, 37.6, 34.1, 33.7, 25.85, 25.8, 21.0. Anal. Calcd. C, 62.20; H, 6.71; N, 3.45; O, 19.73; S, 7.91. Found: C, 61.9; H, 6.91; N, 3.24. MS (FD) 405.2 (100) C₂₁H₂₇NO₅S requires 405.1610.

Radiosynthesis: ¹⁸F-fluoride was produced via proton bombardment of an enriched [¹⁸O]H₂O target via the ¹⁸O(p,n)¹⁸F nuclear reaction. The ¹⁸F-Fluoride containing target water was passed through a Waters accell plus QMA strong anion exchanger, preconditioned with 1 M potassium carbonate solution (10 ml) followed by MilliQ-water (20 ml). The trapped fluoride was eluted directly into a 5 ml Wheaton[®] reactivial in a mixture of acetonitrile (1 ml), containing K222 Kryptofix[®] cryptant (15 mg, 0.04 mmol) and 1 M potassium carbonate solution (15 μl, 0.015 mmol). The vial was tightly capped and the acetonitrile was evaporated at 90 °C in a gentle stream of nitrogen (300 ml/min) at a reduced pressure of 10⁴ Pa. Drying of the [K⁺⊂K222][¹⁸F]F⁻ was accomplished via the addition and evaporation of two additional portions of acetonitrile, followed by high vacuum for 3 min. The colourless solid residue was redissolved in acetonitrile with stirring and transferred into a second 5 ml Wheaton[®] reactivial containing labelling precursor **7** (4.5 mg, 0.0115 mmol). The vial was tightly capped and heated to 120 °C for 3 min after which the oil bath was replaced by a water bath. After cooling of the reaction mixture for 90 s, the reaction mixture was diluted with 1 ml of HPLC-eluent (1 ml, MeCN-0.05 M ammonium acetate solution pH 4.5; 6:4). This solution was directly injected into a semipreparative HPLC-system (4.7 ml/min, Phenomenex[®] Luna[®] RP18 250x10 mm, 10 μ) and the product fraction was collected after a total purification time of 14 min. The product fraction was diluted with MilliQ[®]-water (1:1) and passed through a

VWR Lichrolut[®] SCX strong cation exchanger, preconditioned with 1 M hydrochloric acid (5 ml) followed by water (20 ml). The cartridge was washed with water (3 ml) prior to the elution of the trapped product in sterile DPBS directly through a serially connected vented Millex[®] sterile filter into a multi-injection vial. The product [¹⁸F]PR04.MZ was obtained ready for injection in a non decay-corrected yield of 13±3 % and a specific activity of 18-95 GBq/μmol.

Animal studies: All animal experiments were in compliance with the German and European legislation concerning animal experiments. Animals were housed under standard conditions (access to standard food and water, 55±5 % humidity, 21 °C, lights on 6:00, lights off 18:00).

Biodistribution in rats: A dose of 4-9 MBq of [¹⁸F]PR04.MZ in sterile PBS (100 μl) was injected into the tail vein of 13 male, healthy Sprague-Dawley rats (300±50 g) anaesthetised with isoflurane. The animals were allowed to wake up subsequently. All subjects were decapitated under isoflurane anaesthesia at 5, 15, 30 and 60 min p.i. (n = 3). Blood, organs, tail and bone were removed and transferred into weighed well-counter tubes. The radioactivity in each fraction was measured for 90 s in a self-built well counter (NaI(Tl), window range 380-550 keV). The radioactivity distribution was expressed as percentage of the individual injected dose per gram of tissue (and bone). Mean values were calculated for three individual experiments and one standard deviation (S.D.) was given as error.

Metabolite analysis: 300 μl of full blood were centrifuged at 5000 rpm for 5 min. 150 μl of the supernatant were withdrawn and transferred into 400 μl acetonitrile. The obtained slurry was centrifuged again at 5000 rpm for 5 min to remove the precipitated proteins and the supernatant was analysed by radio-TLC (Et₂O-Hexanes, 2:8, 10 % NEt₃) to determine the amount of intact tracer at 5, 15, 30 and 60 min p.i.. An aliquot of the dissected brain was homogenised, sonicated in MeCN and centrifuged at 5000 rpm for 5 min. The supernatant was analysed by radio-TLC.

Ex vivo autoradiography, baseline and block: Male, healthy wildtype mice were used for the assessment of the DAT-selectivity and target-specific uptake of [¹⁸F]PR04.MZ into the brain. Therefore, three subjects were i.p. injected with 5±0.2 MBq of [¹⁸F]PR04.MZ and decapitated under CO₂-anaesthesia 35 min p.i. For blocking experiments, three mice were pretreated with 1 mg/kg β-CFT (1 % DMSO in 0.9% NaCl-solution) 20 min prior to the i.p. injection of 6.5 MBq of [¹⁸F]PR04.MZ and equally decapitated 35 min p.i.. The brains were taken out and immediately frozen on an aluminium ingot at -80 °C. Brains were mounted on a sample holder of a cryomicrotome and dissected into 14 μm coronal sections. The sections were placed on glass sample holders, smoothed, digitally photographed and some slices were washed with assay buffer (50 mM tris/HCl buffer, pH 7.4 containing 120 mM NaCl and 5 mM KCl) for 20 min, followed by 0.01 % Triton-X in water for one minute to remove non-specific binding. Sections were shortly dipped into deionised water and dried in a stream of cold air. A Fuji BAS-TR 2025 phospho-imaging plate was exposed to the sections for 180 min in the dark. For quantitative evaluation, nine samples of [¹⁸F]PR04.MZ in ascending concentration (0.3 nM, 0.1 nM, 0.03 nM, 0.01 nM, 0.003 nM, 0.001 nM, 0.0003 nM, 0.0001 nM, 0.00003 nM) were codetected. The phospho-imager-plates were read out using a Fuji FLA-7000 analyser and Fuji Multigauge V 3.0. Representative sections were stained with 1 % thionine (Lauth's stain-solution) and photographed. For clarity, chosen examples were fused with the corresponding radioactivity distribution as shown in fig. 5.

In vitro autoradiography: Male, healthy Wistar rats were used for the preparation of cryo-sections. Typically, 280 to 300 g rats were anaesthetised with carbon dioxide and decapitated immediately. The subject's brains were taken out and frozen on an aluminium ingod at -80 °C. Either 14 µm coronal or sagittal sections were prepared in a cryo-microtome at -20 °C. The sections were transferred to microscope sample holders, the outlines of the sections were surrounded by PapPen® and stored at -80 °C. Series of back-to-back sections were used for autoradiography. Sections were slowly warmed to room temperature and pre-incubated in assay buffer, prior to use. Autoradiography was carried out at room temperature in assay buffer (50 mM Tris/HCl buffer, pH 7.4 containing 120 mM NaCl and 5 mM KCl) with [¹⁸F]PR04MZ. β-CFT (WIN 35,428) was used for displacement studies. Sections with [¹⁸F]PRD04-MZ were washed 1x20 min in reaction buffer containing 0.01 % Triton X-100 and 1x20 min in reaction buffer, shortly dipped into de-ionized water and quickly dried in a stream of cold air. Sections, together with a standard-row of 12 concentrations of [¹⁸F]PR04.MZ (1.0 nm, 0.3 nm, 0.1 nm, 0.03 nm, 0.01 nm, 0.003 nm, 0.001 nm, 0.0003 nm, 0.0001 nm, 0.00003 nm, 0.00001 nm, 0.000003 nm) were exposed to the Fuji phosphor screen BAS-TR 2520 for 3 h. Images were re-constructed and quantified using a Fuji FLA-7000 analyser and Fuji Multigauge V 3.0.

µPET-Imaging: Male, healthy Wistar-rats were used for imaging experiments. The animals were anaesthetised with chloral hydrate 30 min prior to the radiotracer delivery. A venal catheter was attached to the surgically accessed left *vena femoralis*. The anaesthetised animal was fixed top to bottom onto the bed of a Siemens/CTI Focus 120 µ-PET-imager. To maintain a vital body temperature, the animal was irradiated with an IR-heat lamp. A transmission scan was subsequently performed using the build-in rotating ⁵⁷Co- source. The venus line was purged immediately before [¹⁸F]PR04.MZ (25-40 MBq, 200 µl) of sterile PBS followed by 0.9 % sterile NaCl-solution (150 µl) were injected. Data acquisition was initiated simultaneously and a dynamic emission scan was performed for 60 to 120 (n = 5) min. For displacement studies, β-CFT (1 mg/kg) were given as a bolus injection after the striatum-to-cerebellum ratios were in steady-state, followed by continuous application of β-CFT (1 mg/kg) over 45 min via a perfusor. After the PET-scan, animals were sacrificed by overstretching under strong chloral hydrate anaesthesia. Blood samples were withdrawn from the heart and analysed by radio-TLC. Reconstruction of the emission data was conducted via the application of filtered back projection on the attenuation corrected sinograms. Regions of interest (ROI) were drawn onto the corregistered MR-templates and copied into the dynamic PET-images Time activity curves (TACs) for cerebellum, cortical regions, thalamus, and striatum were expressed as percent of the decay corrected injected dose (% ID)/cm³ above time. For comparison, the standard uptake volumes (SUV) were calculated according to equation 1 and plotted versus time in fig. 9.

$$SUV = \frac{\%ID}{cm^3} \times \frac{1}{m_{rat}}; [SUV] = \frac{g}{cm^3} \quad (1)$$

References:

- (1) a) W. Forth, D. Henschler, W. Rummel, K. Starke, *Allgemeine und spezielle Pharmakologie und Toxikologie*. Spektrum Akademischer Verlag **1996**; b) G. Thews, E. Mutschler, P. Vaupel, *Anatomie, Physiologie, Pathophysiologie des Menschen*. Wissenschaftliche Verlagsgesellschaft mbH **1999**; c) J. G. Hardman, L. E. Limbird, A. Goodman Gilman, P. Dominiak, S. Harder, M. Paul, A. Goodman Gilman, *Goodman & Gilman: Pharmakologische Grundlagen der Arzneimitteltherapie* Bd. 1 and 2. McGraw-Hill **1999**; d) F. M. Benes, *Trends Pharmacol. Sciences* **2001**, 22, 46, e) S. R. Neves, P. T. Ram, R. Iyengar, G protein pathways, *Science* **2002**, 296, 1636; f) J. Girault, P. Greengard, *Arch. Neurol.* **2004**, 61, 641
- (2) a) U. Gether, P. H. Andersen, O. M. Larsson, A. Schousboe, *Trends Pharmacol. Sci* **2006**, 27, 375-383; b) N. Chen, M. E. A. Reith, *Eur. J. Pharmacol.* **2000**, 329-339.
- (3) a) J. S. Fowler, N. D. Volkow, A. P. Wolf, S. L. Dewey, D. J. Schlyer, R. R. Macgregor, R. Hitzemann, J. Logan, B. Bendriem, S. J. Gatley, et al. *Synapse* **1989**, 4, 371-77; b) N. D. Volkow, J. S. Fowler, S. J. Gatley, J. Logan, G.-J. Wang, Y.-S. Ding, S. Dewey, *J. Nucl. Med.* **1996**, 37, 1242-1256.
- (4) a) J. S. Fowler, N. D. Volkow, G.-J. Wang, S. J. Gatley, J. Logan, *Nucl. Med. Biol.* **2001**, 28, 561-572; b) P. H. Elsinga, K. Hatano, K. Ishiwata, *Curr. Med. Chem.* **2006**, 13, 2139-2153.
- (5) G.-J. Wang, N. D. Volkow, P. K. Thanos, J. S. Fowler, *Journal of addictive diseases* **2004**, 23, 39-53.
- (6) a) N. Haberland, L. Hetey; *J. Neural Transmission* **1987**, 68, 3-4; b) G. Grunder, D. F. Wong, *Fortschr. Neurol. Psychiat.* **2003**, 71, 415-420.
- (7) S. Kapur, J. Mann, *J. Biol. Psychiatry* **1992**, 32, 1-17.
- (8) a) H. Bernheimer, W. Birkmayer, O. Hornykiewicz, K. Jellinger, F. Seitelberger, *J. Neurol. Sci.* **1973**, 20, 415-455; b) T. D. Reisine, J. Z. Fields, L. Z. Stern, P. C. Johnson, E. D. Bird, H. I. Yamamura, *Life Sci.* **1977**, 21, 1123-1128.
- (9) a) J. M. Swanson; *The Lancet* **2000**, 355, 1461; b) Madras, Bertha K.; Miller, Gregory M.; Fischman, Alan, *J. Biological Psychiatry* **2005**, 57, 1397-1409.
- (10) a) H. B. Niznik, E. F. Fogel, F. F. Fassos, P. Seeman *J. Neurochem.* **1991**, 56, 192-198; b) J. O. Rinne, J. Bergman, H. Ruottinen, M. Haaparanta, E. Eronen, V. Oikonen, P. Sonninen, O. Solin; *Synapse* **1999**, 31, 119 - 124. c) M J Kaufman, B K Madras, *Synapse* **1991**, 9, 43-49.
- (11) a) S. Thobois, S. Guillouet, E. Broussolle, *Neurophysiol. Clin.* **2001**, 31, 321-340; b) J. Booij, G. Tissingh, A. Winogrodzka, E. A. van Royen, *Eur. J. Nucl. Med* **1999**, 26, 171-182; c) P. K. Morrish, *Mov. Disord.* **2003**, 18, S63-S70; d) K. Tatsch, *Eur. J. Nucl. Med.* **2002**, 29, 711-714; e) K. A. Frey, *Eur. J. Nucl. Med.* **2002**, 29, 715-717.
- (12) P. O. Allard, J. Rinne, J. O. Marcusson, *Brain Res.* **1994**, 637, 262-266.
- (13) a) S. Nikolaus, R. Larisch, M. Beu, C. Antke, K. Kley, F. Forutan, A. Wirrwar, H.-W. Mueller, *Rev. Neurosci.* **2007**, 18, 473-504; b) S. Nikolaus, C. Antke, K. Kley, T. D. Poeppel, H. Hautzel, D. Schmidt, H.-W. Mueller, *Rev. Neurosci.* **2007**, 18, 439-472.
- (14) a) E. S. Garnett, G. Firnau, C. Nahmias, *Nature* **1983**, 305, 137-138.

- (15) a) V. Sossi, J. E. Holden, G. J. Topping, M.-L. Camborde, R. A. Kornelsen, S. E. McCormick, J. Greene, A. R. Studenov, T. J. Ruth, D. J. Doudet, *J. Cerebr. Blood Flow Metab.* **2007**, *27*, 1407-1415; b) H. Kung, M. P. Kung, B. Lieberman, C. Hou, D. Ponde, R. Goswami, D. Skovraonsky, S. Deng, J. Markammn, M. Kilborn, Abstracts of Papers, 234th ACS National Meeting, Boston, MA, United States.
- (16) P. H. Elsinga, K. Hatano, K. Ishiwata, *Curr. Med. Chem.* **2006**, *13*, 2139-2153.
- (17) D. Sulzer, *Clin. Neurosci. Res.* **2005**, *5*, 117-121.
- (18) a) S. M. Aquilonius, K. Bergstrom, S. A. Eckernas, P. Hartvig, K. L. Leenders, H. Lundquist, G. Antoni, A. Gee, A. Rimland, J. Uhlin, B. Langstrom; *Acta. Neurol. Scand.* **1987**, *76*, 183-287; b) M. R. Kilbourn, J. E. Carey, R. A. Koeppe, M. S. Haka, G. A. Hutchins, P. S. Sherman, D. E. Kuhl, *Nucl. Med. Biol.* **1989**, *16*, 569-576; c) Y.-S. Ding, J. S. Fowler, N. D. Volkow, J. Logan, S. J. Gatley, Y. Sugano, *J. Nucl. Med.* **1995**, *36*, 2298-2305.
- (19) F. Wuest, M. Berndt, K. Strobel, J. van den Hoff, X. Peng, J. L. Neumeyer, R. Bergmann, *Bioorg. Med. Chem.* **2007**, *15*, 4511-4519.
- (20) D. F. Wong, B. Yung, R. F. Dannals, E. K. Shaya, H. T. Ravert, C. A. Chen, B. Chan, T. Folio, U. Scheffel, G. A. Ricaurte, J. L. Neumeyer, H. N. Wagner, M. J. Kuhnar, *Synapse* **1993**, *15*, 185-191.
- (21) L. Müller, C. Halldin, L. Farde, P. Karlsson, H. Hall, C. G. Swahn, J. Neumeyer, Y. Gao, R. Milius, *Nucl. Med. Biol.* **1993**, *20*, 249-255.
- (22) M. M. Goodman, C. D. Kilts, R. Keil, B. Shi, L. Martarello, D. Xing, J. Votaw, T. D. Ely, P. Lambert, M. J. Owens, V. M. Camp, E. Malveaux, J. M. Hoffman, *Nucl. Med. Biol.* **2000**, *27*, 1-12.
- (23) a) C. Lundquist, C. Halldin, C. G. Swahn, H. Hall, P. Karlsson, Y. Nakashima, S. Wang, R. A. Milius, J. L. Neumeyer, L. Farde, *Nucl. Med. Biol.* **1995**, *22*, 905-913; b) M. Yaqub, R. Boellaard, B. N. M. van Berckel, M. M. Ponsen, M. Lubberink, A. D. Windhorst, H. W. Berendse A. A Lammertsma; *J. Cerebr. Blood Flow Metab.* **2007**, *27*, 1397-1406.
- (24) a) P. Emond, L. Garreau, S. Chalon, M. Boazi, M. Caillet, J. Bricard, Y. Frangin, L. Mauclaire, J.-C. Besnard, D. Guilloteau, *J. Med. Chem.* **1997**, *40*, 1366-1372.
- (25) S. Chalon, H. Hall, W. Saba, L. Garreau, F. Dolle, C. Halldin, P. Emond, M. Bottlaender, J.-B. Deloye, J. Helfenbein, J.-C. Madelmont, S. Bodard, Z. Mincheva, J.-C. Besnard, D. Guilloteau, *J. Pharmacol. Exp. Ther.* **2006**, *317*, 147-152.
- (26) M. M. Goodman, P. Chen, Fluoroalkenyl nortropanes. *PCT Int. Appl.* **2000**, 37 pp. WO 2000064490 [*Chem. Abstr.* **2000**, 133, 331552]; b) P. Chen, C. Kilts, V. M. Camp, T. Ely, R. Keil, E. Malveaux, D. Votaw, J. M. Hoffman, M. M. Goodman, *J. Labelled Compd. Radiopharm.* **1999**, *42*, S400-S402; c) J. S. Stehouwer, P. Chen, R. J. Voll, L. Williams, J. R. Votaw, L. L. Howell, M. M. Goodman; *J. Labelled Compd. Radiopharm.* **2007**, *50*, S1, S335.
- (27) a) P. Frankhauser, Y. Grimmer, P. Bugert, M. Deuschle, M. Schmidt, P. Schloss, *Neuroscience Letters* **2006**, *399*, 197-201; b) D. Marazziti, S. Baroni, L. Fabbrini, P. Italiani, M. Catena, B. Dell'Osso, L. Betti, G. Giannaccini, A. Lucacchini, G. B. Cassano, *Neurochem. Res.* **2006**, *31*, 361-365.

- (28) C. Freed, R. Revay, R. A. Vaughan, E. Kriek, S. Grant, G. R. Uhl, M. J. Kuhar, *J. Comp. Neurol.* **1995**, 359, 340-349
- (29) P. C. Meltzer, A. Y. Liang, A. L. Brownell, D. R. Elmaleh, B. K. Madras, *J. Med. Chem.* **1993**, 36, 855-862.
- (30) L. Xu, M. L. Trudell, *J. Heterocycl. Chem.* **1996**, 33, 2037-2039.
- (31) www.loni.ucla.edu/ratdata/Rat.html

4.4 [¹¹C]PR04.MZ, a promising DAT-ligand for low concentration imaging: Synthesis, efficient ¹¹C-*O*-methylation and initial small animal PET studies

[¹¹C]PR04.MZ, a promising DAT-ligand for low concentration imaging: Synthesis, efficient ¹¹C-O-methylation and initial small animal PET studies

Patrick J. Riss,^{1,2*} Jacob M. Hooker¹, David Alexoff¹, Sun-Wong Kim¹, Joanna S. Fowler¹ and Frank Roesch²

¹ Medical Department, Brookhaven National Laboratory, Upton, NY 11973, USA

² Institute of Nuclear Chemistry, University of Mainz, Fritz-Strassmann-Weg 2, D-55128 Mainz, Germany

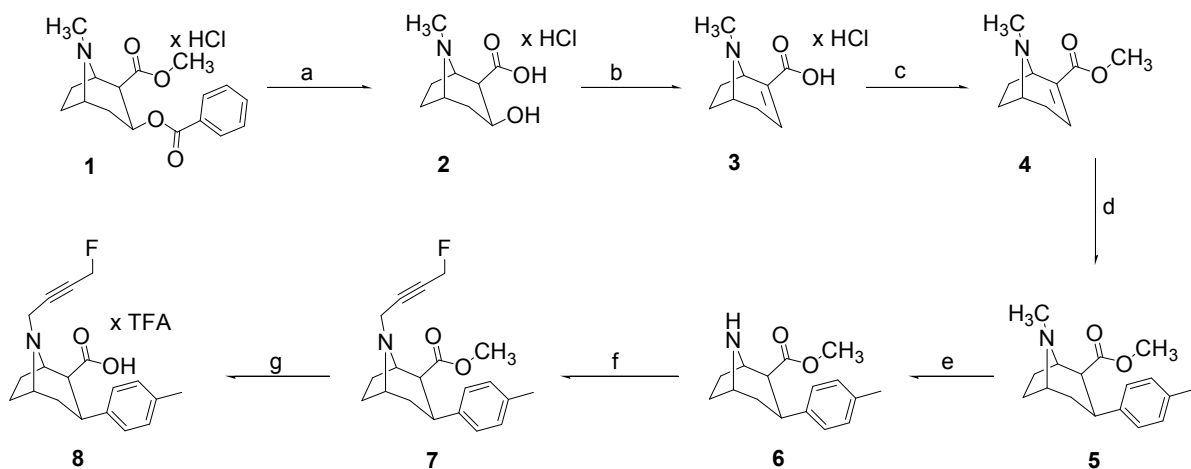
Abstract: PR04.MZ was designed as a highly selective dopamine transporter inhibitor, derived from natural cocaine. As a key feature, its structural design facilitates both, labelling with fluorine-18 at its terminally fluorinated butynyl moiety and carbon-11 at its methyl ester function. The present report concerns the efficient [¹¹C]MeI mediated synthesis of [¹¹C]PR04.MZ from an O-desmethyl precursor trifluoroacetic acid salt with Rb₂CO₃ in DMF in up to 95 ± 5 % labelling yield. A preliminary μPET-experiment demonstrates the reversible, highly specific binding of [¹¹C]PR04.MZ in the brain of a male Sprague-Dawley rat. [¹¹C]PR04.MZ may be suited as a PET-radioligand for the non-invasive exploration of striatal and extrastriatal DAT-populations.

Introduction: Non-invasive molecular imaging is an emerging interdisciplinary field of research. Among the available techniques for the visualisation of the biochemical and physiological function of biological tissue approached by suitable imaging probes, positron emission tomography (PET) provides great potential in terms of quantification, sensitivity, temporal and lateral resolution.¹ The dopaminergic system and in particular the presynaptic dopamine transporter (DAT) represent an important biological target for the development of specific PET-radioligands, due to its role in a variety of pathologies.²

PR04.MZ (**7**) is a highly potent (IC₅₀(hDAT) = 3 nM) selective DAT inhibitor (DAT/SERT > 100, DAT/NET ~10) derived from a new series of conformationally restricted cocaine derivatives for the application as PET-radioligands.³ It is currently under investigation for its suitability as a PET-tracer for in vivo imaging of the DAT in rodents and primates. Although it was specifically designed as an ¹⁸F-labelled radiopharmaceutical, one of its key features is the possibility to incorporate two different radiolabels. In this regard, both, ¹¹C labelling as well as ¹⁸F-fluorination provide specific advantages. The shorter half-life of ¹¹C permits multiple tracer injections into the same subject on the same day.⁴ Thereby, a variety of high value protocols for scientific studies, i.e. test-retest, test-block or baseline-challenge, can be performed in the same subject without altering the orientation within the gantry of a PET-camera. In contrast, fluorine-18 provides a more convenient half-life with regard to the total duration of the radio-synthesis, delivery to off-site PET-centers and total acquisition time of clinical PET examinations.⁵

The present work is concerned with a) the synthesis of non-radioactive **7** as reference, b) the synthesis of the carbon-11 labelling precursor, c) the highly efficient O-methylation of the carboxylic acid function of **8** and d) an initial, preliminary PET-study that underlines the feasibility of exploring the DAT using [¹¹C]-**7**.

The synthetic route to PR04.MZ (**7**) is illustrated in Scheme 1.



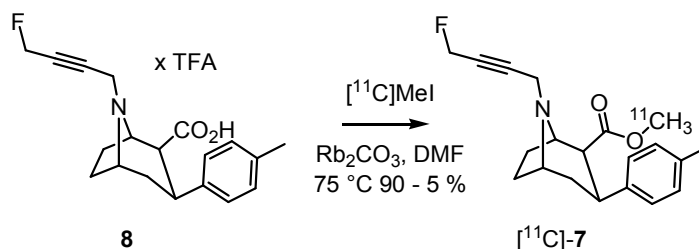
Scheme 1 Synthesis route to PR04MZ (**7**) and labelling precursor **8**; (a) 0.8 M HCl_{aq}, 14 h, reflux, 'quant'; (b) POCl₃, reflux, 90 min 'quant' (c) MeOH/HCl, -78 °C to RT, 14 h, 80 %; (d) 1. p-tolylMgBr, Et₂O/CH₂Cl₂, -43 °C, 3.5 h; 2. TFA/CH₂Cl₂, -78 °C, 30 min, 75 %; (e) 1. ACE-Cl, DiPEA, C₂H₄Cl₂, reflux, 90 min; 2. MeOH (anhydrous), 90 % (f) 4 Fluoro-but-2-ynyl chloride; DiPEA, MeCN, 70 °C, 12 h, 95 %; (g) 1 M HCl, reflux 1 d, 75 %.

Commercially available cocaine hydrochloride (**1**) was hydrolysed to ecgonine (**2**) using dilute hydrochloric acid. Subsequent 1,2-elimination in refluxing POCl₃ afforded the α,β -unsaturated acid anhydroecgonine (**3**) which was re-esterified under Fischer-conditions to afford the Michael-acceptor (**4**) in 80 % yield over three steps.^{7a} The latter was subsequently exposed to a two-fold excess of p-tolyl magnesium bromide in CH₂Cl₂/Et₂O at low temperature. The use of p-tolyl lithium via transmetalation to the Gillman-cuprate was also examined. Careful protonation followed by chromatographic purification afforded 75 % of the desired exo-isomer **5**.^{7b} Demethylation of **5** in refluxing dichloroethane containing 1-chloroethyl chloroformate (ACE-Cl) gave nortropine **6** in up to 90 % yield. PR04MZ (**7**) was obtained from (**6**) via alkylation with 4-fluoro-but-2-ynyl chloride in MeCN at 75 °C in a yield of 95%.³ Finally, the labelling precursor **8** was obtained by aqueous acidic hydrolysis of methyl ester **7** in refluxing dilute hydrochloric acid. HPLC-purification on a Phenomenex Luna[®] RP18 5 μ semipreparative column (10 x 250 mm, eluent: 40 % MeOH in 0.05 % TFA_{aq}) afforded the pure, slightly hygroscopic precursor in 60 % overall yield.⁸

Several groups have reported disappointingly low yields when employing an ammonium salt precursor for O-methylation.^{6a,b} In particular, the [¹¹C]MeI methylation of a variety of carboxylic acid functions demanded liberation of the free base prior to labelling.^{6a} In some cases, the highly reactive [¹¹C]methyl-source [¹¹C]methyltriflate ([¹¹C]MeOTf) had to be used.⁶

Analogous results were found when the initial labelling of PR04.MZ was conducted with an organic nitrogen base or common inorganic bases, such as sodium hydroxide or potassium carbonate. However, it was discovered that a system consisting of rubidium carbonate (Rb₂CO₃) as base, combined with dry DMF as solvent, affords [¹¹C]PR04MZ in high yield

(Scheme 2). Contrary to earlier reports, these conditions facilitate the use of readily available, high-specific-activity [^{11}C]MeI, together with a stable and insensitive TFA-salt precursor. Isolation of the free base can be avoided.



Scheme 2 Carbon-11 labelling of [^{11}C]PR04.MZ.

[^{11}C]Methyl iodide was obtained 14 - 18 min after EOB from a common GE [^{11}C]methyl iodide module (GE box). The radioactivity was trapped in DMF at room temperature and partitioned over multiple reaction vessels to facilitate screening.⁹ Appropriate labelling conditions were elucidated and verified in duplicate. Reaction of precursor **8** with [^{11}C]MeI in DMF or a 1:1 mixture of DMF and DMSO using common bases like sodium hydroxide, triethylamine, sodium or potassium carbonate or potassium hydrogen carbonate did not lead to acceptable radiochemical yields (0-7 %, Table 1). Following solubility considerations, we examined rubidium carbonate and cesium carbonate as alternatives. The use of these highly soluble bases strikingly increased the labelling yields for [^{11}C]MeI methylation. Initially, 1 mg of precursor **8** was used. In a typical synthesis for biological studies, 55 ± 10 mCi of [^{11}C]-**7** were obtained 45 min after the end of [^{11}C]CO₂-production (end of bombardment, EOB). HPLC-purification was performed using a Phenomenex[®] Luna[®] RP 18 semipreparative HPLC-column (dimensions 10 x 250 mm) as stationary phase. The mobile phase consisted of 0.1 M ammonium formate solution (36 % v:v) in acetonitrile. At a flowrate of 4.7 ml/min, the product eluted after a reasonable purification time (t_r ([^{11}C]-**7**) 13 ± 1 min) in a radiochemical purity of > 98 %.

Table 1: Impact of various bases on the radiochemical yield (RCY) of [^{11}C]MeI-supported methylation of precursor **8**

entry	base	solvent	RCY ^a / %
	1 M		
a	NaOH _{aq}	DMF	0
b	Na ₂ CO ₃	DMF	3 ± 1
c	K ₂ CO ₃	DMF	7 ± 1
d	Cs ₂ CO ₃	DMF	90 ± 8
e	Rb ₂ CO ₃	DMF	95 ± 5
f	Rb ₂ CO ₃	DMF/DMSO	92 ± 6

a: errors are given as one SEM.

All further reactions were carried out using system **e**, rubidium carbonate in DMF with a precursor concentration of 0.66 mg / ml. In a typical production run, base and precursor were weighed into a V-shaped borosilicate vial and 450 μl DMF were added. The volume was increased from 300 μl to 450 μl to increase the trapping efficiency. This vial was thoroughly

vortexed and connected to the [^{11}C]MeI delivery tubing. [^{11}C]MeI was directly trapped in this suspension. Subsequently, the vial was placed in an oil bath and heated to 75 °C for 5 min. The reaction mixture was quenched with HPLC-eluent, purified by HPLC and concentrated by rotary evaporation. After evaporation to dryness, the product was dissolved in sterile sodium chloride solution and passed through a small Millipore[®] sterile filter (0.22 μm) into a multi-injection vial (MIV). This simple process afforded [^{11}C]-7 in a total, non-decay corrected yield of 20 % and a radiochemical purity of greater than 98 % after 45 min of total synthesis duration. The specific activity of [^{11}C]PR04MZ at this point exceeded 1.8 Ci / μmol . A 300 g male adult Sprague-Dawley rat was used for a preliminary μPET -study in a CTI Focus 120 μImager . In a test-block experiment, the 300 g rat was anaesthetised with ketamine/xylazine (90/10, 100 mg/kg), and injected with approximately 1 mCi of the radiotracer, directly into the tail vein. A full-dynamic scan was performed for 60 min. Subsequently, the same animal was pretreated with 1.5 mg/kg of GBR12909, 45 min prior to the injection of a second 1 mCi dose of [^{11}C]PR04MZ. Data acquisition was started simultaneous to the injection of tracer and continued for 60 min.

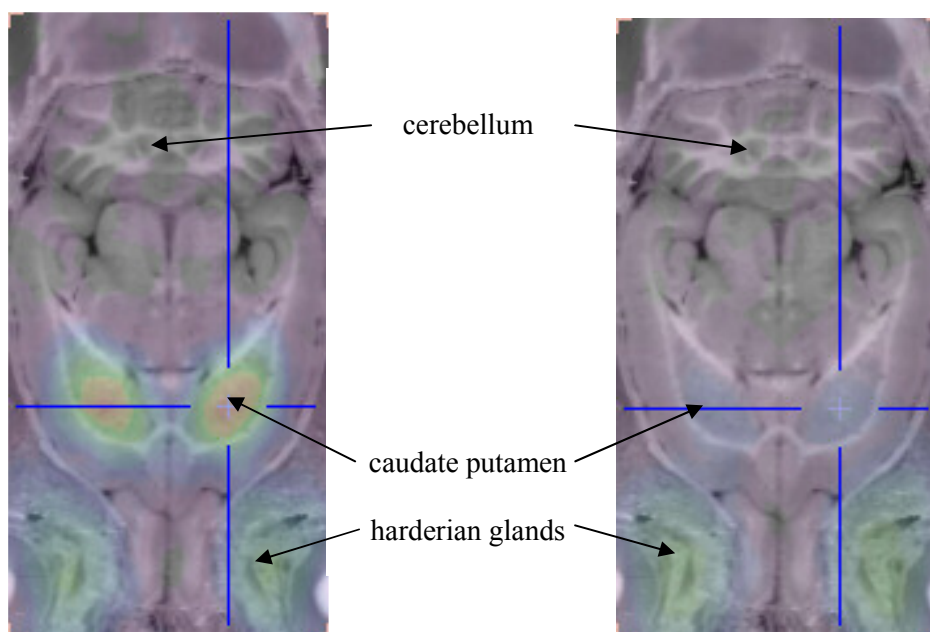


Figure 1: PET/MR-Fusion of brain images of [^{11}C]PR04.MZ (left: baseline; right: block)

Image reconstruction and coregistration was performed using the commercial image processing software p-mod (www.pmod.com). The LONI (www.loni.ucla.edu/ratdata/Rat.html) anatomical MR-atlas of the rat brain was used for PET/MR-fusion and the identification of brain regions. Regions of interest were drawn onto a MRI-template and copied into the co-registered μPET -datasets. The results are shown in figure 1. Peak uptake of 2.22 %ID/ cm^3 was achieved in the baseline scan 4 min post injection. The results clearly indicate the highly specific binding of [^{11}C]PR04.MZ to striatal DAT-binding sites in the rat brain. Figure 1 clearly illustrates the effect of GBR12909 pretreatment. In comparison to the baseline scan, a significant reduction in striatal radioactivity concentration can be observed within the blocking study. In contrast, the radioactivity accumulation in the harderian glands is increased in the pretreated animal compared to the

baseline scan. Furthermore, the radioactivity concentration ratios between the *striatum* and the *cerebellum* after pretreatment are significantly lower (cf. table 2). Pre-treatment with the highly selective DAT-inhibitor leads to a significant decrease in the total activity accumulation in the basal ganglia. These findings may indicate the highly selective binding of PRD04 to rat dopamine transporters (rDAT).

In conclusion, an acid ammonium salt labelling precursor for [¹¹C]PR04.MZ has been prepared and successfully labelled with [¹¹C]methyl iodide in high yield. In a typical production run, 55 ± 10 mCi of injectable radiotracer were obtained after 44 min.

Table 2: Quantitative uptake of [¹¹C]PR04.MZ and distribution volume ratios for striatum and cerebellum, derived from the preliminary μPET-study. a) time-frame of the μPET-scan; b) radioactivity-concentration ratio

aquisition time	%ID(striatum) / cm ³	Striatum / Cerebellum	BP(striatum)	%ID(striatum) / cm ³	Striatum / Cerebellum	BP(striatum)
15 min	2.03	2.41	3.4	2.11	1.25	2.25
30 min	2.13	3.55	4.6	1.59	1.67	2.67
60 min	2.06	5.03	6.0	1.15	1.61	2.61

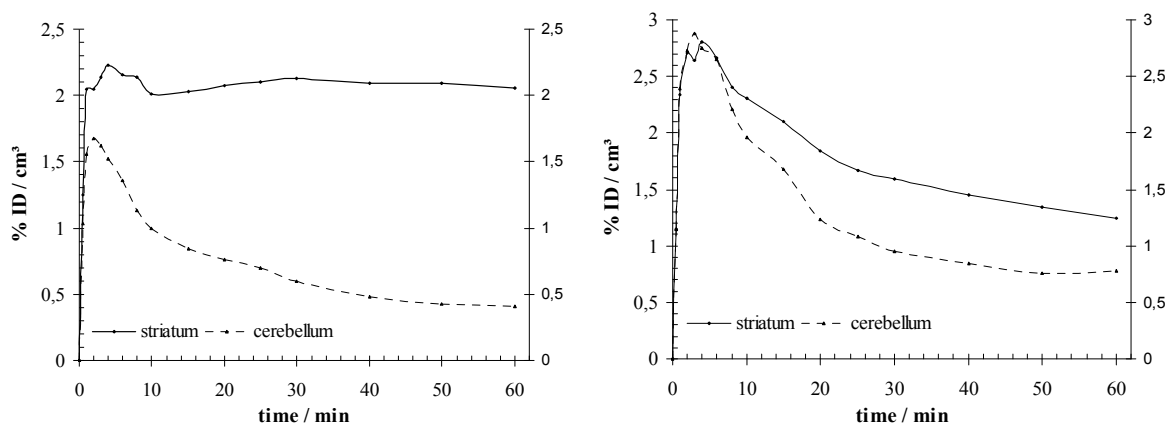


Figure 2: time activity curve for [¹¹C]PR04MZ for the baseline scan compared to time activity curve for the blocking study

The value [¹¹C]PR04MZ as a highly selective probe for the presynaptic DAT has been assessed by an preliminary rat study. The results indicate highly selective binding at rat dopamine transporters. The reversibility of the highly selective DAT-ligand was proved by pretreatment with a structurally non-analogous DAT-inhibitor (GBR12909).

References and Notes

- (1) a) M.-C. Lasne, C. Perrio, J. Rouden, L. Barré, D. Roeda, F. Dolle, C. Crouzel, *Top. Curr. Chem.* **2002**, 222, 201; b) L. Cai, S. Lu, V. W. Pike, *Eur. J. Org. Chem.* **2008**, 2853.
- (2) a) J. S. Fowler, N. D. Volkow, A. P. Wolf, S. L. Dewey, D. J. Schlyer, R. R. Macgregor, R. Hitzemann, J. Logan, B. Bendriem, S. J. Gatley, et al. *Synapse* **1989**, 4, 371-77; b) N. D. Volkow, J. S. Fowler, S. J. Gatley, J. Logan, G.-J. Wang, Y.-S. Ding, S. Dewey, *J. Nucl. Med.* **1996**, 37, 1242-1256; c) J. O. Rinne, J. Bergman, H. Ruottinen, M. Haaparanta, E. Eronen, V. Oikonen, P. Sonninen, O. Solin; *Synapse* **1999**, 31, 119 – 124.
- (3) P. J. Riss, R. Hummerich, P. Schloss, F. Roesch, *ChemMedChem* **2008**, in press, DOI:
- (4) G. Antoni, T. Kihlberg, B. Langstrom in *Handbook of Nuclear Chemistry* 4, Kluwer Academic Publishers, Dordrecht, **2003**, pp. 119-165.
- (5) H. J. Wester in *Handbook of Nuclear Chemistry* 4, Kluwer Academic Publishers, Dordrecht, **2003**, pp. 166-202.
- (6) a) F. Dolle, M. Bottlaender, S. Demphel, P. Emond, C. Fuseau, C. Coulon, M. Ottaviani, H. Valette, C. Loc'h, C. Halldin, L. Mauclaire, D. Guilloteau, B. Maziere, C. Crouzel, *J. Labelled Compd. Radiopharm.* **2000**, 43, 997-1004; b) C. Lundkvist, J. Sandell, K. Nagren, V. W. Pike, C. Halldin, *J. Labelled Compd Radiopharm.* **1998**, 41, 545-556; c) K. Nägren, C. Halldin, L. Müller, C.-G. Swahn, P. Lehtikoinen, *Nucl. Med. Biol.* **1995**, 22, 965-970.
- (7) a) P. C. Meltzer, A. Y. Liang, A. L. Brownell, D. R. Elmaleh, B. K. Madras, *J. Med. Chem.* **1993**, 36, 855; b) L. Xu, M. Trudell, *J. of Heterocycl. Chem.* **1996**, 33, 2037-2039.
- (8) ¹H-NMR(CDCl₃, 300 MHz) δ in ppm: 10.09 (brs, 1H), 4.95 (d, *J*_{HF} = 47.5 Hz, 2H), 4.34 – 4.18 (m, 2H), 3.81 – 3.66 (m, 1H), 3.36 – 3.24 (m, 1H), 3.16 – 2.98 (m, 2H), 2.78 (dt, *J* = 12.5 Hz, *J* = 2.9 Hz), 2.39 – 2.29 (m, 2H), 2.27 (s, 3H), 1.98 – 2.18 (m, 3H), 1.96 – 1.84 (m, 2H). ¹³C-NMR(CDCl₃, 100 MHz) δ in ppm: HRMS(ESI): 316.1723 (M⁺) C₁₉H₂₃FNO₂ requires 316.1713.
- (9) **Base screening experiments were conducted as follows:** Standard 5 ml screw-cap vials were charged with base (2 equiv.), x-y mmol) and **8** was added (0.3-1 mg,). The solids were suspended in either DMF (0.15 ml, for reactions in pure DMF) or DMSO (0.15 ml, for reactions in a mixture of DMSO and DMF). These vials were placed in a self-made multi-vial holder and placed above an oil bath, prior to the addition of 150 µl of DMF, containing [¹¹C]MeI (1-2 mCi). The oil bath was elevated and the vials were heated for 5 min at 75 °C. The heat-source was removed subsequently, and the reaction was immediately quenched by the addition of HPLC-eluent (1 ml). At this point, the activity inside the vial was measured and an aliquote was withdrawn to determine the radiochemical yield by HPLC and TLC. The results are summarised in Table 1.

**4.5 Comparison of [¹¹C]PR04.MZ and [¹⁸F]PR04.MZ
in *anubis papio* baboons:
A selective high-affinity DAT-ligand for low concentration
imaging of the extra-striatal dopamine transporter**

Comparison of [^{11}C]PR04.MZ and [^{18}F]PR04.MZ in *anubis papio* baboons: A selective high-affinity DAT-ligand for low concentration imaging of the extra-striatal dopamine transporter

P. J. Riss^{1,2}, J. M. Hooker², C. Shea², Y. Xu², P. Carter³, D. Warner³, S.-W. Kim²,
J. S. Fowler^{2,3} and F. Roesch¹

¹Institut für Kernchemie, Johannes Gutenberg University, Fritz Strassmann Weg 2, D-55128 Mainz, Germany

²Medical Department and ³PET-Imaging Group, Brookhaven National Laboratory, Upton, NY 11973, USA

Abstract: N-(4-fluorobut-2-yn-1-yl)-2b-carbomethoxy-3b-(4'-tolyl)nortropane (PR04.MZ) is a novel candidate for the non-invasive exploration of the cerebral dopamine transporter (DAT). An adult female *papio anubis* baboon was studied using a test-retest protocol with [^{11}C]PR04.MZ and [^{18}F]PR04.MZ. The injected doses ranged from 5.44 mCi to 0.51 mCi. Dynamic listmode PET was conducted on a Siemens ECAT HR+ PET camera. Automated blood sampling was performed throughout the studies for plasma input and metabolite analysis. Metabolite-corrected plasma input functions were derived from the blood samples. The initial frames of the dynamic PET data were summed for coregistration with [^{18}O]H₂O cerebral perfusion images and the obtained transformations (PET-PET) were used for coregistration of the individual dynamic PET data with the LONI-MR-atlas of the baboon brain. Regions of interest were drawn onto the anatomical MR-image and copied into the dynamic PET data. Time-activity curves and distribution volumes (DVs) were derived for the putamen, the caudate nucleus, the nucleus accumbens, the midbrain and the cerebellum. Distribution volumes (DV) for various brain regions were obtained from Logan-plot analysis and binding potentials were calculated according to the two compartment simplified-reference-tissue-model (SRTM). [^{11}C]PR04.MZ and [^{18}F]PR04.MZ show a rapid, relatively high uptake into the DAT-containing brain regions inside and outside the striatum and low non-specific binding.

Introduction

Presynaptic transmembrane transporter mediated neurotransmitter reuptake is crucial for the mediation of monoamine signal transduction (Hersch et al. 1997). This class of neurotransmitter sodium symporters has attracted a veritable interest for the visualisation of either reuptake dysfunction or downstream visualisation of monoamine transporter effecting pathologies with positron emission tomography (PET) (Laakso et al. 2000, Marshall et al. 2003a, Bergstrom et al. 2001, Laruelle et al. 2002). In this regard, the dopamine transporter (DAT) is related to a variety of neuro-degenerative and psychiatric diseases (Laakso et al. 2003). Radiolabelled DAT-ligands are established for the early clinical diagnosis of Parkinson's disease (PD) and the differentiation of the former from symptomatically related disorders. Although a variety of compounds has already been evaluated and successfully utilised for studies of the striatal DAT, the search for an ideal high affinity candidate, suitable

[¹⁸F]PR04.MZ in the same *papio anubis* baboon has been conducted.

Methods and Results

Chemistry

[¹¹C]PR04.MZ and [¹⁸F]PR04.MZ were obtained as published elsewhere (Riss et al. 2008b,c).

In vitro studies

Prior to the baboon imaging studies, PR04.MZ was screened for hDAT, hSERT and hNET-inhibition potency as well as binding affinity in HEK 293 cells, stably transfected with hDAT, hSERT and hNET (Frankhauser et al. 2006, Hummerich et al. 2004). For clarity, these results are summarised in table 1. An experimental log D_{7.4}, determined by HPLC (OECD 2004) and the plasma protein binding results are also shown. The plasma-protein binding of PR04.MZ was determined in baboon plasma, during the first baboon study. Neostigmine was added to the baboon plasma to inhibit the acetylcholine esterase-mediated cleavage of the [¹¹C]methyl ester label (Ambre et al. 1986, Schwartz et al. 1996). It was found, that approximately 4.5 % of the total injected radioactivity dose was free in the plasma.

Plasma protein binding of [¹¹C]PR04.MZ

The percentage of unbound, available tracer in baboon plasma was determined in two independent experiments, wherein one experiment was conducted in the presence of 10 µl neostigmine to inhibit enzymatic metabolism of [¹¹C]PR04.MZ. Therefore the amount of plasma, used for the determination was spiked with neostigmine, 2 min prior to the addition of radioactivity. Each experiment was performed in duplicate as follows: Baboon plasma (600 µl) was charged with an aliquot of known activity of the formulated radiotracer. This mixture was incubated at room temperature for 10 min. Three aliquots (30 µl) of the plasma containing [¹¹C]PR04.MZ were transferred into vials for measuring radioactivity. An aliquot (200 µl) of the incubated mixture was transferred into a centrifuge tube and centrifuged for 10 min at 5000 rpm. Three samples (20 µl) of the fraction containing the unbound radiotracer were withdrawn and measured. The amount of free radiotracer was calculated according to equation 1:

$$\%_{unbound} = \frac{I_{(unbound)}}{(I_{(bound)} + I_{(unbound)})} \times 100\%; \quad I = \text{decay and efficiency corrected impulse rate (1)}$$

Metabolite analysis

The percentage of intact radiotracer in the plasma of the baboon was determined according to a literature solid phase extraction (SPE) procedure (Alexoff et al. 1995). The plasma was passed through a Waters SepPak C-18 solid phase extraction (SPE) cartridge to trap the organic, radioactive content. The cartridge was sequentially eluted with decreasing polarity and the fractions were counted (Alexoff et al. 1995). The results were validated via an HPLC-method (Ding et al 2003). For HPLC-analyses a Spherex[®] 5µ C18 column was used as stationary phase. The mobile phase consisted of methanol-0.1 ammonium formate buffer, 8:2 at a flow rate of 1.0 ml/min). The sampled radioactivity from the blood was spiked with the non-radioactive reference compound PR04.MZ to confirm the retention time of the intact tracer by co-elution with the UV-reference. The metabolite-corrected plasma radioactivity is

plotted in Figure 2. Furthermore the integral blood input curve was derived from these data. To estimate the cerebral metabolism of [¹¹C]PR04.MZ and potential penetration of a polar metabolite into the brain, a male Sprague Dawley rat was anaesthetised with khetamine/xylazine, injected with 1 mCi of [¹¹C]PR04.MZ, allowed to wake up and to move freely within the cage for 60 min.. The animal was sacrificed 60 minutes p.i. and the brain was rapidly dissected. The rat brain was homogenised by grinding under methanol. The supernatant was cleared by centrifugation and an aliquot was analysed by HPLC. It was found, that about 95 % of the tracer remained intact in the brain, whereas no intact tracer was found in the rat blood at this time-point. No major metabolite was found in the brain. Furthermore, the potential metabolite O-[¹¹C]methyl 3exo-phenyl-8-azabicyclo[3.2.1]octane-2exo-carboxylate was neither found in the blood nor in the brain of both species, rat and baboon.

Animal studies

All animal studies were approved by the Brookhaven Animal Care and Use Committee. All experiments were conducted according to the legislation for animal handling and care. Rats were obtained from Charles River Laboratories and housed under standard conditions (access to standard food and water, 55±5 % humidity, 21 °C, lights on 6:00, lights off 18:00). An adult, female *papio anubis* baboon (“Daisy”, 17.3±0.1 kg) was used for PET imaging experiments and allowed to rest for at least four weeks in between two studies. The animal was kept under standard conditions and supplied with compensatory food (vitamins and iron).

Primate imaging

An adult female baboon was immobilised via an intra-muscular injection of ketamine hydrochloride (10 mg/kg), weighed, intubated and transported to the PET facility. The head of the baboon was positioned in the center of the field of view of a Siemens ECAT EXACT HR+ high resolution (63 slices, 4.5×4.5×4.8 mm) pet camera. For attenuation correction of the emission data, a transmission scan was conducted with a rotating ⁶⁸Ge/⁶⁸Ga rotating source. The animal was kept on isoflurane anaesthesia (oxygen and isoflurane) throughout the PET study, and vital signs (blood pressure, heart rate, respiration) were monitored. A venus line was attached to an antecubital vein for i.v. injection and a arterial line was introduced into the radial artery for blood sampling. Dynamic emission scans were conducted for 90 min with [¹¹C]PR04.MZ (2 x 35 frames: 1 x 10 s, 12 x 5 s, 1 x 20 s, 1 x 30 s, 8 x 60 s, 4 x 300 s, 8 x 450 s; 1 x 39 frames: 1 x 10 s, 12 x 5 s, 1 x 20 s, 1 x 30 s, 8 x 60 s, 16 x 300 s) and for 180 min with [¹⁸F]PR04.MZ (57 frames: 1 x 10 s, 12 x 5 s, 1 x 20 s, 1 x 30 s, 8 x 60 s, 34 x 300 s). A displacement study was conducted, consisting of a dynamic emission scan for 60 min with [¹⁸F]PR04.MZ (20 frames: 10 x 60 s, 10 x 300 s). A test-retest protocol was conducted in a female adult baboon (“Daisy, 17.3 ± 0.1 kg”) with [¹¹C]PR04MZ. The dynamic imaging data were co-registered with a MR-atlas of the baboon brain and regions of interest (ROI) were drawn into the MR-template, copied to the dynamic data and quantified. The resultant time-activity-curves are shown in Figure 3. The dose accumulation within the brain regions containing the DAT in lower concentrations is equally rapid but the washout rate is steeper compared to the DAT-rich brain regions. In contrast, hippocampal as well as cortical radioactivity remains slightly below the cerebellum level throughout the whole study (not shown).

Image and data analysis

Reconstruction of the listmode data was conducted via the application of filtered back projection on the attenuation corrected sinograms. The initial PET frames were summed and coregistered with a H₂[¹⁵O] cerebral perfusion image of the LONI baboon atlas (www.LONI-atlases.org). An MR-template was copied into the co-registered PET images and the dynamic data was loaded. Regions of interest (ROI) were drawn onto the co-registered MR-templates and copied into the dynamic PET-images using the commercial image processing software p-mod (www.pmod.com). Time activity curves (TACs) for cerebellum, frontal cortex, midbrain, thalamus, and striatum were expressed as percent of the decay corrected injected dose (% ID)/cm³ above time. For comparison, the standard uptake volumes (SUV) were calculated according to equation 2 and plotted versus time.

$$SUV = \frac{\%ID}{cm^3} \times \frac{1}{m_{rat}}; [SUV] = \frac{g}{cm^3} \quad (2)$$

Distribution volumes and K_1 for brain ROIs were calculated from the TACs and the metabolite-corrected plasma-input function using Logan plot analysis (1990). The TACs, plasma-input function and metabolite profiles of [¹¹C]PR04.MZ and [¹⁸F]PR04.MZ were compared. Quantification of the images was conducted via Logan Plot analysis (Logan et al 1996, Logan 2000) and distribution volumes (DV), binding potentials (BP, from simplifies two compartment reference tissue model) as well as influx and efflux constants were determined for various brain regions.

Discussion and Conclusion

The present study is concerned with the successful initial evaluation of the compound PR04.MZ in the primate brain. PR04.MZ is a high affinity (IC₅₀_{hDAT}: 2 nM) DAT-selective (SERT/DAT-selectivity: >50; NET/DAT-selectivity: >10) monoamine transporter ligand. Its affinity exceeds those reported for other high-affinity DAT-ligands for PET of similar selectivity, such as PE2I (K_d: 4 nM), FECNT (K_i: 8 nM) or LBT-999 (K_d: 9 nM).

Table 1: *In vitro*-affinity data for PR04.MZ

hDAT _{IC50}	hDAT _{IC50}	hSERT _{IC50}	hSERT _{IC50}	hNET _{IC50}	hNET _{IC50}	% unbound	logD _{7.4}
[3H]DA	[3H]WIN	[3H]5-HT	[3H]Citalopram	[3H]NE	[3H]Nisoxetine	in plasma	HPLC
3.26±0.49	1.93±0.2	239.77±3.67	108.4±1.3	31.04±0.58	22.48±0.83	4.4±0.1	2.7±0.2

PR04.MZ offers two sites for the convenient covalent introduction of a positron emitting radionuclide. In particular, the terminally fluorinated fluorobut-2-yn-1-yl chain facilitates the use of the longer-lived fluorine-18-tag, whereas the methyl-ester function can be substituted for an [¹¹C]methyl label. In general, both radionuclides are well suited for PET. However, each label provides specific advantages related to its half-life. Furthermore, the differential structural location of both different labels allows insights into the metabolism of the compound *in vivo*. Therefore, the DAT-ligand was labelled in these positions with either carbon-11 or fluorine-18 to obtain [¹¹C]PR04.MZ and [¹⁸F]PR04.MZ, respectively. These two

compounds were applied in a baboon PET study to further elucidate the characteristics of the tracers in the primate brain.

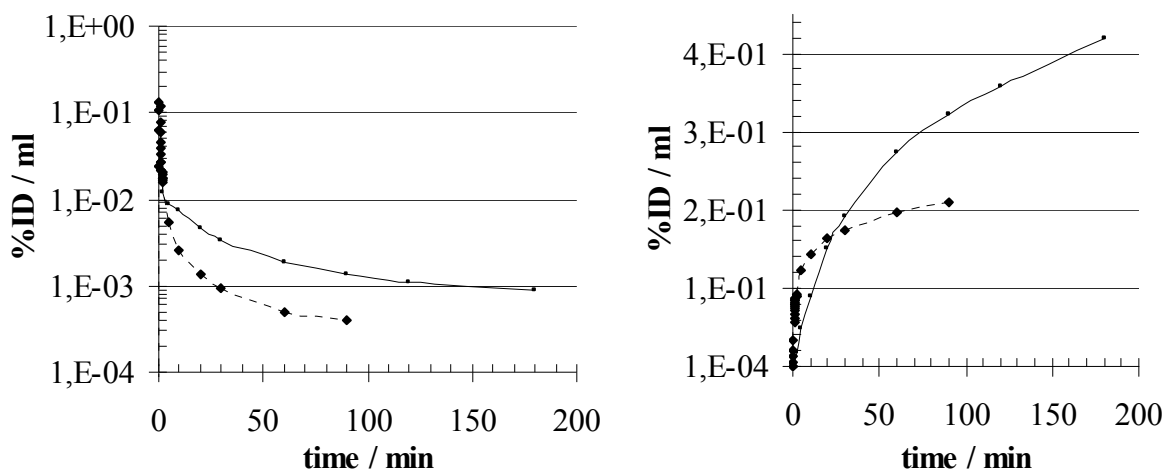


Figure 2: Metabolite corrected plasma activity curve (left) and integral input curve (right) for [^{11}C]PR04.MZ (dashed line) and [^{18}F]PR04.MZ (continuous line)

The plasma metabolism of the two different compounds was assessed via online blood sampling throughout the scan. The blood plasma was analysed and the percentage of intact tracer at each time-point was used to derive the plasma input function for both compounds. [^{11}C]PR04.MZ is rapidly metabolised in the plasma as illustrated in figure 2. Only 33 % of the intact tracer were found in the plasma at 30 min p.i..

However, no major metabolite of [^{11}C]PR04.MZ or [^{18}F]PR04.MZ has crossed the blood brain barrier in Sprague-Dawley rats 60 min p.i. (Riss et al. 2008c). Instead, more than 95 % of the intact tracer was present in the brain at this timepoint. The same might be expected for the baboon brain. [^{18}F]PR04.MZ instead is metabolised less rapid. Up to 45 % of the intact tracer were found within the blood even 180 min p.i. Apart from the different localisation of the radionuclide within the chemical structure of the tracer that can lead to different radioactive metabolites, the extensive metabolism of [^{11}C]PR04.MZ, including potential metabolites could also be related to methyl-ester cleavage by acetylcholine esterase, as reported for [^{11}C]cocaine (Fowler et al, date). N-desalkylation however did obviously not occur, as shown by comparison of the HPLC-metabolite profile with the retention time of the N-desalkyl nortropane-skeleton of PR04.MZ. Nevertheless, a similar rapid metabolism has also been reported for PE2I, FECNT and LBT-999 (Chalon et al. 1999, Goodman et al. 2000, Saba et al. 2007). Wherein especially LBT999, PE2I and PR04.MZ contain activated allylic sites at the tolyl moiety which might be sensitive to oxidative metabolism. The olefinic residues in all mentioned compound might furthermore be sensitive to p450 mediated degradation. In contrast to e.g. N- ^{11}C cocaine, one potential metabolite resulting from N-desalkylation, can be excluded for PR04.MZ. It was found that no radioactive metabolite was formed from [^{11}C]PR04.MZ that corresponded to this retention time. This hints on an increased stability towards N-desalkylation compared to N- ^{11}C cocaine (Gatley et al. 1994)

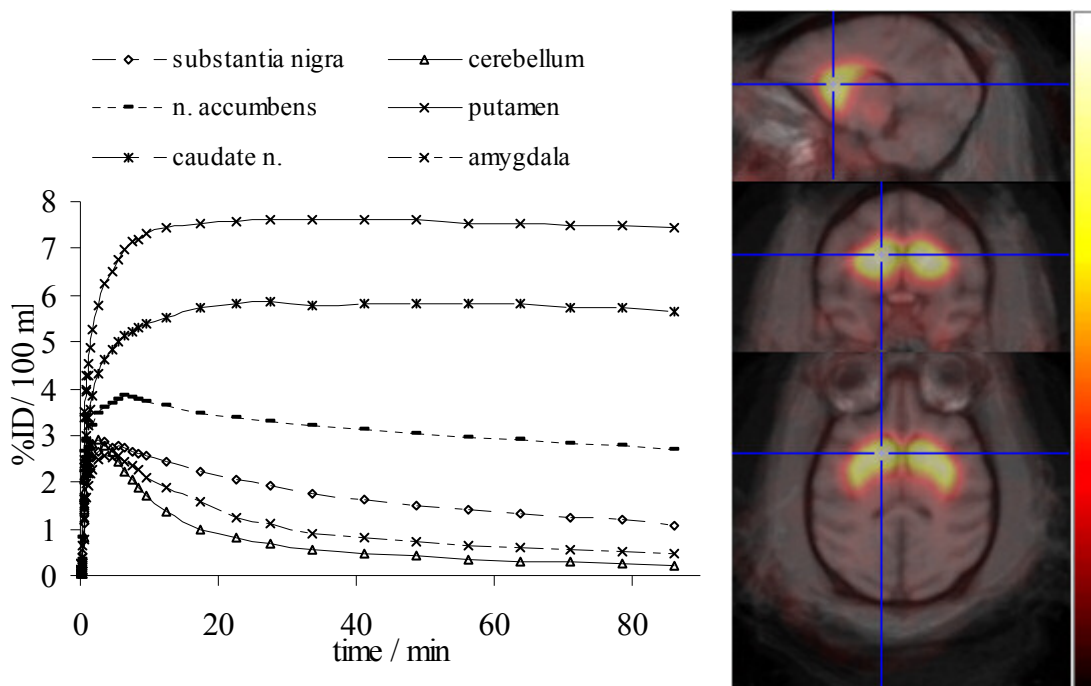


Figure 3: Time activity curves for $[^{11}\text{C}]$ PR04.MZ in various baboon brain regions (left) and sagittal, transversal and coronal view on MR/PET-fusion images of the basal ganglia.; Results are mean values from a test-retest protocol.

The uptake kinetics for both compounds were recorded in the striatal and extra-striatal DAT-domains in the same baboon. Tissue-to-reference ratios were determined for the DAT-containing regions of the basal ganglia, the thalamus as well as the extra-striatal domains located in the midbrain. The midbrain consists of two brain regions that have been identified as the origins of the three different dopaminergic signal pathways. In particular, the tegmental area can be regarded as the source region for the meso-cortico-limbic pathway. These dopaminergic neurons project into the nucleus accumbens and from there into some cortical regions. Dysfunction and alterations of this pathway have been brought into relation with mood-disorders, drug abuse, eating disorders and psychosis. Furthermore, the substantia nigra contains the origins of the nigro-striatal dopaminergic pathway, which is involved with the inhibitory regulation of movement. Today, the degradation of the striatal dopamine biosynthesis is regarded as a downstream effect of the depletion of dopaminergic neurons in this brain region in Parkinson's disease (PD). Furthermore, PET-imaging has revealed a relationship between lesions in the substantia nigra and the abundance of ADHD in children.

Therefore, a significance of radioactive markers for the integrity of midbrain DA-neurons can be deduced. In this regard, the novel radiotracers $[^{11}\text{C}]$ PR04.MZ and $[^{18}\text{F}]$ PR04.MZ may provide quantitative, dynamic insights into the pathobiochemistry of the described pathologies and furthermore enable the exploration of the upstream causes of the effects in the basal ganglia observed in earlier studies.

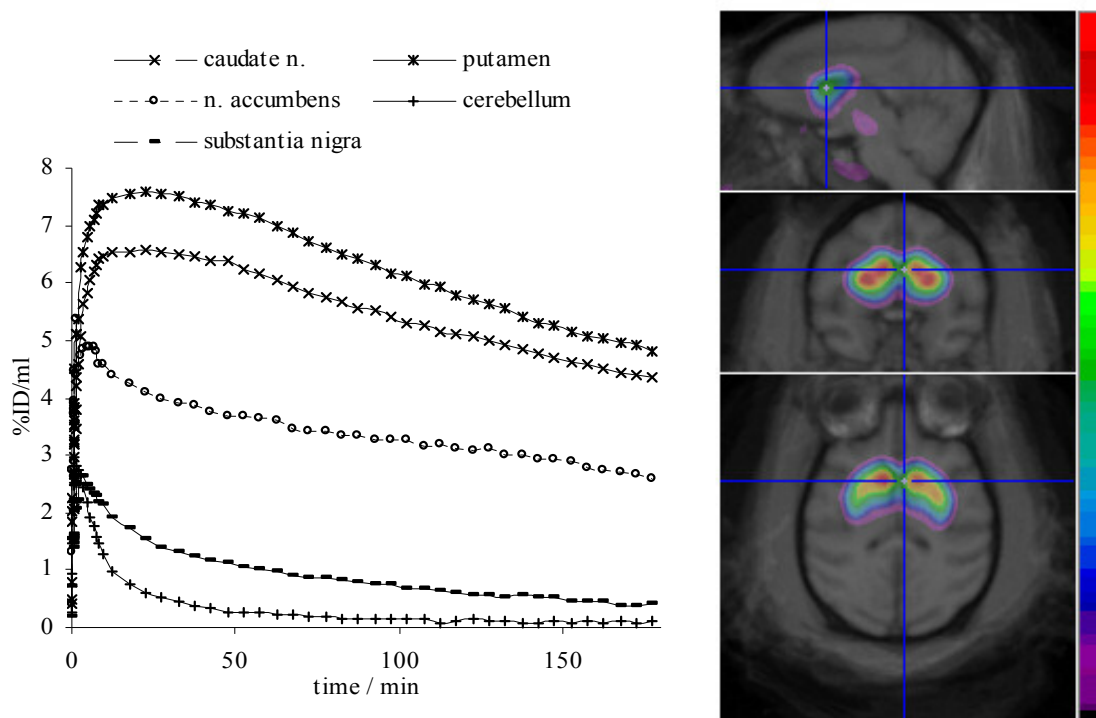


Figure 4: Long-term scan with $[^{18}\text{F}]\text{PR04.MZ}$, time activity curves (left) for various baboon brain regions and sagittal, coronal and transversal view on PET/MR-fusion images of the basal ganglia

Table 2: Region-to-cerebellum ratios for various baboon brain regions for $[^{11}\text{C}]\text{PR04.MZ}$

timeframe	Ptm/Cbl	Cdt/Cbl	Acb/Cbl	Mbn/Cbl
12.5	5.4	4.0	2.6	1.8
17.5	7.5	5.6	3.5	2.2
22.5	9.4	7.1	4.2	2.5
45.0	17.3	13.3	7.0	3.6
71.3	25.8	20.0	9.7	4.3
86.3	31.7	24.1	11.5	4.6

Both compounds show a high uptake into the DAT-rich brain regions (cf. Figures 4 and 5), such as the putamen ($[^{11}\text{C}]\text{PR04.MZ}$: 7.6 %ID / 100 ml, 27.5 min p.i.; $[^{18}\text{F}]\text{PR04.MZ}$: 7.6 %ID/ 100 ml, 22.5 min p.i.) and the caudate nucleus ($[^{11}\text{C}]\text{PR04.MZ}$: 6.8 %ID / 100 ml, 27.5 min p.i.; $[^{18}\text{F}]\text{PR04.MZ}$: 6.6 %ID/ 100 ml, 22.5 min p.i.). The whole brain uptake peaked in the early time frames for both compounds, for $[^{11}\text{C}]\text{PR04.MZ}$ 22.6 %ID/ 100 ml after 3.5 min and for $[^{18}\text{F}]\text{PR04.MZ}$ 29.6 %ID/ 100 ml after 2.5 min, respectively. Both radiotracers exhibit a very low non-specific binding, which is convincingly underlined by the fast washout from the brain regions with a very low DAT-density, such as the cerebellum. In this regard, the cerebellum can be used as reference region for the simplified quantification using the two compartment reference-tissue-model. (Logan et al. 1996, Logan 2000)

Table 3: [¹¹C]PR04.MZ: Distribution volumes (DV) from Logan plots after an acquisition time of 30 min, binding potentials (BP) from simplified reference tissue model (STR-model), influx constant K₁ and efflux constant k₂ from two compartment reference tissue model)

[¹¹ C]PR04.MZ	DV (Logan)	BP (SRT-model)	K ₁	k ₂
cerebellum	4	1	0.144	0.036
midbrain	12.4	3.1	0.064	0.016
accumbens	35.8	8.9	0.030	0.0076
caudate n.	118	29.5	0.017	0.004
putamen	147.6	36.9	0.015	0.004

Values from three independent studies with [¹¹C]PR04.MZ.

These findings are in accordance with the results reported for the mouse and the rat brain as reported previously (Riss et al. 2008). As a result from the low non-specific accumulation, remarkable tissue-to-cerebellum ratios were achieved within the domains of the dopamine transporter in the mammalian brain (tables 2 and 3). These are higher than those reported for PE2I (Chalon et al. 1999), FBCNT (Goodman et al. 2000) and LBT-999 (Saba et al 2007), although FBCNT and LBT-999 show a higher dose uptake into the corresponding brain regions. Freed and coworkers have reported the immunochemical detection of the DAT-RNA in rat brain sections by autoradiography (Freed et al. 1995). The results reported by these investigators are in good accordance with the regional distribution found for PR04.MZ in the primate brain. These are furthermore comparable to the cerebral distributions reported for similar DAT-ligands such as PE2I (Chalon et al. 1999), FECNT (Goodman et al. 2000) and LBT-999 (Saba et al. 2007). As expected, both ligands are significantly retained within the midbrain (striatum-to-cerebellum ratios: [¹¹C]PR04.MZ: 4.6 ± 0.3 , 90 min p.i.; [¹⁸F]PR04.MZ: 4.6, 90 min p.i.). The binding equilibrium necessary for quantitative studies within this brain region is already reached 20 min p.i. The midbrain is clearly distinguishable from the surrounding tissue within the summed PET images, as shown in figures 4 and 5.

Table 4: [¹⁸F]PR04.MZ: Distribution volumes (DV) from Logan plot analysis, binding potentials from simplified reference tissue model (BP (SRT-model)) influx constant (K₁) and efflux constant (k₂) for various DAT-containing brain regions

[¹⁸ F]PR04.MZ	DV (Logan)	BP (SRT-model)	K ₁	k ₂
cerebellum	1.6	1	0.08	0.049
midbrain	4.8	3.1	0.062	0.038
accumbens	19.8	12.1	0.026	0.016
caudate n.	32.9	20.5	0.024	0.015
putamen	37.6	23.5	0.025	0.015

To verify the specific, reversible binding of the compound to the DAT, a displacement study has been conducted with the structurally non-analogue DAT-ligand GBR12909 after a 3 h long-term scan with [¹⁸F]PR04.MZ. The specifically bound tracer was successfully challenged with 2.0 mg/kg of GBR12909 and more than 80% of the bound radioactivity were displaced and washed out of the brain. However, the two different compounds do not behave equal in terms of uptake kinetics and equilibrium. [¹⁸F]PR04.MZ rapidly accumulates in the DAT-containing brain regions. In contrast to the carbon-11 labelled analogue, [¹⁸F]PR04.MZ shows a significantly more rapid washout behaviour. In numbers, the high initial uptake of 7.6 % ID/ 100 ml, 22.5 min p.i., is reduced to 6.1 % after 100 min and to 4.8 % after 180 min.

This kinetic profile is predominantly beneficial for clinical routine applications of [¹⁸F]PR04.MZ, with respect to more rapid binding equilibria. This will certainly result in shorter clinical PET-data acquisition times and yield a reduced scanner occupation.

In order to assess the main feature of the carbon-11 labelled analogue, a test-retest study was conducted with [¹¹C]PR04.MZ in the same baboon on the same day. The acquisition time was 90 min for the test-scan, followed by a 30 min break and a 90 min retest scan. The injected doses were 5.44 mCi and 4.70 mCi, respectively, for test and retest. [¹¹C]PR04.MZ shows a rapid accumulation into the DAT-containing brain regions followed by differential washout rates among the different regions of interest (Figure 4). In general, the washout is slower than for the fluorine-18 labelled analogue and basically the same dose concentrations are found within the striatum from 25 min p.i (7.52 %ID/100ml) to 90 min (7.48 %ID/ 100 ml). The time activity curves for both scans were compared to calculate the test-retest reliability. Both scans showed almost perfect correlation (0.89) and a reliability of 0.94 has been calculated using the split-halves method. These findings indicate the suitability of [¹¹C]PR04.MZ for multi-injection or multi-tracer PET protocols.

In conclusion, both radiotracers provide specific advantages, ¹¹C is particularly suited for multi-tracer studies or multi-injection protocols, such as test-retest, baseline-block or baseline-challenge.

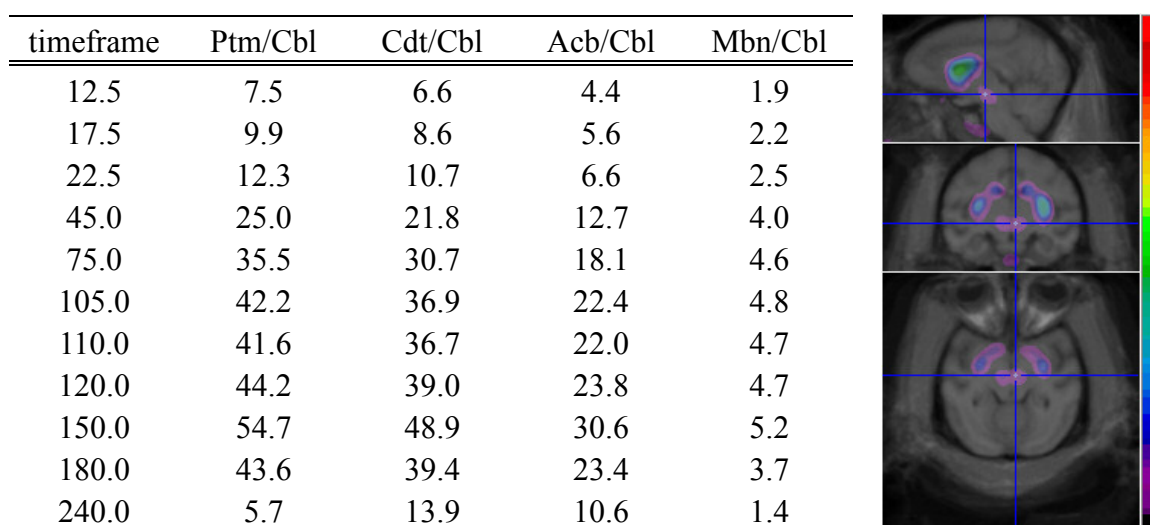


Figure 5: Region-to-cerebellum ratios for various brain regions for [¹⁸F]PR04.MZ and sagittal, transversal and coronal view on PET/MR-fusion images of the midbrain region.

In conclusion, [¹¹C]PR04.MZ displays good test-retest reliability and visualises the DAT-containing brain regions in the primate brain. The ¹⁸F-version shows a faster washout, which is beneficial for the routine application of the tracer in molecular diagnostics. The visualisation of the extra-striatal DAT in the midbrain might contribute to a more detailed, more sensitive exploration of neurodegenerative disorders with PET. Furthermore, the former facilitates the quantitative investigation of extrastriatal contributions to a variety of psychiatric diseases.

References

- (1) Alexoff DL, Shea C, Wolf AP, Fowler JS, King P, Gatley SJ and Schlyer DJ. 1995. Plasma Input Function Determination for PET Using a Commercial Laboratory Robot. *Nucl. Med. Biol.* 22:
- (2) Ambre J, Fischman M, Ruo T-I. Urinary excretion of ecgonine methyl ester, a major metabolite of cocaine in humans. *J. Anal. Toxicol.* 8: 23-25, 1984
- (3) Bergstrom KA, Tupala E; Tiihonen J. 2001. Dopamine Transporter in vitro Binding and in vivo Imaging in the Brain. *Pharmacol Toxicol.* 88:287-293.
- (4) Chalon S, Garreau L, Emond P, Zimmer L, Vilar MP, Besnard JC, Guilloteau D. 1999. Pharmacological characterisation of (E)-N-(3-iodoprop-2-enyl)-2b-carbomethoxy-3-(4'-methylphenyl)nortropine as a selective and potent inhibitor of the neuronal dopamine transporter. *J Pharmacol Exp Ther* 291:648-654
- (5) Ding YS, Lin KS, Garza V, Carter P, Alexoff D, Logan J et al. 2003 Evaluation of a new norepinephrine transporter PET ligand in baboons, both in brain and peripheral organs, *Synapse.* 50:345–352.
- (6) Ernst M, Zametkin AJ, Matochik JA, Pascualvaca D, Jons PA, Cohen RM. 1999. High Midbrain [¹⁸F]DOPA Accumulation in Children With Attention Deficit Hyperactivity Disorder. *Am J Psychiatry* 156:1209-1215
- (7) Fowler JS, Volkow ND, Wolf AP, Dewey SL, Schlyer DJ, MacGregor RR, Hitzemann R, Logan J, Bendriem B, Gatley SJ, Christman D. 1998. Mapping cocaine binding sites in human and baboon brain in vivo. *Synapse* 4:371-77
- (8) Frankhauser P, Grimmer Y, Bugert P, Deuschle M, Schmidt M, Schloss P. 2006. Characterization of the neuronal dopamine transporter DAT in human blood platelets. *Neurosci Lett.* 399:197-201
- (9) Freed C, Revay R, Vaughan RA, Kriek E, Grant S, Uhl GR, Kuhar MJ. 1995. Dopamine Transporter Immunoreactivity in Rat Brain. *J. Comp. Neurol.* 359:340-349
- (10) Gatley SJ, Yu D-W, Fowler JS, MacGregor RR, Schlyer DJ, Dewey SL, Wolf AP, Martin T, Shea CE, Volkow ND. 1994. Studies with Differentially Labeled [¹¹C]Cocaine, [¹¹C]Norcocaine, [¹¹C]Benzoylecgonine, and [¹¹C]-and 4'-[¹⁸F]Fluorococaine to Probe the Extent to Which [¹¹C]Cocaine Metabolites Contribute to PET Images of the Baboon Brain. *J. Neurochem.* 62:1154-1162
- (11) Goodman MM, Kilts CD, Keil R, Shi B, Martarello L, Xing D, Votaw J, Ely TD, Lambert P, Owens MJ, Camp VM, Malveaux E, Hoffman JM. 2000. 18F-labelled FECNT: A Selective Radioligand for PET Imaging of Brain Dopamine Transporters. *Nucl. Med. Biol.* 27:1-12
- (12) Hersch SM, Yi H, Heilman CJ, Edwards RH, Levey AI. 1997. Subcellular localisation and molecular topology of the dopamine transporter in the substantia nigra and the striatum. *J. Comp. Neurol.* 388:211-227
- (13) Hummerich R, Reischl G, Ehrlichmann W, Machulla HJ, Heinz A, Schloss P. 2004. DASB- in vitro binding characteristics on human recombinant monoamine transporters with regard to its potential as positron emission tomography (PET) tracer. *J Neurochem.* 90:1218-1226

- (14) Kilbourn MR, Carey JE, Koeppe RA, Haka MS, Hutchins GD, Sherman PS, Kuhl DE. 1989. Biodistribution, dosimetry, metabolism and monkey PET studies of [¹⁸F]GBR13119. Imaging the dopamine uptake system in vivo. *Int J Rad Appl Instrum B* 16:569–576.
- (15) Laakso A, Hietala J. 2000. PET Studies of Brain Monoamine Transporters. *Curr Pharm Des.* 6:1611-1623
- (16) Laakso A, Bergman J, Haaparanta M, Vilkmann H, Solin O, Syvalahti E, Hietala J. 2001. Decreased striatal dopamine transporter binding in vivo in chronic schizophrenia. *Schizophr Res* 52:115–120.
- (17) Laruelle M, Slifstein M, Huang Y. 2002. Positron emission tomography: imaging and quantification of neurotransmitter availability. *Methods.* 27:287-299
- (18) Logan J. 2000. Graphical analysis of PET data applied to reversible and irreversible tracers. *Nucl Med Biol* 27: 661–670
- (19) Logan J, Fowler JS, Volkow ND, Wang G-J, Ding Y-S, Alexoff DL. 1996. *J. Cerebr. Blood Flow Metab.* 16:834-840
- (20) Marshall V, Grosset D. 2003. Role of dopamine transporter imaging in routine clinical practice. *Mov Disord.* 18:1415-1423
- (21) OECD guidelines for the testing of chemicals 2004. Partition Coefficient (n-octanol/water) High Performance Liquid chromatography (HPLC) Method. #117
- (22) Okada T, Shimada S, Sato K, Schloss P, Watanabe Y, Itoh Y. 1998 Assessment of affinities of beta-CIT, beta-CIT-FE, and beta-CIT-FP for monoamine transporters permanently expressed in cell lines. *Nucl Med Biol*, 25:53 - 58
- (23) Riss PJ, Hummerich R, Schloss P, Roesch F. 2008. Synthesis and monoamine transporter inhibition of conformationally restricted 2β-carbomethoxy-3β-phenyltropanes for in vivo imaging of the dopamine transporter. 2008. *ChemMedChem* submitted.
- (24) Riss PJ, Hooker MJ, Alexoff D, Kim S-W, Fowler JS, Roesch F. 2008 [¹¹C]PR04.MZ, a promising DAT-ligand for low concentration imaging: Synthesis, efficient ¹¹C-O-methylation and initial small animal PET studies. *Bioorg. Med. Chem.* Submitted
- (25) Riss PJ, Debus F, Hummerich R, Schmidt U, Lüddens H; Schloss P, Roesch F. 2008. Ex vivo and in vivo evaluation of [¹⁸F]PR04.MZ in rodents: A novel highly selective dopamine transporter ligand for PET. 2008 *Nucl. Med Biol.* Submitted
- (26) Saba W, Valette H, Schöllhorn-Peyronneau, M-A, Coulon C, Ottaviani M, Chalon S, Dolle F, Emond P, Halldin C, Helfenbein J, Madelmont J-C, Deloye J-B, Guilloteau D, Bottlaender M. 2007. [¹¹C]LBT-999: A Suitable Radioligand for Investigation of Extra-Striatal Dopamine Transporter With PET. *Synapse* 61:17-23
- (27) Schwartz HJ, Johnson D. 1996. In vitro competitive inhibition of plasma cholinesterase by cocaine: normal and variant genotypes. *Clin. Toxicol.* 34: 77-81.
- (28) Yaquib M, Boellaard R, van Berckel BNM, Ponsen MM, Lubberink M, Windhorst AD, Berendse HW, Lammertsma AA. 2006. Quantification of dopamine transporter binding using [¹⁸F]FP-β-CIT and positron emission tomography. *J Cerebr Blood Flow Metab* 27:1397–1406

**4.6 Efficient microwave-assisted direct fluorination of
[¹⁸F]PRD04 and [¹⁸F]LBT999:
Highly selective dopamine transporter ligands for PET**

Efficient microwave-assisted direct fluorination of [¹⁸F]PRD04 and [¹⁸F]LBT999: Highly selective dopamine transporter ligands for PET

Riss, Patrick J¹; Roesch, Frank¹

¹*Institute of Nuclear Chemistry, Mainz University, Fritz Strassmann-Weg 2, 55128 Mainz; Germany*

Summary: PR04.MZ 8-(4-fluoro-but-2-ynyl)-3-p-tolyl-8-aza-bicyclo[3.2.1]octane-2-carboxylic acid methyl ester (**1**) and LBT-999 8-((E)-4-fluoro-but-2-enyl)-3b-p-tolyl-8-aza-bicyclo[3.2.1]octane-2β-carboxylic acid methyl ester (**2**) are highly selective dopamine reuptake inhibitors, derived from cocaine. **1** and **2** were labelled with fluorine-18 at their terminally fluorinated N-substituents employing microwave enhanced direct nucleophilic fluorination. K[¹⁸F]F-Kryptofix[®] 222 cryptate, tetrabutyl ammonium [¹⁸F]fluoride and caesium [¹⁸F]fluoride were compared as fluoride sources under conventional and microwave enhanced conditions. Fluorination yields were remarkably increased under microwave irradiation for all three fluoride salts. Radiochemically pure (> 98%) [¹⁸F]PRD04 (0.95 – 1.09 GBq, 42 – 135 GBq/μmol) was obtained in 34 – 40 min starting from 3.0 GBq [¹⁸F]fluoride (32 – 36 % non-decay-corrected overall yield) using K[¹⁸F]F-Kryptofix[®] 222 cryptate in MeCN.

Introduction

During the last decades, molecular imaging of the dopaminergic signalling has attracted considerable attention.¹ Dopaminergic pathologies are related to several neurodegenerative and psychiatric disorders.² In particular, the presynaptic dopamine transporter (DAT), a transmembrane protein belonging to the family of neurotransmitter-sodium symporters, remains an important target. Cocaine-analogue radioligands, labelled with short-lived positron emitters have shown to be the most promising lead for the development of selective probes for the DAT.³ State-of-the-art in fluorine-18 labelling of tropane-analogue DAT-ligands is N-alkylation with an appropriate secondary labelling synthon, e.g. 2-[¹⁸F]fluoroethyl tosylate.⁴ However, recent studies elucidated direct nucleophilic aliphatic fluorination routes with analogue compounds. Nevertheless, radiolabelling of cocaine-analogue radioligands with fluorine-18 was often complicated by a) low N-alkylation yields, b) poor accessibility of sp²-carbon-bound fluorine, resulting in laborious reaction pathways, and c) α/β-epimerisation at the C-2 position in the tropane skeleton,⁵ due to the inherent basicity of activated, nucleophilic [¹⁸F]F⁻.

The present report is concerned with a reliable, microwave enhanced high yield direct fluorination method for the recently introduced moderate to high potency tropane-analogue DAT-inhibitors LBT999 and PRD04.⁶

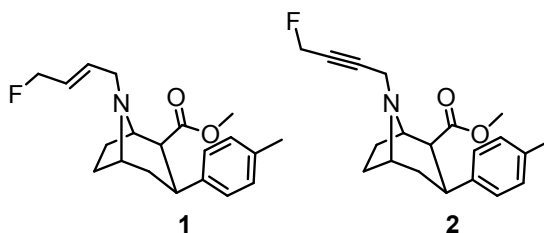


Figure 1: PRD04 (1) and LBT999 (2)

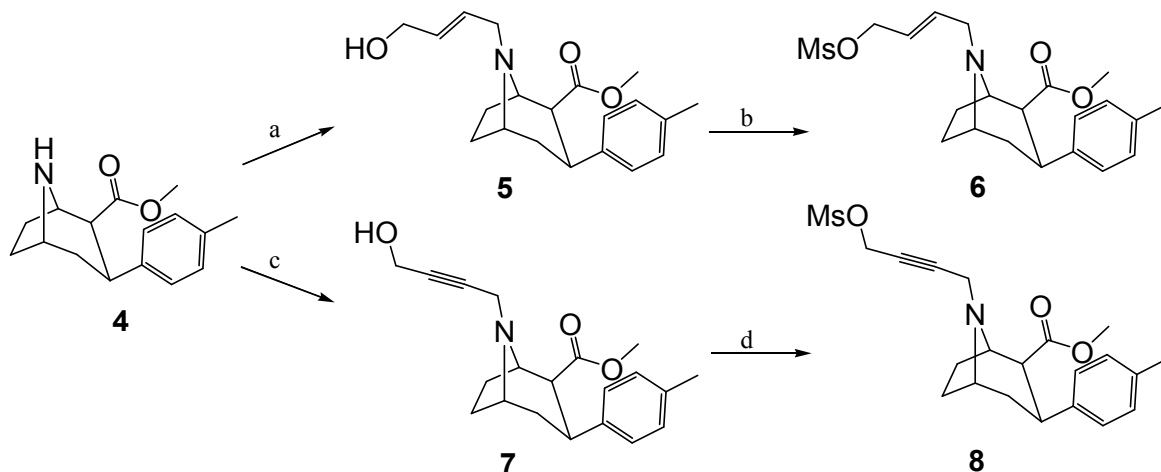
Initial direct aliphatic nucleophilic radiofluorination of PR04.MZ, was performed under conventional conditions. Unfortunately, only low radiochemical yields of 19 ± 3 % were obtained after 60 to 70 min radiosynthesis.^{6c} Similar yields have also been reported in a simple one-step fluorine-18-labelling of LBT-999, based on a chlorine-for-fluorine nucleophilic substitution.^{4b} Reaction of $K[^{18}F]F$ Kryptofix[®]222 with the chlorinated precursor at $165^{\circ}C$ in DMSO for 10 min followed by C-18 solid phase extraction and final semi-preparative HPLC separation afforded $[^{18}F]2$ in 10-16 % non decay corrected radiochemical yield after ~65 min. In order to increase the radiochemical yield, we considered the use of microwave enhanced conditions for nucleophilic aliphatic radiofluorination.⁷

Microwave assisted synthesis has evolved as a powerful tool in the development of fast, chemo-selective synthetic methods.⁷ Compared to conventional heating, energy transfer does not proceed gradually from the outside of the vessel to the inside. Instead, the microwave directly interacts with dipoles or charged species inside the reaction mixture. Thus, the direct energy transfer to a reaction center, a reactant or an intermediate is possible. Furthermore, the amount of activation energy, necessary for the conversion of a given molar amount of reactants can be provided within a shorter time, due to the high performance of focussed microwaves. The high energy influx facilitates different reaction pathways. In opposite to conventional conditions, thermodynamic reaction routes are preferred and kinetic side reactions are disfavoured.⁷ In general, commercially available microwave-reactors provide monomodal electromagnetic radiation ($\lambda = 12.2$ cm, $\nu = 2450$ MHz), representing the energy spectrum of molecular rotation. Therefore, it is unlikely that microwave irradiation results in cleavage of covalent bonds.⁷ Most striking with regard to radiosynthesis employing lived isotopes is the high, direct transfer of activation energy to the reactants, which mostly results in remarkably shortened reactions times.⁷

Results and Discussion

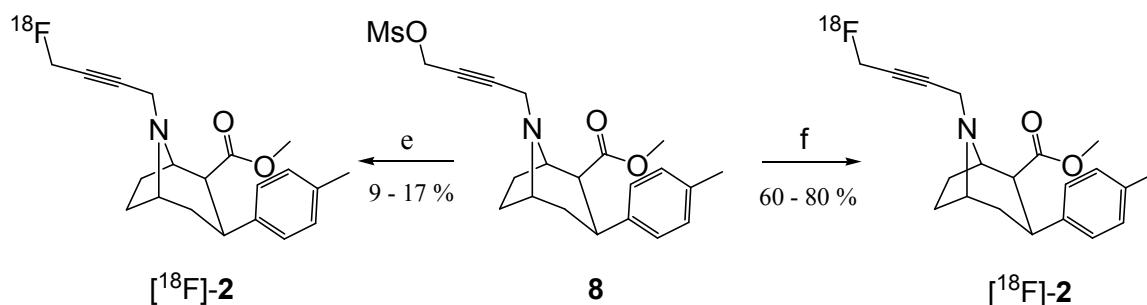
Chemistry

Reference compounds **1-2** and nortropane **4** were synthesised from natural cocaine as published somewhere else.⁸ The LBT999 labelling precursor 8-(4-methanesulfonyloxy-but-2-enyl)-3-exo-p-tolyl-8-aza-bicyclo[3.2.1]octane-2-exo-carboxylic acid methyl ester (**6**) was obtained from nortropane **4** via alkylation with 4-bromo but-2-ene-1-ol in 74 % yield, followed by Lewis-acid catalysed esterification with methanesulfonyl anhydride in 67 % yield. (Scheme 1) The labelling precursor for PRD04 8-(4-methanesulfonyloxy-but-2-ynyl)-3-p-tolyl-8-aza-bicyclo[3.2.1]octane-2-carboxylic acid methyl ester (**8**) was synthesised according to scheme 1. **4** was reacted with 4-chlorobut-2-ynyl alcohol to afford **7** in 95 % yield. Subsequent mesylation in dichloromethane using methansulfonyl chloride and triethylamine afforded **8** in 94 % yield.



Scheme 1: Synthesis of precursors for LBT999 and PRD04; a) DiPEA, 4-hydroxybut-2-ene-1-yl bromide, MeCN; b) Ms₂O, Yb(OTf)₃, CH₂Cl₂, 0 °C, 1 d; c) DiPEA, MeCN, 4-hydroxybut-2-yne-1-yl chloride; c) MsCl, NEt₃, CH₂Cl₂, 0 °C, 25 min

Radiochemistry



Scheme 2: [¹⁸F]fluorination of PRD04 precursor **8**; conventional conditions, (e) 120 °C, MeCN, K₂CO₃, [K⁺cK222][¹⁸F]F⁻, 3 min; microwave conditions, (f) 175 °C, 18 bar, MeCN, K₂CO₃, [K⁺cK222][¹⁸F]F⁻, 0.75 min.

PRD04 (**1**) was labelled with fluorine-18 at its 4-fluorobut-2-ynyl residue, using a CEM discover focussed microwave reactor. The maximum pressure during the labelling reaction was 20 bar, the maximum temperature at the end of microwave irradiation was 175 °C.

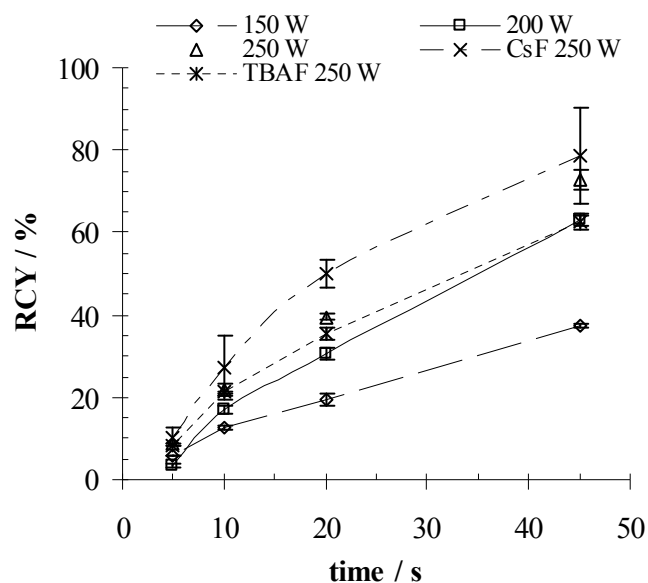


Figure 2: Labelling kinetics of [^{18}F]PRD04 in a CEM Discover® focussed microwave. Settings: pressure reaction, $T_{\text{max}} = 175\text{ }^{\circ}\text{C}$, $p_{\text{max}} = 1.8 \times 10^6\text{ Pa}$, moderate stirring, no cooling.

The optimal microwave performance was found to be 255 W (Figure 2). The labelling reaction is outlined in figure 1. Labelling precursor **8** was exposed to cyclotron-produced [^{18}F]fluoride as n.c.a. $\text{K}[\text{K}^+\text{C}222][\text{F}^-]$, tetrabutyl ammonium [^{18}F]fluoride complex ($[\text{F}]\text{TBAF}$) or cesium [^{18}F]fluoride salt ($[\text{F}]\text{CsF}$). Labelling was performed under constant microwave irradiation at 255 W for up to 45 seconds in a pressure-tight microwave reaction vial. The maximum pressure during the labelling reaction was $1.8 \times 10^6\text{ Pa}$. After heating for various time-periods (5 s, 10 s, 20 s, 45 s), an aliquot of the remaining radioactivity was measured by TLC. The relative reaction yield was determined on silica gel 60 coated aluminium plates. A mixture of diethyl ether (Et_2O) and hexanes containing 10 % of triethylamine (NEt_3) was used as mobile phase. The conversion to the desired fluorine-18 labelled compound was expressed as percentage of total radioactivity in the TLC lane. Volatile side products were neglected, because the head space of the vial did not contain any radioactivity. The relative radiochemical yield was determined from the radio-TLC as the ratio of radioactivity area of [^{18}F]**2** over total fluorine-18 radioactivity area within the lane. The radiochemical yield after 45 seconds of heating was 40–80%. The reaction mixture was then withdrawn into a automated syringe containing 300 μl of sterile water and directly transferred into the sample loop of a semipreparative HPLC-System. Three to ten percent of the starting activity routinely remained in the microwave reaction vessel.

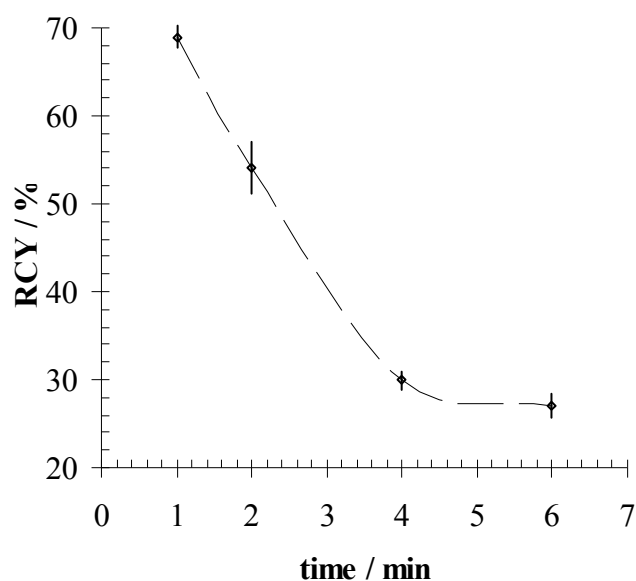


Figure 3: Product degradation under prolonged reaction time

Later on it was found, that the bulk of n.c.a. fluoride had been incorporated into the molecule, at this point. Prolonged heating resulted in thermal degradation to form an additional polar side product. This might lead to false interpretation of the thin layer chromatogram. The latter eluted shortly after the HPLC-inject-signal and displayed up to 20 % of starting radioactivity. [^{18}F]**1** eluted after a reasonable purification time (t_{R} :13.5 – 14.5 min) with a radiochemical purity of > 98 %. The product fraction did not contain any chemical impurities. In some runs, a non-significant by-product was formed which was assigned to the saponified [^{18}F]PR04.MZ acid. For concentration and isolation of the radiotracer, the product fraction was diluted with water and passed through a proton-loaded Merck-Lichrolut SCX strong cation exchanger. About 95 % of the total radioactivity in the product fraction were retained on the SCX resin. Subsequently, the cartridge was washed with 3 ml of water. Sterile, isotonic PBS was used for elution of the product. A sterile filter was serially connected to the cartridge and the [^{18}F]PR04.MZ containing PBS was collected in a multi injection vial. At this point an aliquot of the sterile filtered solution was guided into a screw-cap vial, containing 1 ml of 30 % ammonium formate buffer in MeCN. This sample was used for quality control. Less than 5 % of the total trapped radioactivity remained on the SCX-cartridge. The radiotracer formulation was a colourless, clear solution with a pH-value of 7.3. Quality control by analytical HPLC proved, that [^{18}F]**1** was > 98 % radiochemically pure (**1**, t_{R} :10 min). The preparation was shown to be free of non-radioactive labelling precursor. Specific radioactivities ranged from 42 to 135 GBq/ μmol at the end of the synthesis. [^{18}F]LBT-999 ([^{18}F]**2**) was obtained under the same conditions in 19 % non-decay-corrected yield. The retention time for preparative purification was 8 min, and the radiochemical purity was comparable to the radiochemical purity of [^{18}F]**1**. Interestingly, the total radioactivity incorporation was remarkably lower in this case.

Comparison of fluoride sources

Initially, the microwave enhanced method was optimised using the well established potassium Kryptofix[®] cryptate [^{18}F]F⁻ complex ($[\text{K}^+\subset\text{K222}]^{18}\text{F}^-$). The reaction outcome, as percentage of

total ^{18}F radioactivity that was converted to the desired product, was determined as a function of reaction time, precursor amount, microwave energy and temperature. During these investigations it was found, that the reaction between precursors **6** and **8** proceeded very fast. Actually, almost quantitative incorporation of the employed fluoride occurred within the first 55 seconds. Upon prolonged heating, the product degraded to a polar side product. The latter has also been found with thermal heating. Dolle et al. describe a similar effect within the radiosynthesis of LBT-999, where prolonged heating led to product degradation.¹⁷ In the present case, a maximum radioactivity incorporation of 80 % was observed with $[\text{K}^+\text{C}222]^{18}\text{F}^-$.

The reactions with ^{18}F CsF and ^{18}F TBAF were performed analogously to the conditions described above. For comparison, labelling was performed under thermal conditions with all three fluoride sources. Representative results are summarised in figure 4.

Virtually, the use of ^{18}F CsF gave the highest radiochemical yields. Unfortunately, ^{18}F CsF proved to be less stable with regard to the reaction outcome than ^{18}F TBAF and K^{18}F Kryptofix[®] 222 cryptate. Thus, although the highest yields can be ascribed to CsF, this salt also claims the highest SEM.

^{18}F TBAF proved a better reliability, in addition the reaction worked well in low boiling THF and almost equal results were found in MeCN. However, the total reaction yields were substantially lower than with the standard ^{18}F fluoride source K^{18}F Kryptofix[®] 222 cryptate. For these reasons, we conclude, that K^{18}F Kryptofix[®] 222 cryptate is the most efficient source for n.c.a. fluoride in microwave assisted radiofluorinations of tropane analogue DAT ligands.

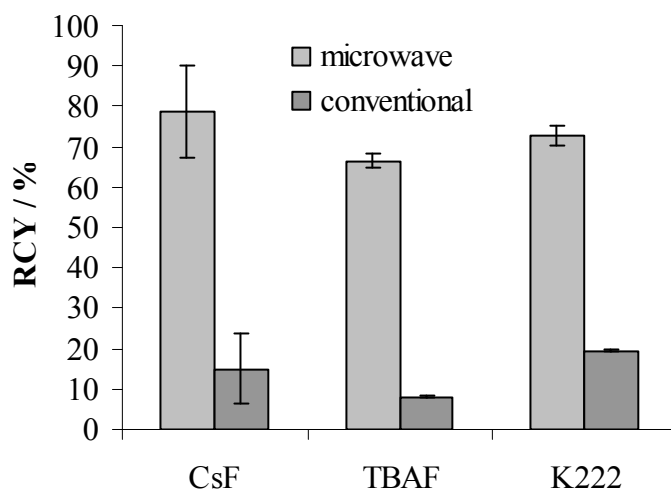


Figure 4: Comparison of maximum yields after 1 minute of microwave irradiation and 20 minutes of conventional heating in MeCN.

Conclusions

^{18}F PRD04 and ^{18}F LBT999 have been prepared using a novel, highly efficient and time effective microwave assisted labelling method. The use of direct molecular heating significantly increased the radiochemical yield and remarkably reduced the reaction time. Radiosynthesis of ^{18}F PRD04 was performed under pressure in a CEM discover[®] focussed

microwave reactor. [¹⁸F]**1** was rapidly formed within the first 45 seconds of microwave irradiation and degraded when a high microwave-intensity was maintained. The formulated tracer was obtained in a non-decay corrected yield of 32 % to 36 %, 40 minutes after EOB

Experimental

LBT999: methyl 8-((E)-4-hydroxybut-2-enyl)-3-p-tolyl-8-aza-bicyclo[3.2.1]octane-2-carboxylate, 5: DiPEA (129.1 mg, 1 mmol) was added to nortropine **4** (260 mg, 1 mmol) and 4 bromobut-2-enol dissolved in acetonitrile (5 ml). The reaction mixture was heated to 45 °C for 3 h. After completion of the reaction, the reaction mixture was concentrated to approximately 500 µl, which were directly transferred to a 20 g silical gel column and eluted with MeOH/CHCl₃ 1:6, rf =. 79% yield. ¹H-NMR: (300 MHz, CDCl₃) δ (in ppm): 7.13 (d, J = 8 Hz, 2 H, ArH), 7.05 (d, J = 8 Hz, 2 H, ArH), 5.78 - 5.57 (m, 2 H), 4.1 (t, J = 5,5 Hz, 2 H), 3.65 (brs, 1H), 3.47 (s, 1H, OCH₃), 3.40 (brs, 1 H), 3.03 – 2.92 (m, 2 H), 2.90 - 2.77 (m, 2 H), 2.57 (dt, J = 12.5 Hz, J = 2.9 Hz, 1 H), 2.27 (s, 3 H), 2.10 – 1.91 (m, 2 H), 1.77 - 1.55 (m, 3 H). ¹³C-NMR: (100 MHz, CDCl₃) δ (in ppm): 172.0, 139.9, 135.2, 134.4, 128.6, 127.2, 126.3, 126.0, 84.2, 82.1, 62.3, 61.3, 54.9, 52.7, 50.9, 34.1, 33.8, 26.1, 25.9, 21.0 .

(E)-4-(2-(methoxycarbonyl)-3-p-tolyl-8-aza-bicyclo[3.2.1]octan-8-yl)but-2-enyl methane sulfonate, 6: Alcohol **5** was dissolved in dichloromethane and methanesulfonyl anhydride was added. The reaction was initiated by the addition of 1 mol% of ytterbium triflate. After stirring the reaction mixture for 5 h, the reaction was terminated and the reaction mixture was concentrated in vacuo. The residue was re-dissolved in a small amount of dichloromethane and purified by flash chromatography on a silica gel column. 63 % of **6** were obtained as colourless crystals.

¹H-NMR: (300 MHz, CDCl₃) δ (in ppm): 7.13 (d, J = 8 Hz, 2 H, ArH), 7.05 (d, J = 8 Hz, 2 H, ArH), 5.78 - 5.57 (m, 2 H), 4.1 (t, J = 5,5 Hz, 2 H), 3.65 (brs, 1H), 3.47 (s, 1H, OCH₃), 3.40 (brs, 1 H), 3.03 – 2.92 (m, 2 H), 2.90 - 2.77 (m, 2 H), 2.57 (dt, J = 12.5 Hz, J = 2.9 Hz, 1 H), 2.27 (s, 3 H), 2.10 – 1.91 (m, 2 H), 1.77 - 1.55 (m, 3 H). ¹³C-NMR: (100 MHz, CDCl₃) δ (in ppm): 172.0, 139.9, 135.2, 134.4, 128.6, 127.2, 126.3, 126.0, 84.2, 82.1, 62.3, 61.3, 54.9, 52.7, 50.9, 34.1, 33.8, 26.1, 25.9, 21.0

2-exo-carboxymethyl-3-(4-methylphenyl)-8-(4'-hydroxybut-2-yne-1-yl)-8-azabicyclo [3.2.1]octane, 7: Nortropine **4** (260 mg, 1 mmol) was added to 1.05 eq. of DiPEA, dissolved in acetonitrile (5 ml). 4-hydroxybut-2-yne-1-yl chloride was added subsequently and the reaction mixture was heated to 75 °C for 13 h. After completion of the reaction the reaction mixture was concentrated to approximately 500 µl, which were directly transferred to a 20 g silical gel column and eluted with MeOH/CHCl₃ 1:6, rf =. 89% yield. ¹H-NMR: (300 MHz, CDCl₃) δ (in ppm): 7.14 (d, J = 8.5 Hz, 2 H, ArH), 7.06 (d, J = 8.5 Hz, 2 H, ArH), 5.02 (t, J = 1.5 Hz, J_{H-F} = 47.8 Hz, 1 H), 4.86 (t, J = 1.5 Hz, J_{H-F} = 47.8 Hz, 1 H), 3.89 (brs, 1 H), 3.51 (s, 3 H, OCH₃), 3.47 (brs, 1 H), 3.25 (ddt, J = 1.5 Hz, J = 7.5 Hz, J = 16.5 Hz, 1 H), 3.10 (ddt, J = 1.5 Hz, J = 7.5 Hz, J = 16.5 Hz, 1 H), 2.98 (dt, J = 5 Hz, J = 12.9 Hz, 1 H), 2.94 – 2.89 (m, 1 H), 2.62 (td, J = 2.9 Hz, J = 12.5 Hz, 1 H), 2.27 (s, 3 H, ArCH₃), 2.16 – 1.92 (m, 2 H), 1.82 – 1.61 (m, 3 H). ¹³C-NMR: (100 MHz, CDCl₃) δ (in ppm): 171.7, 139.6, 135.3, 128.7, 127.2, 127.1, 87.7, 87.5, 69.7, 62.6, 61.2, 52.8, 52.6, 51.1, 42.9, 34.1, 33.7, 25.9, 25.7, 21.0. Anal. Calcd. C, 72.92; H, 7.34; F, 5.77; N, 4.25; O, 9.71. Found: C, 72.79; H, 8.03; N, 4.53. MS (FD) 327.2 (100) C₂₀H₂₆NO₃ requires 327.1834.

2-exo-carboxymethyl-3-(4-methylphenyl)-8-(4'-methanesulfonyloxybut-2-yn-1-yl)-8-azabicyclo[3,2,1]octane, 8: Alcohol 7 was added to 1.05 eq. of triethylamine dissolved in dry dichloromethane (1 ml/mmol) and cooled to 0 °C. After stirring at 0°C for 30 min, neat methanesulfonyl chloride 1 eq. was added drop by drop without interruption. After completion of the addition the reaction mixture was stirred for 5 additional minutes when all alcohol had been consumed (TLC-monitoring). The reaction was quenched by the addition of 1 ml/mmol cold water with vigorous stirring. Subsequently, the reaction mixture was diluted with dichloromethane. After separation of the aqueous phase, the reaction mixture was washed with 5 % sodium carbonate solution, dried over potassium carbonate and concentrated in vacuo to leave a residue that was quickly chromatographed on silica gel to yield precursor **8** in 90 % yield. ¹H-NMR: (300 MHz, CDCl₃) δ (in ppm): 7.15 (d, J = 8 Hz, 2 H, ArH), 7.08 (d, J = 8 Hz, 2 H, ArH), 4.23 (t, J = 2 Hz, 2 H), 3.91 (brs, 1 H), 3.52 (s, 3 H, OCH₃), 3.50 (brs, 1 H), 3.22 (dt, J = 2 Hz, J = 16 Hz, 1 H), 3.10 (dt, J = 2 Hz, J = 16 Hz, 1 H), 3.02 (dt, J = 12.5 Hz, J = 5 Hz, 1 H), 2.93 ("t", J = 4 Hz, 1 H), 2.89 (s, 3 H, SO₂CH₃), 2.61 (td, J = 2.9 Hz, J = 12.5 Hz, 1 H), 2.29 (s, 3 H, CH₃), 2.21 - 2.10 (m, 1 H), 2.07 - 1.95 (m, 1 H), 1.83 - 1.59 (m, 3 H). ¹³C-NMR: (100 MHz, CDCl₃) δ (in ppm): 172.1, 139.7, 135.3, 129.0, 128.6, 127.2, 82.7, 81.7, 62.5, 60.9, 52.8, 51.2, 50.9, 42.9, 37.6, 34.1, 33.7, 25.85, 25.8, 21.0. Anal. Calcd. C, 62.20; H, 6.71; N, 3.45; O, 19.73; S, 7.91. Found: C, 61.9; H, 6.91; N, 3.24. MS (FD) 405.2 (100) C₂₁H₂₇NO₅S requires 405.1610.

Representative protocol for microwave assisted fluorination of tropanes: [¹⁸O]H₂O containing [¹⁸F]fluoride were passed through a waters accel plus light QMA strong anion exchange cartridge, preconditioned with 10 ml of 1 M potassium carbonate solution followed by 20 ml of sterile water. The trapped fluoride was eluted in a acetonitrile solution containing 40 μmol of cryptand kryptofix® K222 and 15 μmol of potassium carbonate, directly into a supelco 5 ml reactivial. A reduced pressure of 100 mbar was applied to the tightly closed vial in an oil bath at 90 °C while a stream of 300 ml nitrogen per minute was applied. After the complete evaporation additional MeCN (1 ml) was added (two times). After evaporation of the third amount of MeCN, the nitrogen inlet was closed and full vacuum was applied to the reaction vial for 3 minutes. Afterwards, the dried radioactivity was re-dissolved in 1 ml of MeCN and stirred at RT for 5 minutes. This stock solution was transferred into a CEM pressure-reaction vial containing 4.5 mg of labelling precursor and an 8 mm stirring magnet. The vial was placed inside the cavity of a CEM discover® laboratory microwave and irradiated with microwaves at 250 W for approximately 45 s after which the preset maximum pressure and temperature were reached. After cooling down of the vial for 90 s in a stream of air, the reaction mixture was taken up into a syringe containing 300 μl of cold water and directly injected into a Dionex p680 HPLC-system equipped with a Dionex UVD 170U UV-detector and a Raytest Gabi Star radioactivity detector. Dionex Chromeleon software was used for UV-data analysis and Raytest Gina-star software was used for radioactivity detection. A semipreparative Phenomenex Luna RP 18 10 μ HPLC column was used as stationary phase. The dimensions were 250 x 10 mm. 40 % 0.1 M ammonium acetate buffer at pH 4.7 in acetonitrile was used as mobile phase. The product fraction was collected after a total retention time of 14 min, taken up into a syringe containing 10 ml of water and passed through a Merck Lichrolute SCX strong cation exchange cartridge (200 mg), preconditioned with 5 ml of 1 M hydrochloric acid and neutralised with 20 ml of water. Subsequently, the cartridge was washed with 3 ml of water. At this point usually >95% of radioactivity were trapped on the cartridge.

Formulation of [¹⁸F]PRD04: Elution of the radiotracer was performed using 5 ml of sterile phosphate buffered saline. A sterile filter was serially connected to the cartridge, to obtain the injectable radiotracer formulation containing [¹⁸F]PRD04 in a non decay corrected yield of 32 % to 36 %. The maximum specific activity of product [¹⁸F]1 at end of synthesis was up to 135 GBq/μmol, depending on the quality of [¹⁸F]fluoride.

Quality control of [¹⁸F]PRD04: The radiochemical purity and the specific radioactivity of [¹⁸F]PRD04, [¹⁸F]1, were determined using a Sykam S1100 HPLC-pump, a Berthold Flow Star LB 513 radioactivity detector and a Knauer K 2501 UV-detector. A Phenomenex Luna RP 18 5 μ 250 x 4.6 mm analytical HPLC column was used as stationary phase. The mobile phase consisted of 30 % 0.05 molar ammonium acetate buffer at pH 4.6 in acetonitrile. An aliquot of 20 μl was withdrawn from the sterile filtered formulated tracer solution and diluted with eluent. Approximately 50 kBq of this solution were injected into the HPLC. The product which was > 97 % radiochemically pure eluted after 10 min.

Acknowledgement: This work was financially supported by the DFG-grant Ro985 / 21. The authors are grateful to the Fonds der Chemischen Industrie for the donation of various chemicals and solvents.

References:

- (1) a) N. D. Volkow, J. S. Fowler, G. J. Wang, R. Baler, F. Telang, *Neuropharm.* **2008**, in press; doi: 10.1016/j.neuropharm.2008.05.022; b) J. S. Fowler, N. D. Volkow, A. P. Wolf, S. L. Dewey, D. J. Schlyer, R. R. Macgregor, R. Hitzemann, J. Logan, B. Bendriem, S. J. Gatley, et al. *Synapse* **1989**, *4*, 371; c) D. Sulzer, *Clin. Neurosci. Res.* **2005**, *5*, 117; d) S. M. Aquilonius, K. Bergstrom, S. A. Eckernas, P. Hartvig, K. L. Leenders, H. Lundquist, G. Antoni, A. Gee, A. Rimland, J. Uhlin, B. Langstrom; *Acta. Neurol. Scand.* **1987**, *76*, 183; e) M. R. Kilbourn, J. E. Carey, R. A. Koeppe, M. S. Haka, G. A. Hutchins, P. S. Sherman, D. E. Kuhl, *Nucl. Med. Biol.* **1989**, *16*, 569; f) Y.-S. Ding, J. S. Fowler, N. D. Volkow, J. Logan, S. J. Gatley, Y. Sugano, *J. Nucl. Med.* **1995**, *36*, 2298; g) J. O. Rinne, J. Bergman, H. Ruottinen, M. Haaparanta, E. Eronen, V. Oikonen, P. Sonninen, O. Solin; *Synapse* **1999**, *31*, 119 – 124.
- (2) a) K. A. Bergstrom, E. Tupala, J. Tiihonen, *Pharmacol Toxicol.* **2001**, *88*, 287-293; b) V. Marshall, D. Grosset, *Mov. Disord.* **2003**, *18*, 1415-1423; c) A. Laakso, J. Hietala, *Curr. Pharm. Des.* **2000**, *6*, 1611-1623; d) A. Laakso, J. Bergman, M. Haaparanta, H. Vilkmann, O. Solin, E. Syvalahti, J. Hietala, *Schizophr. Res.* **2001**, *52*, 115–120.
- (3) a) M. F. Chesselet, J. M. Delfs, *Trends Neurosci.* **1996**; *19*, 417-22. b) L. Müller, C. Halldin, C. Lundquist, C.-G. Swahn, C. Foged, H. Hall, P. Karlsson, N. Ginovart, Y. Nakashima, T. Suhara, L. Farde, *J. Radioanal. Nucl. Chem.* **1996**, *206*, 133-144; c) A. Abi-Dargham, M. S. Gandelman, G. A. DeErausquin, Y. Zea-Ponce, S. S. Zoghbi, R. M. Baldwin, M. Laruelle, D. S. Charney, P. B. Hoffer, J. L. Neumeyer, *J. Nucl. Med.* **1996**; *37*, 1129-1133.
- (4) a) L. Cai, S. Lu, V. W. Pike, *Eur. J. Org. Chem.* **2008**, 2853; b) F. Dollé, J. Helfenbein, F. Hinnen, S. Mavel, Z. Mincheva, W. Saba, M.-A. Schöllhorn-Peyronneau, H. Valette, L. Garreau, S. Chalon, C. Halldin, J.-C. Madelmont, J.-B. Deloye, M. Bottlaender, J.

Le Gailliard, D. Guilloteau, P. Emond, *J. Labelled Compd. Radiopharm.* **2007**, 50, 717-723

- (5) a) F. Dollé, F. Hinnen, P. Emond, S. Mavel, Z. Mincheva, W. Saba, M.-A. Schöllhorn-Peyronneau, H. Valette, L. Garreau, S. Chalon, C. Halldin, J. Helfenbein, J. Legailard, J.-C. Madelmont, J.-B. Deloye, M. Bottlaender, D. Guilloteau, *J. Labelled Compd. Radiopharm.* **2006**, 49, 687-698 ; b) R. P. Klok, P. J. Klein, J. D. M. Herscheid, A. D. Windhorst, *J. Labelled Compd. Radiopharm.* **2006**, 49, 77-89 c) F. Wuest, M. Berndt, K. Strobel, J. van den Hoff, X. Peng, J. L. Neumeyer, R. Bergmann, *Bioorg. Med. Chem.* **2007**, 15, 4511-4519
- (6) a) S. Chalon, H. Hall, W. Saba, L. Garreau, F. Dolle, C. Halldin, P. Emond, M. Bottlaender, J.-B. Deloye, J. Helfenbein, J.-C. Madelmont, S. Bodard, Z. Mincheva, J.-C. Besnard, D. Guilloteau, *J. Pharmacol. Exp. Ther.* **2006**, 317, 147-152 b) P. J. Riss, R. Hummerich, P. Schloss, F. Roesch, *ChemMedChem* **2008**, submitted. c) P. J. Riss, F. Debus, R. Hummerich, U. Schmidt, H. Lüddens, P. Schloss, F. Roesch, *Nucl. Med Biol.* **2008**, submitted d) P. J. Riss, M. J. Hooker, D. Alexoff, S.-W. Kim, J. S. Fowler, F. Rösch, *Bioorg. Med. Chem. Letters* **2008**, submitted.
- (7) a) N. Elander, J. R. Jones, S.-Y. Lu, S. Stone-Elander, *Chem. Soc. Rev.* **2000**, 29, 239–249, b) F. Dollé, *Cur. Pharm. Des.* **2005**, 11, 3221-3235, c) B. Hayes, *Microwave Synthesis*, CEM Publishing: Matthews 2002; d) P. Lidström, J. Tierney, B. Wathey, J. Westman, *Tetrahedron* **2001**, 57, 9225–9283.
- (8) a) P. C. Meltzer, A. Y. Liang, A. L. Brownell, D. R. Elmaleh, B. K. Madras, *J. Med. Chem.* **1993**, 36, 855-62; b) L. Xu, M. L. Trudell, *J. Heterocycl. Chem.* **1996**, 33, 2037-2039.

**4.7 NODAPA-OH and NODAPA-(NCS)_n: Synthesis,
⁶⁸Ga-radiolabelling and in vitro characterisation of novel
versatile bifunctional chelators for molecular imaging**

NODAPA-OH and NODAPA-(NCS)_n: Synthesis, ⁶⁸Ga-radiolabelling and *in vitro* characterisation of novel versatile bifunctional chelators for molecular imaging

Patrick Riss, Carsten Kroll, Verena Nagel and Frank Roesch

Institute of Nuclear Chemistry, University of Mainz, Fritz-Strassmann-Weg 2, 55128 Mainz, Germany

Abstract: This report concerns synthesis, ⁶⁸Ga-radiolabelling and stability data of 1,4,7-triazacyclononane-1,4-diacetic acid-7-p-isothio-cyanatophenyl-acetic acid (NODAPA-NCS), 1,4,7-triazacyclononane-1-acetic acid-4,7-di-p-isothiocyanatophenyl-acetic acid (NODAPA-(NCS)₂) and 1,4,7-triazacyclononane-1,4-diacetic acid-7-p-hydroxyphenyl-acetic acid (NODAPA-OH), versatile bifunctional chelators with potential for molecular imaging. Protein binding and exemplified conjugation is also reported.

Non-invasive molecular imaging of biochemical mechanisms and pathologies *in vivo* is an emerging interdisciplinary field of research. Among the available techniques for a sensitive, quantitative visualisation of the biochemical and physiological function of biological tissue approached by suitable imaging probes, positron emission tomography (PET) provides great potential in terms of quantification, sensitivity, temporal and lateral resolution. The commercially available ⁶⁸Ge/⁶⁸Ga radionuclide generator systems and its recent improvement concerning on-line processing and labelling,¹ may provide a beneficial complement to nuclear imaging with established, cyclotron produced PET nuclides like ¹¹C and ¹⁸F. ⁶⁸Ga provides a high positron abundance of 89 % and an intermediate positron maximum energy. With its half-life (1.13 h) lying perfectly in between the half-lives of the most frequently used ¹¹C (0.33 h) and ¹⁸F (1.82 h), it provides excellent decay characteristics as a PET-radiolabel. In addition, its most promising advantage is its availability via a radionuclide generator system. The mother nuclide ⁶⁸Ge has a half-life of 270.8 d, guaranteeing prolonged use of generator set-ups in action (ca. 1 year). Consequently, ⁶⁸Ga provides an economical alternative to the cyclotron produced radionuclides. On the other hand, radiolabelling of molecular probes with ⁶⁸Ga requires a completely different synthesis route. The main group metal rapidly forms chelate-complexes with hard donor functions of four to six coordinating chelators. Adequate radioligand precursors meeting the coordination chemistry of gallium(III) with versatile conjugation possibilities are of high interest. To reinforce the flow of novel tracer candidates to biological evaluation, a convenient, time efficient route to various chelator conjugated potential targeting vectors would be desirable.

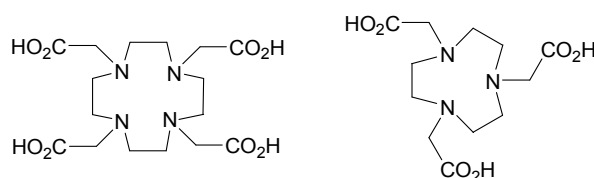


Figure 1 (4,7,10-tris-carboxymethyl-1,4,7,10-tetraaza-cyclododec-1-yl)-acetic acid (DOTA) and (4,7-bis-carboxymethyl-[1,4,7]-triazanon-1-yl)-acetic acid (NOTA)

The macrocyclic chelators DOTA and NOTA (Fig. 1) are established as frequently considered routes for the introduction of a ^{68}Ga -tag. Compared to open chain acyclic analogues, both provide complexes of superior kinetic and thermodynamic stability since gallium is irreversibly complexed at room temperature. DOTA remains the most frequently used chelator because of its better commercial availability and less challenging synthesis. Its six-coordinate nine-ring analogue NOTA forms slightly distorted octahedral complexes with gallium which display higher stabilities and faster incorporation of Ga(III) at lower temperatures.² Thus, we were interested in a time-saving and cost-effective access to a versatile gallium chelator allowing convenient conjugation to various targeting molecules.

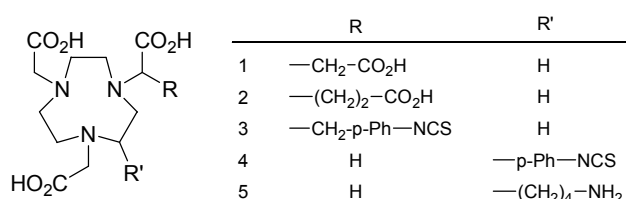
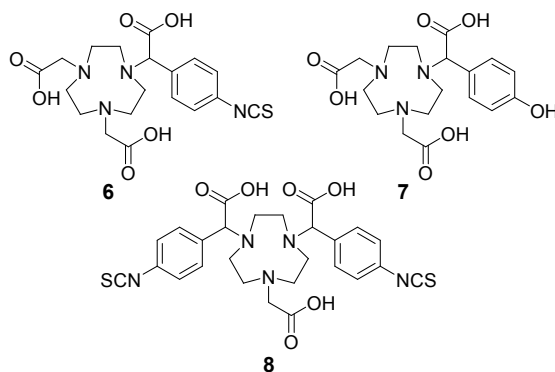


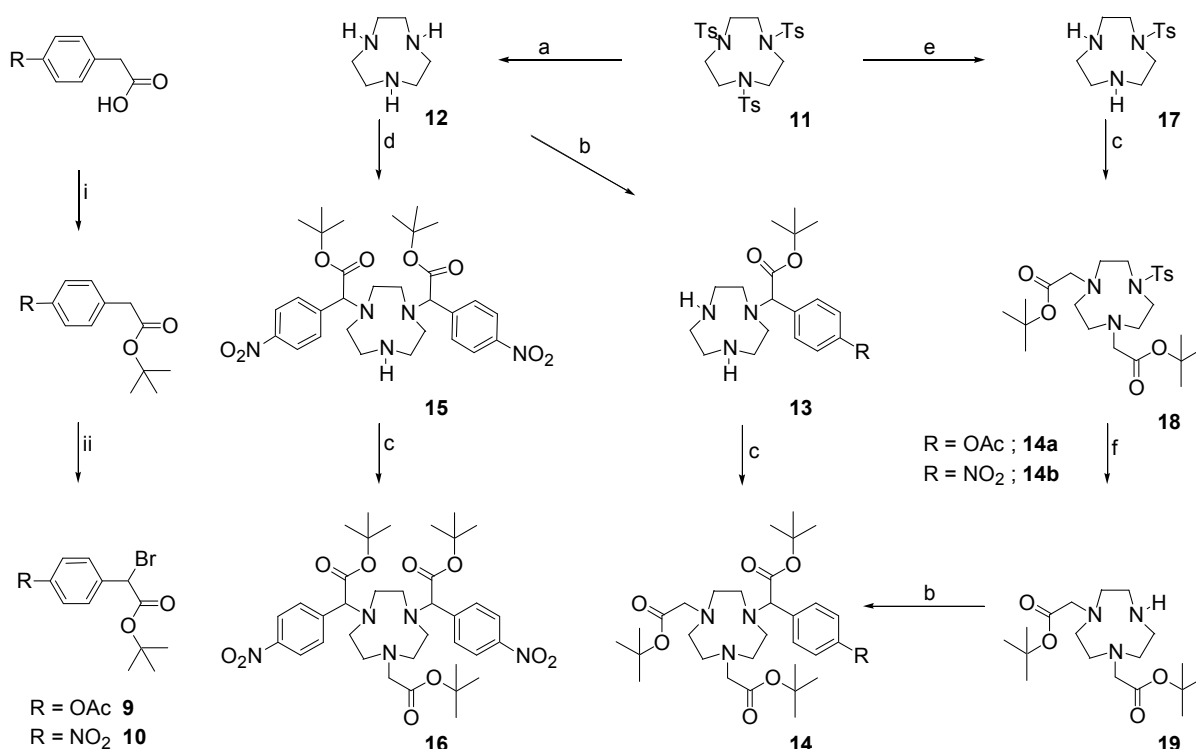
Figure 2 NOTA-based bifunctional chelators

Specific bifunctional derivatives of NOTA, published so far, are surveyed in figure 2. NODAGA (**1**) and NODASA (**2**) are limited to coupling peptides through an amide bond.^{3,4} The value of NODAGA has been demonstrated convincingly. The isothiocyanatophenyl derivative **3** has been introduced by Brechbiel et al. but no further use has been reported yet.⁵ The C-substituted analogue **4** is commercially available. The synthesis of C-substituted NOTA derivative **5** was reported by Parker et al. in 7.7 % yield.⁶ Brechbiel et al. also reported very low cyclisation yields of C-substituted 9-membered rings due to transannular condensation.⁵ Consequently, we were interested in a cost-effective concept for an easy access to a bifunctional derivative of NOTA, starting from bulk chemicals.

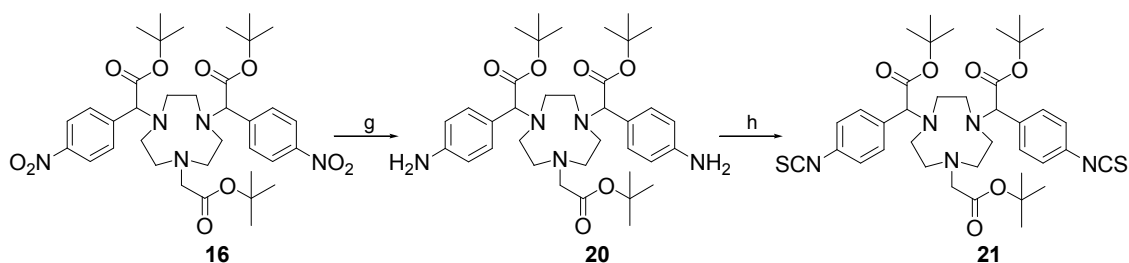


Scheme 1 Novel NOTA-derived bifunctional chelators NODAPA-NCS (**6**), NODAPA-OH (**7**) and NODAPA-(NCS)₂ (**8**)

Therefore a straightforward and economical synthesis of a bifunctional chelator was developed. Orthogonally reactive phenol as well as isothiocyanate functions were included for conjugation. The intended bifunctional chelators are illustrated in scheme 1. The gallium core forms stable five-ring chelates with the nitrogen and the adjacent carboxylate donors in NOTA and its analogues. Introduction of a conjugation functionality in a pendant arm branch into NOTA-analogue chelators following nucleophilic N-alkylation, requires a secondary leaving group in α -position to the carboxylate function. In addition, the planar phenylene subunit provides a non-flexible initial spacer, complementary to **2**, that can be combined with a variety of additional spacer functions via the included conjugation functionality. Both linkers, 2-bromo-(4-acetoxy-phenyl)-*t*-butylacetate (**9**) and 2-bromo-2-(*p*-nitrophenyl)-*t*-butylacetate (**10**) were easily synthesised from the corresponding acetic acid derivatives via *t*-butyl protection under Steglich conditions (i) in up to 80 % yield, followed by Wohl-Ziegler bromination (ii) in 90 % yield (Scheme 2).⁷⁻¹⁰ Cyclisation of 1,4,7-tritosyl-1,4,7-triazacyclononane (**11**) was achieved according to the well known procedure reported by Richman and Atkins.¹¹ Full detosylation (a) was performed in concentrated sulphuric acid (110°C, 2 h; Scheme 2).¹² The polyhydrogensulfate of 1,4,7-triazacyclononane (TACN, **12**) was precipitated in ethanol and diethylether,¹³ dissolved in a small amount of water and basified (pH = 13) with sodium hydroxide. After exposure to activated carbon under reflux followed by extraction with predistilled 1-butanol, **12** was obtained as colourless crystals displaying sufficient purity for all further reactions. Statistical alkylation (b) with **9** or **10** was carried out in the presence of potassium carbonate over three days in dichloromethane, using a threefold excess of TACN (**12**). Employing a lower excess of **12**, (d) the yield of the dialkylated product **15** increased.^{***} Thereby, a convenient access to multivalent [⁶⁸Ga]chelates is provided. The trialkylated product was not observed. Introduction of the *t*-butyl protected acetic acid donor functions (c) was performed in acetonitrile with stoichiometric amounts of 2-bromo-*t*-butyl acetate and potassium carbonate as base to afford **14**, **16** or **18** in a yield of up to 90 %.⁴ Although all NODAPA derivatives presented herein were successfully synthesised via statistical alkylation, the latter remains somewhat unfavourable for the synthesis of mono-functionalised derivatives **14**. Furthermore, a large excess of **12** has to be employed. Therefore, an alternative route was examined. The key step involved selective detosylation at two ring-nitrogens to facilitate stoichiometrical alkylation. First, 1,4,7-tritosyl-TACN (**11**) was reacted with HBr in glacial acetic acid containing an eight-fold excess of phenol (Scheme 2, e). The reaction proceeded straightforwardly to afford 88 % of 1-tosyl-1,4,7-triazacyclononane (**17**), as determined by ESI-MS and proton-NMR. Subsequent exposure of **17** to *t*-butyl bromoacetate in acetonitrile followed by SET-reduction (f) with sodium naphthalenide in dimethoxyethane or lithium in propylamine/ ethylenediamine gave secondary amine **19**. The latter was converted into the protected chelators **14a** and **14b** by reaction with bromides **9** and **10**, respectively, in 27 % overall yield. Catalytic hydrogenation of **16** was conducted under basic conditions (g) to give the desired aniline **20** in good yield (90 %) as shown in scheme 3.⁸



Scheme 2 Synthesis route to mono-functionalised and di-functionalised NOTA derivatives; (a) H₂SO₄, 2 h, 110 °C; (b) *t*-butyl 2-bromo-2-(4'-nitrophenyl) acetate, CH₂Cl₂, K₂CO₃, 3 d; (c) *t*-butyl bromoacetate, MeCN, K₂CO₃; (d) 2 eq. *t*-butyl 2-bromo-2-(4'-nitrophenyl) acetate, CH₂Cl₂, K₂CO₃, 3 d; (e) PhOH, HBr/AcOH, 1.5 d, 90 °C, (f) dimethoxyethane, Na, C₁₀H₈; (i) *t*BuOH, CH₂Cl₂, DCC, DMAP, 3 h; (ii) CCl₄ (distilled from P₄O₁₀), NBS, AIBN



Scheme 3 Synthesis of di-functionalised NOTA derivatives, (g) 2 mM KOH in MeOH, 10 % Pd/C, H₂, RT, 4 h, (h) Ca₂CO₃, Me₂CO, H₂O, thiophosgen

Subsequent conversion to an isothiocyanate **21** was carried out using thiophosgene in 85 % yield (Scheme 3, h).^{†††} The *t*-butyl esters were deprotected in trifluoroacetic acid and the trifluoroacetic acid salts were removed using an ion exchange resin, to afford **6** and **8** in up to 23% overall yield. **7** was obtained in similar yield after deacetylation in 10 % KOH in methanol, prior to deprotection in TFA.^{††} The desalted precursors were directly used for radiolabelling without further purification. In order to analyse whether the chain branch, containing the coupling moiety in one pendant arm, affects the kinetic and thermodynamic characteristics of [⁶⁸Ga]NOTA-complex formation, labelling of NODAPA-NCS (**6**),

NODAPA-OH (**7**), NODAPA-NCS₂ (**8**) and NODAPA-NO₂ (**14b**) with generator produced and purified Gallium-68 was carried out in aqueous solution at pH = 2.8.

Quality control was performed using an Agilent Zorbax C 8 column using 50 mM phosphate buffer and MeOH as eluent at 0.5 ml/min. Yields were very high (85±5 % after 3 min) and comparable to those achieved for NOTA (Fig. 3).

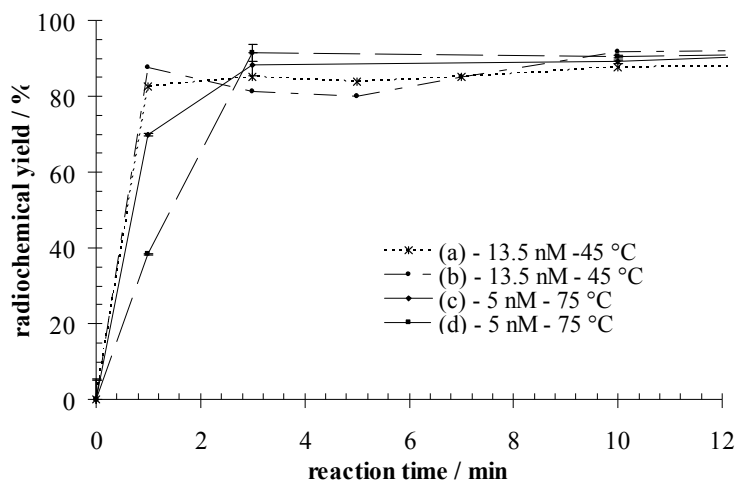


Figure 3 Time-dependency of ⁶⁸Ga-labelling of (a) NOTA, (b) NODAPA-OH (**7**), (c) NODAPA-NCS (**6**) and (d) NODAPA-NCS₂ (**8**) pH 2.8, 5 - 13.5 nmol ligand, 5 ml H₂O, 400 μl [⁶⁸Ga]GaCl₃ in N₂-solution.¹

The stability of both novel ⁶⁸Ga chelates was determined in a DTPA-challenge study at 25 °C and 37 °C employing 1 mM, 10 mM and 100 mM solutions of DTPA in water, indicating >94% complex stability, in a similar range as the congener NOTA (Fig. 4).

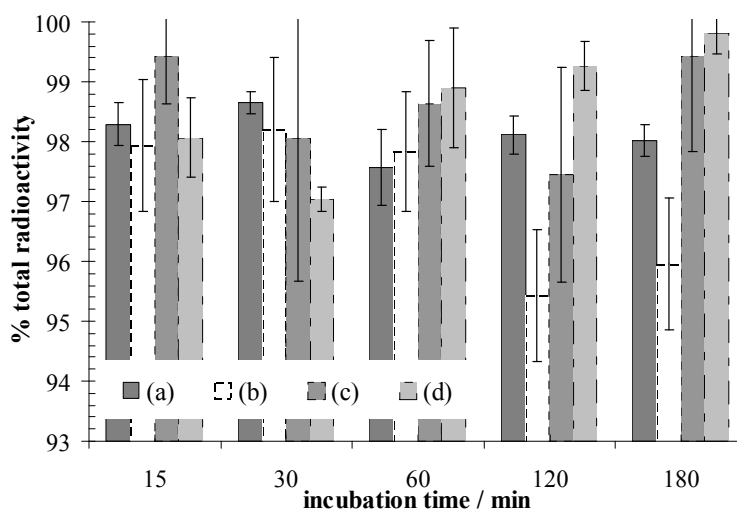
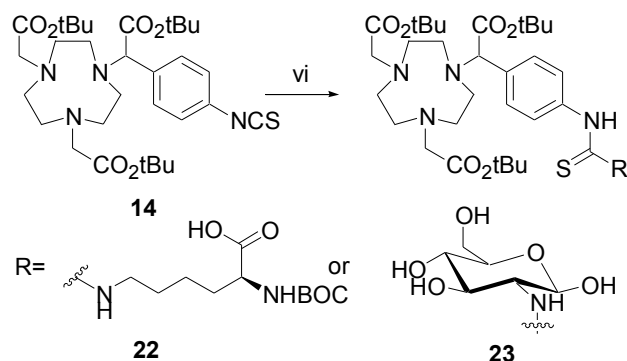


Figure 4 Stability of [⁶⁸Ga]NOTA (a), [⁶⁸Ga]NODAPA-OH (b), [⁶⁸Ga]NODAPA-NCS (c) and [⁶⁸Ga]NODAPA-(NCS)₂ (d); 10 mM DTPA in DPBS (pH 7.4) at 37 °C (n = 3).

Plasma protein binding and transchelation to serum proteins *in vitro* was examined under physiological conditions in rat plasma. 4 MBq of [⁶⁸Ga]NODAPA-OH were incubated in 300 μL of rat plasma from male adult Wistar rats, obtained via centrifugation of full blood. Samples of 50 μL were withdrawn after 1, 30, 60, 90 and 180 min and analysed by radio-TLC (silica gel 60, 5% aqueous NaCl-EtOH, 3:1).



Scheme 4 Conjugation of NODAPA-NCS to model substrates, (vi) Ca₂CO₃, MeOH: H₂O: NEt₃, 7:1:1,(65-73 %)

In correlation to the DTPA-challenge, less than 2 % of non-[⁶⁸Ga]NODAPA-OH radioactivity was observed after 3 h.

In conclusion, three novel NOTA-based bifunctional chelators have been obtained via a simple and efficient synthesis route. **6**, **7** and **8** provide excellent ⁶⁸Ga labeling and stability parameters. While offering –NCS and –OH functionalities, covalent coupling to various potential targeting vectors is possible. As a proof-of-concept, NODAPA-NCS was conjugated to L-lysine (**22**) and glucosamine (**23**) (Scheme 4).^{††††} The latter symbolise the first bioconjugates with the promising novel NOTA based bi-functional chelators introduced in the present work.

References and Notes

- (1) Zhernosekov, K. P., Filosofov, D. V., Baum, R. P., Aschoff, P., Bihl, H., Razbash, A., Jahn, M., Jennewein, M. and Rösch, F.; *J. Nucl. Med.*, **2007**, 48.
- (2) Craig, A. S., Parker, D., Adams, H., Bailey, N. A.; *J. Chem. Soc. Chem. Commun.* **1989**, 1793
- (3) Eisenwiener, K.-P., Prata, M. I. M., Buschmann, I., Zhang, H. W., Santos, A. C., Wenger, S., Reubi, J. C. and Mäcke, H. R.; *Bioconjugate Chem.*, **2002**, 13, 530
- (4) André, J. P., Maecke, H. R., Zehnder, M., Macko, L. and Akyel, K. G.; *Chem. Commun.*, **1998**, 1301
- (5) Brechbiel, M. W., McMurry, T. J. and Gansow, O. A.; *Tetrahedron* **1993**, 34, 3691
- (6) Cox, J. Craig, A., Helps, I. M., Jankowski, K., Parker, D., Eaton, M., Millican, A., Millar, K., Beeley, N. and Boyce, B.; *J. Chem. Soc., Perkin Trans. 1*, **1990**, 2567
- (7) Ziegler, K., Schenck, G., Krockow, E. W., Siebert, A., Wenz, A.; and Weber, H.; *Liebig's Annalen*, **1942**, 551, 1

- (8) Helps, I. M.; Parker, D., Morphy, J. R. and Chapman, J.; *Tetrahedron* **1989**, 45, 219
- (9) Neises, A., Steglich, W.; *Angew. Chem. Int. Ed. Engl.* **1978**, 17, 52213.
- (10) Wohl, A.; *Chem. Ber.* **1919**; 52, 51
- (11) Richman, J. E., Atkins, T. J.; *J. Am. Chem. Soc.*, **1974**, 96, 2268
- (12) Raßhofer, W., Vögtle, F.; *Liebigs Ann. Chem.*, **1977**, 1340
- (13) Diril, H., Chang, H. R., Nilges, M. J., Zhang, X., Potenza, J. A., Schugar, H. J., Isied, S. S. and Hendrickson, D. N.; *J. Am. Chem. Soc.*, **1989**, 111, 5102
- (14) Horner, L., and Winkelmann, E. H., *Angew. Chem.*, **1959**, 7, 349
- (15) ‡ (**14b**) δ_{H} (300 MHz; CDCl_3) 1.40 (9 H, s, t-Bu), 1.42 (18 H, s, t-Bu), 2.78 – 3.25 (16 H, m, N- CH_2 , N-CH), 4.10 (1 H, s, N-CH-Ar), 7.15 (2 H, d, $J = 8$ Hz, Ar), 7.40 (2 H, d, $J = 8$ Hz, Ar); m/z (ESI) 606.32 ($[\text{M}+\text{H}]^+$ $\text{C}_{31}\text{H}_{48}\text{N}_4\text{O}_6\text{S}$ requires 606.33, 100 %), 606.34 (96.1); 607.38 (58.0), 608.40 (12.9), 549.29
- ‡‡ (**14a**) δ_{H} (300 MHz; CDCl_3) 1.41 (9 H, s, t-Bu), 1.42 (9 H, s, t-Bu), 1.43 (9 H, s, t-Bu) 2.70 – 3.04 (12 H, m, N- CH_2), 3.25 (2 H, br s, $\text{CH}_2\text{-C}(\text{O})$) 3.30 (2 H, s, $\text{CH}_2\text{-C}(\text{O})$) 4.41 (1 H, dd, $J = 6$ Hz, N-CH-Ar), 6.74 (2 H, d, $J = 8$ Hz, ArH), 7.20 (2 H, d, $J = 8$ Hz, ArH); m/z (ESI) 564.37 ($[\text{M}+\text{H}]^+$ $\text{C}_{30}\text{H}_{49}\text{N}_3\text{O}_7$ requires 563.36, 100 %), 565.37 (35 %); 556.38 (8 %)
- ‡‡‡ (**21**) δ_{H} (300 MHz; CDCl_3) 1.41 (s, 9H, t-Bu), 1.415 (s, 9 H, t-Bu), 1.42 (s, 9 H, tBu), 3.10-2.60 (m, 12 H), 3.2 (m, 4 H, N- $\text{CH}_2\text{-COOtBu}$), 4.41 (s, 1 H, N- $\text{CH}'\text{-Ar}$), 4.41 (s, 1 H, N- $\text{CH}'\text{-Ar}$), 4.42 (s, 1 H, NCH-Ar); 7.57 (m, 4 H, Ar); 8.16 (m, 4 H, Ar) m/z (ESI) 738.30 (100 %); 739.33 (947 %); 740.35 (58.8 %); 741.37 (10.8 %); ($[\text{M}+\text{H}]^+$ $\text{C}_{38}\text{H}_{51}\text{N}_5\text{O}_6\text{S}_2$ requires 737.33, 100.0%), 738.33 (41,1%), 739.32 (9.0%), 739.33 (8.2%), 740.33 (37%)
- ‡‡‡‡ (**22**) δ_{H} (300 MHz; CDCl_3): 1.25 (m, 2 H, Lys-g- CH_2), 1.34 (s, 9 H, OtBu), 1.40 (s, 18 H, OtBu) 1.42 (s, 9 H, OtBu), 1,7 – 1,5 (m, 4 H, $\beta\text{-CH}_2$, $\delta\text{-CH}_2$), 3,0 – 2,65 (m, 12 H, N- $\text{CH}_2\text{-CH}_2$), 3,25 (4 H, s, N- $\text{CH}_2\text{-COOtBu}$); 3,50 (t, $J = 5$ Hz, 2 H, $\varepsilon\text{-CH}_2$); 4,05 (s, 1 H, N- CH-Ar); 4,34 (t, 1 H, $\alpha\text{-CH}$); 7,40 – 7,25 (m, 4 H, Ar); m/z (ESI) 851,6 $[\text{M}+\text{H}]^+$ $\text{C}_{42}\text{H}_{70}\text{N}_6\text{O}_{10}\text{S}$ requires 850,49. (**23**) m/z(ESI): 784,43 $[\text{M}+\text{H}]^+$ $\text{C}_{37}\text{H}_{61}\text{N}_5\text{O}_{11}\text{S}$ requires 783,41.

4.8 Studies towards the synthesis of lipophilic bifunctional chelators for ^{68}Ga

Studies towards the synthesis of lipophilic bifunctional chelators for ^{68}Ga

P. J. Riss, N. Hanik, F. Roesch

Institute of Nuclear Chemistry, Johannes Gutenberg University, 55128 Mainz, Germany

Abstract: The present study is concerned with charge-neutral, lipophilic, macrocyclic bifunctional chelators, suitable for the introduction of a gallium-68 label into small molecules. The synthesis of a novel bifunctional N_3S_3 -type chelator, derived from 1,4,7-triazacyclononane, initial ^{68}Ga -radiolabelling and the determination of stability and lipophilicity of the compound are described. The ^{68}Ga -labelled chelate was obtained in a radiochemical yield of $80 \pm 5\%$ after a reaction time of 7 minutes. It remained intact over 3 h in a DTPA-challenge experiment, indicating sufficient stability for PET studies.

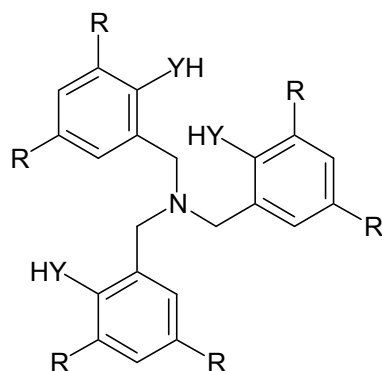
In the present years, the positron-emitter ^{68}Ga undergoes a renaissance as generator-derived PET-nuclide for clinical routine. This is due to recent improvements in generator performance of commercially available $^{68}\text{Ge}/^{68}\text{Ga}$ -generator systems, and post-processing of generator eluents. The latter includes purification of the ^{68}Ga by separation of metal contaminants as well as eluate concentration for labelling purpose.¹ Thereby a chemical generator system is transformed into a medical one.

The idea of lipophilic metal-chelates, dedicated for molecular imaging is not new. However, most of the earlier approaches did not specifically target bifunctional chelators, but elucidated the synthesis of rather lipophilic complex-precursors. The stability constants of various metal complexes formed by the former have also been accessed. These investigations yielded two main approaches with potential for successful application in imaging.

1) Tripodal, tetradentate NY_3 -type chelators (Figure 1), wherein Y is a substitute for O or S. These chelators yield highly stable complexes with trivalent metals, however, crystal structures of the non-radioactive complexes show bulky structures, that easily excel many bioactive small molecules by both, size and molecular weight.²⁻³

2) Chelators derived from the macrocyclic polyamine 1,4,7-triazacyclononane (TACN). Stable complexes can be obtained from the macrocyclic, hexachelating N_3Y_3 -type precursors (Figure 3). Unfortunately, some of these i.e. compounds **4** and **5** are even more sterically demanding and exhibit a higher molecular weight than the tripodal chelators mentioned earlier. Moore and coworkers have introduced compound **6a**, and a more lipophilic analogue was later on studied in rats with regard to a potential application as radio-gallium labelled tracer for hepatobiliary imaging by John et al.^{6,7} The ^{67}Ga -chelate displays rather lipophilic properties, is mainly excreted via the liver and remained stable versus trans-chelation to the iron binding sites of transferrin. Nevertheless, the compound did not show any uptake into the brain.⁵⁻⁷

Table 1: Tripodal, monofunctional tetradentate NY₃-type chelators



entry	Y	R	Reference
1	O	H	2a-b
2	O	CH ₃	2a
3	S	H	2b, 3

Recent progress includes the work of Luyt and Katzenellenbogen, who described a bifunctional chelator based on the first approach (Figure 2).⁴

Despite the potential value of the ligand for the intended use as labelling agent for peptides and proteins, the high molecular weight and the particular requirements for conjugation utilising the included aniline-NH₂ donor-function limits the value of this compound for labelling of small molecules.⁴

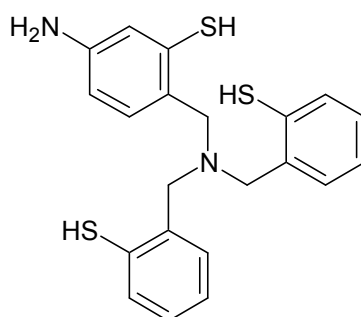
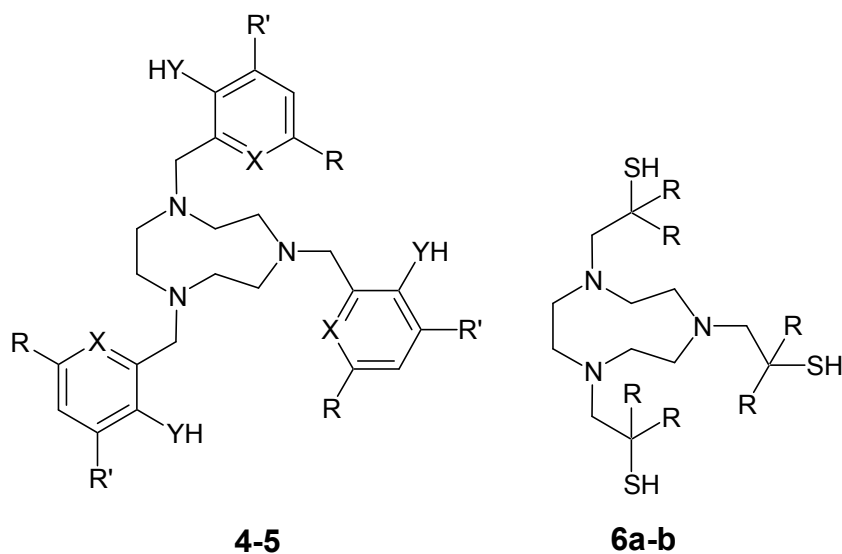


Figure 2: Tripodal, bifunctional NS₃-type chelator

Figure 3: Hexadentate N3S3-type chelators based on 1,4,7-triazacyclononane

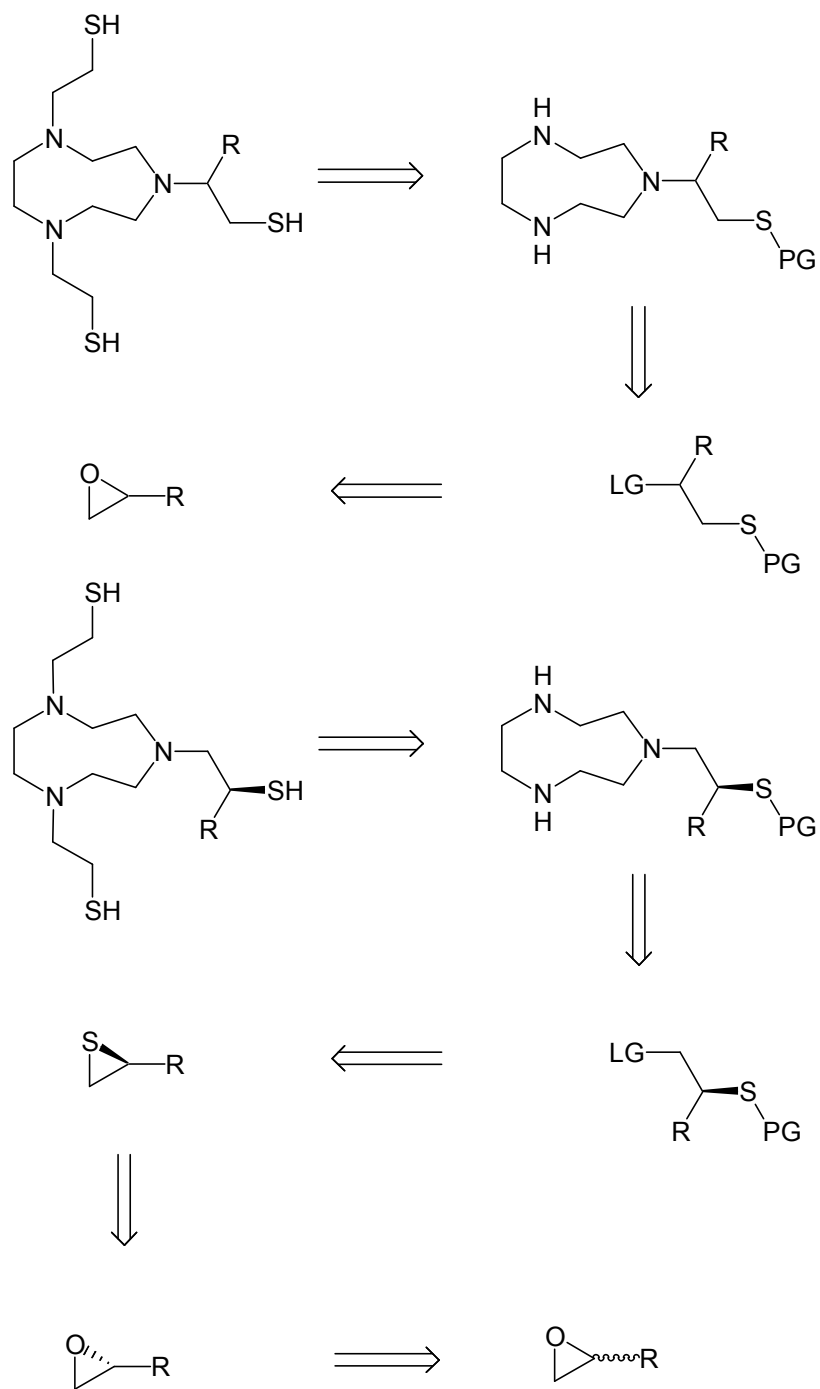


entry	X	Y	R	R'	Reference
4	N	O	CH ₃	H	5a-b
5	CH	O	CH ₃	CH ₃	5b-c
6a	-	-	H	-	5b, 6, 7
6b	-	-	CH ₃	-	7

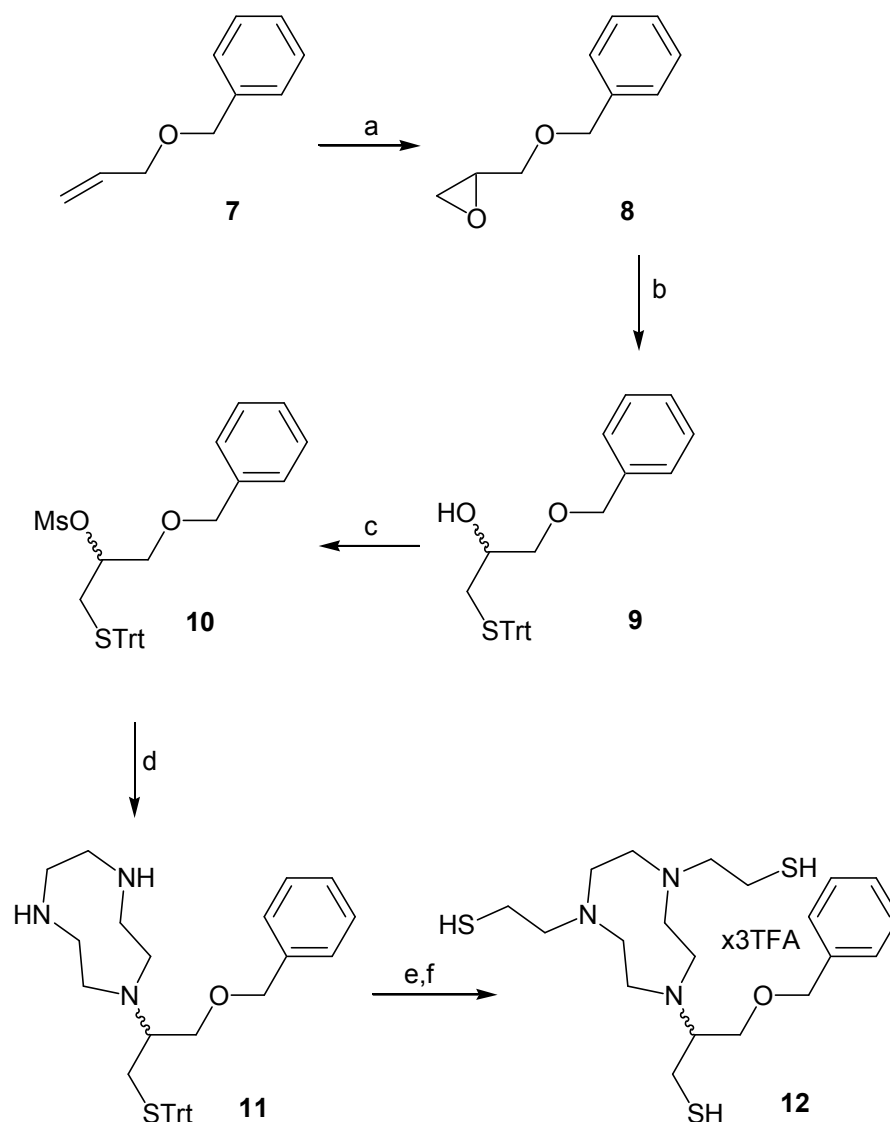
The present work is concerned with charge-neutral, lipophilic, macrocyclic bifunctional chelators, suitable for the introduction of a charge-free gallium label into small molecules. The corresponding gallium-chelate should possess a reasonably low molecular weight, a low tendency to form intermolecular hydrogen-bonds, kinetic inertness and sufficient thermodynamic stability to facilitate PET-imaging.

A bifunctional derivative of compound **6** was synthesised, labelled with generator-derived ⁶⁸Ga, tested for stability and the octanol-water partition coefficient was determined at pH 7.4 via HPLC.

The synthesis of the bifunctional pendant arms was straightforward from commercially available starting materials. Two routes were planned as shown in Scheme 1, including one approach to an enantiomerically enriched chelator. For further functionalisation of the chelator, an asymmetric alkylation approach was chosen, wherein one pendant arm was branched with an adjacent hydroxymethyl substituent. Thereby, various donor and acceptor function can be incorporated by interconversion of the versatile hydroxyl-group.



Scheme 1: Retrosynthetic approach to pendant arm functionalised bifunctional chelators based on TACN (**13**). The racemic route is shown on the left, whereas the enantioselective route is shown on the right. PG = protective group.



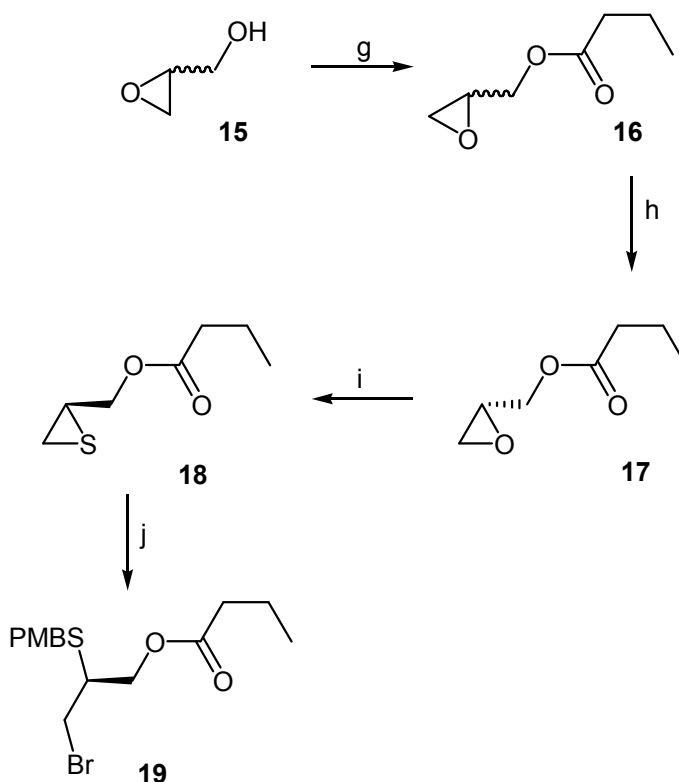
Scheme 2: Synthesis of racemic model compound **12**; a) mCPBA, CHCl₃, r.t., 14 h; b) 1. *n*-BuLi, heptane, THF, TrtSH, 0 °C, 30 min, 2. THF, **8**, 0 °C to r. t.; c) MsCl, NEt₃, CH₂Cl₂, 0 °C, 15 – 30 min; d) N₂, **13**, CH₂Cl₂, reflux 3 d; e) 1. N₂, C₂H₄S (2 equiv.), benzene, 50 °C, 2 h, 2. MeCN, anisole, TFA, Et₃SiH, -20 °C to 0 °C, 15 min.

To get an initial impression on the feasibility of the synthesis and an estimate on the properties of a potential bio-molecule conjugated 1,4,7-tris(mercaptoethyl)-1,4,7-triazacyclononane (TACN-TM, **6a**), model compound **12** was synthesised.

Therefore allyl-benzyl ether (**7**) was epoxidised with *meta*-chloroperbenzoic acid (**a**) to obtain **8** in 95 % yield.^{8a} Subsequent ring-opening with lithium triphenylmethyl mercaptate (**b**) afforded compound **9** in 88 % yield.^{8b} Mesylation of alcohol **9** under standard conditions (**c**) gave sulphide **10** in 97 % yield.^{8c} Compound **11** was obtained in only 33 % yield by asymmetric alkylation of **13** in dichloromethane (**d**).¹⁰ The final chelator **12** was obtained from **11** in 55 % yield via alkylation of the remaining secondary amines with ethylene sulphide (**e**) followed by immediate deprotection of the mono-thiol-protected intermediate (**f**),^{7,8d} resulting in an overall yield of 15 %.

1,4,7-triazacyclononane (**13**) was synthesized via the common route described by Richman et al.. Deprotection and work up was slightly modified to result in a reproducible yield of 83 ± 5 %. The reaction time for deprotection in concentrated sulphuric acid was reduced to 120 min at 110 °C. The conversion of the protected polyaminomacrocycle was monitored using the method of Voegtle and co-workers. The sulphuric acid was removed by two subsequent reprecipitations in Et₂O and MeOH. The obtained colourless slurry was taken up in water and made alkaline, prior to the extraction with n-butanol to obtain compound **13** as colourless crystals of sufficient purity for all further reactions.¹⁰

All initial labelling and stability experiments were carried out with **12**. The compound includes a benzyl group at the intended coupling moiety, which should, in theory, result in a high-lipophilicity analogue of the hydroxymethylene functionalised TACN-TM. Most bioactive molecules suitable for conjugation with an appropriate radiolabel are less lipophilic than the simple aromatic hydrocarbon used as model. Therefore, representative values obtained for the model conjugate are expected to be higher than those obtained with real targeting vectors.



Scheme 3: Synthesis of chiral, orthogonally protected building block **19** for the synthesis of enantiomerically enriched chelators; g) DMAP, pyridine, dichloromethane, butyric anhydride, 0 °C to r.t., 14 h; h) PPL, pH 7.8, NaOH, 6 h; i) N₂, SC(NH₂)₂, MeCN, RT, 14 h; j) N₂, PMB-Br (neat), r.t., 14 h.

The synthesis of the chiral building-block **19** was initiated from *rac*-glycidol **15**. The compound was acylated with butyric acid anhydride under mild conditions in 95 % yield, followed by kinetic resolution of the racemic ester **16** using pig liver esterase (PLE, E.C. 3.1.1.1).^{8e} The enantio-enriched product **17** was obtained in 36 % yield. **17** displayed an

enantiomeric excess of approximately 90 % ($[\alpha]_D^{20} = -2.8^\circ \text{ cm}^2 \text{ g}^{-1}$). The oxirane **17** was converted into thiirane **18** via exposure to thiourea in 95 % yield,^{8f} followed by the simultaneous introduction of the para-methoxy benzyl protective group into the thiol and bromide as leaving group.^{8g} Compound **19** was obtained in an overall yield of 18.5 %.

Compound **19** can serve as linker/donor moiety and allows pre-conjugation to an appropriate biomolecule prior to the attachment of the macrocycle as shown in Scheme 5. This approach would have the particular advantage of increased ease of synthesis, due to the fact that fewer steps would have to be performed on the macrocycle.

The TFA salt **12** was labelled in anhydrous chloroform as described previously, isolated by solid phase extraction and analysed by HPLC and TLC.¹² The radiochemical purity of the product exceeded 98 % and the specific activity of the product was $\geq 7 \text{ GBq}/\mu\text{mol}$.

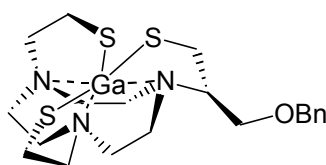


Figure 4: Potential structure of the Gallium complex **14**

Compound **12** was labelled with generator derived and prepurified $^{68}\text{Ga}(\text{III})$. The time dependency of the radiochemical yield is shown in Figure 5. The TFA salt **12** was dissolved in acetonitrile (1 mg/ml) and directly used for radio-labelling without further purification. Radiolabelling was conducted as recently reported.⁹ Briefly, the 0.1 M hydrochloric acid containing $[^{68}\text{Ga}]\text{Ga}(\text{III})$ was passed through and Biorad AG 50 W8 cation exchanger resin to trap the $^{68}\text{Ga}^{3+}$. The resin was subsequently eluted with N1 solution followed by air to remove the non-gallium-metal contamination. The n.c.a. radionuclide was eluted in a mixture of 2 % acetylacetonate and 5 mg of phenol in acetone, directly into a round-bottom, pressure-tight glass vial. Evaporation of the volatiles followed by reconditioning in dry chloroform (5 ml) afforded n.c.a. $[^{68}\text{Ga}]\text{Ga}(\text{acac})_3$. Precursor solution (10 μl , 13 nmol) were added to the reaction mixture and the reaction was conducted under microwave irradiation (CEM discover focussed microwave, 300 W, 2 min). The chloroform was evaporated and the product was taken up in purified water and passed through an acidic strong cation exchanger (Merck Lichrolut SCX, 200 mg).*

The product was formulated in DPBS, filtered through a Millex[®] sterile filter and the formulated tracer was analysed for radiochemical purity and specific activity by radio-HPLC (Merck Lichrocart RP-18, 7 μ , 150 x 4.6 mm, 25 % MeOH in PBS at pH 7.4) and radio-TLC (silica-gel 60, 0.1 M citrate solution pH 4, 30 % EtOH in 5% NaCl).

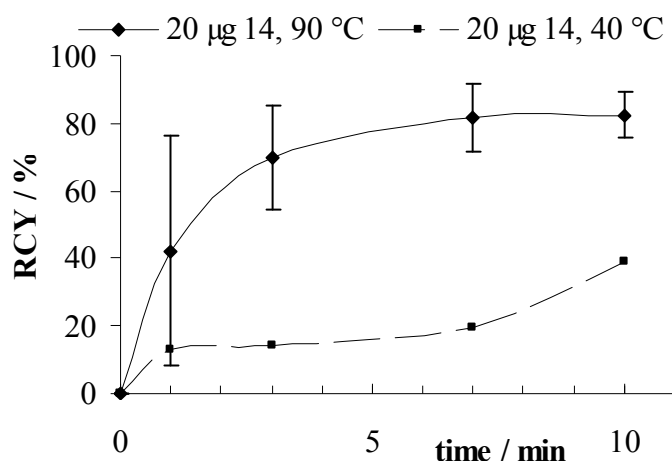


Figure 5: Gallium labelling of chelator **12** at two different temperatures

The stability of product [^{68}Ga]**14** was determined via a DTPA-challenge experiment.¹⁰ Therefore, aliquots of the radioactive product were added to 1 nM, 10 nM, 100 nM and 1 μM concentrations of DTPA in PBS at pH 7.4 and incubated for 180 min. Samples were withdrawn from the solutions after 5 min, 15 min, 30 min, 60 min, 120 min and 180 min. The percentage of intact complex [^{68}Ga]**14** were determined by TLC. It was found that virtually no transchelation occurred between [^{68}Ga]**14** and DTPA, indicating that the known high stability for the non-modified 1,4,7-trismercaptopethyl-1,4,7-triazacyclononane was retained within the introduction of the pendant arm branch.

The octanol-water partition coefficient was determined in triplicate using the OECD-HPLC-method. Unfortunately the measured $\log D_{7.4}$ was only 0.12, about two orders of magnitude lower than the required value of 2-3.¹¹

These above findings support the utility of **14** as a Gallium-label for blood-brain-barrier-penetrating small molecules, as the obtained product [^{68}Ga]**14** does display much less hydrophilic properties than reported for carboxylate-analogues.¹³ However, the compound might be of higher utility in other cases, i.e. for perfusion imaging or in the development of liver-function tracers. The approach to the enantioenriched chelator is clearly favourable compared to the racemic route, because the obtained primary, aliphatic bromide is significantly more reactive for N-alkylation of the nine-ring or direct attachment to a biomolecule. Furthermore, orthogonal protection at the sulphur and the oxygen facilitates maximum flexibility in further synthetic steps.

References and Notes:

- (1) (a) K. P. Zhernosekov, D. V. Filosofov, R. P. Baum, P. Aschoff, H. Bihl, A. Razbash, M. Jahn, M. Jennewein, F. Rösch, *J. Nucl. Med.* **2007**, 48, 1741, (b) F. Roesch: *Handbook of Nuclear Chemistry* 4, Kluwer Academic Publishers: Dordrecht **2003**; (c) M. J. Welch, C. S. Redvanly, *Handbook of Radiopharmaceuticals: Radiochemistry and Applications*, Wiley: New York **2002**
 - (2) (a) J. W. Hwang, K. Govindaswamy, S. A. Koch, *Chem. Commun.* **1998**, 1667 - 1668; (b) R. J. Motekaitis, A. E. Martell, S. A. Koch, J. W. Hwang, D. A. Quarless, M. J. Welch, *Inorg. Chem.* **1998**, 37, 5902 – 5911
 - (3) (a) N. Govindaswamy, D. A. Quarless, and S. A. Koch, *J. Am. Chem. Soc.* **1995**, 117, 8468 – 8469.
 - (4) L. G. Luyt, J. A. Katzenellenbogen, *Bioconjugate Chem.* **2002**, 13, 1140 – 1145.
 - (5) (a) R. J. Motekaitis, Y. Sun, A. E. Martell, *Inorg. Chim. Acta*, **1992**, 421, 198 - 200; (b) A. E. Martell, R. J. Motekaitis, E. T. Clarke, R. Delgado, Y. Sun, R. Ma, *Supramol. Chem.* **1996**, 6, 353 – 363; (c) D. A. Moore, P. E. Fanwick, M. J. Welch, *J. Inorg. Chem.* **1989**, 28, 1504
 - (6) (a) D. A. Moore, P. E. Fanwick, M. J. Welch, *J. Inorg. Chem.* **1990**, 29, 672 - 676; (b) U. Bossek, D. Hanke, K. Wiegardt, B. Nuber, *Polyhedron* **1993**, 12, 1-5; (c) R. Ma, M. J. Welch, J. Riebenspies, A. E. Martell, *Inorg. Chim. Act.* **1995**, 236, 75 – 82.
 - (7) C. S. John, S. Kinuya, G. Minear, R. K. Keast, C. H. Paik, *Nucl. Med. Biol.* **1993**, 20, 217-223.
 - (8) (a) M. Muehlbacher, C. D. Poulter, *J. Org. Chem.* 1988, **53**, 1026; (b) T. G. M. Dhar, L. A. Borden, S. Tyagarajan, K. E. Smith, T. A. Brancheck, R. L. Weinshank, C. Gluchowskit, *J. Med. Chem.* **1994**, 37, 2334-2342; (c) P. J. Riss, F. Rösch, *Org. Biomol. Chem.* **2008**, in press (d) B. J. Cleynhens, G. M. Bormans, H. P. Vanbilloen, D. V. Vanderghinste, D. M. Kieffer, T. J. De Groot, A. M. Verbruggen, *Tetrahedron Letters* **2003**, 44, 2597-2600; (f) D. Herault, C. Saluzzo, M. Lemaire, *Tetrahedron: Asymmetry* **2006**, 17, 1944-1951; (g) D. A. Trujillo, W. A. McMahon, R. E. Lyle, *J. Org. Chem.* **1987**, 52, 2932-2933.
 - (9) F. Zoller, P. Riss, F.-P. Montforts, F. Rösch, *Dalton Trans.* **2008**, submitted
 - (10) (a) P. Riss, C. Kroll, V. Nagel, F. Rösch, *Bioorg. Med. Chem. Letters* **2008**, 18, 5364-5367; (b) W. Raßhofer, F. Vögtle, *Liebigs Ann. Chem.* **1977**, 1340.
 - (11) C. A. Lipinski, F. Lombardo, B. W. Dominy, P. J. Feeney, *Adv. Drug Del. Rev.* **2001**, 46, 3-26.
 - (12) Proof of identity for compound **14**: MS(ESI) = 430.21 (100) [M+H]⁺ C₂₀H₃₅N₃OS₃ requires 429.1942; ¹H-NMR (400 MHz, CDCl₃): δ (in ppm) = 7.05 – 7.2 (m, 5 H, ArH), 4.5 (s, 2 H, ArCH₂-O), 3.58 – 3.46 (m, 1 H, OCH₂), 3.38 – 3.24 (m, 2 H, OCH₂, NC-H), 3.1 - 2.7 (m, 22 H, CH₂-S, NCH₂), 1.8 (brs, CH₂SH).
- * Notably, the trapped non-reacted gallium can be eluted from the cartridge with N1-solution and the non-reacted precursor can be recovered by alkaline elution to some extend.

- (13) E. Dadachova, C. Park, N. Eberly, D. Ma, C. H. Paik, M. W. Brechbiel, *Nucl. Med. Biol.* **2001**, 28, 695-701.

4.9 Radioaktiv-markierte Cyclopropan-Derivate DAT-affiner Tropane

Radioaktiv-markierte Cyclopropan-Derivate DAT-affiner Tropane

Patrick J. Riss, Frank Roesch

Institut für Kernchemie, Johannes Gutenberg Universität, 55128 Mainz, BRD

Die vorliegende Erfindung betrifft eine radioaktiv-markierte Verbindung für die quantitative, nicht-invasive Darstellung striataler und extrastriataler Dopamintransporter (DAT) in Menschen und Versuchstieren mittels Positronenemissionstomographie (PET), Einzelphotonenemissionstomographie (SPECT), Autoradiographie oder Radioassay. Die erfindungsgemäße Verbindung beinhaltet einen neuen, hochselektiven und hochaffinen Liganden, der für die radioaktive Markierung u.a. mit Fluor-18 (^{18}F) und mit Kohlenstoff-11 (^{11}C) geeignet ist.

Ein für die Quantifizierung erforderliches Gleichgewicht zwischen Bindung und Dissoziation eines Liganden zum Dopamintransporter in den DAT-reichen Hirnregionen wird in Nagetieren bereits wenige Minuten nach der intravenösen Applikation erreicht, in nichtmenschlichen Primaten nach weniger als einer Stunde. In den extrastriatalen DAT-haltigen Regionen wird das Bindungsgleichgewicht in Primaten in weniger als 30 Minuten erreicht. Die Pharmakokinetik in nicht-menschlichen Primaten ist mit der menschlichen vergleichbar. Die quantitative Visualisierung der dopaminergen Signaltransduktion im lebenden Menschen kann eine experimentelle Grundlage für die Beantwortung verschiedenster Fragestellungen liefern, die mit der dopaminergen Signaltransduktion verknüpft sind. Im Falle von Parkinson-Krankheit führt eine Schädigung dopaminergener Neuronen in der Substantia Nigra zur nichtreversiblen Erschöpfung der striatalen Dopaminsynthese, die mit Hilfe von 6- ^{18}F]L-DOPA und PET im fortgeschrittenen Stadium der Krankheit sichtbar wird. Die Substantia Nigra ist mit dem Striatum als so genannte nigro-striatale dopaminerge Bahn verknüpft und wird in erster Linie mit dem Bewegungsapparat, bzw. der inhibitorischen Dämpfung von durch Acetylcholin vermittelten, exzitatorischen Bewegungsreizen in Verbindung gebracht. Fehlfunktionen dieser Nervenbahn führen auch zu der für Parkinson typischen Bewegungsbeschränkung. Der Mangel an Dopamin führt zu einer übersteigerten Acetylcholinaktivität und somit zum charakteristischen Zittern. Im Gegensatz zu markierten L-DOPA-Derivaten kann die molekulare Bildgebung durch Messung der DAT-Verfügbarkeit mittels SPECT oder PET bereits im frühesten Stadium der entstehenden Parkinsonschen Krankheit positive Befunde liefern.

Die mesocorticolimbische, dopaminerge Bahn wird u.A. mit Suchterkrankungen und dem Belohnungseffekt (Belohnungsbahn) von suchterzeugenden Substanzen in Verbindung gebracht. In diesem Zusammenhang ist die Verfügbarkeit von Dopaminrezeptoren und -transportern im nucleus accumbens von Bedeutung, da diese Hirnregion in dem oben genannten Zusammenhang eine zentrale Stellung einnimmt. Dopaminerge Axone projizieren, ausgehend vom ventralen tegmentalen Areal mit hoher Dichte in den Nucleus accumbens und von dort aus weiter zu dem Corpus amygdaloideum, dem Septum, dem vorderen Gyrus cinguli und dem frontalen Cortex. In diesem Zusammenhang kann die Messung der Verfügbarkeit dopaminergener Transporter zum Verständnis von Substanz-vermittelten

Suchterkrankungen und ähnlichen Krankheitsbildern beitragen.

Schizophrenie und andere Psychosen werden ebenfalls mit Fehlfunktionen dieser Bahn in Verbindung gebracht. Neben dem Verständnis zugrunde liegender neuronaler Prozesse auf Basis des Dopamintransporters kann die PET in dieser Fragestellung insbesondere zur Aufklärung von Wirkmechanismen, Therapiekontrolle und Dosisbestimmung der gegen Psychosen eingesetzten Psychotherapeutika (Neuroleptika, Dopaminantagonisten) beitragen. Der DAT kann auch hier als ein wichtiger Bestandteil des Krankheitsbildes aufgefasst werden, da er die präsynaptische Ausschüttung des endogenen Dopamins reguliert, dessen Bindung an postsynaptische Rezeptoren durch Neuroleptika herabgesetzt wird.

Das Aufmerksamkeitsdefizits/Hyperaktivitätssyndrom ADHS wird ebenfalls mit dopaminergen Fehlfunktionen erklärt. Beispielsweise können mit DAT-affinen Liganden für SPECT und PET deutlich erhöhte DAT-Verfügbarkeiten im Striatum gemessen werden, die mit einer verringerten Dopaminkonzentration korrelieren und die erhöhte Motivation von ADHS-Patienten erklären. Das ADHS-Therapeutikum Methylphenidat (Ritalin[®]) blockiert DAT und Noradrenalintransporter im Gehirn und kann somit den akuten Symptomen entgegenwirken. Neben der Therapiekontrolle mittels DAT-PET, erscheint die Messung und Bewertung der DAT-Verfügbarkeit im Mittelhirn mittels bildgebender Verfahren im oben genannten Krankheitsbild jedoch vielversprechender, z.B. zeigt sich in Kindern mit Läsionen in Bereichen des Mittelhirns, Substantia nigra, erhöhtes Auftreten von ADHS. Studien am extrastriatalen DAT im Mittelhirn können in diesem Zusammenhang zum Verständnis der neurochemischen Störung beitragen.

Zusätzlich ermöglichen DAT-Liganden die klinische Bewertung neuer Arzneistoffe hinsichtlich ihrer Charakteristika im Bezug auf die Beeinflussung des dopaminergen Systems, eines Wirkmechanismus im Bereich des DAT oder ihres suchterzeugenden Potentials.

DAT-Liganden sind im Stand der Technik bekannt.

Kommerziell ist beispielsweise ein SPECT-Radiotracer verfügbar in Form des als DATscan[®] vertriebenen 8-(3-Fluorpropyl)-2 β -carboxymethyl-3 β -(4'-[¹²³I]iodphenyl)-nortropan. Neben der eingeschränkten Quantifizierbarkeit der mittels SPECT gemessenen Radioaktivitätsverteilung im Gehirn und der deutlich schlechteren Auflösung der SPECT-Bildgebung im Vergleich zur PET, sind die langsame Gleichgewichtseinstellung und vor allem die mangelnde Bindungselektivität des Liganden nachteilig für die sensitive Befundung der Patienten. Die Darstellung des extrastriatalen Bestandteils der nigro-striatalen Bahn ist durch dieses Radiopharmakon ebenfalls nicht möglich, wodurch speziell die Bewertung eines extrastriatalen Fortschreitens der Krankheit mit Hilfe von DATscan[®] unmöglich ist. Typischerweise wird der Radiotracer DATscan[®] bereits einen Tag vor der eigentlichen Messung appliziert, um zum Zeitpunkt der Messung ein ausreichendes Gleichgewicht sicher zu stellen.

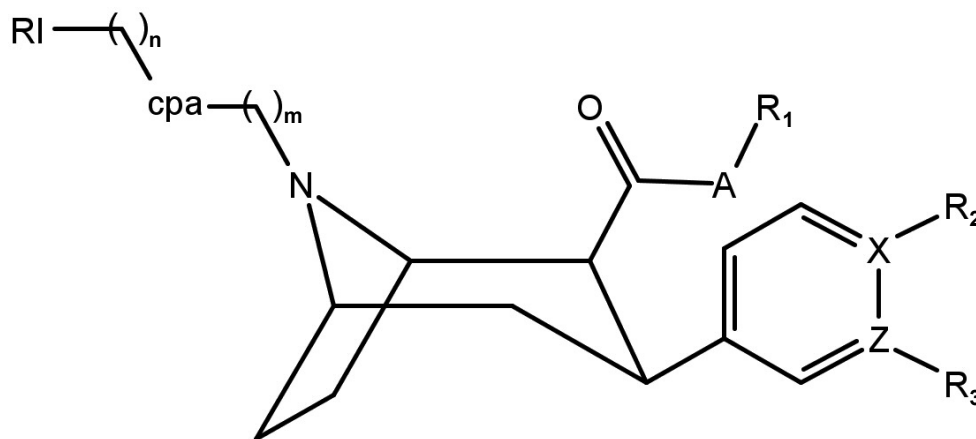
Im Weiteren schlägt WO 00/64490 Fluoralkenyl-nortropane als Radiotracer für PET vor, wobei das Radioisotop, bei dem es sich bevorzugt um ¹⁸F handelt, über ein Alkenyl der Struktur (CH₂)R(CH₂) an den Stickstoff des Tropyls gebunden ist. R ist eine ein- oder mehrfach ungesättigte Kohlenwasserstoffverbindung mit 2 bis 6 Kohlenstoffatomen (C₂-C₆), die eine oder mehrere Ethylen-, Acetylen- oder Allen-Gruppen enthält.

EP 1 212 103 offenbart 4-Fluoralkyl-3-halogenphenylnortropane, die sich für die in situ Bildgebung mittels PET und SPECT eignen. In den beschriebenen 4-Fluoralkyl-3-halogenphenylnortropanen sind radioaktive Halogenisotope an den Phenylring gebunden.

Die im Stand der Technik bekannten Radiotracer erfüllen nicht alle Anforderungen für die quantitative Visualisierung der dopaminergen Signaltransduktion in lebenden Organismen.

Dementsprechend hat die vorliegende Erfindung die Aufgabe, radioaktiv markierbare Liganden bereitzustellen, die die Anforderungen für die quantitative Visualisierung der dopaminergen Signaltransduktion in lebenden Organismen in höherem Maße erfüllen; insbesondere sollen Radiotracer mit hoher Selektivität und Affinität geschaffen werden.

Diese Aufgabe wird gelöst durch eine Verbindung der Struktur:



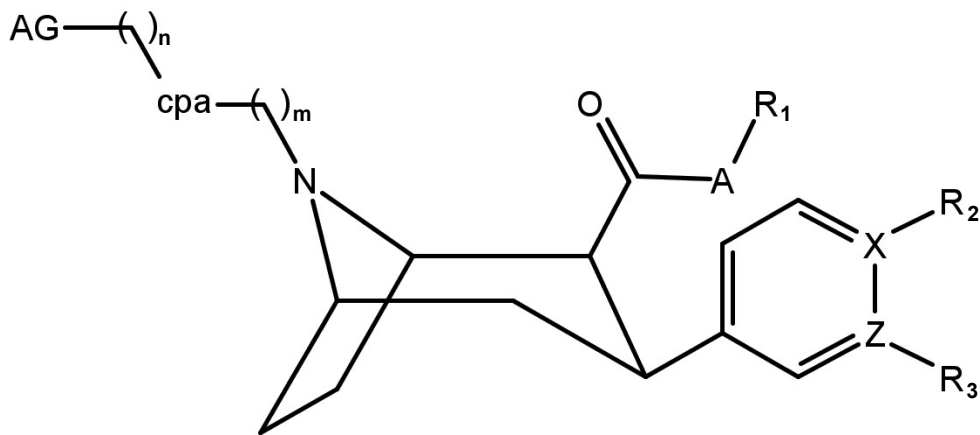
worin RI ein Radioisotop umfasst; cpa gleich Cyclopropan-1,2-diyl ist; und m und n eine natürliche Zahl größer gleich 0 sind. N und m können dabei gleich oder voneinander verschieden sein.

Vorzugsweise ist RI ein Radioisotop, das aus der Gruppe, bestehend aus ^1H , ^{11}C , ^{14}C , ^{13}N , ^{18}F , ^{76}Br , $^{123-131}\text{I}$, ausgewählt ist. In einer anderen bevorzugten Ausführungsform der Erfindung ist RI ein Komplex eines metallischen Radioisotops, das aus der Gruppe, bestehend aus ^{44}Sc , ^{64}Cu , ^{55}Co , ^{66}Ga , ^{67}Ga , ^{68}Ga , $^{99\text{m}}\text{Tc}$, ^{111}In , ausgewählt ist. Bei dem Komplex handelt es sich insbesondere um einen Komplex der einen makrozyklischen Chelator auf Basis des Cyclens (1,4,7,11-Tetraazacyclododecan) oder TACN (1,4,7-Triazacyclononan) beinhaltet.

Weiterbildungen der Erfindung sind dadurch gekennzeichnet, dass:

- R_1 ein einwertiger Rest einer Kohlenwasserstoffverbindung, ausgewählt aus der Gruppe, bestehend aus CH_3 , CH_2CH_3 , $(\text{CH}_2)_2\text{CH}_3$, $\text{CH}(\text{CH}_3)_2$, $\text{C}(\text{CH}_3)_3$, $(\text{CH}_2)_2\text{F}$, $(\text{CH}_2)_3\text{F}$, Phenyl, ist, wobei A ein O (Sauerstoff) oder ein N (Stickstoff) sein kann;
- X gleich C (Kohlenstoff) und R_2 ein Atom oder eine Verbindung, ausgewählt aus der Gruppe, bestehend aus H, CH_3 , F, Cl, Br, I, NO_2 , NH_2 , $\text{CH}(\text{CH}_3)_2$, $\text{C}(\text{CH}_3)_3$, CHO, COOH, COOR, CH_2F , CH_2Cl , CH_2Br , CH_2I , Phenyl, OH, OCH_3 ist;
- X gleich N (Stickstoff) ist;
- Z gleich C (Kohlenstoff) und R_3 ein Atom oder eine Verbindung, ausgewählt aus der Gruppe, bestehend aus H, CH_3 , F, Cl, Br, I, NO_2 , NH_2 , $\text{CH}(\text{CH}_3)_2$, $\text{C}(\text{CH}_3)_3$, CHO, COOH, COOR, CH_2F , CH_2Cl , CH_2Br , CH_2I , Phenyl, OH, OCH_3 ist; und
- Z gleich N (Stickstoff) ist.

- Im Weiteren betrifft die Erfindung einen Markierungsvorläufer für die Synthese der voranstehend beschriebenen, radioaktiv markierten Verbindungen. Der erfindungsgemäße Markierungsvorläufer umfasst ein Reagenz und eine Verbindung der Struktur:



worin cpa gleich Cyclopropan-1,2-diyl ist; und m und n eine natürliche Zahl größer gleich 0 sind; AG eine Abgangsgruppe ist, die durch einen radioaktiven Substituenten ersetzt wird; und das Reagenz geeignet ist, die Abgangsgruppe AG durch einen radioaktiven Substituenten zu ersetzen.

Alternativ kann der Zugang zu dieser Struktur auch erfolgen, indem die AG-(CH₂)_n-cpa-(CH₂)_m-Gruppierung zuerst insgesamt synthetisiert und anschließend als Ganzes an das Stickstoffatom gebunden wird.

Insbesondere handelt es sich bei dem radioaktiven Substituenten des Markierungsvorläufer um ein Radioisotop, das aus der Gruppe, bestehend aus ³H, ¹¹C, ¹⁴C, ¹³N, ¹⁸F, ⁷⁵Br, ⁷⁶Br, ¹²³⁻¹³¹I, ausgewählt ist; oder um einen Komplex eines metallischen Radioisotops, das aus der Gruppe, bestehend aus ⁴⁴Sc, ⁶⁴Cu, ⁵⁵Co, ⁶⁷Ga, ⁶⁸Ga, ^{99m}Tc, ¹¹¹In, ausgewählt ist.

Zudem wird ein Verfahren zum Durchführen einer Positronenemissions-Tomographieabbildung, einer Einzelphotonenemissions-Tomographieabbildung, einer Autoradiographie oder eines Radioassays eines Subjektes vorgeschlagen. Das Verfahren umfasst das Verabreichen einer abbildungserzeugenden Menge einer Verbindung nach Anspruch 1, welche mindestens ein Radioisotop oder einen Komplex eines metallischen Radioisotops enthält, an das Subjekt und das Messen der Verteilung und gegebenenfalls des Gehalts der Verbindung innerhalb des Subjekts mittels Positronenemissions-Tomographie, Einzelphotonenemissions-Tomographie, Autoradiographie oder Radioassay.

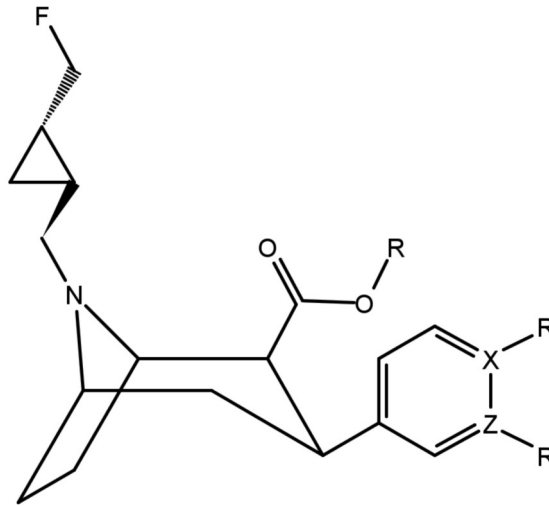
In bevorzugten Ausführungsformen es erfindungsgemäßen Verfahrens wird:

- die Verteilung der Verbindung mittels Positronenemissions-Tomographie gemessen, wobei das Radioisotop aus der Gruppe, bestehend aus ³H, ¹¹C, ¹⁴C, ¹³N, ¹⁸F, ⁷⁵Br, ⁷⁶Br, ¹²⁰I, ¹²⁴I, ⁴⁴Sc, ⁶⁴Cu, ⁵⁵Co, ⁶⁶Ga, ⁶⁸Ga ausgewählt ist;
- die Verteilung der Verbindung innerhalb des Subjekts mittels Einzelphotonenemissions-Tomographie gemessen, wobei das Radioisotop aus der

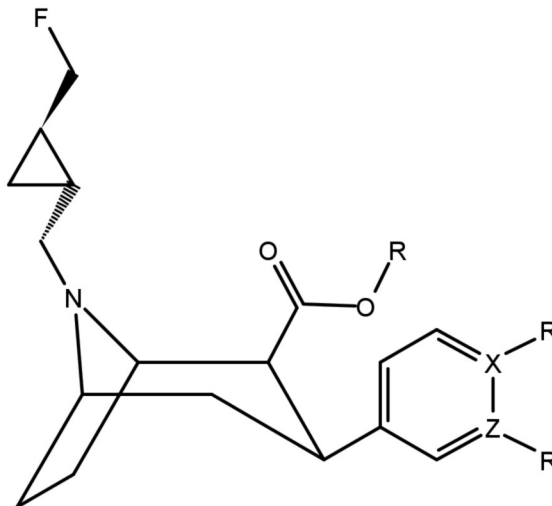
Gruppe, bestehend aus ^{123}I , ^{131}I , ^{67}Ga , $^{99\text{m}}\text{Tc}$, ^{111}In ausgewählt ist; und

- die Verteilung und der Gehalt der Verbindung innerhalb des Subjekts mittels Autoradiographie oder Radioassay gemessen, wobei das Radioisotop aus der Gruppe, bestehend aus ^3H , ^{14}C ausgewählt ist.

Für PET sind erfindungsgemäße Radiotracer der folgenden Strukturen besonders geeignet:



oder



Wie der Fachliteratur zu entnehmen ist, wurden zahlreiche Anstrengungen unternommen, Tropane bzw. Nortropane zu modifizieren, um ihre Selektivität und Affinität für Dopaminrezeptoren zu erhöhen. Diese Bemühungen waren bislang nur in beschränktem Maße erfolgreich.

Völlig überraschend wurde nun gefunden, dass die Platzierung von Cyclopropan-Einheiten

am Stickstoffatom des Tropyls die Selektivität und Affinität von Nortropanen in erheblichem Maße erhöht und zugleich ihre Anreicherungskinetik stark beschleunigt. Des Weiteren wird die metabolische Stabilität gegenüber oxidativer Metabolisierung der Doppelbindung erhöht.

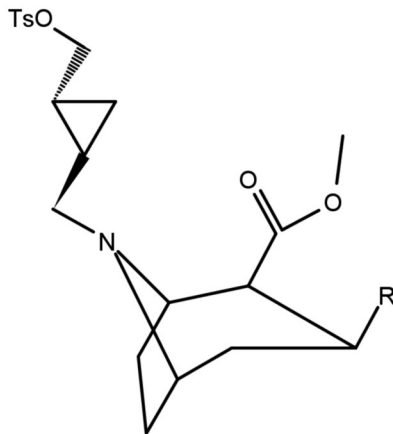
Die herausragende Selektivität der erfindungsgemäßen Liganden wird durch strukturelle Modifikation der darin verwendeten Nortropane erreicht, die zu einer Versteifung der räumlichen Struktur des Moleküls führen. Diese rigide Konformation ermöglicht die für die Bindung an den DAT erforderliche „induced-fit“-Interaktion, erschwert jedoch gleichzeitig die Bindung an ähnliche Bindungsstellen der analogen Monoamintransporter SERT und NET, sowie die Bindung an andere biologische Targets. Zusätzlich besitzen die Liganden eine auf die schnelle Penetration der Blut-Hirn-Schranke angelegte Lipophilie und ein geringes Molekulargewicht, um einer langsamen Kinetik entgegen zu wirken. Die hohe Affinität der Liganden begünstigt auch die Visualisierung solcher Hirnregionen, die eine geringe Dichte an DAT aufweisen. Mit den erfindungsgemäßen Liganden wird das erforderliche Gleichgewicht innerhalb erheblich kürzerer Zeiten erreicht. Zudem sind die Radiotracer hochaffin und binden selektiv an den DAT, so dass neben den DAT-reichen Regionen auch die schwächeren Populationen des Dopamintransporters abgebildet werden können. Sie sind daher für die oben genannten Anwendungen von herausragendem Interesse.

Zusätzlich soll die Anwendung zweier PET-Radionuklide mit unterschiedlicher Halbwertszeit den Untersuchungs-spezifischen Einsatz der Radioaktivität ermöglichen. Während Fluor-18 (^{18}F) die hochaufgelöste Darstellung selbst solcher Regionen ermöglicht, bei denen die Pharmakokinetik eher langsam ist und zusätzlich über Entfernungen von mehreren hundert Kilometern zwischen dem Standort der Produktion und dem Standort der PET-Kamera transportiert werden kann, ermöglicht Kohlenstoff-11 (^{11}C) durch seine kurze Halbwertszeit den aufeinanderfolgenden Einsatz verschiedener Radiotracer im gleichen Patienten am gleichen Tag. Dadurch werden umfassende Studien neurologischer Prozesse erheblich erleichtert. Die schnelle Kinetik des Liganden im Bereich der extrastriatalen Bindungsstellen ist dabei zusätzlich von Vorteil.

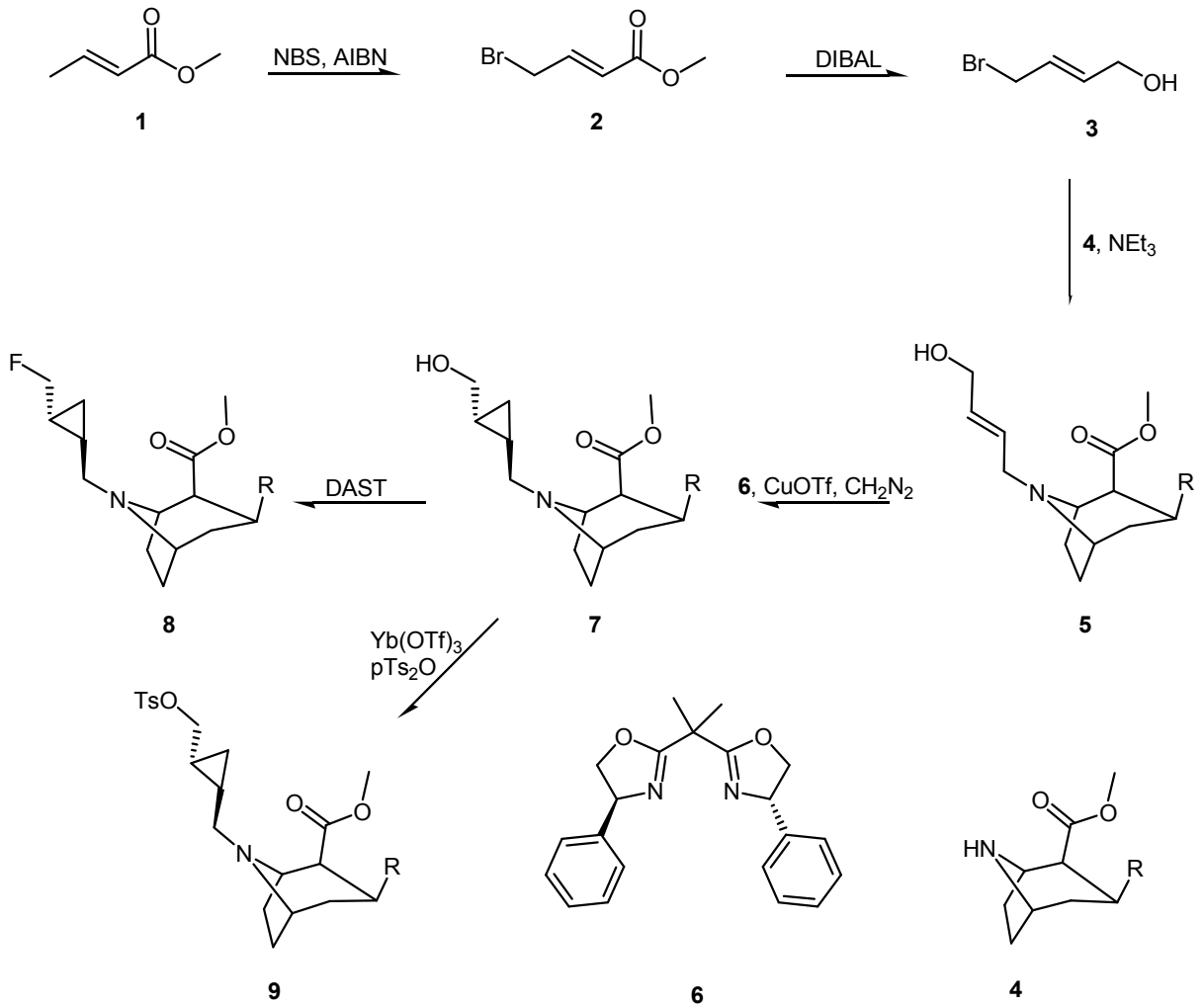
Begünstigt wird eine systematische Anwendung in der klinischen Diagnostik, der Arzneimittel-Evaluierung und der Grundlagenforschung durch die relativ einfache Synthese in hoher Ausbeute und Reinheit.

Neben der Bildgebung mittels PET eignen sich die erfindungsgemäßen Liganden als hochaffine und hochselektive Referenzliganden für molekularbiologische Studien, da sie keine störenden Kreuzaffinitäten zu anderen Neurotransmittersystemen aufweisen. Analog zur Markierung mit Kohlenstoff-11 (^{11}C) ist hier eine Markierung mit Tritium oder Kohlenstoff-14 (^{14}C) in einer metabolisch stabilen Position des Moleküls möglich.

Beispiel: Synthese eines N-cyclopropan-derivatisierten Tropan-Markierungsvorläufers



Das Syntheschema ist im Folgenden zusammengefasst:



Methylcrotonat (1) wird mit 0,7 Äquivalenten N-Bromsuccinimid in Tetrachlorkohlenstoff gelöst und bis zum Rückfluss erhitzt. Die Reaktion wird durch Zugabe von einer Spatelspitze AIBN initiiert. Nach einer Reaktionszeit von einer Stunde wird das entstandene N-Hydroxysuccinimid abfiltriert und das Filtrat wird eingeeignet. Methyl-4-bromcrotonat (2) wird durch Vakuumdestillation in 80 % Ausbeute isoliert.

Zu einer Lösung von (2) in Toluol werden zwei Äquivalente einer 1 molaren Lösung von Diisobutylaluminiumhydrid unter Kühlung so zugetropft, dass die Reaktionsmischung eine Temperatur von $-78\text{ }^{\circ}\text{C}$ beibehält. Anschliessend wird die Lösung langsam auf Raumtemperatur erwärmt. Nach Beendigung der Reaktion werden sechs Äquivalente Methanol, gelöst in THF, gefolgt von sechs Äquivalenten Wasser, ebenfalls gelöst in Toluol langsam unter Kühlung zugetropft. Die entstandene Lösung wird noch vier Stunden bei Raumtemperatur gerührt. Anschließend wird der feine Aluminiumhydroxid-Niederschlag über Celite® abfiltriert, das Filtrat wird getrocknet und eingeeignet. Der Rückstand wird im Vakuum destilliert. Man erhält 4-Brombut-2-en-1-ol (3) in 78 % Ausbeute.

Das 2-Carboxymethyl-nortropan (4) wird bei Raumtemperatur in Ethanol gelöst und mit einem Äquivalent Triethylamin versetzt. Anschließend wird (3) gelöst in Ethanol zugetropft und die Reaktionslösung wird zum Rückfluss erhitzt. Nachdem alles (4) umgesetzt ist, wird die Reaktionslösung konzentriert und der Rückstand säulenchromatographisch aufgereinigt. Man erhält den Alkohol (5) in 90 % Ausbeute.

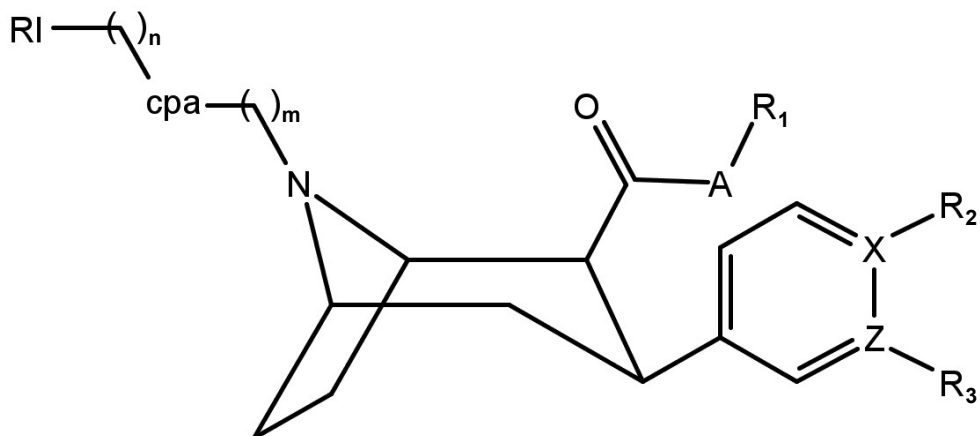
Cu(I)OTf und (6) werden in Dichlormethan vorgelegt, eine Lösung von (5) in Dichlormethan wird zugegeben und die Reaktionsmischung wird auf $-40\text{ }^{\circ}\text{C}$ gekühlt. Anschließend wird eine 2 molare etherische Diazomethanlösung im Argonstrom durch die Lösung geleitet. Nachdem die Reaktion beendet wurde, wird der Ansatz auf Raumtemperatur erwärmt und im Vakuum konzentriert. Der Rückstand wird säulenchromatographisch aufgereinigt. Man erhält 80 % des Cyclopropan (7).

(7) wird in Dichlormethan gelöst und bei $-78\text{ }^{\circ}\text{C}$ langsam zu einer Lösung von Diethylaminoschwefeltrifluorid (DAST) in Dichlormethan getropft. Nach erfolgter Zugabe wird noch ein Stunde bei dieser Temperatur gerührt. Die Reaktionslösung wird schrittweise auf Raumtemperatur erwärmt. Nach vollständigem Umsatz wird die Reaktionslösung mit 5 % Natriumhydrogencarbonatlösung behandelt und die organische Phase wird abgetrennt. Nach Trocknung über Natriumsulfat und Konzentration im Vakuum wird der erhaltene Rückstand säulenchromatographisch aufgereinigt. Man erhält Fluorid (8) in 90 % Ausbeute.

Triethylamin und ein Äquivalent (7) wird in Dichlormethan gelöst und auf $0\text{ }^{\circ}\text{C}$ gekühlt. Anschliessend werden 1,5 Äquivalente p-Toluensulfonylchlorid portionsweise zugegeben. Nach beendeter Zugabe wird noch 4 h gerührt. Die Reaktion wird mit Wasser gequench und die organische Phase wird abgetrennt. Nach einmaligem Waschen mit 1 molarer Natriumcarbonatlösung wird die organische Phase getrocknet und im Vakuum eingeeignet. Der Rückstand wird flashchromatographisch aufgereinigt. Man erhält den Markierungsvorläufer (9) in 75 % Ausbeute.

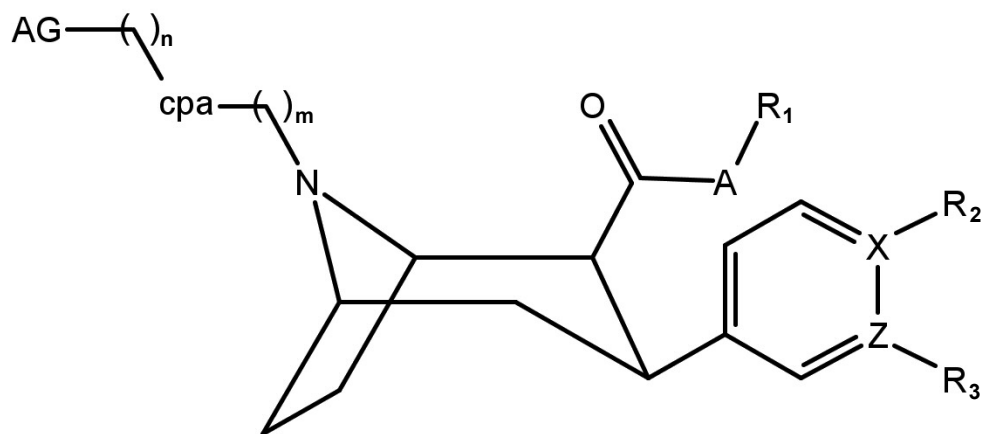
Patentansprüche

1. Eine Verbindung der Struktur:



- Worin RI ein Radioisotop umfasst; cpa gleich Cyclopropan-1,2-diyl ist; und m und n eine ganze Zahl größer gleich 0 ist, und m und n gleich oder verschieden sind.
2. Eine Verbindung nach Anspruch 1, dadurch gekennzeichnet, dass RI ein Radioisotop ausgewählt aus der Gruppe, bestehend aus ^1H , ^{11}C , ^{14}C , ^{13}N , ^{18}F , ^{76}Br , $^{120-131}\text{I}$, ist.
 3. Eine Verbindung nach Anspruch 1, dadurch gekennzeichnet, dass RI ein Komplex eines metallischen Radioisotops, ausgewählt aus der Gruppe, bestehend aus ^{44}Sc , ^{64}Cu , ^{55}Co , ^{66}Ga , ^{67}Ga , ^{68}Ga , $^{99\text{m}}\text{Tc}$, ^{111}In ist.
 4. Eine Verbindung nach Anspruch 3, dadurch gekennzeichnet, dass der Komplex einen bifunktionellen Chelator, insbesondere einen makrozyklischen Chelator auf Basis des Cyclen (1,4,7,11-Tetraazacyclododecan) oder TACN (1,4,7-Triazacyclononan) beinhaltet.
 5. Eine Verbindung nach Anspruch 1, dadurch gekennzeichnet, dass R_1 ein einwertiger Rest einer Kohlenwasserstoffverbindung, ausgewählt aus der Gruppe, bestehend aus CH_3 , CH_2CH_3 , $(\text{CH}_2)_2\text{CH}_3$, $\text{CH}(\text{CH}_3)_2$, $\text{C}(\text{CH}_3)_3$, $(\text{CH}_2)_2\text{F}$, $(\text{CH}_2)_3\text{F}$, Phenyl ist.
 6. Eine Verbindung nach Anspruch 5, dadurch gekennzeichnet, dass A ein O (Sauerstoff) ist.
 7. Eine Verbindung nach Anspruch 5, dadurch gekennzeichnet, dass A ein N (Stickstoff) ist.
 8. Eine Verbindung nach Anspruch 1, dadurch gekennzeichnet, dass X gleich C (Kohlenstoff), und R_2 ein Atom oder eine Verbindung, ausgewählt aus der Gruppe, bestehend aus H, CH_3 , F, Cl, Br, I, NO_2 , NH_2 , $\text{CH}(\text{CH}_3)_2$, $\text{C}(\text{CH}_3)_3$, CHO, COOH, COOR, CH_2F , CH_2Cl , CH_2Br , CH_2I , Phenyl, OH, OCH_3 ist.
 9. Eine Verbindung nach Anspruch 1, dadurch gekennzeichnet, dass X gleich N (Stickstoff) ist.
 10. Eine Verbindung nach Anspruch 1, dadurch gekennzeichnet, dass Z gleich C (Kohlenstoff), und R_3 ein Atom oder eine Verbindung, ausgewählt aus der Gruppe, bestehend aus H, CH_3 , F, Cl, Br, I, NO_2 , NH_2 , $\text{CH}(\text{CH}_3)_2$, $\text{C}(\text{CH}_3)_3$, CHO, COOH, COOR, CH_2F , CH_2Cl , CH_2Br , CH_2I , Phenyl, OH, OCH_3 ist.

11. Eine Verbindung nach Anspruch 1, dadurch gekennzeichnet, dass Z gleich N (Stickstoff) ist.
12. Ein Markierungsvorläufer für die Synthese einer radioaktiv markierten Verbindung nach Anspruch 1, umfassend ein Reagenz und eine Verbindung der Struktur:



worin cpa gleich Cyclopropan-1,2-diyl ist; n eine natürliche Zahl größer gleich 0 ist; m eine natürliche Zahl größer gleich 1 ist, m und n gleich oder voneinander verschieden sind, AG eine Abgangsgruppe ist, die durch einen radioaktiven Substituenten ersetzt wird; und das Reagenz geeignet ist, die Abgangsgruppe AG durch einen radioaktiven Substituenten zu ersetzen.

13. Markierungsvorläufer nach Anspruch 12, dadurch gekennzeichnet, dass der radioaktive Substituent ein Radioisotop, ausgewählt aus der Gruppe, bestehend aus ^3H , ^{11}C , ^{14}C , ^{13}N , ^{18}F , ^{75}Br , ^{76}Br , $^{120-131}\text{I}$, oder ein Komplex eines metallischen Radioisotops, ausgewählt aus der Gruppe, bestehend aus ^{44}Sc , ^{64}Cu , ^{55}Co , ^{66}Ga , ^{67}Ga , ^{68}Ga , $^{99\text{m}}\text{Tc}$, ^{111}In ist.
14. Verfahren zum Durchführen einer Positronenemissions-Tomographie-Abbildung, einer Einzelphotonenemissions-Tomographieabbildung, einer Autoradiographie oder eines Radioassays eines Subjekts, umfassend das Verabreichen einer abbildungserzeugenden Menge einer Verbindung nach Anspruch 1, welche mindestens ein Radioisotop oder einen Komplex eines metallischen Radioisotops enthält, an das Subjekt und das Messen der Verteilung und gegebenenfalls des Gehalts der Verbindung innerhalb des Subjekts mittels Positronenemissions-Tomographie, Einzelphotonenemissions-Tomographie, Autoradiographie oder Radioassay.
15. Verfahren nach Anspruch 14, worin das Radioisotop ausgewählt ist aus der Gruppe, bestehend aus ^3H , ^{11}C , ^{14}C , ^{13}N , ^{18}F , ^{75}Br , ^{76}Br , ^{120}I , ^{124}I , ^{44}Sc , ^{64}Cu , ^{55}Co , ^{66}Ga , ^{68}Ga und die Verteilung der Verbindung mittels Positronenemissions-Tomographie gemessen wird.
16. Verfahren nach Anspruch 14, worin das Radioisotop ausgewählt ist aus der Gruppe, bestehend aus ^{123}I , ^{131}I , ^{67}Ga , $^{99\text{m}}\text{Tc}$, ^{111}In und die Verteilung der Verbindung innerhalb des Subjekts mittels Einzelphotonenemissions-Tomographie gemessen wird.
17. Verfahren nach Anspruch 14, worin das Radioisotop ausgewählt ist aus der Gruppe, bestehend aus ^3H , ^{14}C und die Verteilung und der Gehalt der Verbindung innerhalb des Subjekts mittels Autoradiographie oder Radioassay gemessen wird.

Referenzen

- (1) W. Saba, H. Valette, M.-A. Schollhorn-Peyronneau, C. Coulon, M. Ottaviani, S. Chalon, F. Dolle, P. Emond, C. Halldin, J. Helfenbein, J.-C. Madelmont, J.-B. Deloye, D. Guilloteau, M. Bottlaender, *Synapse* **2006**, 61, 17.
- (2) T. Beuming, J. Kniazeff, M. L. Bergmann, L. Shi, L. Gracia, K. Raniszewska, A. H. Newman, J. A. Javitch, H. Weinstein, U. Gether, C. J. Loland, *Nature Neuroscience* **2008**, 11, 780
- (3) F. Dolle, P. Emond, S. Mavel, S. Demphel, F. Hinnen, Z. Mincheva, W. Saba, H. Valette, S. Chalon, C. Halldin, J. Helfenbein, J. Legailard, J. C. Madelmont, J.-B. Deloye, M. Bottlaender, D. Guilloteau, *Bioorg. Med. Chem.* **2006**, 14, 1115
- (4) T. J. Volz, J. O. Schenk, *Synapse* 2005, 58, 72
- (5) S. Singh, *Chem. Rev.* **2000**, 100, 925
- (6) G. F. Morgan, D. P. Nowotnik, *Drug News & Perspectives* **1999**, 12, 137
- (7) V. Marshall, D. Grosset, *Movement Disord.* **2003**, 18, 1415
- (8) M. Yaqub, R. Boellaard, B. N. M. van Berckel, M. M. Ponsen, M. Lubberink, A. D. Windhorst, H. W. Berendse, A. A. Lammertsma, *J. Cerebr. Blood Flow Metab.* **2007**, 27, 1397

5 Summary and Conclusions

The present thesis deals with the development of improved Dopamine-transporter ligands for the visualisation of extra-striatal and striatal DAT populations. Tropane derivatives have been selected as lead, and radiolabelling was designed for ^{11}C , ^{18}F and ^{68}Ga .

A particular aspect was concerned with studies towards the synthesis of lipophilic [^{68}Ga]Ga(III)-labelled chelator-DAT-ligand conjugates, to combine the high relevance of clinical Parkinson diagnosis with the potential of the cost-effective and generator-derived positron-emitter ^{68}Ga .

The initial task within the present work was the design and the synthesis of novel cocaine-derived structures. This included retrosynthetic approaches to synthetic routes for all required building blocks. As a result, a novel stereoselective route towards the synthesis of terminally-fluorinated trans-1,2-disubstituted cyclopropanes has been developed. These were the prerequisites for eight novel phenyltropanes.

Furthermore, a synthetic route to a linear C_4 -segment, namely the 4-fluorobut-2-yn-1-yl-chain has been developed. Both synthons were utilised for the synthesis of novel cocaine derivatives, bearing an inflexible substituent at the position-8 nitrogen of 2-exo-carboxymethyl-3-exo-phenyl-8-azabicyclo[3.2.1]octanes. The derivatives obtained via the introduction of a linear alkyne segment were subsequently reduced to the saturated butyl analogues. Selective reduction of the alkyne to an (E)-configured double bond afforded LBT-999. Thus, the versatile 4-fluoro-but-2-yn-1-yl moiety provided access to the residual derivatives via the convenient reduction/hydrogenation of the triple bond. The new derivatives were subsequently converted into water-soluble hydrochloride salts and assayed in human embryonic kidney (HEK 293) cell lines, stably transfected with either human dopamine transporter (hDAT) RNA, or human 5-HT transporter (hSERT) RNA or human noradrenalin transporter (hNET) RNA. The tritiated natural substrates [^3H]dopamine, [^3H]serotonin and [^3H]noradrenalin were used as radioligands to determine the uptake inhibition potency and thereby the affinity of the new compounds. The selectivities were calculated as the affinity ratios of hSERT versus hDAT and hNET versus hDAT. Among the tested structures, two candidates emerged as interesting compounds in terms of affinity and selectivity. These were termed PR04.MZ (**13e**) and PR17.MZ (**13l**).

Compared to the most recently established candidate LBT-999 (**13q**), **13e** provides an eight-fold increase in DAT affinity, a three-fold increase in SERT selectivity and a two-fold increase in NET-selectivity. PR17.MZ provides a twofold higher affinity than **13q**, combined with a 5 fold improvement in SERT selectivity and a three-fold higher NET-selectivity.

The improvements are even more striking when compared to the clinically established gold-standard **7g**. In this regard **13e** exhibits a seven-fold increase in DAT affinity, a 37-fold increase in SERT selectivity and a 16 fold improvement in NET-selectivity. Compound **13l** provides a three-fold improved DAT affinity of even better improvements in SERT and NET selectivity of 77-fold and 30-fold, respectively.

Table 2: IC₅₀ values and monoamine transporter selectivity of novel phenyl tropanes, as determined in human embryonic kidney cells (HEK 293) stably transfected with hDAT, hSERT and hNET-RNA.

entry	structure	R	hDAT _{IC50} (hDAT _{Ki}) / nM	hSERT _{IC50} (hSERT _{Ki}) / nM	hNET _{IC50} (hNET _{Ki}) / nM	SERT / DAT	NET /DAT
13a		Me	7.8±0.3	810±5	37±0.9	104	5
13b		Cl	22±0.9	1400±0.3	29±1.2	64	1.5
13c		F	19±0.9	2600±0.4	31±1.1	137	1.5
13d		H	33±0.9	4000±0.5	136±0.8	121	4
13e		Me	3.3±0.5	240±4	31±0.6	74	10
13f		Cl	17±1	270±0.2	41±0.7	17	2.5
13g		F	16±0.9	1400±0.2	21±1.3	89	1.5
13h		H	5.8±0.6	250±0.1	13±0.5	44	2
13i		Me	14±0.5	950±3	56±0.4	70	4
13j		Cl	4.3±0.5	220±0.4	16±0.4	50	3.5
13k		F	31±1	690±5	76±1	22	2.5
13l		H	11±0.5	1400±3	175±0.8	134	17
13m		Me	5.7±0.3	290±4	25±0.5	51	4.5
13n		Cl	8.9±0.3	160±2	24±0.8	18	3
13o		F	12±0.6	420±2	37±0.9	34	3
13p		H	34±0.9	560±3	84±0.7	16	2.5
13q			26±0.9	700±2	150±2	27	6
7a		F	40±0.9	2300±0.3	120±2	57	3
7b ^a		I	(6.3±1.7)	(29±6.4)	(33±13)	4.5	5
7b ^c		I	(0.5)	(0.7)	(474)	1.5	1000 ^d
7h ^a		I	(91±5)	(130±31)	(130±49)	1.5	1.5
7k ^c		Cl	(1.53)	(39.1)	(240)	25.5	157 ^d
7g ^a		I	(28±7)	(110±64)	(70±15)	4	2.5
3 ^a			(320±130)	(580±110)	(180±25)	2	0.6

a) Taken from Ref. [16z]: IC₅₀ and values were converted to K_i values using the Cheng and Prusoff equation, $K_i = IC_{50} / (1 + [L] / K_m)$ (where [L] is concentration of [³H]DA, [³H]5-HT or [³H]NE; K_m values from Eadie-Hofstee-plots. b) Values are mean ± SD (nM). c) Taken from Ref. [16o] K_i from murine kidney cells transfected with hDAT, hSERT and hNET, [³H]Win 35,428, [³H]Citalopram and [³H]Nisoxetine were used as radioligands. d) the systematically higher values might be related to the use of a different assay.

The main effort for radiolabelling and further characterisation, however, was focussed on PR04.MZ. This was due to the fact, that the publication of the cyclopropane containing PR17.MZ was postponed due to the patent submission.

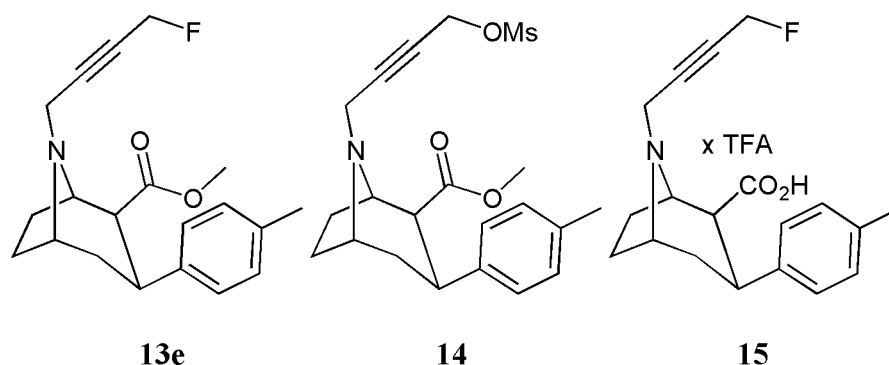


Figure 1: The target compound PR04.MZ (**13e**) and precursors for fluorine-18 (**14**) and carbon-11 (**15**) labelling; R = Me, Cl, F, H

For these reasons, a mesylate labelling precursor for [^{18}F]PR04.MZ was prepared and directly labelled with [^{18}F]F $^-$ (cf. Figures 1 and 2).

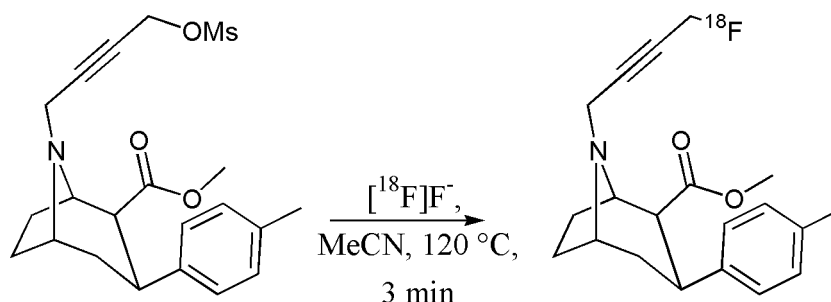


Figure 2: Direct nucleophilic radiofluorination of precursor **7**, conditions h) [$\text{K}^+\text{K}222$][^{18}F]F $^-$ cryptate complex, K_2CO_3 , MeCN, 120 °C, 3 min, ~20 % radiochemical yield

The labelled product was separated and transferred into injectable sterile formulation via cation exchange and online sterile filtration. In parallel, the reference compound PR04.MZ was assayed in a binding study to validate the affinity and selectivity obtained from the uptake inhibition assay. The initial characterisation included *in vitro* autoradiography in male, healthy Wistar rat brain sections, to access the specific binding characteristics of [^{18}F]PR04.MZ. Brain uptake and selectivity for the DAT were elucidated via a baseline-block study with a known selective DAT ligand in wildtype mice. To evaluate the peripheral biodistribution, the excretion route as well as plasma and cerebral metabolism, an *ex vivo* biodistribution was conducted in healthy, mal Sprague-Dawley (SD) rats.

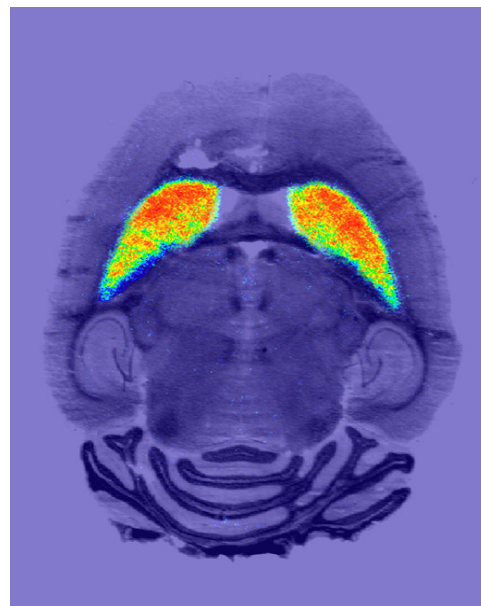
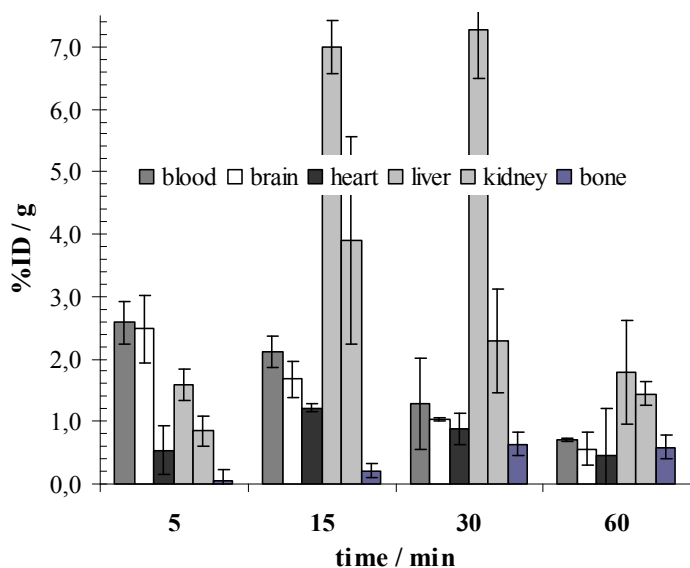


Figure 3: Ex vivo biodistribution in Sprague-Dawley rats (left) and ex vivo autoradiography (right) in wildtype mice (AR-image shows overlay of radioactivity distribution above the stained brain-section)

Encouraged by the positive finding during the initial biological characterisation, the first μ PET-studies were conducted in male, healthy Wistar rats. The cerebral distribution was analysed and it was found that the tracer specifically accumulates in the rat striatum.

In conclusion, it was found that the novel candidate provides a very high ratio between the specific accumulation within the target region and non-specific binding in non-target regions. The accumulation is reasonably fast and blocking, as well as displacement with other selective DAT-inhibitors leads to significant reductions in the radioactivity concentration within the target regions. This indicates an outstanding selective binding profile. The candidate is well suited for the non-invasive exploration of the rat dopamine transporter (rDAT).

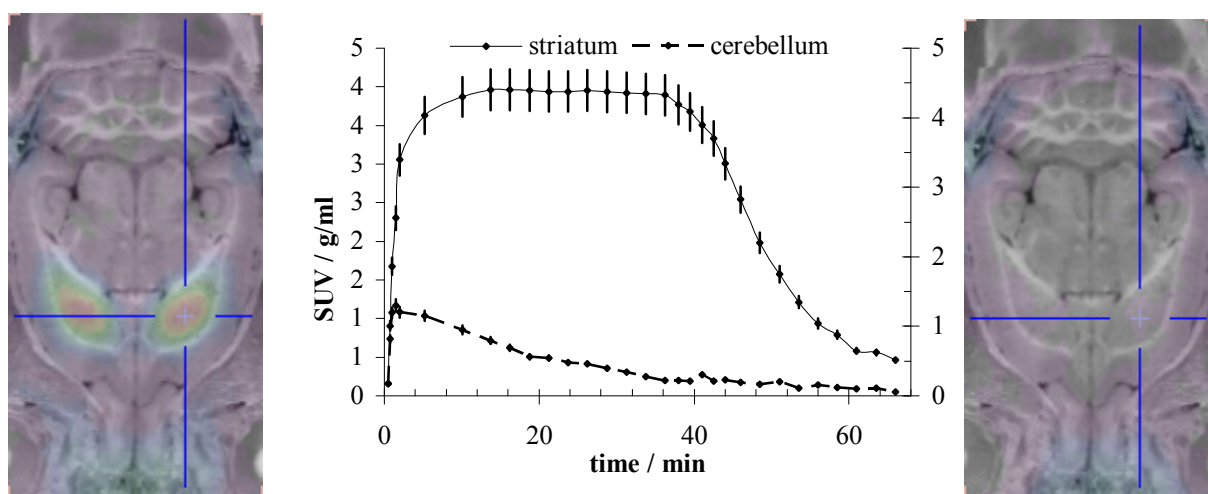


Figure 4: left: PET/MR-fusion, summed frames from 10 to 30 min, middle: time-activity-curve, right: PET/MR-fusion, summed frames from 45-65 min.

After this suitability of [^{18}F]PR04.MZ had been shown in the rodent brain, carbon-11 labelling was examined, to investigate the suitability of [^{11}C]PR04.MZ for multi-injection studies and to conduct a primate study in *anubis papio* baboons. Thereby, the comparison of [^{11}C]PR04.MZ and [^{18}F]PR04.MZ would be possible under representative conditions. The latter allows further information on potential metabolism of the compound due to the different labelling positions. Furthermore, the baboon brain enables the visualisation of the midbrain region with high-resolution PET (Siemens ECAT exact HR+, 63 slice PET scanner). Furthermore, plasma protein binding, metabolism and plasma concentration of the radiotracer can be determined online, throughout every baboon study. In addition, multi-injection protocols are conveniently feasible. This plan required efficient carbon-11 labelling of the radiotracer and screening for labelled metabolites in the brain, which originate from differential metabolism of the carbon-11 labelled analogue. The carboxylic acid function is the most convenient site for the introduction of the [^{11}C]methyl label into PR04.MZ. However, several groups have encountered issues when labelling carboxylic acids with readily available [^{11}C]MeI, in many cases, the elaborate use of [^{11}C]MeOTf was necessary to obtain moderate yields. During the method development for ^{11}C methylation of PR04.MZ, a yield of $95 \pm 5\%$ was achieved after 5 min at $75\text{ }^\circ\text{C}$, using a system consisting of Rb_2CO_3 dissolved in DMF. Thereby high-yield labelling of the carboxylic acid function, even in a readily available ammonium salt precursor was possible (cf. Figure 5). This is a remarkable improvement in both, labelling yield and precursor preparation.

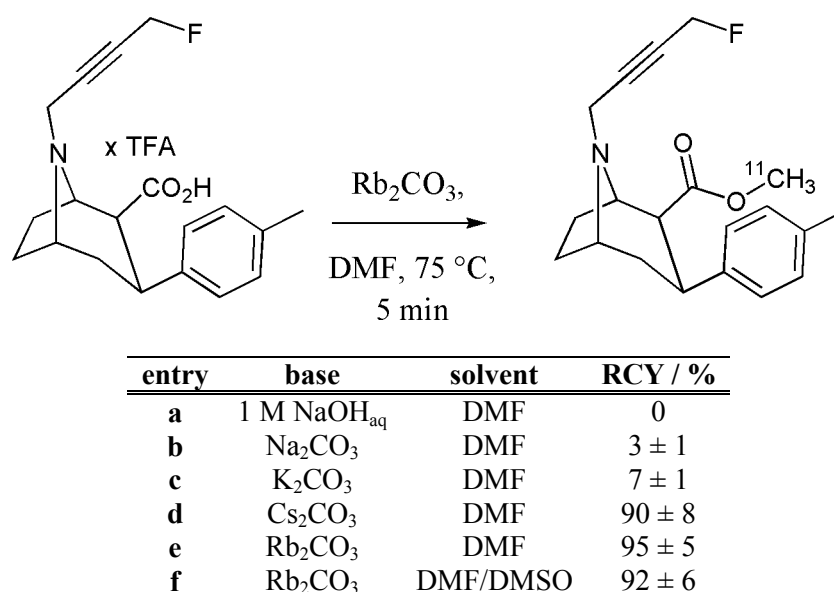


Figure 5: Carbon-11 labelling reaction and screening parameters

With [^{11}C]PR04.MZ synthesised, a multi-injection test-retest PET-scan was conducted in a single female baboon (Daisy, 17.2 kg) at Brookhaven National Laboratory, Medical Department. Three sequential radiosyntheses were conducted on the same day to provide high specific activity for each scan. The same baboon was scanned again after four weeks of rest and recovery.

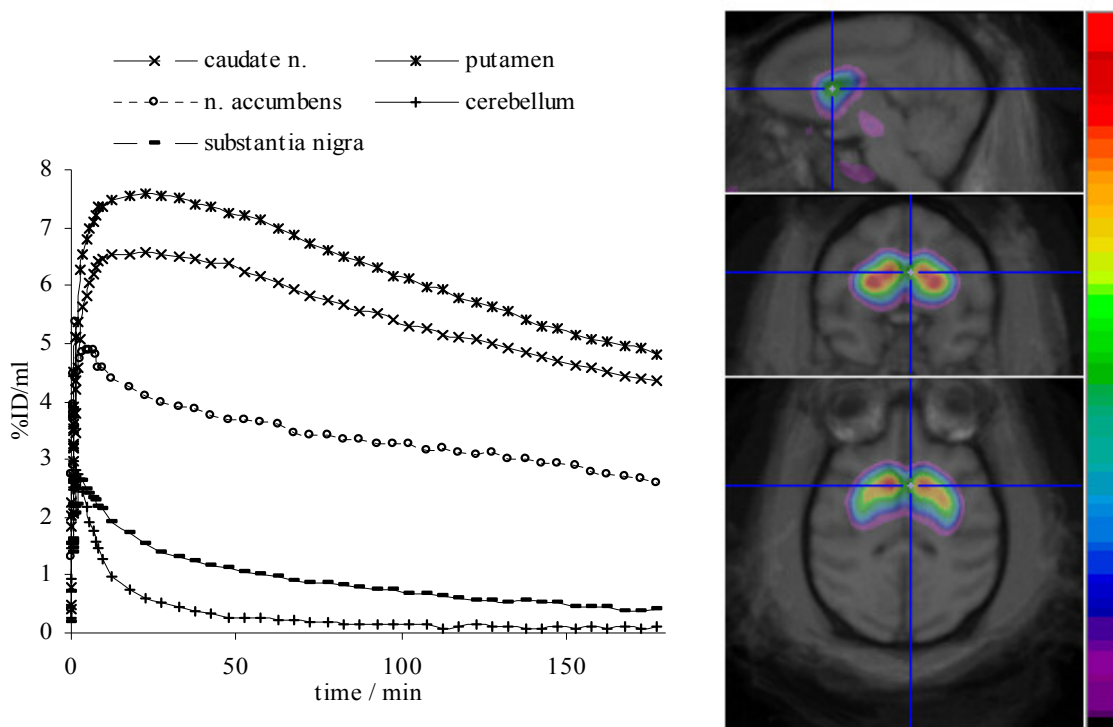


Figure 6: Long-term scan with $[^{18}\text{F}]\text{PR04.MZ}$, time activity curves (left) for various brain regions and sagittal, coronal and transversal view on PET/MR-fusion images of the basal ganglia

The Distribution Volumes (DV) obtained from the quantitative evaluation of the PET-data are comparable to those obtained for $[^{11}\text{C}]\text{LBT999}$ (cf. Table 3). In contrast the binding potentials (BP; from SRTM) obtained for $[^{11}\text{C}]\text{PR04.MZ}$ in the DAT-containing brain regions are significantly higher, indicating a lower non-specific contribution to the cerebral distribution of $[^{11}\text{C}]\text{PR04.MZ}$. These data reflect the main advantage of the new ligand compared to $[^{11}\text{C}]\text{LBT999}$, $[^{11}\text{C}]\text{PR04.MZ}$ is even more suited for the exploration of the extrastriatal DAT.

Table 3: Distribution volumes (DV) from Logan plots after an acquisition time of 30 min, binding potentials (BP) from simplified reference tissue model (STR-model), influx constant K_1 and efflux constant k_2 from two compartment reference tissue model)

$[^{11}\text{C}]\text{PR04.MZ}$	DV (Logan)	BP (SRTM)	K_1	k_2
cerebellum	4	1	0.144	0.036
midbrain	12.4	3.1	0.064	0.016
n. accumbens	35.8	8.9	0.03	0.0076
caudate nucleus	118	29.5	0.017	0.004
putamen	147.6	36.9	0.015	0.004

Values from three independent studies with $[^{11}\text{C}]\text{PR04.MZ}$ in the same baboon.

This time, a 90 min $[^{11}\text{C}]\text{PR04.MZ}$ scan was conducted, followed by a long term scan with $[^{18}\text{F}]\text{PR04.MZ}$ for 3 h and subsequent displacement with a structurally non-analogue DAT-inhibitor. It was found that both tracers visualise the relevant striatal and extra-striatal DAT. $[^{11}\text{C}]\text{PR04.MZ}$ is reliable for multi-injection or multi-tracer studies and $[^{18}\text{F}]\text{PR04.MZ}$ might

be particularly suited for routine applications in diagnostic imaging.

At this point the last potential drawback of [^{18}F]PR04.MZ was identified as the comparably low labelling yield for nucleophilic fluorination. Therefore, the reaction was transferred into a focussed microwave reactor and the synthesis conditions were optimised. Finally, a new labelling method was developed that resulted in a radiochemical yield of $80\pm 10\%$ after a microwave irradiation for only 45 seconds. Thereby, a five-fold improvement of radiochemical yields for [^{18}F]PR04.MZ was achieved, whereas the total synthesis duration was shortened to 35 min. This may not only have an impact on the routine batch production of [^{18}F]PR04.MZ, but also for a variety of different radioligands, such as LBT999.

After the successful synthesis and characterisation of fluorine-18 and carbon-11 labelled tropanes, the feasibility of lipophilic, hexadentate N_3S_3 -chelators for ^{68}Ga was examined.

Initial experiments towards the development of a Ga-chelate conjugated DAT-ligand involved the optimisation and establishment of synthetic routes to the required chelators. Apart from low published yields, most reports of charge neutral gallium complexes are concerned with monofunctional chelators. These might complex gallium on the one hand, but are not suited for conjugation to biomolecules on the other. Therefore a new concept for versatile bifunctional chelators was introduced. Based on this concept and the optimisation of the literature known procedures, retrosynthetic analysis yielded a convenient route to a potentially lipophilic chelator with a built-in conjugation site.

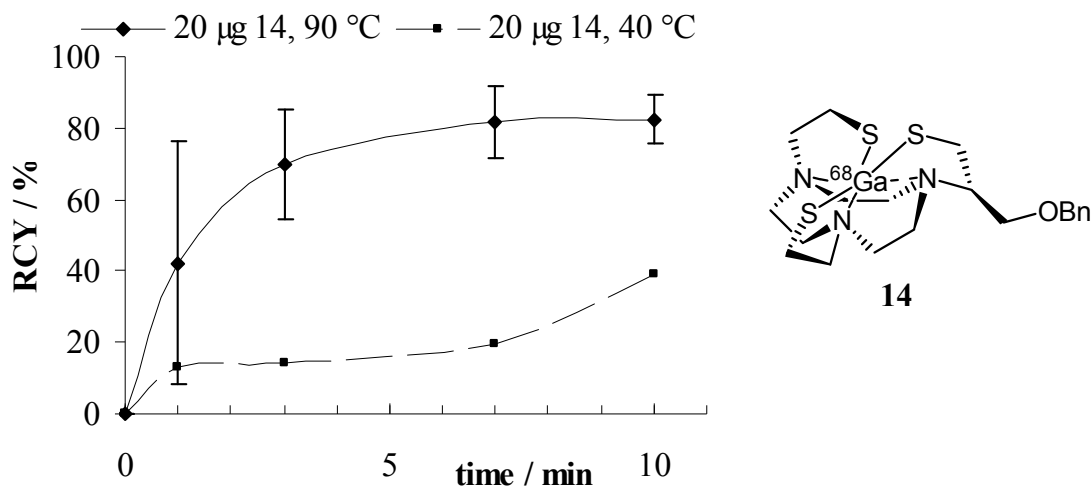


Figure 7: Plot of radiochemical yield as a function of reaction time for a novel N_3S_3 -type chelator. (^{68}Ga 14)

This new chelator was synthesised, labelled and the lipophilicity was measured via an OECD HPLC-method. As a result it was found, that the chelate does not exhibit pronounced hydrophilic properties as in the case of its carboxylate or phosphonate congeners. Although sufficient lipophilicity for the penetration of the blood brain barrier was not achieved, the final product shows remarkable increases in lipophilicity, indicating validity for the N_3S_3 -approach. Furthermore, this is the first successful synthesis of a 1,4,7-based bifunctional chelator bearing mercaptoethyl donor pendant arms.

In conclusion, novel highly promising candidate DAT-ligands were synthesised and characterised. Among these, two compounds emerged as outstandingly selective. The novel cocaine derivative [¹⁸F]PR04.MZ provides appropriate characteristics for routine PD-diagnosis with PET. The disadvantageous, slow equilibria, as well as the non-selective binding profile that has limited the use of many of its congeners are not an issue with the new compound. This might be particularly useful for the accurate and sensitive determination of therapeutic doses for PD-medication and the rating of therapeutic success and for imaging of low density, extra-striatal DAT. Furthermore, the novel imaging agent can be used as versatile tool for the development of new pharmaceuticals which interact with the dopaminergic system in general and in particular with the reuptake of DA. The novel, microwave enhanced labelling method for the nucleophilic aliphatic fluorination with [¹⁸F]F⁻ affords high labelling yields in shorter reaction times, which is beneficial for the routine production of [¹⁸F]PR04.MZ and similar compounds.

In contrast, the carbon-11 labelled analogue can reliably be utilised for multi-injection studies in psychiatric and neuro-scientific research. Thereby new insights into the extra-striatal contributions to a variety of the dopaminergic system affecting pathologies might be provided. In this relationship, improved conditions for the ¹¹C-methylation were developed that utilise the readily available [¹¹C]MeI, which can be produced in high specific activity.

Furthermore the initial aspects towards the development of a ⁶⁸Ga-labelled DAT-ligand for routine diagnostic applications were conducted. With the obtained informations in hand, the further improvement of the required lipophilic bifunctional chelator and the subsequent introduction of the chelating moiety into the tropane body are the next milestones. The ⁶⁸Ga-labelled compound would possess a remarkable impact on the clinical availability of DAT-ligands for routine PD diagnosis. Thereby, a generator based low-cost alternative to ¹⁸F-fluorinated DAT-ligands would be provided for PET imaging.

6 References

- (1) O. Loewi, *Pflügers Arch. Ges. Physiol.* **1921**, 189, 239
- (2) M. M. Ter-Pogossian, M. E. Phelps, E.J. Hoffman, *Radiology* **1975**, 114, 89
- (3) M. E. Phelps, E.J. Hoffman, N.A. Mullani, M.M. Ter-Pogossian, *J. Nucl. Med.* **1975**, 16, 210
- (4) H. Levi, *Eur. J. Nucl. Med.* **1976**, 1, 3
- (5) (a) M.-C. Lasne, C. Perrio, J. Rouden, L. Barré, D. Roeda, F. Dolle, C. Crouzel, *Topics in Current Chemistry* **2002**, 222, 201; (b) L. Cai, S. Lu, V. W. Pike, *Eur. J. Org. Chem.* **2008**, 2853; (c) F. Roesch: *Handbook of Nuclear Chemistry* 4, Kluwer Academic Publishers: Dordrecht **2003**; (d) M. J. Welch, C. S. Redvanly, *Handbook of Radiopharmaceuticals: Radiochemistry and Applications*, Wiley: New York **2002**
- (6) Philips Medical Systems and Jens Langer, *Master-thesis* TU-Dresden **2003**
- (7) H. Herzog, *Rad. Phys. Chem.* **2006**, 76, 337
- (8) L. Sokoloff, *J. Cereb. Blood Flow Metab.* **1981**, 1, 7
- (9) (a) B. M. Gallagher, A. Ansari, H. Atkins, V. Casella, D. R. Christman, J. S. Fowler, T. Ido, R. R. MacGregor, P. Som, C.-N. Wan, A. P. Wolf, D. E. Kuhl, M. Reivich, *J. Nucl. Med.* **1977**, 18, 990; (b) T. Ido, C.-N. Wan, V. Casella, J. S. Fowler, A. P. Wolf, M. Reivich, D. E. Kuhl, *J. Labelled Compd. Radiopharm.* **1978**, 14, 175
- (10) (a) W. Forth, D. Henschler, W. Rummel, K. Starke, *Allgemeine und spezielle Pharmakologie und Toxikologie*. Spektrum Akademischer Verlag **1996**; (b) G. Thews, E. Mutschler, P. Vaupel, *Anatomie, Physiologie, Pathophysiologie des Menschen*. Wissenschaftliche Verlagsgesellschaft mbH **1999**; (c) J. G. Hardman, L. E. Limbird, A. Goodman Gilman, P. Dominiak, S. Harder, M. Paul, A. Goodman Gilman, *Goodman & Gilman: Pharmakologische Grundlagen der Arzneimitteltherapie* Bd. 1 and 2. McGraw-Hill **1999**; (d) F. M. Benes, *Trends Pharmacol. Sciences* **2001**, 22, 46, (e) S. R. Neves, P. T. Ram, R. Iyengar, G protein pathways, *Science* **2002**, 296, 1636; (f) J. Girault, P. Greengard, *Arch. Neurol.* **2004**, 61, 641; (g) H. Gray, *Gray's Anatomy*, 20, Lea & Febiger: Philadelphia **1918**.
- (11) (a) E. R. Kandel, J. H. Schwartz, T. M. Jessell. *Principles of Neural Science*, 4th edition, New York: McGraw-Hill **2000**; (b) S. G. Hormuzdi, M. A. Filippov, G. Mitropoulou, H. Monyer, R. Bruzzone, *Biochim. Biophys. Acta* **2004**, 1662, 113-137.
- (12) (a) F. Roesch, G. Gründer, M. Schreckenberger, G. Dannhardt, *Pharmazie in unserer Zeit* 2005, 6, 474-483; (b) R. A. Koeppe, K. A. Frey, T. M. Vander Borcht, A. Karlamangla, D. M. Jewett, L. C. Lee, M. R. Kilbourn, D. E. Kuhl, *J. Cerebr. Blood Flow Metab.* **1996**, 16, 1288-1299.
- (13) (a) N. D. Volkow, J. S. Fowler, G. J. Wang, R. Baler, F. Telang, *Neuropharm.* **2008**, in press; doi: 10.1016/j.neuropharm.2008.05.022; (b) K. Tatsch, *Eur. J. Nucl. Med.* **2002**, 29, 711-714; c) K. A. Frey, *Eur. J. Nucl. Med.* **2002**, 29, 715-717
- (14) (a) J. S. Fowler, N. D. Volkow, A. P. Wolf, S. L. Dewey, D. J. Schlyer, R. R. Macgregor, R. Hitzemann, J. Logan, B. Bendriem, S. J. Gatley, et al. *Synapse* **1989**, 4, 371; (b) D. Sulzer, *Clin. Neurosci. Res.* **2005**, 5, 117; (c) S. M. Aquilonius, K.

- Bergstrom, S. A. Eckernas, P. Hartvig, K. L. Leenders, H. Lundquist, G. Antoni, A. Gee, A. Rimland, J. Uhlin, B. Langstrom; *Acta. Neurol. Scand.* **1987**, 76, 183; (d) M. R. Kilbourn, J. E. Carey, R. A. Koeppel, M. S. Haka, G. A. Hutchins, P. S. Sherman, D. E. Kuhl, *Nucl. Med. Biol.* **1989**, 16, 569; (e) Y.-S. Ding, J. S. Fowler, N. D. Volkow, J. Logan, S. J. Gatley, Y. Sugano, *J. Nucl. Med.* **1995**, 36, 2298.
- (15) (a) B. K. Madras, A. G. Jones, A. Mahmood, R. E. Zimmerman, B. Garada, B. L. Holman, A. Davison, P. Blundell, P. C. Meltzer, *Synapse* **1996**, 22, 239; (b) P. C. Meltzer, P. Blundell, A. G. Jones, A. Mahmood, B. Garada, R. E. Zimmerman, A. Davison, B. L. Holman, B. K. Madras, *J. Med. Chem.* **1997**, 40, 1835; (c) H. F. Kung, H. J. Kim, M. P. Kung, S. K. Meegalla, K. Plossl, H. K. Lee, *Eur. J. Nucl. Med.* **1996**, 23, 1527; (d) S. K. Meegalla, K. Plossl, M. P. Kung, S. Chumpradit, D. A. Stevenson, S. A. Kushner, W. T. McElgin, P. D. Mozley, H. F. Kung, *J. Med. Chem.* **1997**, 40, 9 (e) M. P. Kung, D. A. Stevenson, K. Plossl, S. K. Meegalla, A. Beckwith, W. D. Essman, M. Mu, I. Lucki, H. F. Kung, *Eur. J. Nucl. Med.* **1997**, 24, 372.
- (16) (a) R. F. Dannals, J. L. Neumeyer, R. A. Milius, H. T. Ravert, A. A. Wilson, H. N. Wagner, *J. Labelled Compd. Radiopharm.* **1993**, 33, 147; (b) P. C. Meltzer, A. Y. Liang, A. L. Brownell, D. R. Elmaleh, B. K. Madras, *J. Med. Chem.* **1993**, 36, 855. (c) L. Muller, C. Halldin, L. Farde, P. Karlsson, H. Hall, C. G. Swahn, J. Neumeyer, Y. Gao, R. Milius, *Nucl. Med. Biol.* **1993**, 20, 249. (d) L. Farde, L.; C. Halldin, L. Muller, T. Suhara, P. Karlsson, H. Hall, *Synapse* **1994**, 16, 93. (e) S. P. Hume, S. K. Luthra, D. J. Brown, J. Opacka-Juffry, S. Osman, S. Ashworth, R. Myers, F. Brady, F. I. Carroll, M. J. Kuhar, D. J. Brooks, *Nucl. Med. Biol.* **1996**, 23, 377 (f) R. D. Schönbachler, P. M. Gucker, M. Arigoni, S. Kneifel, F. X. Vollenweider, A. Buck, C. Burger, T. Berthold, M. Brühlmeier, P. A. Schubiger, S. M. Ametamey, *Nucl. Med. Biol.* **2002**, 29, 19. (g) R. Schönbachler, S. M. Ametamey, P. A. Schubiger, *J. Labelled Compd. Radiopharm.* **1999**, 42, S447. (h) A. D. Gee, D. F. Smith, A. Gjedde, *J. Labelled Compd. Radiopharm.* **1997**, 39, 89. (i) T. Chaly, V. Dhawan, K. Kazumata, A. Antonini, C. Margouleff, J. R. Dahl, A. Belakhlef, D. Margouleff, A. Yee, S. Wang, G. Tamagnan, J. L. Neumeyer, D. Eidelberg, *Nucl. Med. Biol.* **1996**, 23, 999. (j) C. Lundkvist, C. Halldin, C. G. Swahn, H. Hall, P. Karlsson, Y. Nakashima, S. Wang, R. A. Milius, J. L. Neumeyer, L. Farde, *Nucl. Med. Biol.* **1995**, 22, 905 (k) Y. Ma, V. Dhawan, M. Mentis, T. Chaly, P. G. Spetsieris, D. Eidelberg, *Synapse* **2002**, 45, 125 (l) C. Lundkvist, J. Sandell, K. Nagren, V. W. Pike, C. Halldin, *J. Labelled Compd. Radiopharm.* **1998**, 41, 545 (m) A. L. Brownell, D. R. Elmaleh, P. C. Meltzer, T. M. Shoup, G. L. Brownell, A. J. Fischman, B. K. Madras, *J. Nucl. Med.* **1996**, 37, 1186 (n) A. J. Fischman, A. Bonab, J. W. Babich, E. Livni, N. M. Alpert, P. C. Meltzer, B. K. Madras, *Synapse* **2001**, 39, 332. (o) M. M. Goodman, C. D. Kilts, R. Keil, B. Shi, L. Martarello, D. Xing, J. Votaw, T. D. Ely, P. Lambert, M. J. Owens, V. M. Camp, E. Malveaux, J. M. Hoffman, *Nucl. Med. Biol.*, **2000**, 27, 1-12 (p) N. Harada, H. Ohba, D. Fukumoto, T. Kakiuchi, H. Tsukada, *Synapse* **2004**, 54, 37 (q) T. Chaly, R. Matakchieri, R. Dahl, V. Dhawan, D. Eidelberg, *Appl. Radiat. Isot.* **1999**, 51, 299. (r) M. M. Goodman, G. W. Kabalka, M. P. Kung, H. F. Kung, M. A. Meyer, *J. Labelled Compd. Radiopharm.* **1994**, 34, 488 (s) T. Chaly, R. M. Baldwin, J. L. Neumeyer, M. J. Hellman, V. Dhawan, P. K. Garg, G. Tamagnan, J. K. Staley, M. S. Al-Tikriti, Y. Hou, S. S. Zoghbi, X. H. Gu, R. Zong, D. Eidelberg, *Nucl. Med. Biol.* **2004**, 31, 125. (t) X. Peng, A. Zhang, N. S. Kula, R. J. Baldessarini, J. L. Neumeyer, *Bioorg. Med. Chem. Lett.* **2004**, 14, 5635 (u) F. Wuest, M. Berndt, K. Strobel, J. van den Hoff, X. Peng, J.

- L. Neumeyer, R. Bergmann, *Bioorg. Med. Chem.* **2007**, 15, 4511-4519. (v) M. Mitterhauser, W. Wadsak, L. K. Mien, A. Hoepfing, H. Viernstein, R. Dudczak, K. Kletter, *Synapse* **2005**, 55, 73, (w) A. A. Wilson, J. N. DaSilva, S. Houle, *Nucl. Med. Biol.* **1996**, 23, 141. (x) A. A. Wilson, J. N. DaSilva, S. Houle, *Appl. Radiat. Isot.* **1995**, 46, 765, (y) D. Xing, P. Chen, R. Keil, C. D. Kilts, B. Shi, V. M. Camp, G. Malveaux, T. Ely, M. J. Owens, J. Votaw, M. Davis, J. M. Hoffman, R. A. BaKay, T. Subramanian, R. L. Watts, M. M. Goodman, *J. Med. Chem.* **2000**, 43, 639; (z) T. Okada, S. Shimada, K. Sato, P. Schloss, Y. Watanabe, Y. Itoh, *Nucl Med Biol* **1998**, 25, 53 - 58
- (17) (a) Der Spiegel online 9.11.2005; IBMP (Institut für Biomedizinische und Pharmazeutische Forschung) Flusswasserstudie 2005; (b) R. L. Clarke, S. J. Daum, A. J. Gambino, M. D. Aceto, J. Pearl, M. Levitt, W. R. Cumiskey, E. F. Bogado, *J. Med. Chem.* **1973**, 16, 1260.
- (18) (a) S. Singh, *Chem. Rev.* **2000**, 100, 925; (b) F. Dollé, P. Emond, S. Mavel, S. Demphel, F. Hinnen, Z. Mincheva, W. Saba, H. Valette, S. Chalon, C. Halldin, J. Helfenbein, J. Legaillard, J.-C. Madelmont, J.-B. Deloye, M. Bottlaender, D. Guilloteau, *Bioorg. Med. Chem.* **2006**, 14, 1115
- (19) K. P. Zhernosekov, D. V. Filosofov, R. P. Baum, P. Aschoff, H. Bihl, A. Razbash, M. Jahn, M. Jennewein, F. Rösch, *J. Nucl. Med.* **2007**, 48, 1741